Molecular Phylogeny, Evolution and Biogeography of the Andean Gynoxyoid Group (Compositae, Asteroideae-Senecioneae).

Inaugural-Dissertation to obtain the academic degree

Doctor rerum naturalium (Dr. rer. nat.)

Submitted to the Department of Biology, Chemistry, Pharmacy

of the Freie Universität Berlin

by

Andrea Belen Escobari Vargas

2022

1st reviewer: Prof. Dr. Thomas Borsch

2nd reviewer: Prof. Dr. Julien Bachelier

Date of disputation: 08.12.2022

Acknowledgements

I would like to express my deepest gratitude to Prof. Dr. Thomas Borsch who gave me the chance to carry out my investigation at the Botanical Garden and Botanical Museum Berlin – BGBM. I am evenly grateful for his guidance during the design and development of this work. The interest and time he invested in each stage of this study gave rise to useful discussions that made this work possible and let me grow as a scientist and develop new skills in this wonderful science of Botany.

I am extremely grateful to Dr. Norbert Kilian who was a great advisor and stand next to me in every phase of this life stage starting with picking me in the airport, accompanying me during fieldwork, advising me in difficult situations and helping me until the defense of this work. His advices and support made this work possible, and I am convinced I could not have had a better and more patient advisor. I further acknowledge the support of PhD. Michael Grünstäudl during the first state of my research, his huge knowledge and abilities facilitated and sped up the data analysis.

I would like to thank the Herbario Nacional de Bolivia at the head of Dr. Carla Maldonado who supported this investigation in processing the collection permits for our fieldtrip in Bolivia, and Dr. Daniel Montesinos for the fieldtrip in Peru. Specially I am grateful to Dr. Stephan Beck from La Paz, Huber Vilca and Beatriz Nieto from Cochabamba for all his support during the collection trips. Further acknowledgements go to Magaly Mercado (BOLV), Eric Rodriguez (HUT) and Dr. Asuncion Cano (USM) who gave me the chance to check relevant collections for this investigation in their respective herbaria.

Special thanks to Dr. Tilo Henning, Dr. Robert Lücking, Ing. Kim Govers, Dr. Jeannine Marquardt, Wolf-Henning Kusber and Dr. Nadja Korotkova who supported me not only on a professional but personal way, and motivated me to overcome the frustration and many times the sadness as well. I will always be thankful for your time, for every supporting word, laughs, games and coffees we shared.

Thank should also go to Aydah Sabah, Julia Dietrich, Bettina Giesicke and Juliane Bettig who accompanied and assisted me with the laboratory work and with whom I could build a nice friendship. I specially would like to thank Sabine Scheel from the bottom of my heart, with whom I shared all my disappointment during my failed laboratory work and who worked very hard to find solutions to my problems. Thanks for carrying the cross with me, for being a good friend and for believing in me even when I could not. I am of course equally thankful for all the nice times and laughs we shared.

I further thank Robert Vogt and Katharina Rabe for taking care of all specimens loan formalities, as well as all herbaria which shared material for this study.

Funding for this project was provided by the Julia Krieg Forschungsfond of the BGBM in the context of the collaboration with the Herbario Nacional de Bolivia. Fieldtrips were additionally supported by the by the association Friends of the Botanical Garden of the BGBM.

Mi eterna gratitud a mi mamá Nancy, mi hermana Paola, mi tío Wilfredo, mi tía Jacqueline, mis primos Andreas y Claudia, y mis hijos Cachuchin, Eddy, Tequila y Nicolas que a pesar de la distancia me dieron ánimos y motivación para seguir hasta el final y nunca dudaron de creer en mí.

Estos seis años han sido un camino de aprendizaje no solo en el aspecto profesional sino también en lo personal. Este trayecto no hubiera sido posible sin el apoyo de la familia que pude hacer fuera de mi país, quienes estuvieron para mi hasta en los momentos más amargos de esta etapa y que me hicieron sentir que no estaba tan lejos de mi hogar. Mi inmensa gratitud a Ricardo Carrillo, Karina Sánchez y Patrick Plitzner por hacerme sentir parte de sus hogares, por el tiempo compartido con sus familias y por todas las horas de terapia escuchando penas y problemas. Mis peores momentos siempre se volvieron los más felices por qué los pasaba con ustedes. Un agradecimiento desde el corazón a mi amiga Blanca Behrends quien hizo mis días en el BGBM más livianos y con quién las horas pasaban volando charlando. Finalmente, pero no menos importantes agradezco a mis amigos Sergio Ávila, Georgia Fassou, Alvaro Martinez, Mirka Slowik y Taleja Brandenburger por todos los momentos compartidos y su sincera amistad

I would like to extend my thanks to the Botanic Garden and Botanic Museum which received my and hosted my six years. I had the chance to meet nice and friendly collages who offered me their help in any situation.

Declaration of Independence

Herewith I certify that I have prepared and written my thesis independently and that I have not used any sources and aids other than those indicated by me.

Summary

This study is focused on the Gynoxyoid group a species-rich lineage with low genetic distances within the subtribe Tussilaginineae. The Andean clade within the Asteraceae family comprises four genera and ca. 160 species. The genus *Paracalia* represents the smallest genus within the Gynoxyoid comprising only two species, the genera *Aequatorium* and *Paragynoxys* include 12 and 13 species respectively, and the largest genus *Gynoxys* contains 131 species. This group includes shrubs to big trees and eventually scandent shrubs (meanly *Paracalia*) which are distributed from north to south Andes, representing important components of the Andean vegetation. Analyses on plastid and nuclear data have retrieved this group as monophyletic, nevertheless these studies include only some representatives of this clade as part of their investigations. In that sense, the phylogenetic relationships at inter- and infrageneric level remained largely unresolved. Likewise, the morphological studies within this group is limited to close-distributed group of species.

The aim of this study is to elucidate the phylogenetic relationships of the Gynoxyoid clade and define genera and (for a reduced group) species limits within it. In that sense, 21 complete annotated chloroplast genomes from a representative subgroup of the Gynoxyoids and four related members of the Tussilaginineae were generated. Thereafter, phylogenetic analyses were performed under maximum likelihood and Bayesian approaches. In order to estimate the strength of the phylogenetic signal in each genome partition trees topologies supported by gene, intron, and intergenic spacer partitions were compared. In a second instance, the impact of indel coding as well as manual adjustments of multiple automatic DNA sequence on the reconstruction of phylogenetic tree was evaluated. Given the phylogenetic backbone retrieved in the first phase of this study, genera delimitation was evaluated. Morphological variation among genera was evaluated by selecting a representative group of members of the Gynoxyoids and searching for discontinuities. The set of characters contributing to the discontinuities and already stated diagnostic characters in prologues were evaluated with a character reconstruction analysis. A second evaluation of the potential set of morphological characters retrieved in the previous analysis was further extended to all remaining members of the Gynoxyoids. Consequently, a revision of the current genera and species circumscription is made and a checklist including all members of the clade is provided. When necessary, new circumscriptions were proposed. Finally, species delimitation was evaluated for a reduced number of species distributed exclusively in Bolivia. The Asteraceae checklist for Bolivia was the basis for the species selection. A morphological revision as described for the genera evaluation was carried out at species level. Based on the discontinuities, morpho-species were defined. Additionally, phylogenetic inferences were reconstructed on the nuclear markers ETS and ITS. The set of putative characters suitable for morpho-species was tested with a principal component analysis in order to test the clustering of morpho-species and phylogenetic clades. The results of all analyses resulted in the elaboration of a taxonomic treatment for all supported Bolivian species.

The phylogenetic results resolve the Gynoxyoid group as monophyletic. Phylogenetic trees on all three plastid genomic partitions retrieved well-supported clades. Nevertheless, incongruences in tree topologies were found among all three partitions. Moreover, significant differences were found among tree inferences before and after the manual curation of the alignments, meaning that the automatic multiple sequence alignment failed at the assessment of homology. Furthermore, the results show that a manual alignment correction is essential for phylogeny reconstruction, specially for closely related taxa. The phylogeny retrieved in this study is partially incongruent with the current generic classification, which was purely based on morphological data. The genus *Aequatorium* was represented by only one representative and its monophyly could not be tested, nevertheless, this unique specimen was retrieved as an independent clade. The genus *Paragynoxys* was retrieved as monophyletic. All members of the genus *Nordenstamia* were retrieved as being part of the *Gynoxys* clade, as well as one of the two members of the genus *Paracalia*. The second member of the genus *Paracalia* was retrieved as basal clade of the tree inference. In the second part of the study, the ancestral character reconstruction suggested a set of potential characters for genera delimitation. After testing the validity of this characters set in all members of the Gynoxyoids the delimitation and characterization of four genera was achieved. In that sense, the genus *Aequatorium* comprises all species with radiate white capitula, *Paragynoxys* includes trees with discoid white capitula distributed in Colombia and Venezuela, *Paracalia* characterizes by the absence of outer phyllaries and a central (Bolivia and Peru) distribution, and finally all members with yellow capitula are included in *Gynoxys.* The checklist resulted in a total of 158 species belonging to the four previously mentioned genera. The genus *Nordenstamia* was synonymized under *Gynoxys* and so all its members were newly synonymized in this study. Finally, although the phylogeny on the ETS and ITS markers of the Bolivian species retrieved incongruent topologies, it supported the circumscription of some species. The results of the principal component analysis supported most of the morpho-species, but vaguely the clades retrieved in the phylogenetic inference. Interestingly, both molecular and morphological analysis suggested the presence of at least one putative hybrid species. Based on these results, the taxonomic treatment for the Bolivian species of the Gynoxyoid clade resulted in 14 species belonging to *Paracalia* (1 sp) and *Gynoxys* (13 sp). This represented a reduction on the species number stated in the Asteraceae checklist for Bolivia as seven names were synonymized, and three names were excluded because of misidentifications.

This investigation represents the first comprehensive study on the Gynoxyoid clade. It includes a phylogenetic backbone, character states reconstruction and a morphological analysis. The molecular datasets reveled closely relationships among species, suggesting rapid-radiating evolution, which was supported by morphological data. Furthermore, based on this analysis we were able to delimit genera and in a more reduced geographic scale, at species level.

This study aims to contribute to the Flora de Bolivia which is part of the cooperation agreement between the Botanic Garden and Botanical Museum Berlin (Germany), the "Herbario Nacional de Bolivia" and the "Instituto de Ecología" de La Paz-Bolivia. That aims of this association are to collaborate in the formation of professionals in the area of botany for the subsequent application of knowledge.

Zusammenfassung

Diese Studie konzentriert sich auf die Gynoxyoid-Gruppe, eine artenreiche Linie mit geringen genetischen Abständen innerhalb der Untertribe Tussilaginineae. Die Andenklade innerhalb der Familie der Asteraceae umfasst vier Gattungen und ca. 160 Arten. Die Gattung Paracalia ist mit nur zwei Arten die kleinste Gattung innerhalb der Gynoxyoide, die Gattungen Aequatorium und Paragynoxys umfassen 12 bzw. 13 Arten, und die größte Gattung Gynoxys enthält 131 Arten. Diese Gruppe umfasst Sträucher bis hin zu großen Bäumen und schließlich skandierenden Sträuchern (gemeinhin als Paracalia bezeichnet), die vom Norden bis in den Süden der Anden verbreitet sind und wichtige Bestandteile der Andenvegetation darstellen. Analysen von Plastiden- und Nukleardaten haben diese Gruppe als monophyletisch herausgestellt, dennoch umfassen diese Studien nur einige Vertreter dieser Gruppe als Teil ihrer Untersuchungen. In diesem Sinne blieben die phylogenetischen Beziehungen auf inter- und infragenerischer Ebene weitgehend ungelöst. Auch die morphologischen Untersuchungen innerhalb dieser Gruppe beschränken sich auf eng verteilte Artengruppen.

Ziel dieser Studie ist es, die phylogenetischen Beziehungen der Gynoxyoid-Gruppe aufzuklären und Gattungen und (für eine reduzierte Gruppe) Artgrenzen innerhalb dieser Gruppe zu definieren. Zu diesem Zweck wurden 21 vollständige annotierte Chloroplastengenome von einer repräsentativen Untergruppe der Gynoxyoiden und vier verwandten Mitgliedern der Tussilaginineae erstellt. Anschließend wurden phylogenetische Analysen mit Hilfe von Maximum-Likelihood- und Bayes'schen Ansätzen durchgeführt. Um die Stärke des phylogenetischen Signals in jeder Genompartition abzuschätzen, wurden die durch Gen-, Intron- und intergene Spacer-Partitionen unterstützten Topologien verglichen. In einem zweiten Schritt wurden die Auswirkungen der Indel-Kodierung sowie manueller Anpassungen mehrerer automatischer DNA-Sequenzen auf die Rekonstruktion des phylogenetischen Baums bewertet. Angesichts des phylogenetischen Rückgrats, der in der ersten Phase dieser Studie gewonnen wurde, wurde die Abgrenzung der Gattungen bewertet. Die morphologische Variation zwischen den Gattungen wurde durch die Auswahl einer repräsentativen Gruppe von Mitgliedern der Gynoxyoiden und die Suche nach Diskontinuitäten bewertet. Der Satz von Merkmalen, der zu den Diskontinuitäten beiträgt, und bereits in Prologen angegebene diagnostische Merkmale wurden mit einer Zeichenrekonstruktionsanalyse bewertet. Eine zweite Bewertung der potenziellen morphologischen Merkmale, die in der vorherigen Analyse ermittelt wurden, wurde auf alle verbleibenden Mitglieder der Gynoxyoiden ausgeweitet. Infolgedessen wird eine Revision der aktuellen Gattungs- und Artenumschreibung vorgenommen und eine Checkliste mit allen Mitgliedern der Gattung vorgelegt. Soweit erforderlich, wurden neue Umschreibungen vorgeschlagen. Schließlich wurde die Abgrenzung der Arten für eine reduzierte Anzahl von Arten, die ausschließlich in Bolivien verbreitet sind, bewertet. Die Checkliste der Asteraceae für Bolivien bildete die Grundlage für die Artenauswahl. Auf Artniveau wurde eine morphologische Revision wie bei der Gattungsbewertung beschrieben durchgeführt. Auf der Grundlage der Diskontinuitäten wurden Morpho-Arten definiert. Zusätzlich wurden phylogenetische Rückschlüsse anhand der Kernmarker ETS und ITS rekonstruiert. Die für Morpho-Spezies geeigneten Merkmale wurden mit einer Hauptkomponentenanalyse untersucht, um das Clustering von Morpho-Spezies und phylogenetischen Kladen zu testen.

Die Ergebnisse aller Analysen führten zur Ausarbeitung einer taxonomischen Behandlung für alle unterstützten bolivianischen Arten.

Die phylogenetischen Ergebnisse weisen die Gynoxyoid-Gruppe als monophyletisch aus. Phylogenetische Bäume auf allen drei Plastiden-Genom-Partitionen ergaben gut unterstützte Kladen. Dennoch wurden zwischen allen drei Partitionen Inkongruenzen in den Baumtopologien festgestellt. Darüber hinaus wurden signifikante Unterschiede zwischen den Bauminferenzen vor und nach der manuellen Bearbeitung der Alignments festgestellt, was bedeutet, dass das automatische Multiple Sequence Alignment bei der Bewertung der Homologie versagt hat. Darüber hinaus zeigen die Ergebnisse, dass eine manuelle Alignment-Korrektur für die Rekonstruktion der Phylogenie unerlässlich ist, insbesondere bei eng verwandten Taxa. Die in dieser Studie ermittelte Phylogenie stimmt teilweise nicht mit der aktuellen Gattungsklassifikation überein, die rein auf morphologischen Daten beruht. Die Gattung Aequatorium war nur durch einen einzigen Vertreter vertreten, so dass ihre Monophylie nicht geprüft werden konnte; dennoch wurde dieses einzige Exemplar als eigenständige Klade ermittelt. Die Gattung Paragynoxys wurde als monophyletisch eingestuft. Alle Mitglieder der Gattung Nordenstamia wurden der Gynoxys-Klade zugeordnet, ebenso wie eines der beiden Mitglieder der Gattung Paracalia. Das zweite Mitglied der Gattung Paracalia wurde als basale Klade der Bauminferenz ermittelt. Im zweiten Teil der Studie wurde anhand der Rekonstruktion der Vorfahren eine Reihe potenzieller Merkmale für die Abgrenzung der Gattungen vorgeschlagen. Nachdem die Gültigkeit dieses Zeichensatzes bei allen Mitgliedern der Gynoxyoiden getestet wurde, konnte die Abgrenzung und Charakterisierung von vier Gattungen erreicht werden. In diesem Sinne umfasst die Gattung Aequatorium alle Arten mit strahligen weißen Körbchen, Paragynoxys umfasst Bäume mit scheibenförmigen weißen Körbchen, die in Kolumbien und Venezuela verbreitet sind, Paracalia zeichnet sich durch das Fehlen äußerer Phyllarien und eine zentrale (Bolivien und Peru) Verbreitung aus, und schließlich werden alle Mitglieder mit gelben Körbchen in Gynoxys aufgenommen. Die Checkliste ergab insgesamt 158 Arten, die zu den vier zuvor genannten Gattungen gehören. Die Gattung Nordenstamia wurde unter Gynoxys synonymisiert, so dass alle ihre Mitglieder in dieser Studie neu synonymisiert wurden. Die Phylogenie der bolivianischen Arten auf der Grundlage der ETS- und ITS-Marker ergab zwar inkongruente Topologien, unterstützte aber die Umschreibung einiger Arten. Die Ergebnisse der Hauptkomponentenanalyse unterstützten die meisten Morpho-Arten, aber nur vage die Kladen, die in der phylogenetischen Schlussfolgerung gefunden wurden. Interessanterweise deuteten sowohl die molekulare als auch die morphologische Analyse auf das Vorhandensein von mindestens einer mutmaßlichen Hybridart hin. Auf der Grundlage dieser Ergebnisse führte die taxonomische Behandlung der bolivianischen Arten der Gynoxyoid-Klade zu 14 Arten, die zu Paracalia (1 sp) und Gynoxys (13 sp) gehören. Dies bedeutet eine Verringerung der in der Checkliste der Asteraceae für Bolivien angegebenen Artenzahl, da sieben Namen synonymisiert und drei Namen aufgrund von Fehlbestimmungen ausgeschlossen wurden.

Diese Untersuchung stellt die erste umfassende Studie über die Gynoxyoid-Klade dar. Sie umfasst ein phylogenetisches Grundgerüst, die Rekonstruktion von Merkmalsausprägungen und eine morphologische Analyse. Die molekularen Datensätze ergaben enge Beziehungen zwischen den Arten, was auf eine sich schnell ausbreitende Evolution hindeutet, die durch morphologische Daten bestätigt wurde. Darüber hinaus konnten wir auf der Grundlage dieser Analyse Gattungen und in einem kleineren geografischen Maßstab auf Artniveau abgrenzen.

Diese Studie soll einen Beitrag zur Flora de Bolivia leisten, die Teil des Kooperationsabkommens zwischen dem Botanischen Garten und Botanischen Museum Berlin (Deutschland), dem "Herbario Nacional de Bolivia" und dem "Instituto de Ecología" de La Paz-Bolivia ist. Ziel dieses Vereins ist es, bei der Ausbildung von Fachleuten im Bereich der Botanik für die spätere Anwendung des Wissens zusammenzuarbeiten.

Contents

Chapter 1: General introduction

1.1 The Tussilagininae subtribe of the Senecioneae tribe

The Senecioneae tribe is subdivided in four subtribes: Abrotanellinae, Tussilagininae, Othonninae and Senecioninae (Pelser et al., 2007, 2010) each distinguished by morphological characters (see García-Mendoza et al., 2020). Early characterization of the Tussilagininae subtribe was based on morphological characters such as polarized endothecial cell wall thickenings, cylindrical filament collar and a chromosome number x = 30 (Jeffrey and Chen 1984). Bremer (1994) supported this hypothesis based on a morphological analysis including a set of morphological characters that were traditionally used for the characterization of the subtribe. Based on his results, the author additionally transferred all genera from Tephroseridinae to Tussilagininae. In that sense, the author recognized 48 genera and ca. 730 species distributed worldwide and expanded the ancient morphological characters set. Robinson et al. (1997) evaluated the chromosome number of Tussilagininea sensu Bremer (1994). Their results characterized the Tussilagininae based on a chromosome number of x = 30 and supported the results of Jeffrey and Chen (1984). Nevertheless, Robinson et al. (1997) reported aneuploid reductions within the subtribe variating from x = 15 to 30. Pelser et al. (2007) reconstructed the phylogeny of the Senecioneae tribe on molecular data (ITS) and retrieved Tussilagininae sensu Bremer (1994) as non-monophyletic. The phylogenetic analysis recovered two subtribes (Othonninae and Senecioninae) nested within Tussilagininae. In that sense, the authors informally named Tussilagininae s.str. to a monophyletic group comprising the greatest number of taxa belonging to Tussilagininae. Although the Tussilagininae s.str. was supported as monophyletic, the internal relationships among the 34 genera contained within were largely unresolved as they show mixed supported values. These results were confirmed by Pelser et al. (2010) based on an expanded sampling and increasing the molecular markers to the nuclear marker ETS and five plastid markers. According to Funk et al. (2009) the Tussilaginineae includes nowadays mostly shrubs and in less quantity, tree forms that occur meanly in the Gynoxyoid group (growing until 18 m). Among the morphological characters that distinguish the clade are phyllaries with a medial rib thickened at the base; florets yellow or whitish; (García-Mendoza 2020), anther collar cylindrical, endothecial tissue polar; branches of the style with continuous stigma surface (Funk et al., 2009, García-Mendoza 2020), style branches often glabrous except for the apical appendages (sweeping hairs, papillate, or hairy structures) (Funk

et al., 2009). The predominant distribution of the subtribe is in Central America with a center of diversity in Mexico (Funk et al., 2009, Pelser et al., 2007, Pelser et al., 2010). The Gynoxyoid group was retrieved within the Tussilagininae as sister clade of eight genera from Central and North America (e.g., *Arnoglossum*, *Pittocaulon*, and *Roldana*) by Pelser et al. (2007, 2010).

1.2 The Gynoxyoid group

The Gynoxyoid group was defined by Jeffrey (1992) on the combination of cylindrical anther-collars and polar endothecial thickenings in addition to a chromosome number based on x = 10. Jeffrey included six genera within this clade *Alciope* DC. Ex Lindl. from South Africa, *Herodotia* Urb. & Eckm., from Haiti, and *Aequatorium* B. Nord., *Gynoxys* Cass., *Paracalia* Cuatrec. and *Paragynoxys* Cuatrec. from South America. Moreover, the author includes a set of characters suitable for genera recognition. Later, Robinson et al. (1997) studied the chromosome numbers in the Senecioneae tribe and included the Gynoxyoid group defined by Jeffrey (1992), nevertheless including exclusively the South American genera. The authors supported Jeffrey´s hypotheses while characterizing the group as having n= 40 or ca. 40. Furthermore, Robinson et al. (1997) complemented the morphological character set as describing the inside of the style branches with a single continuous stigmatic surface.

The first genus of this group to be described was *Gynoxys* Cass. (1827) including six species of which five were initially placed in the genus *Senecio*. Since then, the species number have gradually incremented over time reaching ca. 160 species. Cuatrecasas (1955) described the second genus of this group i.e., *Paragynoxys* and he transferred six *Senecio* species to the new genus. Shortly after, the same author described the genus *Paracalia* including two species (Cuatrecasas 1960). *Aequatorium* was described by Nordenstam (1978) including one *Senecio* species and a newly described species. Finally, Lundin (2006) segregated 12 species previously placed in *Aequatorium*, and in addition to three *Gynoxys* species stablished the genus *Nordenstamia.*

The Gynoxyoid group spreads along the Andes including north, central and south Andes from Venezuela to Argentina with a higher concentration in Peru (66), Colombia (43) and Ecuador (32). The species span from 500 to 4500 m, but the vast majority are found between 2500-3900 m. The main habitats of the Gynoxyoids are the Páramos and Humid Forest representing important components of Andean highlands and having high levels of endemism.

1.2.1 Morphological studies

Since the former description of the Gynoxyoid oldest genus (i.e., *Gynoxys*) a great number of new species have been described. Nevertheless, the information available on this group is exclusively based on individual or local studies that comprehend a limited number of species or species from a reduced area of distribution. One of the most important botanists to contribute to the history of this group was José Cuatrecasas. His publications: Studies on Andean Compositae I (1950) and II (1951), represent the most completely taxonomic treatment of all *Gynoxys* species described until his time. Cuatrecasas described a considerable number of new species (see checklist in chapter 2). Likewise, for *Gynoxys* the same author made the first taxonomic treatment for *Paracalia* and *Paragynoxys*. Correa (2003) updated the revision on *Paragynoxys* including all species and discussing taxonomic changes among *Paragynoxys* and *Paracalia* resulting in the transfer of one species to *Paragynoxys*. Further contribution to this group, specially to the genus *Gynoxys* was made by Herrera (1980). Specifically, the author provides a taxonomic treatment for all *Gynoxys* species described for Peru representing this the unique taxonomic treatment for any of the Gynoxyoid genera for Peru. Likewise, the genus *Aequatorium* was studied in Colombia by Díaz-Piedrahíta and Cuatrecasas (1990), and in Ecuador by Nordenstam (1997).

The customized studies within this group, in addition to the constant description of new species, lead to the different taxa hypotheses. Moreover, due to the lack of a morphological analysis at a higher level the definition of diagnostic characters was based on each author´s observations and experience. The differences on perspectives caused species delimitations hypotheses followed by constant nomenclatural changes.

1.2.2 Molecular studies

Few authors have focused their studies on phylogenetic relationships within this clade. Kadereit and Jeffrey (1996) used chloroplast restriction sites on the phylogenetic study of the Senecioneae tribe and included one species of *Gynoxys.* Their analysis retrieving this unique species as closely related to other members of the Tussilagininae (*Tussilago* L., *Roldana* La Llave, and *Brachyglottis* J.R. Forst. & G. Forst.). Pelser et al. (2007) extended the sampling and included at least one member of four (out of five) Gynoxyoid genera. Specifically, the authors reconstructed phylogenies within the Senecioneae using the nuclear marker ITS. Their results retrieved the Gynoxyoid group, comprised by *Aequatorium*, *Gynoxys*, *Nordenstamia* and

Paragynoxys (*Paracalia* which was not represented in this study) as monophyletic. Pelser et al. (2010) increased the taxon sampling including one species of *Paracalia* and sequenced five plastid regions additionally to the ITS and ETS nuclear markers. Although the Gynoxyoid group was supported as monophyletic on both phylogenies (nuclear and plastid markers), the tree topologies retrieved on each dataset were incongruent among them.

1.3 Background, aims and framework of the study

The Botanical Garden and Botanical Museum Berlin has established the basis of a scientific cooperation with the Herbario Nacional de Bolivia to contribute to the study of plants diversity in that country. In the frame of this cooperation, the high Andean *Gynoxys* clade of the Asteraceae tribe Senecioneae was selected as subject for a joint study, to be conducted in the Asterales Research Group at the BGBM lead by Dr. Norbert Kilian. This *Gynoxys* project combined the phylogenetic and taxonomic investigation of this clade and also aimed to contribute a treatment of this clade for the Flora of Bolivia. This objective could not have been achieved based merely on morphological data, hence a robust phylogenetic backbone based on plastid and nuclear phylogenetics was needed to support the conclusions.

In order to achieve these aims, a representative number of species of the Gynoxyoid group were required. The need for a large number of specimens led us to the planification of fieldtrips in Bolivia and Peru. Representatives of species that could not be collected during the fieldtrips were requested on loan to different herbaria.

Chapter 1 comprises the general introduction. Chapter 2 to 4 correspond to three research manuscripts, and Chapter 5 comprises the general conclusion. Chapter 2 to 4 follow a journal structure and each of them include its own summary, introduction, material and methods, results, discussion, conclusions, references, figures and tables. Appendices are given at the end of this document.

Chapter 2 corresponds to the paper “Plastid phylogenomics of the Gynoxoid group (Senecioneae, Asteraceae) highlights the importance of motif-based sequence alignment amid low genetic distances” published in the American Journal of Botany. This chapter includes the first phylogenetic analysis of the Gynoxyoid clade based on complete plastid genome including 21 members of the group. In this chapter three main objectives could be achieved [1] Elucidate the phylogenetic relationship of the Gynoxyoid group and of the generic relationships within it,

[2] differentiate the phylogenetic hypotheses on different partitions of the plastid genome, [3] evaluate the impact of manual adjustment of MSAs on phylogenetic reconstruction, [4] test the current generic classification based on plastome phylogenetic reconstructions.

Chapter 3 corresponds to the manuscript “Genus concepts and species diversity within the Gynoxyoid clade (Senecioneae, Compositae)”, that will be submitted to Phytokeys. This chapter comprises the ancestral character-state reconstruction of eleven morphological characters based on the phylogenetic backbone generated in the second chapter. Additionally, it includes an evaluation on genera classification. These analyses enabled to [1] evaluate the generic delimitation considering molecular (plastome and nrDNA) and morphological data, and [2] generate a checklist of all species belonging to the Gynoxyoid clade in respective genera.

Chapter 4 corresponds to the manuscript “Intricate species delimitation in Gynoxys (Senecioneae, Asteraceae): insights from a taxonomic revision of the Gynoxyoids for Bolivia” which will be submitted. This chapter presents the taxonomic treatment of the Bolivian Gynoxyoids which was based on the species revision of chapter three. In order to elaborate an inclusive taxonomic treatment, phylogenetic analysis on nuclear markers ETS/ITS was reconstructed. Furthermore, a total of 110 morphological characters on 99 specimens was evaluated and a component principal analysis was performed. Based on these results we could [1] elaborate the first taxonomic treatment for the Gynoxyoids in Bolivia based on morphological and molecular data.

Chapter 5 concludes general results obtained in this study.

Chapter 2. Plastid phylogenomics of the Gynoxoid group (Senecioneae, Asteraceae) highlights the importance of motif-based sequence alignment amid low genetic distances

2.1 Summary

The genus *Gynoxys* and relatives form a species-rich lineage of Andean shrubs and trees with low genetic distances within the sunflower subtribe Tussilaginineae. Previous molecular phylogenetic investigations of the Tussilaginineae have included few, if any, representatives of this Gynoxyoid group or reconstructed ambiguous patterns of relationships for it. We sequenced complete plastid genomes of 21 species of the Gynoxyoid group and related Tussilaginineae and conducted detailed comparisons of the phylogenetic relationships supported by the gene, intron, and intergenic spacer partitions of these genomes. We also evaluated the impact of manual, motif-based adjustments of automatic DNA sequence alignments on phylogenetic tree inference. Our results indicate that the inclusion of all plastid genome partitions is needed to infer well-supported phylogenetic trees of the Gynoxyoid group. Whole plastome-based tree inference suggests that the genera *Gynoxys* and *Nordenstamia* are polyphyletic and form the core clade of the Gynoxyoid group. This clade is sister to a clade of *Aequatorium* and *Paragynoxys* and also includes some but not all representatives of *Paracalia*. The concatenation and combined analysis of all plastid genome partitions and the construction of manually-curated, motif-based DNA sequence alignments are found to be instrumental in the recovery of well-supported relationships of the Gynoxyoid group. We demonstrate that the correct assessment of homology in genome-level plastid sequence data sets is crucial for subsequent phylogeny reconstruction and that the manual post-processing of multiple sequence alignments improves the reliability of such reconstructions amid low genetic distances between taxa.

2.2 Introduction

The Andean region of northwestern South America is one of the most prominent regions of plant diversification in the neotropics (Luebert and Weigend, 2014) and a common location for plant radiations in sunflowers (Asteraceae; e.g., Vargas et al., 2017; Pouchon et al., 2018). The Gynoxyoid group of the sunflower tribe Senecioneae is one such radiation (Vision and Dillon, 1996; Lundin, 2006). The group comprises 150–170 species of shrubs and trees that primarily inhabit high-elevation habitats in the northern and central Andes (Nordenstam et al., 2009). Under the current taxonomic circumscription, the species of the Gynoxyoid group are separated into five closely related genera [i.e., *Aequatorium* B. Nord., *Gynoxys* Cass. *Nordenstamia* Lundin, *Paracalia* Cuatrec., and *Paragynoxys* (Cuatrec.) Cuatrec.]. *Gynoxys* contains the majority of species in the group (Cuatrecasas, 1951; Nordenstam, 2007; Beck and Ibáñez, 2014), and novel species continue to be described (e.g., Beltran and Campos de la Cruz, 2009). Biogeographically, the group ranges from northern Venezuela to northern Argentina, and most of its species are characteristic elements of montane forests or solitary shrubs and trees in the paramo (Tinoco et al., 2013), while only a few exhibit a scandent growth form and inhabit lower-elevation montane forests (Beck and Ibáñez, 2014; Figure 2.1). Most of the species of the Gynoxyoid group are restricted to relatively small distribution ranges and occur in habitats threatened by anthropogenic land use and climate change, thus making this a group of conservation concern (Beltran et al., 2006; Morillo and Briceno, 2000; Hind, 2007). Based on the most recent phylogenetic investigations of the Senecioneae, the Gynoxyoid group is part of the subtribe Tussilagininae (Pelser et al., 2007, 2010), which represents one of four subtribes of the Senecioneae. The phylogenetic relationships and species limits within the Gynoxyoid group are poorly understood because few molecular phylogenetic investigations have included taxa of this group or focused on aspects other than their relationships. Kadereit and Jeffrey (1996) conducted a study on the phylogeny of the Senecioneae using chloroplast restriction site data and included one species of *Gynoxys* in their data set. Their results indicated that *Gynoxys* was most closely related to *Tussilago* L., *Roldana* La Llave, and *Brachyglottis* J.R. Forst. & G. Forst. Similarly, Pelser et al. (2007) aimed to infer relationships within the Senecioneae using the internal transcribed spacer (ITS) region and recovered a clade comprising the genera *Aequatorium*, *Gynoxys*, *Nordenstamia*, and *Paragynoxys*, but with mixed levels of branch support. Their results indicated that the current taxonomic circumscriptions within the Gynoxyoid group were not fully substantiated by DNA sequence data, as *Nordenstamia* was found nested within a paraphyletic *Gynoxys*. Pelser et al. (2010) extended their previous taxon sampling of the Gynoxyoid group by including one sample of *Paracalia* and recovered the group as monophyletic. Recently, Quedensley et al. (2018) included taxa of *Aequatorium* and

Figure 2.1: Morphological variability among three species of the Gynoxyoid group. Displayed are the leaves and capitulescences of *Nordenstamia repanda* (A and D), which represents a characteristic element of upper cloud forests (bosque yungueño de ceja de monte); *Gynoxys asterotricha* (B and E), which represents a characteristic element of lower cloud forests; and *Gynoxys tomentosissima* (C and F), which represents a characteristic element of low montane forests

Gynoxys in a study of North and Central American representatives of the Tussilaginineae and recovered a monophyletic Gynoxyoid group with strong statistical support; however, no insight into the intergeneric relationships of the group was investigated. In summary, the intergeneric relationships of the Gynoxyoid group have remained largely unresolved, and the delimitation of its genera is mostly unsubstantiated by phylogenetic methods. Plastid phylogenomic studies have been shown to be efficient in resolving the phylogenetic relationships of species groups in the Asteraceae. Vargas et al. (2017) investigated the relationships of *Diplostephium* Kunth and related genera that exemplified low levels of molecular variability (Vargas and Madrinan, 2012). The authors sequenced complete plastid genomes of 14 different genera (91 samples) and inferred a highly resolved phylogeny. Similarly, Pouchon et al. (2018) sequenced plastid genomes in an analysis of the phylogenetic relationships of *Espeletia* Mutis ex Bonpl. and relatives, which previous studies could not resolve due to an insufficient number of informative DNA sequence characters available. Specifically, the authors sequenced complete plastid genomes for 41 species among eight genera and recovered well-supported clades. Zhang et al. (2019) sequenced plastid genomes to establish a robust phylogenetic framework for the species-rich genus *Saussurea* DC., for which previous work had generated conflicting infrageneric

classifications. By analyzing complete plastid genomes of 136 species of *Saussurea*, the authors found that approximately 2000 parsimony informative sites were needed to produce a resolved and well-supported phylogeny. More recently, Knope et al. (2020) sequenced plastid genomes to reconstruct the phylogeny of Hawaiian endemics of the genus *Bidens* L. in light of a decade-long effort to clarify the evolutionary history of this rapidly radiating lineage and were able to generate a highly supported phylogeny. Evidently, the use of plastid genomes for phylogenetic inference can be instrumental in clarifying the relationships of plant groups that exhibit low molecular variability. This utility is not restricted to Asteraceae but has been demonstrated in numerous lineages of flowering plants (e.g., Givnish et al., 2018; Yao et al., 2019). The process of sequencing and comparing plastid genomes for the reconstruction of phylogenetic relationships is often perceived as simple, but several studies have indicated that the evolution and structure of plastid genomes and, by extension, their application in phylogenetic inference, is complex. Based on observations that the majority of plastid genomes display strong structural conservation (Mower and Vickrey, 2018), are uniparentally (mostly maternally) inherited (Greiner et al., 2015), and do not experience biparental recombination (Marechal and Brisson, 2010), many investigations have operated under the assumption of a congruent phylogenetic signal across the entire plastid genome. However, several studies have cast doubt on the validity of this assumption and instead highlighted the presence of a discordant phylogenetic signal across different regions of the plastid genome. Investigations on the more variable regions of plastid genomes, for example, found mosaic-like patterns of molecular evolution (Borsch and Quandt, 2009), a hierarchical structure of phylogenetic signal (Müller et al., 2006; Barniske et al., 2012), and lineage-specific lengths and positions of these regions (Korotkova et al., 2014). Recent phylogenomic investigations corroborated these reports by identifying considerable phylogenetic incongruence across different regions of the plastid genome, which may result in inefficient or even incorrect phylogenetic inferences if the entire genome is analyzed under the same model parameters. Goncalves et al. (2019), for example, identified significant incongruence among the gene and species trees of different plastome regions in a phylogenomic study on rosids. The authors reported that the concatenation of all plastid coding regions produced highly supported phylogenies that were nonetheless incongruent to individual plastid gene trees. Similarly, Gruenstaeudl (2019) detected phylogenetic incongruence across different loci of the plastid genome in a phylogenomic investigation of water lilies and relatives. Walker et al. (2019) reported gene tree conflict among various plastid genes based on a broad sampling of angiosperm plastid genomes and noted numerous strongly supported but conflicting nodes between different gene trees. Similar observations were made in plastid phylogenomic analyses

of Fabaceae (Zhang et al., 2020) and Bignoniaceae (Thode et al., 2020). Furthermore, Koehler et al. (2020) identified and ranked plastid genome regions by phylogenetic informativeness and found topological incongruence between the phylogenetic trees inferred from complete plastid genome sequences and those inferred from the five and 10 most variable plastid regions only. Based on these and similar studies, Goncalves et al. (2020) cautioned that "one or a few genes that have high phylogenetic signal may bias the inference" (Goncalves et al., 2020, p. 4) and, thus, recommended the continued exploration of more phylogenetic information among different regions of the plastid genome. The positional homology among the nucleotides of a multiple sequence alignment (MSA) represents an essential aspect of phylogenetic tree inference and has not received sufficient attention in many phylogenomic investigations. Early plastid phylogenomic studies primarily employed the coding regions of the genomes for phylogenetic reconstruction (e.g., Leebens-Mack et al., 2005; Moore et al., 2010), which are largely conserved in their length and sequence and, thus, require relatively little adjustment upon standard MSA. Phylogenetic investigations that employ noncoding plastid DNA, by contrast, routinely inspect software-generated MSAs and adjust them according to the criterion of explicit sequence motifs to ensure correct positional homology (Kelchner, 2000; Loehne and Borsch, 2005; Morrison, 2006). In phylogenomic analyses, such adjustments are sometimes dismissed as impractical due to the large amounts of sequence data involved (Wu et al., 2012), but numerous investigations have demonstrated the impact of alignment errors on phylogenetic inference (reviewed by Wong et al., 2008). To reduce this impact while simultaneously avoiding time-expensive evaluations of the MSAs, many studies tend to automatically exclude nucleotide positions in software-generated MSAs that are deemed unreliable (e.g., Bellot et al., 2020). In practice, such procedures may go as far as excluding alignment positions that exhibit a gap in only one of the aligned sequences, which substantially reduces the proportion of genome sequence employed for phylogenetic reconstruction (e.g., Gernandt et al., 2018). Along with the reduction of potential informativeness, such exclusions do not guarantee correct positional homology in the remaining alignment, as demonstrated for cases of small genomic inversions (Ochoterena, 2008). Given the larger share of noncoding compared to coding DNA in plastid genomes as well as the higher frequency of substitutions and microstructural mutations in noncoding DNA, manual adjustments of software-derived MSAs may even have a considerable impact on plastid phylogenomic reconstruction. In fact, in species groups with low genetic distances, a large proportion of potentially informative sequence characters will likely be encoded in the noncoding regions of the plastid genome. The present investigation had two goals: (1) to infer the phylogenetic relationships within the Gynoxyoid group of the

Tussilaginineae using complete plastid genomes to account for the low genetic distances expected within this group, and (2) to assess the phylogenetic signal of different sections of the plastid genome, particularly with regard to motif-based adjustments of software-generated MSAs. To achieve these goals, we asked four questions: (1) Does phylogenetic analysis of complete plastid genomes yield resolved and well-supported phylogenetic trees for the Gynoxyoid group? (2) Do different partitions of the plastid genome (i.e., coding sequences, intergenic spacers, and introns) support different phylogenetic hypotheses? (3) Does the manual adjustment of MSAs have a measurable impact on phylogenetic reconstruction? (4) Are the results of the plastome-based reconstructions congruent with the current generic classification of the Gynoxyoid group? To address these questions, complete plastid genomes of 17 species of the Gynoxyoid group and four species of closely related members of the Tussilaginineae were sequenced and annotated. These taxa form a taxon set that encompasses the typical genetic distances within the Gynoxyoid group and to other members of the Tussilaginineae. We then used this data set to conduct phylogenetic tree inference based on different coding regions, introns, and intergenic spacers of the plastid genome before and after the manual adjustment of the MSAs and contrast the results.

2.3 Materials and Methods

2.3.1 Taxon sampling DNA and DNA extraction

A total of 21 samples of different species of the Tussilaginineae were collected for DNA extraction and subsequent plastid genome sequencing (Table 2.1). Of these, 17 samples represent genera of the Gynoxyoid group (i.e., *Aequatorium*, *Gynoxys*, *Nordenstamia*, *Paracalia*, and *Paragynoxys*), while four represent other genera of the Tussilaginineae that form the sister clade to the Gynoxyoid group (i.e., *Arnoglossum* Raf., *Roldana* La Llave, and *Telanthophora* H. Rob. & Brettell; see Quedensley et al., [2018] for details). Particular emphasis in our taxon sampling was placed on the inclusion of (1) more than one species per genus, where possible, to approximate the genetic variability within each genus, (2) multiple species of *Gynoxys* to represent its species diversity across the Andes and to accommodate previous results indicating that *Gynoxys* may be non-monophyletic, and (3) the type species of the genera *Gynoxys*, *Nordenstamia*, and *Paracalia* to enable comparisons of our reconstructions with the current taxonomic classification of the Gynoxyoid group. We included the previously published plastid genome of *Ligularia fischeri* (Ledeb.) Turcz. (GenBank accession

NC_039352; Chen et al., 2018) as an outgroup. The taxon names and generic concepts that we applied follow those of Nordenstam (2007). Herbarium vouchers of all newly sequenced samples of the Gynoxyoid group were deposited in B, with duplicates in LPB, USM, HSP, or HUT. Total genomic DNA was extracted from silica gel-dried leaf material using the NucleoSpin Plant II kit (Macherey- Nagel, Dueren, Germany) or from herbarium specimens using the CTAB DNA isolation method as modified by Borsch et al. (2003). A DNA sample for each specimen was deposited in the DNA bank of the Botanic Garden and Botanical Museum Berlin (BGBM; Table 2.1). Unless DNA isolates were fragmented due to age, samples were sheared to an average fragment size of 600 bp using a Covaris S220 sonicator (Covaris, Woburn, MA, USA). Upon shearing, all fragments between 400 and 900 bp were selected and maintained by applying the BluePippin protocol (Sage Science, Beverly, MA, USA). The final concentration of DNA samples was measured using Qubit 2.0 Fluorometer dsDNA BR Assay kits (Life Technologies-Thermo Fisher Scientific, Saint Aubin, France) and the final fragment size distribution using an Agilent 2100 Bioanalyzer (Agilent Technologies, Santa Clara, CA, USA). Manufacturer protocols were followed for all steps of DNA extraction.

2.3.2 Genomic library preparation and DNA sequencing

Plastid genomes were sequenced via a genome skimming approach following the preparation of genomic libraries. For each DNA sample, a barcoded genomic library was constructed using the TruSeq DNA library preparation kit (Illumina, San Diego, CA, USA). Standard indexing adapters were ligated to the fragment ends to generate single- index libraries. Libraries were validated via qPCR on a Mastercycler ep realplex (Eppendorf AG, Hamburg, Germany) using the KAPA library quantification kit (KAPA Biosystems, Wilmington, MA, USA). Following qPCR, indexed DNA libraries were normalized and pooled in equal volumes. Pooled libraries were sequenced as paired-end reads either on an Illumina MiSeq or an Illumina HiSeq X platform. Sequencing was performed in-house at the Berlin Center for Genomics in Biodiversity Research (Berlin, Germany) or the Genome Sequencing and Analysis Facility of the University of Texas at Austin, or outsourced to Macrogen (Seoul, Republic of Korea).

2.3.3 Genome assembly and annotation

After DNA sequencing, raw sequence reads were filtered for quality and successful pairing using scripts 1 and 2 of the pipeline of Gruenstaeudl et al. (2018), followed by a mapping of the quality-filtered reads to the plastid genome of *Jacobaea vulgaris* Gaertn. (accession NC_015543; Doorduin et al., 2011) to extract plastome reads using Bowtie2 v.2.3.4 (Langmead and Salzberg, 2012). Contigs were assembled de novo with either IOGA v.20160908 (Bakker et al., 2015) or NOVOPlasty v.2.7.2 (Dierckxsens et al., 2017) based on the subset of reads that mapped against the reference genome, using a range of different kmer values to optimize contig length (kmer = 33–97, in increments of 4). Unless already circular, final contigs were circularized manually with Geneious v.11.1.4 (Kearse et al., 2012), using the plastid genome of Jacobaea vulgaris as a reference for contig position and orientation. A circular, quadripartite structure of the plastid genome and equality of its inverted repeat (IR) regions were confirmed for each assembly through a blast search against itself using script 4 of the pipeline of Gruenstaeudl et al. (2018). Sequence ambiguities in the final assembly, if present, were resolved by mapping the quality- filtered reads against the circularized assembly using Bowtie2. Final assemblies were annotated via the annotation server DOGMA (Wyman et al., 2004), followed by a manual inspection and, where necessary, correction of the annotations in Geneious. Specifically, sequence annotations were corrected regarding the presence of start and stop codons, the absence of internal stop codons, and their length as a multiple of three for each coding region. This process resulted in a complete and fully annotated plastid genome for each taxon sampled for this study. Upon annotation, all new plastid genomes were deposited to GenBank; their accession numbers are listed in Table 2.1. Plastome maps were drawn with OGDRAW v.1.3.1 (Greiner et al., 2019).

2.3.4 Data partitioning, sequence alignment, and alignment adjustments

The coding and noncoding regions of the plastid genomes were extracted and aligned using a four-step procedure. First, one of the IRs was removed from each genome to avoid redundancy among the extracted loci. Second, all coding and noncoding regions (except tRNAs and rRNAs) were excised bioinformatically from each genome using script 9 of the pipeline of Gruenstaeudl et al. (2018) and then grouped by region name. Third, all sequences of the same region were aligned into preliminary MSAs using MAFFT v.7.394 (Katoh and Standley, 2013) under the default settings of the software. Specifically, MSAs of 81 coding regions, 20 introns, and 111 intergenic spacers, each consisting of the sequences of 22 taxa, were constructed. Fourth, these

Table 1: Species name, collection location and number, herbarium voucher information, and GenBank accession number for each plastid genome sequenced in this investigation. n.a. = not applicable

Species	Taxonomic authority	Location	Collection no.	Herbarium voucher	DNA Bank code	GenBank
Aequatorium jamesonii	(S.F. Blake) C. Jeffrey	Ecuador: Napo, Parque Nacional Llanganates	Vargas H. et al. 2594	MO 2940002 (MO)	DB38638	MT528247
Arnoglossum atriplicifolium	(L.) H.Rob.	USA: Spring LakePark, Omaha, Nebraska	Quedensley T.S. s.n.	TSQ2011cp001 (TEX)	n.a.	MK170176
Gynoxys asterotricha	Sch. Bip.	Bolivia: Parque Nacional Madidi, Laji Sorapata	Escobari B. et al. 36	B 100720926 (LPB,B)	DB27411	MK044798
Gysnoxys baccharoides	(Kunth) Cass.	Ecuador: Azuay, Parque Nacional Cajas	Jorgensen P. et al. 1616	MO 1879904 (AAU,MO)	DB38633	MT528244
Gynoxys ignaciana	Cuatrec.	Ecuador: Loja, Guararas	Emperaire L. 1318	P 03833291 (P)	DB38767	MT528252
Gynoxys longifolia	Wedd.	Peru: Arequipa, Cailloma	Beck S. 26384	LPB0002593 (LPB,MO,US)	DB38565	MT528245
Gynoxys mandonii	Sch. Bip. ex Rusby	Bolivia: La Paz, Nor Yungas, Unduavi	Cayola L. 5570	MO 3151322 (LPB,MO)	DB27416	MK056106
Gynoxys megacephala	Rusby	Bolivia: Nor Yungas, Ecovia	Escobari B. et al. 46	LPB0002594 (LPB)	DB27426	MN328892
Gynoxys sp. SEN301		Peru: Amazonas, Leymebamba	Escobari B. et al. 593	B 101098545 (USM,HUT,B)	DB38744	MN328891
Gynoxys tomentosissima	Cuatrec.	Peru: Amazonas, Leymebamba	Escobari B. et al. 590	B 101098697 (USM,HUT,B)	DB38742	MN328890
Gynoxys violacea	Sch. Bip. ex Wedd.	Venezuela: Merida	Walter E. 166	B 101139853 (B)	DB38780	MT528243
Nordenstamia cajamarcensis	(H. Rob. & Cuatrec.) B. Nord.	Peru: Pasco, Oxapampa	Castillo G. 460	MO 2940516 (F,MO,USM)	DB38626	MT528248
Nordenstamia kingii	(H. Rob. & Cuatrec.) B.Nord.	Bolivia: Cochabamba, Monte Puncu	Solomon J. 18067	LPB0002595 (LPB,MO)	DB38764	MT528249
Nordenstamia repanda	(Wedd.) Lundin	Bolivia: Parque Nacional Madidi, Laji Sorapata	Cayola L. 5585	LPB0002597 (LPB,MO)	DB27409	MK086040
Paracalia jungioides	(Hook. & Arn.) Cuatrec.	Peru: Ancash, Huaraz	Diaz C. 1975	MO 3030471 (LPB,MO)	DB43895	MT528251
Paracalia pentamera	(Cuatrec.) Cuatrec.	Bolivia: Sud Yungas, Chulumani	Gallegos S. 3850	LPB0002596 (LPB)	DB40913	MT942595
Paragynoxys martingrantii	(Cuatrec.) Cuatrec.	Colombia: Cesar	Gentry A. 79156	MO 1962013 (MO)	DB43896	MT528250
Paragynoxys venezuelae	(V.M. Badillo) Cuatrec.	Venezuela: Merida, Paramo de Las Coloradas	Cuatrecasas J. et al. 28996	MA 01 00896838 (MA,S)	DB43902	MT528246
Roldana aschenborniana	(Schauer) H. Rob. & Brettell	Mexico: Oaxaca (cult. ex situ in California)	Quedensley T.S. s.n.	TSQ2011cp002 (TEX)	n.a.	MK170177
Roldana barba johannis	(DC.) H. Rob. & Brettell	Mexico: Oaxaca (cult. ex situ in California)	Quedensley T.S. s.n.	TSQ2011cp003 (TEX)	n.a.	MK170178
Telanthophora grandifolia	(Less.) H. Rob. & Brettell	Mexico: Oaxaca (cult. ex situ in California)	Quedensley T.S. s.n.	TSQ2011cp004 (TEX)	n.a.	MK170179

preliminary MSAs were evaluated by eye and, where necessary, adjusted manually to improve positional homology across nucleotides using PhyDE v.0.9971 (Müller et al., 2010). The adjustments followed the rules of Loehne and Borsch (2005) and included the masking of mutational hotspots for those sections of the MSAs where correct positional homology could not be established. This motif-based alignment approach was based on the assumption that insertions, deletions or inversions of genomic regions do not occur at random, but exhibit recurrent patterns (similar to those found in simple sequence repeats or hairpin-mediated inversions; e.g., Kelchner, 2002; Borsch and Quandt, 2009) and are often caused by structural and functional constraints (invoked, for example, during DNA replication and repair; Smith and Keeling, 2015). Such microstructural mutations may simultaneously encompass multiple nucleotides, contradicting earlier assumptions of a fifth character state per gap position (Barriel, 1994). When adjusting a MSA, microstructural mutations can be expressed by placing inserted elements in their own alignment columns, creating biologically meaningful gaps that can be utilized during indel coding (Simmons and Ochoterena, 2000). Occasionally, microstructural mutations are so frequent within a region that they create overlapping mutations for which positional homology can no longer be established by eye. Such cases are particularly common for mono- or dinucleotide microsatellites (e.g., poly-A repeats) where positional homology is often obscured by the short unit length. The evolution of plastid microsatellites has, thus, been reported as highly homoplastic (e.g., Tesfaye et al., 2007), involving insertions and deletions of one to several repeat units rather than following a stepwise model. Consequently, we excluded regions of uncertain homology from the process of indel coding and tree reconstruction in this investigation. Small sequence inversions, by comparison, were masked through a manual re- inversion of the sequence motifs, followed by a re-alignment to the other sequences and the recording of each inversion as a single-step event that was later added to the indel matrix as a binary character. If such inversions were left unchanged, the presence of incorrect nucleotide substitutions instead of the inversion itself would be implied, resulting in the loss of a relevant phylogenetic character (discussed by Loehne and Borsch, 2005). Examples of the masking of microsatellites and sequence inversions are illustrated in Figure 2.2; a summary of the positions and lengths of masked sequence regions within the MSAs is given in Appendix 2.1. Following these alignment adjustments, all MSAs were assessed for length and sequence variability and excluded from the data set if any of the following criteria were met: lack of sequence variability, length less than 10 bp, more ambiguous than variable nucleotides if length less than 50 bp, and vicinity to trans-spliced genes. For example, the MSAs of the intergenic spacers *ndhH–ndhA*, *rpoB–rpoC1*, *ndhK–psbG*, and *psbF–psbE* were excluded

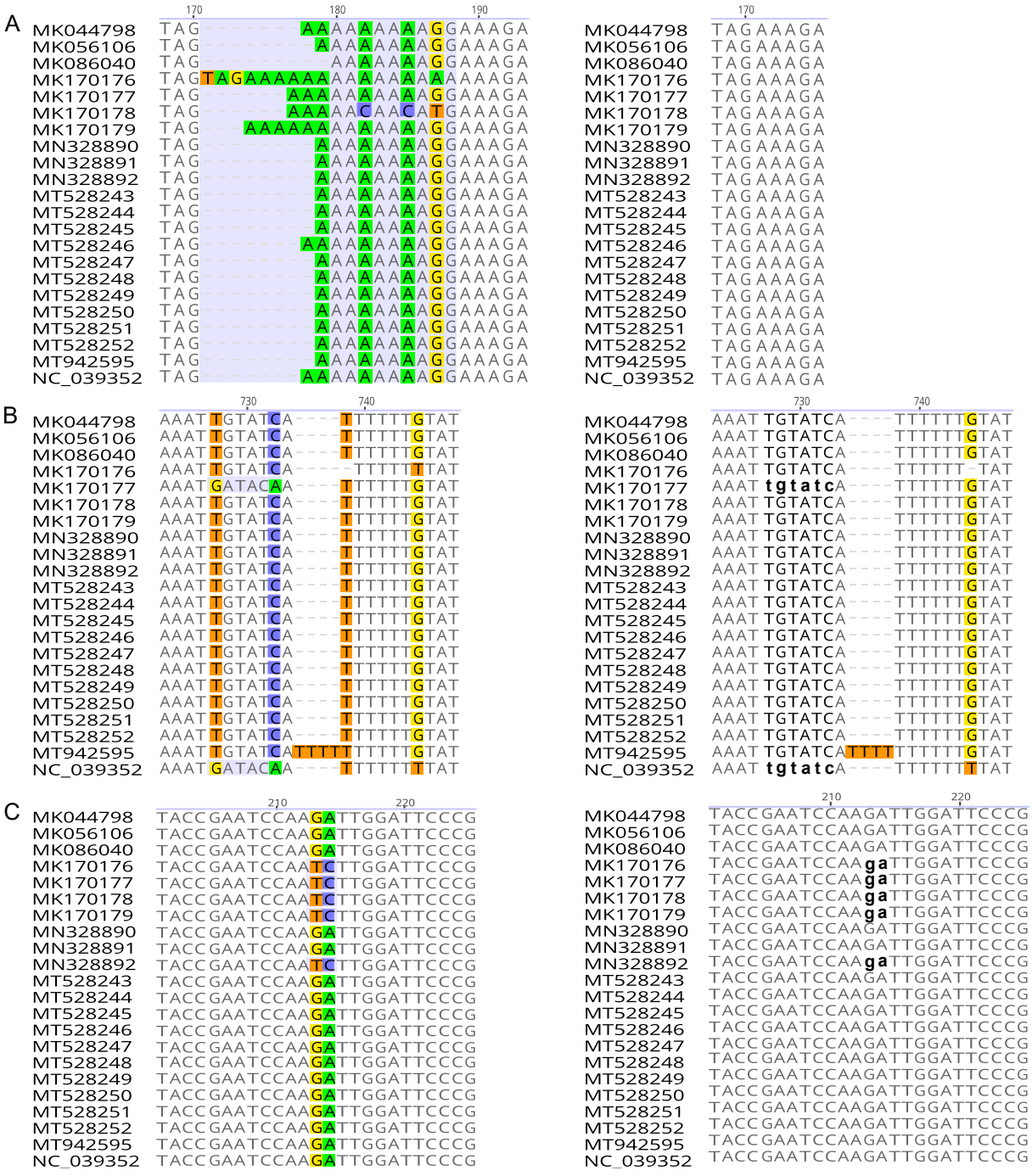

Figure 2.2: Illustration of the manual adjustment of sequence alignments as exemplified by three different intergenic spacers of the plastid genome. For each spacer, the MSA before adjustment is displayed on the left, the MSA after adjustment on the right. Polymorphic nucleotides are highlighted in color. Row (A) illustrates the adjustment of the MSA of spacer *atpI–atpH*, which contains a poly-A region with internal nucleotide polymorphism; this poly-A region (highlighted in blue) was removed due to uncertain positional homology during the adjustment. Row (B) illustrates the adjustment of the MSA of spacer *ndhC–trnV*, which contains shared sequence inversions of a length of six bp (highlighted in blue); these inversions were manually inverted (lower case nucleotides) during the adjustment to avoid incorrect positional homology. Row (C) illustrates the adjustment of the MSA of spacer *psbM–trnD*, which contains shared sequence inversions of a length of two bp (highlighted in blue) as part of a stem-loop structure; these inversions were manually inverted (lower case nucleotides) during the adjustment to avoid incorrect positional homology.

because they were only 1, 5, 7, and 9 bp long, respectively. Similarly, the spacer *psbT–psbN* was excluded due to the combination of a short alignment length and a higher number of ambiguous than variable nucleotides. All tRNA and rRNA genes were excluded due to minimal, if any, sequence variability. The intergenic spacers adjacent to *rps12* (i.e., *rpl20–rps12*, *rps12–clpP*, and *rps7–rps12*) were excluded because rps12 comprises discontinuous group II introns that are often associated with complex secondary DNA structures and may bias the mutational dynamics of the intergenic spacers flanking the trans-spliced exons of this gene (Kelchner, 2002; Glanz and Kueck, 2009). All other MSAs were saved as NEXUS files for further processing. Insertions and deletions in each MSA were coded as binary characters using the simple indel coding (SIC) scheme of Simmons and Ochoterena (2000) as implemented in SeqState v.1.4.1 (Müller, 2005). The complete sets of MSAs representing 81 different coding regions, 20 different introns, and 103 different intergenic spacers were grouped by marker class (hereafter, plastid partitions; i.e., coding regions, introns, and intergenic spacers) and then concatenated with and without indel codes. Specifically, the MSAs were concatenated within each set as well as across the three sets, both with and without the presence of indel codes, generating a total of eight different matrices. All matrices were deposited in Zenodo (https://zenodo.org/record/4428211) and employed for phylogenetic tree reconstruction. For brevity in our analyses, coding regions are abbreviated with "CDS", introns with "INT", and intergenic spacers with "IGS". Similarly, the concatenation of all MSAs of the coding regions is abbreviated as "81 CDS concat", the concatenation of all MSAs of the introns as "20 INT concat", and the concatenation of all MSAs of the intergenic spacers as "103 IGS concat".

2.3.5 Alignment metrics and sequence variability

To assess the reliability of the MSAs and the impact of manual alignment adjustment on them, we calculated a total of eight different alignment metrics for each MSA before and after alignment adjustment. The inferred metrics were (1) alignment length, (2) GC content, (3) fraction of polymorphic sites, (4) fraction of parsimony-informative sites, (5–7) three homoplasy indices—(5) consistency index (CI; Kluge and Farris, 1969), (6) rescaled consistency index (RC), and (7) retention index (RI; both Farris, 1989) in their ensemble form, and (8) the largest uncorrected p-distance between all sequences as defined in equation 3.1 of Nei and Kumar (2000). Each metric was calculated in R (R Core Team, 2019) using the R packages ape v.5.2 (Paradis and Schliep, 2018) or phangorn v.2.4.0 (Schliep, 2011). For each MSA, the three homoplasy indices were calculated on the neighbor-joining tree of that MSA.

The values of the homoplasy indices are negatively correlated with the level of homoplasy in the MSA, with high index values indicating low levels of homoplasy. Indels were taken into account during the calculation of alignment length and the fraction of polymorphic sites but were disregarded in the calculation of all other metrics in accordance with the original settings of the R functions. To quantify sequence variability across the plastid genomes under study, we calculated the nucleotide diversity index n (Nei and Li, 1979) with DnaSP v.6.12.03 (Rozas et al., 2017) for each MSA as well as their concatenation across all partitions using a sliding window algorithm with a step size of 200 bp and window size of 600 bp. To visualize sequence variability across the genomes, we generated variability plots using mVISTA (Frazer et al., 2004) following a global pairwise alignment of the sequences with LAGAN (Brudno et al., 2003). The IRa was excluded from each plastid genome before alignment and visualization with mVISTA; coding regions

2.3.6 Phylogenetic inference and hypothesis testing

Phylogenetic tree inference was conducted under the maximum likelihood (ML) and the Bayesian inference (BI) criterion on the concatenation of all plastid partitions before and after the manual adjustment of the MSAs. Tree inference under ML was also conducted on the independent concatenation of the coding regions, the introns, and the intergenic spacers, before and after the manual alignment adjustment. To infer the homoplasy indices, tree inference under ML was additionally conducted for each individual MSA before and after alignment adjustment. Tree inference under ML was performed using RAxML v.8.2.9 (Stamatakis, 2014), including the option for a thorough optimization of the best-scoring ML tree. Tree inference under BI was performed with MrBayes v.3.2.6 (Ronquist and Huelsenbeck, 2003) using four parallel Markov chain Monte Carlo (MCMC) runs for a total of 50 million generations. Branch support under ML was calculated through 1000 bootstrap (BS) replicates under the rapid BS algorithm (Stamatakis et al., 2008). Branch support under BI was calculated as posterior probability (PP) values. The nucleotide substitution model GTR + G + I was applied by default to model nucleotide substitution rates during tree inference under both optimality criteria. For indel characters, an F81-like binary substitution model with a gamma- shaped rate variation across sites was employed under both optimality criteria (Lewis, 2001). In analyses under BI, the sampling of independent generations and the convergence of the Markov chains were confirmed in Tracer v.1.7 (Rambaut et al., 2018); the initial 50% of all MCMC trees were discarded as burn-in, and post-burn-in trees were summarized as a 50% majority rule consensus

tree. The significance of the topological differences between inferred trees was evaluated with the approximately unbiased (AU) test (Shimodaira, 2002). Specifically, we compared the likelihoods of competing tree topologies based on the concatenation of all plastid partitions using the software CONSEL v.0.20 (Shimodaira and Hasegawa, 2001) and a significance threshold of $\alpha = 0.05$.

2.4 Results

2.4.1 Genome structure and gene content

Genome structure and length, as well as the number of genes per genome, were found to be highly conserved across the plastid genomes of the Gynoxyoid group. The genomes exhibit the standard circular and quadripartite structure, comprising one large (LSC) and one small single-copy (SSC) region, separated by two identical IRs, and display minor, if any, length variability. The variability in total sequence length between the largest and the smallest plastid genome in this group was less than 1 kb (except for *Gynoxys tomentosissima*; Appendix 2.2). All of the genomes of the Gynoxyoid group consist of a total of 81 protein-coding regions (seven of which are duplicated in the IRs), 30 transfer RNA (tRNA) genes (seven duplicated in the IRs), and four ribosomal RNA (rRNA) genes (all duplicated in the IRs), resulting in a total of 133 functional coding regions per genome. Also, the same genes contain one or more introns across the genomes: *atpF*, *ndhA*, *ndhB*, *petB*, *petD*, *rpl2*, *rpoC1*, and *rps16* contain one intron each; *clpP* and *ycf3* contain two introns each. The plastid genome of *Gynoxys tomentosissima* is slightly different than the other genomes of the Gynoxyoid group: with 155,060 bp, making it the largest sequenced in this study. Compared to the other plastid genomes of the Gynoxyoid group, its sequence is approximately 4 kb longer (Appendices 2.2 and 2.3) due to the expansion of its IRs into the LSC, with the genes *rpl14*, *rpl16*, *rps3*, *rpl22*, and *rps19* additionally duplicated in the IRs. The GC content of all plastid genomes of the Gynoxyoid group was between 37.2% and 37.9% and is, thus, within the typical bandwidth of plastid GC content (Smith, 2009).

2.4.2 Sequences variability across genomes

Sequence variability across the plastid genomes of the Gynoxyoid group was low and located almost exclusively in the noncoding regions of the genomes, with coding regions exhibiting

only occasional, if any, nucleotide polymorphism (Figure 2.3). Specifically, the intergenic spacers were the most variable among the three plastid partitions (average n = 0.006; Table 2.2A), followed by the introns (n = 0.004) and the coding regions (n = 0.002). Among the coding regions, only *ycf1* exhibited a modest number of differences across sequences (i.e., proportion of polymorphic sites of 0.08 and 0.07 before and after the alignment adjustment, respectively; Appendix 2.4). Among the intergenic spacers, by contrast, several MSAs exhibited a proportion of polymorphic sites above 0.10 both before and after the alignment adjustment (Appendix 2.5); the MSAs of the intergenic spacers *psbA–trnK-TTT*, *rpl16– rps3*, and *rps18–rpl20*, for example, contained the highest nucleotide diversity (n = 0.20). Some sequence variability was also observed in the MSAs of the introns (e.g., the actual noncoding domains of the intron of *trnK-TTT*), but most introns exhibited a modest number of differences across sequences (i.e., proportion of polymorphic sites below 0.10; Appendix 2.6). Interestingly, the visualization of sequence variability with mVISTA produced somewhat misleading results regarding their phylogenetic utility. The high level of sequence variability indicated for the intergenic spacer *trnT-GGT–psbD* (i.e., position 31,828–33,081 bp) was primarily the consequence of a DNA insertion shared by five sequences and only yields a single variable character for phylogenetic inference upon indel coding. In summary, the plastid genomes of the Gynoxyoid group exhibited relatively low but nonetheless divergent levels of sequence variability across the three plastid partitions.

2.4.3 Effect of alignment adjustment on homoplasy indices

The evaluation and, when required, manual adjustment of the MSAs had a considerable effect on homoplasy in these alignments (Figure 2.4; Appendix 2.7). Specifically, the MSAs of the intergenic spacers *atpB–rbcL*, *ndhC–trnV-TAC*, *psaA–ycf3*, *trnC-GCA–petN*, and *trnL-TAG–rpl32* exhibited considerably reduced levels of homoplasy upon alignment adjustment, with some spacer regions having their homoplasy index values improve by more than 50%. Improvements were particularly noticeable for values of the RC and the RI among the intergenic spacers. The manual adjustment of the MSAs of the introns and the coding regions had less impact but nonetheless resulted in reduced levels of homoplasy for the alignment of three introns and one coding region. Overall, these changes in homoplasy levels due to alignment adjustment should be seen as conservative estimates of improvement, as the corrected positional homology may additionally benefit phylogenetic inference through, among other factors, a better fit of the employed nucleotide substitution models (e.g., Du et al., 2019).

2.4.4 Phylogenetic reconstruction

A comparison of the phylogenetic tree inferences based on each of the three plastid partitions to the inference conducted on their concatenation indicated that each partition contributed informative characters to the phylogenetic reconstruction, albeit in different proportions (Table 2.2). After alignment adjustment, the concatenation of all MSAs of the coding regions had a length of 68,076 bp, of which 1030 (1.51%) were polymorphic sites; the concatenation of all MSAs of the introns had a length of 14,184 bp, of which 318 (2.24%) were polymorphic sites; and the concatenation of all MSAs of the intergenic spacers had a length of 37,033 bp after alignment adjustment, of which 1194 (3.22%) were polymorphic sites. Consequently, the sequence matrix representing the concatenation of the three partitions had a total length of 119,311 bp after alignment adjustment, of which 113,059 (94.8%) were monomorphic sites, 2542 (2.1%) were polymorphic sites, and 3710 (3.1%) gaps or sites of missing data. Among the polymorphic sites, a total of 589 (23.2%) were parsimony informative, of which 248 (42.1%) originated in the coding regions, 275 (46.7%) in the intergenic spacers, and 66 (11.2%) in the introns. Considerable differences in the results of our phylogenetic reconstructions were identified based on the different plastid partitions as well as the adjustment of alignments. First, the phylogenetic reconstructions before and after the adjustment of alignments generally resulted in trees with different topologies and branch support. For example, the best ML tree inferred under the concatenation of all three plastid partitions was significantly different before and after alignment adjustment (Figure 2.5A; Table 2.3). Similarly, the best ML trees based on the concatenation of all coding regions produced different topologies before and after alignment adjustment, while BS support was >50% for all but one node (Appendix 2.8). In the tree inferred before alignment adjustment, *Gynoxys longifolia* was sister to *Nordenstamia kingii* (BS 59%), and a clade comprising *Paragynoxys* and *Aequatorium* was sister to a clade of *G. baccharoides* and *G. violacea* (BS 52%). In the tree inferred after alignment adjustment, fewer nodes with BS support >50% were retrieved, and none of the previously stated relationships were supported. The best ML trees of the concatenation of all introns also exhibited different topologies before and after alignment adjustment, with BS support primarily >50% (Appendix 2.9). By contrast, the best ML trees of the concatenation of all intergenic spacers inferred before and after alignment adjustment were highly similar in topology and generally recovered BS support >50% (Appendix 2.10). Second, the phylogenetic reconstructions based on different plastid partitions resulted in trees with different topologies and branch support. For example, the best ML tree inferred under the concatenation of the coding regions was significantly

different from the best ML tree inferred under the concatenation of all three plastid partitions (Figure 2.5B; Table 2.3). Similarly, the tree topologies inferred under the concatenation of all introns were notably different from the topologies inferred under the concatenation of all coding regions and intergenic spacers, and also exhibited lower branch support (Appendices 2.8–2.10). The average BS support per node in the best ML tree inferred under the concatenation of all introns was considerably lower than the average BS support per node in the trees inferred on the concatenation of all coding regions and all intergenic spacers. Only the sister relationship between the Gynoxyoid group and the North and Central American members of the Tussilaginineae was consistently retrieved across the plastid partitions. In summary, the reconstruction of the phylogenetic relationships of the Gynoxyoid group was strongly dependent on the adjustment of the alignments and the exact plastid partitions employed. By comparison, small, if any, differences in the results of our phylogenetic reconstructions were identified in relation to the coding of indels and between the two tree inference methods employed. First, the coding of indels had only a small impact on tree inference: several trees exhibited minor topological changes upon inclusion of an indel coding matrix in the phylogenetic reconstruction, but the overall relationships, as well as the branch support, exhibited few, if any, differences. For the concatenation of all plastid partitions upon alignment adjustment, the best ML tree before the coding of indels was topologically identical to the best ML tree after indels coding (Table 2.3; Appendix 2.11). Similarly, the phylogenetic trees reconstructed under the concatenation of all coding regions experienced no topological changes upon the coding of indels, whereas trees reconstructed under the concatenation of all introns and all intergenic spacers exhibited differences in one or occasionally multiple nodes (Appendices 2.8–2.10). Second, the phylogenetic reconstructions conducted under different inference methods generated trees that were primarily different with respect to branch support. Branch support for reconstructions under BI was often higher than branch support for reconstructions under ML (Appendices 2.12 and 2.13). For the concatenation of all plastid partitions upon alignment adjustment and the coding of indels, the best ML tree was topologically identical to the best BI tree inferred (Table 2.3; Appendix 2.11). Phylogenetic reconstruction on the concatenation of all plastid partitions resulted in trees that were consistent in topology and similar in branch support across different tree inference methods and the coding of indels after the adjustment of alignments (Appendix 2.11), but inconsistent in topology and branch support before these adjustments (Figure 2.5A; Appendices 2.12 and 2.13). Except for the most recent common ancestor of the two clades containing *Gynoxys* and the node of a clade comprising *Gynoxys asterotricha* and *G. megacephala*, all nodes of the best ML tree based on

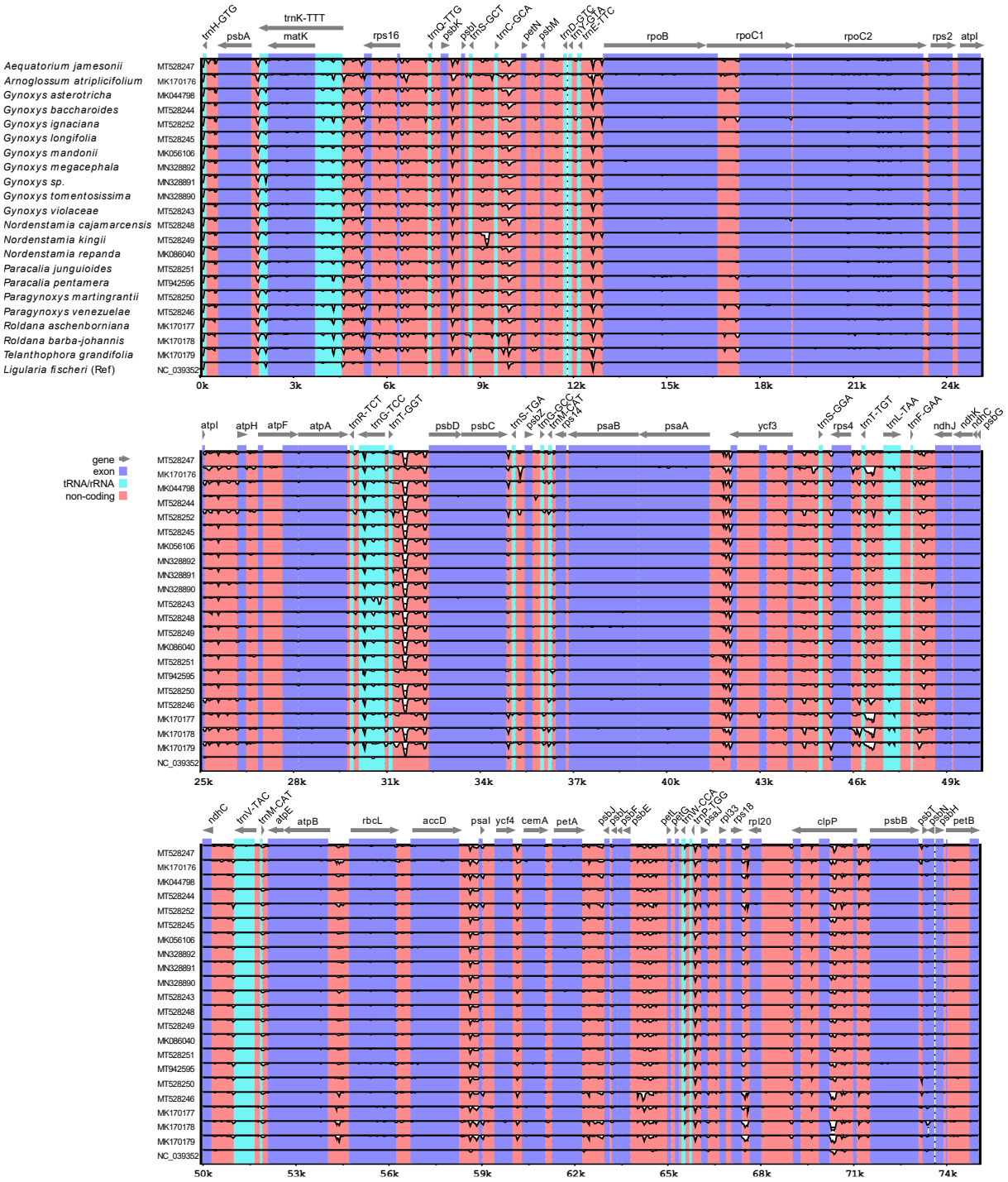

Figure 2.3: Visualization of sequence variability between the plastid genomes under study using mVISTA. The alignment was split into sequence batches of 25 kb length by mVISTA for easier visualization. Each lane represents a genome. In each lane, the proportion of missing similarity is indicated by white color, starting from the top of each lane. Coding regions are represented in blue, transfer and ribosomal RNAs in cyan, and non-coding regions in red. Gray arrows indicate the location and orientation of plastome genes

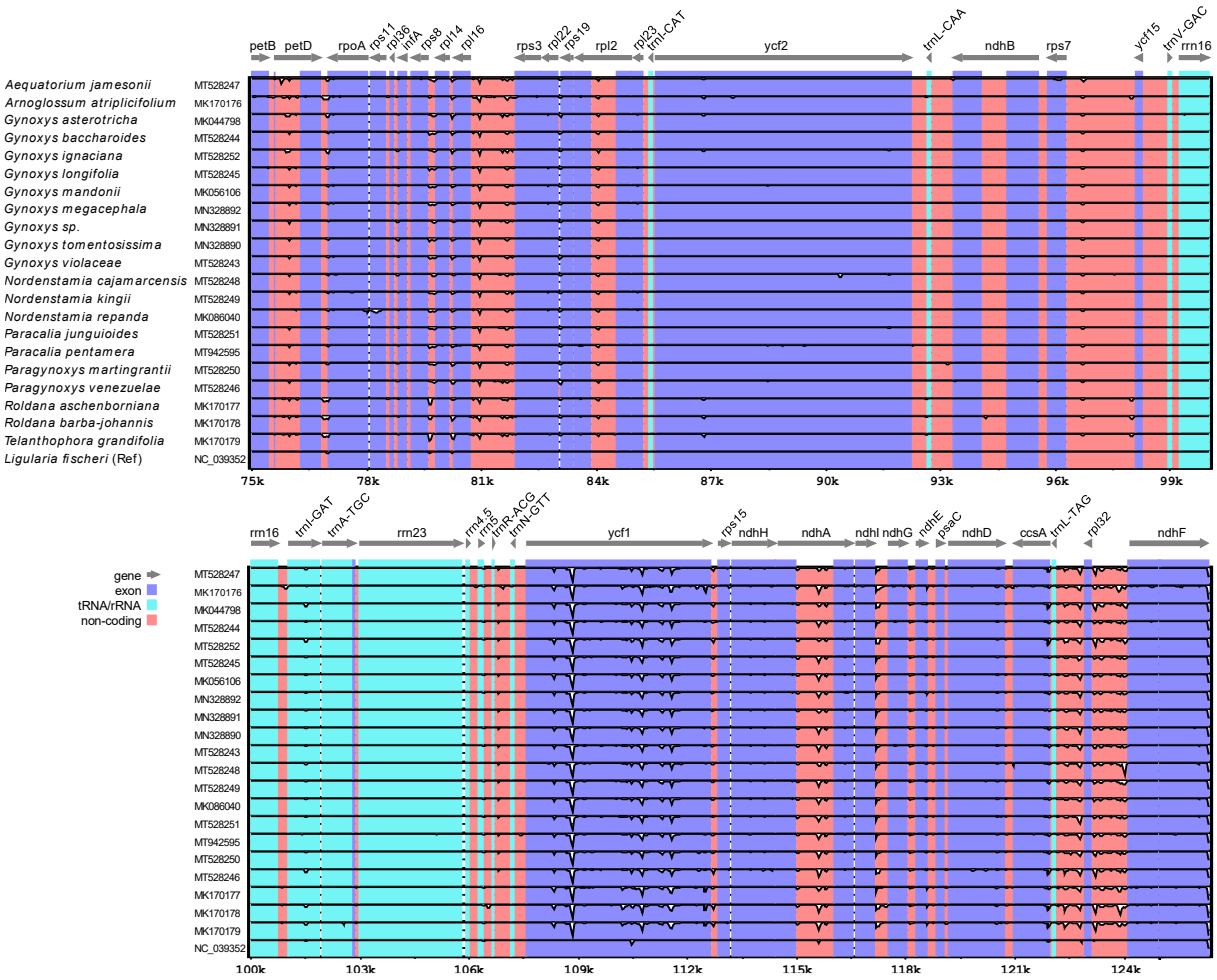

Figure 2.3: Continued

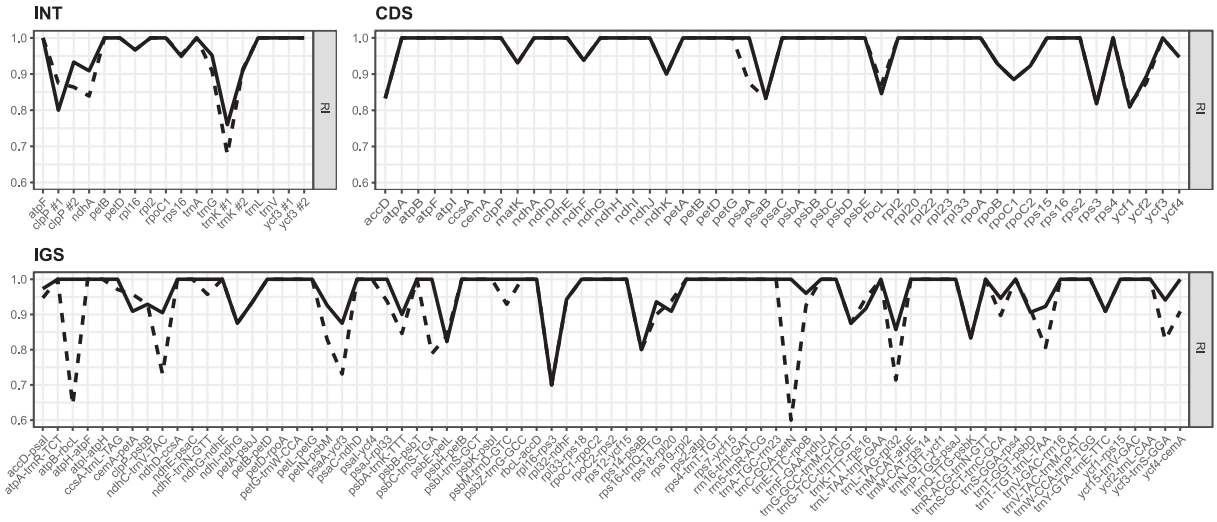

Figure 2.4: Comparison of the RI values across each MSA under study before (dashed lines) and after (solid lines) the alignment adjustment

Table 2.2: Alignment length, sequence variability, and maximum likelihood (ML) tree statistics of the different data sets under study. (A) Alignment length and sequence variability statistics (with percentages shown in parentheses); (B) statistics on ML tree inference before and after alignment adjustment. adj. = adjustment; align. = alignment; BS = bootstrap support; concat. = concatenated; nucl. = nucleotide; PI = parsimony informative

A. Partition	Align. adj.	Align. length (bp)	Gaps/ Missing (%)	Polymorphic sites (%)	PI sites (%)	Nucl. diversity
CDS	Before	68,117	824 (1.21)	1120 (1.64)	270 (0.40)	0.0023
	After	68,076	328 (0.48)	1030 (1.51)	248 (0.36)	0.0022
INT	Before	14,499	470 (3.24)	385 (2.66)	76 (0.52)	0.0037
	After	14,184	428 (3.02)	318 (2.24)	66 (0.47)	0.0032
IGS	Before	38,752	2623 (6.77)	1453 (3.75)	352 (0.91)	0.0056
	After	37,051	2458 (6.63)	1194 (3.22)	275 (0.74)	0.0048
Concat.	Before	121,368	3710 (3.11)	3958 (3.26)	698 (0.58)	0.0035
	After	119,302	3421 (2.82)	2542 (2.13)	589 (0.49)	0.0031

B. Partition	Align. adj	Indel coding	Align. length (bp)	Best ML tree likel. (-lnL)	Best ML tree length (bp)	Avg. BS per node
CDS	Before	no	68,117	103,459.8	0.0193	68
	After	no	68,076	102,518.0	0.0177	66
	Before	yes	68,150	103,736.0	0.0199	68
	After	yes	68,108	102,783.0	0.0182	65
INT	Before	no	14,499	23,560.9	0.0370	45
	After	no	14,184	22,187.8	0.0273	44
	Before	yes	14,658	25,318.6	2.1675	42
	After	yes	14,259	22,760.0	0.0344	43
IGS	Before	no	38,752	66,780.7	0.0580	65
	After	no	37,042	60,729.1	0.0430	63
	Before	yes	39,318	71,559.8	0.0831	62
	After	yes	37,385	63,146.6	0.0556	68
Concat.	Before	no	121,368	194,716.3	0.0337	67
	After	no	119,302	186,078.8	0.0266	73
	Before	yes	122,126	201,615.7	0.0432	68
	After	yes	119,752	189,627.2	0.0315	73

the concatenation of all plastid partitions exhibited BS support >50% upon alignment adjustment (Appendix 2.12). In the 50% majority-rule consensus tree of the posterior tree distribution of the BI, most nodes had PP values ≥ 0.9 (Appendix 2.13). By contrast, the best ML tree inferred before the adjustment of alignments exhibited lower BS support as well as topological incongruence regarding the positions of *Gynoxys mandonii*, *G. longifolia*, *G. megacephala*, and Nordenstamia kingii, and the paraphyly of *Roldana* with respect to *Telantophora* (Appendix 2.12). These differences in tree topology before and after the alignment adjustments were even more pronounced under BI and may be discordant given the high branch support received under this optimality criterion (Appendix 2.13).

Table 2.3: Statistical comparison of competing phylogenetic trees as displayed in Figure 2.5 using the AU test on the concatenation of all three plastid partitions upon the coding of indels and after alignment adjustment. Significant P values are indicated with an asterisk

Constraint	P
Figure 5, left tree (positive control)	0.545
Figure 5A, right tree	0.036*
Appendix S11A, right tree	0.037*
Appendix S11A, right tree	0.545
Appendix S11B, right tree	0.461

2.4.5 Inference of relationships

The phylogenetic relationships recovered through our tree inferences on the concatenation of all plastid partitions resulted in high branch support for most clades (Appendices 2.12 and 2.13). The Gynoxyoid group was recovered as a clade with maximum BS and PP support, comprising the genera *Aequatorium*, *Gynoxys*, *Nordenstamia*, *Paracalia*, and *Paragynoxys*. The non-Gynoxyoid taxa of the Tussilagininae (i.e., *Roldana*, *Telanthophora*, and *Arnoglossum*) were recovered as sister to this Gynoxyoid group in each reconstruction and with maximum support. *Paracalia pentamera*, which constitutes the type species in the genus, was recovered as the earliest-diverging lineage of the Gynoxyoid group in each inference, again with high branch support. Except for *Paragynoxys*, all other genera of the Gynoxyoid group that are represented by two or more species were found to be non-monophyletic. Specifically, *Paragynoxys martingrantii* and *P. venezuelae* were recovered as sister species with maximum branch support and identified to be sister to the specimen of *Aequatorium* included in this study (medium BS support, maximum PP support). *Gynoxys* and *Nordenstamia* were recovered in two separate subclades and found to be either para- or polyphyletic, depending on the reconstruction observed. One subclade comprised four species of *Gynoxys* and two species of *Nordenstamia* and exhibited maximum branch support under both ML and BI. Specifically, it comprised *Gynoxys asterotricha*, *G. longifolia*, *G. mandonii*, and *G. megacephala*, as well as *Nordenstamia kingii* and *N. repanda*, the last of which is the type for the genus. However, the most recent common ancestor of *Nordenstamia kingii* and *Gynoxys megacephala* was poorly supported in this subclade and part of a polytomy under BI upon coding indels. The other subclade comprised five species of *Gynoxys*, one species of *Nordenstamia*, and one species of *Paracalia* and had maximum PP but only medium BS support (BS > 67). This clade comprised

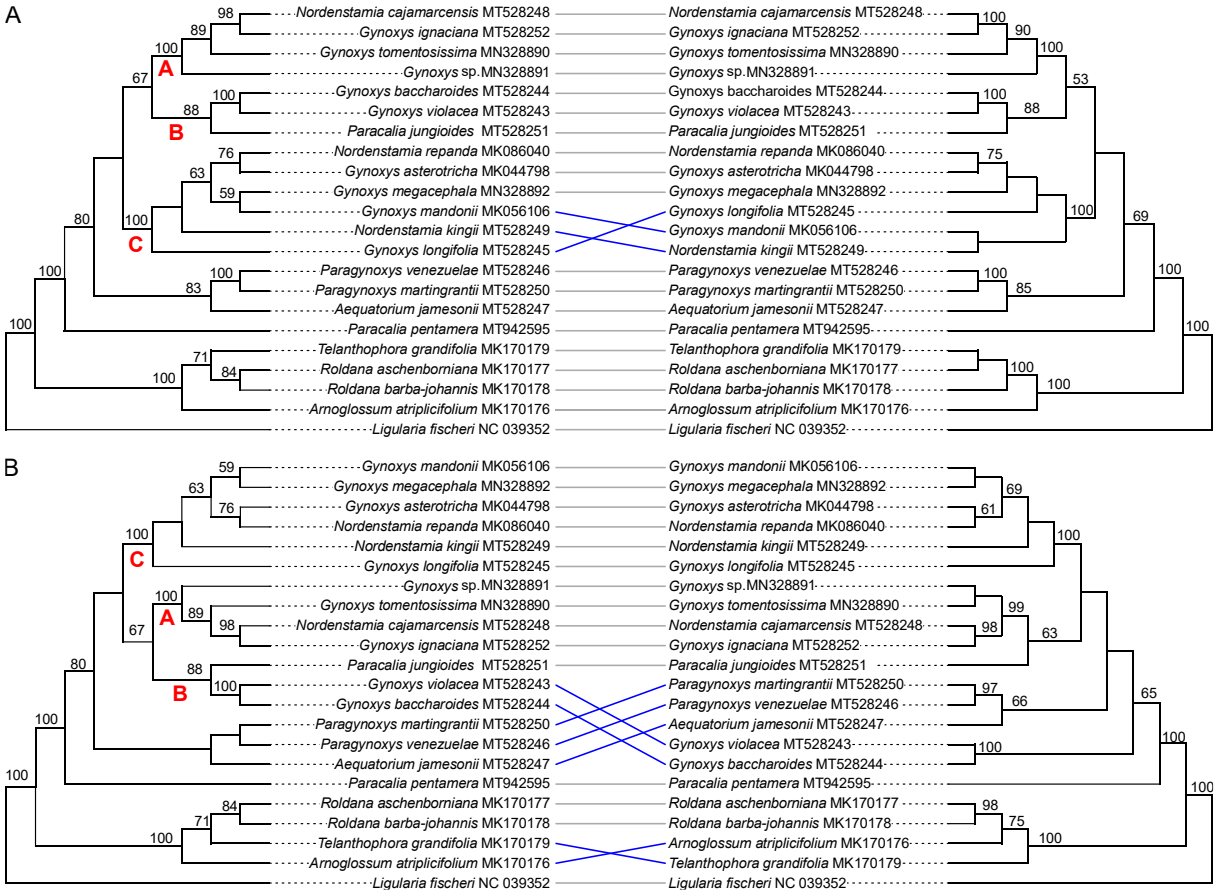

Figure 2.5: Comparison of phylogenetic trees of the Gynoxyoid group inferred before and after alignment adjustment and under different datasets. The tree displayed on the left is held constant across both comparisons and constitutes the tree with the highest likelihood score inferred on the concatenated MSAs of all three plastid genome partitions upon the coding of indels and after alignment adjustment. Three clades (i.e., "A", "B", and "C") are highlighted on this tree by red letters located next to the most recent common ancestor of each clade. (A) Comparison of the best tree against its equivalent inferred before alignment adjustment; and (B) comparison of the best tree against its equivalent inferred on the concatenated MSAs of all coding regions only

G. baccharoides, which constitutes the type species for *Gynoxys*, *G. ignaciana*, *G. tomentosissima*, *G. violacea*, and an unidentified species of *Gynoxys* (i.e., *Gynoxys* sp. SEN301). Moreover, the clade comprised *Paracalia jungioides* and *Nordenstamia cajamarcensis*. The species *Paracalia jungioides*, *Gynoxys baccharoides*, and *G. violacea* formed a clade under both ML and BI, which exhibited maximum PP and high BS support (BS > 81). The other species of this subclade were also recovered as a monophyletic group with maximum branch support.

2.5 Discussion

2.5.1 Plastid genomes of Senecioneae

The present investigation is the first to compare plastid genomes from different genera of the Tussilagininae and to employ their sequences in a phylogenetic analysis. As of December 2020, 29 complete plastid genomes of the Senecioneae have been sequenced and are available through the NCBI Nucleotide database (https://www.ncbi.nlm.nih.gov/ nucleotide/), representing five different genera and two of the four subtribes. Specifically, plastid genomes have been sequenced for *Dendrosenecio* (Hauman ex Hedberg) B. Nord., *Jacobaea* Mill., *Pericallis* D. Don, and *Senecio* L. of the subtribe Senecioninae, and *Ligularia* Cass. of the subtribe Tussilagininae. Gichira et al. (2019), sequenced and compared 11 plastid genomes of *Dendrosenecio* (Hauman ex Hedberg) B. Nord. and *Senecio* to identify variable regions for phylogenetic analysis. Similarly, Chen et al. (2018) generated plastid genomes of six species of *Ligularia* to examine the utility of these genomes as barcodes for identifying individual species. The present investigation expands the list of sequenced plastid genomes of the Tussilagininae by eight genera. All plastid genomes sequenced in this study display a highly conserved genome structure and exhibit the two large inversions that separate the Asteraceae from other flowering plant families (Kim et al., 2005). The size range of these newly sequenced plastid genomes and their gene order and content is highly similar to other Senecioneae (Gichira et al., 2019; Chen et al., 2018).

2.5.2 Phylogenetic position of the Gynoxyoid clade

The results of our phylogenetic reconstructions corroborate the previously supported relationships of the Tussilaginineae as inferred by Pelser et al. (2007). Specifically, our results support the phylogenetic relationships of the *Aequatorium–Arnoglossum* clade that were reported by Pelser et al. (2007) and confirm the Gynoxyoid group as being monophyletic with high statistical support. While previous studies had already reported the Gynoxyoid group as a clade (e.g., Pelser et al., 2010; Quedensley et al., 2018, both primarily based on ITS DNA sequences), their sampling of taxa and genomic regions was generally insufficient to infer the monophyly of the Gynoxyoid group. Moreover, we recovered the Gynoxyoid clade as sister to a clade of North and Central America taxa (i.e., *Arnoglossum*, *Telantophora*, and *Roldana*) that are distributed from the United States (Quedensley et al., 2018) to Panama (Funston, 2009; Clark and Pruski, 2015) and possibly Colombia (Calvo, 2016), and this sister relationship was previously illustrated (Pelser et al., 2010). Quedensley et al. (2018) reported that several genera

in this sister clade to the Gynoxyoid group were highly polyphyletic, and our results support this assessment, as we found *Roldana* non-monophyletic in several reconstructions (e.g., Appendix 2.12). Future studies on the phylogenetic relationships of the Tussilaginineae should further increase the taxon sampling.

2.5.3 Phylogenetic relationships in the Gynoxyoid clade

Our phylogenetic reconstructions recovered several relationships within the Gynoxyoid clade with high clade support. For example, our results suggest that genus *Paracalia* is not monophyletic and that its type species (i.e., *Paracalia pentamera*) is sister to the rest of the Gynoxyoid group, whereas *Paragynoxys* is monophyletic with full support. The monophyly of *Paragynoxys* is also supported by morphological characters such as discoid capitula and deep-lobed white corollas (Cuatrecasas, 1955). The reconstructions based on the full plastid genome revealed that *Aequatorium* and *Paragynoxys* were sister genera (1.0 PP and 80% ML-BS), whereas reconstructions based on individual plastid regions could not resolve this relationship (e.g., Pelser et al., 2010). Moreover, these complete plastome reconstructions identified three highly supported subclades within the Gynoxyoid clade irrespective of the tree inference method applied: subclade A, which comprises *G. ignaciana*, *G. tomentosissima*, *Gynoxys* sp., and *Nordenstamia cajamarcensis* and is also supported by morphological characters such as opposite leaves and granular hairs along the veins on the upper face of the leaves; subclade B, which comprises *G. baccharoides*, *G. violacea*, and *Paracalia jungioides*; and subclade C, which comprises *G. megacephala*, *G. mandonii*, *Nordenstamia repanda*, *G. asterotricha*, *N. kingii*, and *G. longifolia*. All internal nodes in these subclades were found to be well supported, except for the position of *N. kingii* in subclade C (weakly supported in the ML and BI trees when ignoring indel coding and unsupported upon inclusion of the indel coding matrix). The type species of *Gynoxys* and *Nordenstamia* (i.e., *Gynoxys baccharoides* and *Nordenstamia repanda*, respectively) were recovered in a clade in which the species of both genera did not segregate, indicating the non-monophyly of both genera.

2.5.4 Importance of manual alignment adjustment

The present investigation highlights the importance of evaluating and, where necessary, adjusting software- generated MSAs before phylogenomic analysis. While different alignment

algorithms have been implemented in the various software tools available for automatic DNA sequence alignment (e.g., Needleman-Wunsch algorithm in CLUSTAL W; Thompson et al., 1994), their mechanistic processes often depart from the actual biological processes that shape the molecular evolution of DNA sequences. For example, biological processes often comprise the instantaneous insertion, deletion, inversion, or translocation of multiple nucleotides, yet many alignment algorithms cannot replicate these mechanisms (Graham et al., 2000; Borsch and Quandt, 2009; Ochoterena, 2008). Molecular phylogenetic studies, thus, often adjust their DNA sequence alignments manually using motif-based approaches. Such approaches were conceptualized as motif alignments that follow defined rules (e.g., Kelchner, 2000; Loehne and Borsch, 2005; Morrison, 2006, 2015) and aim to improve the alignment of microstructural mutations while assessing positional homology (de Pinna, 1991). Numerous investigations have demonstrated the impact that the selection of alignment method can have on the reconstruction of phylogenetic trees (e.g., Morrison and Ellis, 1997; Simmons et al., 2010a, b; Wong et al., 2008). Moreover, several simulation studies have shown that alignment accuracy is highly dependent on the frequency of genomic insertions and deletions (e.g., Pervez et al., 2014). Hence, the manual adjustment of DNA sequence alignments following a motif- based approach has become a common practice among molecular phylogenetic studies, particularly those based on single genetic markers. Phylogenomic studies, by contrast, often dismiss the practice of manual alignment adjustment, as the amount of sequence data under analysis is considered to outweigh the ability of any researcher to correct software- induced alignment errors for all but the smallest data sets (Wu et al., 2012) or to lead to a lack of repeatability (Edwards et al., 2016). Instead, most phylogenomic studies often exclude those regions of a MSA that are deemed unreliable via positional filtering processes (e.g., Ali et al., 2019). While such a practice may eliminate some of the erroneous statements of positional homology among aligned nucleotides, they often fail to recognize inversions (Figure 2.2) or eliminate positions with sequence gaps although the respective indel motifs allow clear homologous positions. It is, therefore, not surprising that methods for automated alignment filtering, in which a threshold of shared gaps is employed to determine the removal of nucleotides, may actually counteract accurate tree inference (e.g., Tan et al., 2015). The inadvertent analysis of DNA matrices that harbor sequence inversions is particularly problematic, as these inversions can be highly homoplastic (Kelchner and Wendel, 1996) and often lead to spurious phylogenetic results (Joly et al., 2010). Unsurprisingly, the manual examination of the plastid phylogenomic data set of this investigation for alignment errors has led to the identification of numerous sequence

inversions that were not recognized at the stage of the software-driven sequence alignment (Figure 2.2; Appendix 2.1).

2.5.5 Process of manual alignment adjustment

To alleviate the problem of missing positional homology upon automatic sequence alignment, we conducted visual examinations and manual corrections of the software- derived MSAs using a motif approach. Specifically, we removed the nucleotide positions from the final sequence matrix for which positional homology could not be established. For example, we removed or truncated length- variable poly-A/T microsatellites that originated through repeated and independent insertions of single or multiple nucleotides and did not form recognizable sequence motifs. In addition to improving the positional homology for individual MSAs, this strategy allowed us to (1) identify and re-invert naturally occurring sequence inversions that cannot be automatically aligned and would introduce erroneous nucleotide polymorphisms if left unedited (Chen et al., 2016), and (2) mask and, thus, exclude those nucleotide positions for which positional homology could not be reasonably identified. Time-efficient work was facilitated through automatically partitioning of annotated genomic regions into individual data sets, which could then be edited manually in PhyDE without affecting the overall alignment. Upon alignment adjustment, individual MSAs were then concatenated automatically using the pipeline of Gruenstaeudl et al. (2018). The homoplasy indices improved in value upon alignment adjustment (Appendix 2.7), and this change was also seen in the inferred tree topologies when comparing tree inference before and after alignment adjustments (Table 2.2B; Figure 2.5A). Adjusting software- derived alignments may have the effect of avoiding erroneous phylogenetic signal from both substitutions and coded microstructural mutations (i.e., insertions, deletions, and inversions) within the alignable sections of DNA sequences and, additionally, of avoiding spurious signal from the unalignable sections. Moreover, the evaluation and adjustment of sequence alignments may also assist in identifying cases of natural gene rearrangements among plastid genomes, which would lead to MSAs comprising non-homologous sequence elements in noncoding sequence partitions, as such rearrangements are typically not identified through software-derived sequence alignment (Fonseca and Lohmann, 2017). Plastid phylogenomic reconstructions should, thus, consider the evaluation and, where necessary, correction of automatic alignment results.

2.5.6 Mosaic-like evolution of plastid genomes

The large majority of angiosperm plastid genomes display a highly conserved structure, uniparental inheritance, and a general absence of recombination between chromosomes (Marechal and Brisson, 2010, but see Ruhlman et al., 2017; Li et al., 2020). Hence, many researchers assume that the plastid genome evolves as a single linkage unit (Bock, 2007), with different genomic regions sharing the same evolutionary history (e.g., Lu et al., 2018). However, recent studies have reported widespread phylogenetic incongruence between different regions of the plastid genome (e.g., Goncalves et al., 2019; Gruenstaeudl, 2019; Walker et al., 2019), which indicates that the plastid genome may not represent a homogeneous genetic locus. This phylogenetic incongruence may partially be the result of the different mutation rates and selective constraints across the plastid genome, which is illustrated by the co-existence of the relatively slowly evolving gene *rbcL*, the more rapidly evolving gene *matK* with nearly equal site rates in all three codon positions, and the even faster evolving noncoding markers *trnL* intron, *trnT–L* intergenic spacer, and *trnL–F* intergenic spacer in the same genome (Müller et al., 2006). Examples for selective constraints are directed selection on certain nucleotide positions and compensatory base changes (Kelchner, 2002; Borsch et al., 2003), which can cause patterns of homoplasy and lead to a spurious phylogenetic signal, especially when the number of variable nucleotides is limited. This observed phylogenetic incongruence may also be the result of the different structural constraints in the plastid genome, which comprises a succession of conserved and variable elements that can display secondary DNA structure. For example, the highly variable and AT-rich stem loops of noncoding plastid DNA often exhibit accelerated, lineage-specific nucleotide substitution rates and a high frequency of microstructural mutations (Korotkova et al., 2014). The presence of phylogenetic incongruence due to systematic error, such as the selection of incorrect nucleotide substitution models or incorrect homology statements during MSA (e.g., Zhang et al., 2020), represents another possible explanation, and its extent is under active investigation (Goncalves et al., 2020). In summary, the plastid genome seems to exhibit a mosaic-like pattern of molecular evolution, and if that pattern is not adequately modeled during phylogenetic reconstruction, the resulting inferences may be highly supported yet spurious (see discussion by Walker et al., 2019; Thode et al., 2020; Zhang et al., 2020). Plastid phylogenomics may, thus, be facing a new trend in which researchers aim to better account for the differential phylogenetic signal of particular genome regions (Goncalves et al., 2020).

2.5.7 Phylogenetic utility of different plastome regions

The different regions of the plastid genome exhibit different molecular constraints and, thus, a different utility for phylogenetic reconstructions. The coding regions of the plastid genome have traditionally been used for the reconstruction of deep-level phylogenetic relationships (Graham and Olmstead, 2000; Xi et al., 2012; Walker et al., 2019), but these may be biased when genes with incongruent phylogenetic signals coexist in the genome (e.g., Gruenstaeudl, 2019; Goncalves et al., 2019; Walker et al., 2019). Accordingly, Goncalves et al. (2020) suggested to infer phylogenetic relationships on individual genes and to compare the resulting topologies to the reconstructions based on the concatenation of all coding regions. In this regard, it is important to note that gene tree incongruence may have different causes: incongruent signal may be (1) truly phylogenetic in origin (i.e., genes reflect different evolutionary histories), or (2) tree-like and originate from homoplastic nucleotide substitutions, which are often associated with highly unequal substitution rates (Morton and Clegg, 1995). Incongruent, yet tree-like signal may additionally be compounded by inadequate model fit, poor sample size, and other systemic errors during phylogenetic tree inference (Kelchner and Thomas, 2006). Given that the plastid genome as a whole shares a common evolutionary history within our study group (as it does in most plastid phylogenomic investigations on land plant lineages), it is likely that an incongruent, yet tree-like signal is also present in the data sets analyzed here, as evidenced by the incongruent phylogenetic trees inferred from different plastid partitions. Another potential explanation for gene tree incongruence rests with the different quantities of phylogenetic information in genes, introns, and intergenic spacers: the noncoding regions of the plastid genome experience only limited selective pressures and are known to evolve at faster rates than the coding regions (Clegg et al., 1994; Kim et al., 1999), leading to a higher frequency of potentially informative sites in these partitions. On the other hand, different regions of the plastid genome can also differ in the quality of the phylogenetic signal they contain (Barniske et al., 2012), underscoring the different molecular evolutionary patterns acting within them. Most molecular phylogenetic studies preferentially employ noncoding genome regions to reconstruct the relationships of taxa that exhibit shallow levels of sequence divergence (Kelchner, 2002; Shaw et al., 2007; Androsiuk et al., 2020). Such levels are often found among recently radiated plant lineages, and the noncoding portion of the plastid genome is particularly useful in acquiring phylogenetic resolution in such lineages, as demonstrated here for the Gynoxyoid group. However, noncoding regions also exhibit a higher frequency of microstructural mutations and require greater attention when generating MSAs. In this study,

the intron partition contributed fewer potentially informative characters than the other partitions, which corresponds with the lower average variability of introns compared to intergenic spacers. This lower variability is, however, often compounded with very specific mutational dynamics associated with secondary DNA structures and the alternation of highly conserved and highly variable sequence elements (Kelchner, 2002). Nonetheless, many phylogenetic studies have demonstrated that introns can contain high levels of hierarchical phylogenetic signal at various taxonomic levels (Creer, 2007). The intron of *rpl16*, for instance, is one of the fastest-evolving introns in the plastid genome of land plants and has been used extensively for reconstructing phylogenetic relationships at the species level (Kelchner, 2002) and often constitutes the plastome partition with the most useful phylogenetic signal (Korotkova et al., 2011). However, with the extremely low genetic distances present in the Gynoxyoid clade, the potentially higher signal quality in introns seems to have been outcompeted by the more numerous variable sites among the intergenic spacers.

2.5.8 Harnessing all regions of the plastid genome

The results of this investigation suggest that the analysis of all regions of the plastid genome can be highly beneficial for acquiring a well-supported phylogenetic reconstruction of a recently diverged plant lineage. This conclusion can likely be generalized to many plastid phylogenomic studies at the species level, as the phylogenetic signal of any plastid partition individually (i.e., genes, introns, and intergenic spacers alone) is likely insufficient to retrieve fully resolved and well-supported trees. Several studies have demonstrated that phylogenetic tree inference is affected by the selection of plastid genomic regions employed (e.g., Lu et al., 2018; Wikström et al., 2020). Thode et al. (2020), for example, recovered congruent phylogenetic trees from coding and noncoding plastid regions of neotropical lianas, but the nodes exhibited stronger support values in reconstructions using noncoding sequences. Similarly, Koehler et al. (2020) discovered that only a subset of the plastid genome regions was particularly useful in the phylogenetic reconstruction of the subfamily Opuntioideae (Cactaceae). Furthermore, Zhang et al. (2020) encountered considerable phylogenetic incongruence in a phylogenomic analysis of 36 tribes of the Fabaceae, including incongruence among strongly supported nodes and in relation to coding versus noncoding sections of the plastid genome. Despite these findings, many plastid phylogenomic investigations ignore the noncoding sections of the plastid genome during phylogenetic tree inference (e.g., Ma et al., 2014; Ross et al., 2015), often due to challenges in the alignment of these regions (e.g., Zhang

et al., 2017). This preferential selection of coding over noncoding regions in plastid phylogenomic studies may have led to reduced power in many reconstructions, and few, if any, biological reasons exist to exclude such genome regions from phylogenetic analysis. Our study contributes to the ongoing discussion of how the phylogenetic signal of the complete plastid genome can be partitioned and employed more effectively for phylogenetic inference (Koehler et al., 2020; Thode et al., 2020). More research is needed to address this question and should include different lineages of land plants and different levels of genetic distance among taxa and sequences.

2.6 Conclusion

In this plastid phylogenomic investigation, we analyzed the phylogenetic relationships of the Gynoxyoid group, an Andean lineage of the Asteraceae with low genetic distances between taxa. Our results indicated that at least two, and possibly three, of the five genera are polyphyletic. Moreover, our results demonstrated that the inclusion of all plastid genome partitions was needed to infer well-supported phylogenetic trees of the Gynoxyoid group and that manual correction of sequence alignments had a considerable effect on tree inference. Furthermore, our results indicated that the adjustment of software-derived DNA sequence alignments may constitute an important step toward improved phylogenetic analyses in plastid phylogenomic studies. Specifically, the same standards of DNA sequence alignment and matrix construction that have been applied in studies of individual genomic regions should also be applied to plastid phylogenomic data sets. The impact of incorrect positional homology in a sequence matrix may be particularly severe among plastid data sets with low genetic distances, as the misaligned regions may contain a high proportion of the potentially informative sites. Consequently, species-level investigations that require the analysis of complete plastid genomes to resolve phylogenetic relationships should apply the utmost rigor in the motif-based alignment of nucleotide sequences and consider excluding areas of uncertain homology from their alignments.

2.7 References

Ali, R., M. Bogusz, and S. Whelan. 2019. Identifying clusters of high confidence homologies in multiple sequence alignments. Molecular Biology and Evolution 36: 2340–2351.

Androsiuk, P., J. Jastrzebski, L. Paukszto, K. Makowczenko, A. Okorski, A. Pszczolkowska, K. Chwedorzewska, et al., 2020. Evolutionary dynamics of the chloroplast genome sequences of six *Colobanthus* species. Scientific Reports 10: 11522.

Bakker, F., D. Lei, J. Yu, S. Mohammadin, Z. Wei, S. van de Kerke, B. Gravendeel, et al., 2015. Herbarium genomics: plastome sequence assembly from a range of herbarium specimens using an iterative organelle genome assembly pipeline. Biological Journal of the Linnean Society 117: 33–43.

Barniske, A., T. Borsch, K. Müller, M. Krug, A. Worberg, C. Neinhuis, and D. Quandt. 2012. Phylogenetics of early branching eudicots: comparing phylogenetic signal across plastid introns, spacers, and genes. Journal of Systematics and Evolution 50: 85–108. 2252

Barriel, V. 1994. Molecular phylogenies and nucleotide insertion–deletion. Comptes rendus de l'Academie des sciences, III, Sciences de la vie 317: 693–701.

Beck, S., and D. Ibáñez. 2014. Asteraceae. In P. M. Jorgensen, M. H. Nee, and S. G. Beck [eds.], Catálogo de las plantas vasculares de Bolivia. Monographs in Systematic Botany from the Missouri Botanical Garden 127: 290–382.

Bellot, S., T. Mitchell, and H. Schaefer. 2020. Phylogenetic informativeness analyses to clarify past diversification processes in Cucurbitaceae. Scientific Reports 10: 1–13.

Beltran, H., and J. Campos de la Cruz. 2009. *Nordenstamia magnifolia* (Asteraceae: Senecioneae), una especie nueva del norte de Peru. Arnolda 16: 37–40.

Beltran, H., A. Granda, B. León, A. Sagástegui, I. Sanchez, and M. Zapata. 2006. Asteraceas endémicas de Perú. Revista Peruana Botanica 13: 64–164.

Bock, R. 2007. Structure, function, and inheritance of plastid genomes. In R. Bock [ed.], Cell and molecular biology of plastids, 29–63. Springer Verlag, Heidelberg, Germany.

Borsch, T., K. Hilu, D. Quandt, V. Wilde, C. Neinhuis, and W. Barthlott. 2003. Noncoding plastid *trnT-trnF* sequences reveal a well resolved phylogeny of basal angiosperms. Journal of Evolutionary Biology 16: 558–576.

Borsch, T., and D. Quandt. 2009. Mutational dynamics and phylogenetic utility of noncoding chloroplast DNA. Plant Systematics and Evolution 282: 169–199.

Brudno, M., C. Do, G. Cooper, M. Kim, E. Davydov, NISC Comparative Sequencing Program, E. Green, et al., 2003. LAGAN and Multi-LAGAN: Efficient tools for large-scale multiple alignment of genomic DNA. Genome Research 13: 721–731.

Calvo, J. 2016. A new combination in *Roldana* (Compositae, Senecioneae). Phytotaxa 272: 225–227.

Chen, R., Y. Lau, Y. Zhang, and W. Yang. 2016. SRinversion: a tool for detecting short inversions by splitting and re-aligning poorly mapped and unmapped sequencing reads. Bioinformatics 32: btw516.

Chen, X., J. Zhou, Y. Cui, Y. Wang, B. Duan, and H. Yao. 2018. Identification of *Ligularia* herbs using the complete chloroplast genome as a super-barcode. Frontiers in Pharmacology 9: 695–706.

Clark, B., and J. Pruski. 2015. *Telanthophora* H. Rob. et Brettell. In J. Pruski and H. Robinson [eds.], Flora mesoamericana, 427–469. Missouri Botanical Garden Press, St. Louis, MO, USA.

Clegg, M., B. Gaut, G. Learn, and B. Morton. 1994. Rates and patterns of chloroplast DNA evolution. Proceedings of the National Academy of Sciences, USA 91: 6795–6801.

Creer, S. 2007. Choosing and using introns in molecular phylogenetics. Evolutionary Bioinformatics Online 3: 99–108.

Cuatrecasas, J. 1951. Contributions to the flora of South America: studies on Andean Compositae, II. Studies in South American plants, III. Fieldiana 27: 1–74.

Cuatrecasas, J. 1955. A new genus and other novelties in Compositae. Brittonia 8: 151–163.

de Pinna, M. 1991. Concepts and tests of homology in the cladistic paradigm. Cladistics 7: 367–394.
Dierckxsens, N., P. Mardulyn, and G. Smits. 2017. NOVOPlasty: de novo assembly of organelle genomes from whole genome data. Nucleic Acids Research 45: e18.
Doorduin, L., B. Gravendeel, Y. Lammers, Y. Ariyurek, T. Chin-A-Woeng, and K. Vrieling. 2011. The complete chloroplast genome of 17 individuals of pest species *Jacobaea vulgaris*: SNPs, microsatellites and barcoding markers for population and phylogenetic studies. DNA Research 18: 93–105.
Du, Y., S. Wu, S. Edwards, and L. Liu. 2019. The effect of alignment uncertainty, substitution models and priors in building and dating the mammal tree of life. BMC Evolutionary Biology 191: 203.
Edwards, S., Z. Xi, A. Janke, B. Faircloth, J. McCormack, T. Glenn, B. Zhong, et al., 2016. Implementing and testing the multispecies coalescent model: a valuable paradigm for phylogenomics. Molecular Phylogenetics and Evolution 94: 447–462.
Farris, J. 1989. The retention index and the rescaled consistency index. Cladistics 5: 417–419.
Fonseca, L., and L. Lohmann. 2017. Plastome rearrangements in the Adenocalymma-Neojobertia clade (Bignonieae, Bignoniaceae) and its phylogenetic implications. Frontiers in Plant Science 8: 1875.
Frazer, K., L. Pachter, A. Poliakov, E. Rubin, and I. Dubchak. 2004. VISTA: computational tools for comparative genomics. Nucleic Acids Research 32: W273–W279.
Funston, A. 2009. Taxonomic revision of *Roldana* (Asteraceae: Senecioneae), a genus of the southwestern U.S.A., Mexico, and Central America. Annals of the Missouri Botanical Garden 95: 282–337.
Gernandt, D., X. Aguirre-Dugua, A. Vazquez-Lobo, A. Willyard, A. Moreno-Letelier, J. Perez de la Rosa, D. Pinero, and A. Liston. 2018. Multi-locus phylogenetics, lineage sorting, and reticulation in *Pinus* subsection Australes. American Journal of Botany 105: 711–725.
Gichira, A., S. Avoga, and Z. Li. 2019. Comparative genomics of 11 complete chloroplast genomes of Senecioneae (Asteraceae) species: DNA barcodes and phylogenetics. Botanical Studies 60: 1–17.
Givnish, T., A. Zuluaga, D. Spalink, M. Soto, V. Lam, J. Saarela, C. Sass, et al., 2018. Monocot plastid phylogenomics, timeline, net rates of species diversification, the power of multi-gene analyses, and a functional model for the origin of monocots. American Journal of Botany 105: 1888–1910.
Glanz, S., and U. Kueck. 2009. Trans-splicing of organelle introns—a detour to continuous RNAs. Bioessays 31: 921–934.
Goncalves, D., R. Jansen, T. Ruhlman, and J. Mandel. 2020. Under the rug: abandoning persistent misconceptions that obfuscate organelle evolution. Molecular Phylogenetics and Evolution 151: 106903.
Goncalves, D., B. Simpson, E. Ortiz, G. Shimizu, and R. Jansen. 2019. Incongruence between gene trees and species trees and phylogenetic signal variation in plastid genes. Molecular Phylogenetics and Evolution 138: 219–232.
Graham, S., and R. Olmstead. 2000. Utility of 17 chloroplast genes for inferring the phylogeny of the basal angiosperms. American Journal of Botany 87: 1712–1730.
Graham, S., P. Reeves, A. Burns, and R. Olmstead. 2000. Microstructural changes in noncoding chloroplast DNA: interpretation, evolution, and utility of indels and inversions in basal angiosperm phylogenetic inference. International Journal of Plant Science 161: 83–96.
Greiner, S., Lehwark, P., and Bock, R. 2019. OrganellarGenomeDRAW (OGDRAW) version 1.3.1: expanded toolkit for the graphical visualization of organellar genomes. Nucleic Acids Research 47: 59–64.
Greiner, S., Sobanski, J., and Bock, R. 2015. Why are most organelle genomes transmitted maternally? BioEssays 37: 80–94.
Gruenstaeudl, M. 2019. Why the monophyly of Nymphaeaceae currently remains indeterminate: an

assessment based on gene-wise plastid phylogenomics. Plant Systematics and Evolution 305: 827–836.
Gruenstaeudl, M., N. Gerschler, and T. Borsch. 2018. Bioinformatic workflows for generating complete plastid genome sequences: an example from *Cabomba* (Cabombaceae) in the context of the phylogenomic analysis of the water-lily clade. Life 8: 1–17.
Hind, N. 2007. An annotated preliminary checklist of the Compositae of Bolivia, version 2. Website: https://www.kew.org/sites/default/files/ 2019-01/Bolivian%20compositae%20checklist.pdf [accessed 05 November 2021].
Joly, S., B. Pfeil, B. Oxelman, T. Mclenachan, and P. Lockhart. 2010. Erratum: A statistical approach for distinguishing hybridization and incomplete lineage sorting. American Naturalist 174: 621–622.
Kadereit, J., and C. Jeffrey. 1996. A preliminary analysis of cpDNA variation in the tribe Senecioneae (Compositae). In D. Hind and H. Beentje [eds.], Compositae: Systematics. Proceedings of the International Compositae Conference, vol. 1, 349–360. Royal Botanic Gardens, Kew, UK.
Katoh, K., and D. Standley. 2013. MAFFT multiple sequence alignment software version 7: improvements in performance and usability. Molecular Biology and Evolution 30: 772–780.
Kearse, M., R. Moir, A. Wilson, S. Stones-Havas, M. Cheung, S. Sturrock, S. Buxton, et al., 2012. Geneious Basic: an integrated and extendable desktop software platform for the organization and analysis of sequence data. Bioinformatics 28: 1647–1649.
Kelchner, S. 2000. The evolution of non-coding chloroplast DNA and its application in plant systematics. Annals of the Missouri Botanical Garden 87: 482–498.
Kelchner, S. 2002. Group II introns as phylogenetic tools: structure, function, and evolutionary constraints. American Journal of Botany 89: 1651–1669.
Kelchner, S., and M. Thomas. 2006. Model use in phylogenetics: nine key questions. Trends in Ecology and Evolution 22: 87–94.
Kelchner, S., and J. Wendel. 1996. Hairpins create minute inversions in non-coding regions of chloroplast DNA. Current Genetics 30: 259–262.
Kim, K., K. Choi, and R. Jansen. 2005. Two chloroplast DNA inversions originated simultaneously during the early evolution of the sunflower family (Asteraceae). Molecular Biology and Evolution 22: 1783–1792.
Kim, S., D. Crawford, R. Jansen, and A. Santos-Guerra. 1999. The use of a non-coding region of chloroplast DNA in phylogenetic studies of the subtribe Sonchinae (Asteraceae: Lactuceae). Plant Systematics and Evolution 215: 85–99.
Kluge, A., and J. Farris. 1969. Quantitative phyletics and the evolution of anurans. Systematic Zoology 18: 1–32.
Knope, M., M. Bellinger, E. Datlof, T. Gallaher, and M. Johnson. 2020. Insights into the evolutionary history of the Hawaiian *Bidens* (Asteraceae) adaptive radiation revealed through phylogenomics. Journal of Heredity 111: 1–19.
Koehler, M., M. Reginato, T. Chies, and L. Majure. 2020. Insights into chloroplast genome evolution across Opuntioideae (Cactaceae) reveals robust yet sometimes conflicting phylogenetic topologies. Frontiers in Plant Science 11: 1–20.
Korotkova, N., T. Borsch, D. Quandt, N. Taylor, K. Mueller, and W. Barthlott. 2011. What does it take to resolve relationships and to identify species with molecular markers? An example from the epiphytic Rhipsalideae (Cactaceae). American Journal of Botany 98: 1549–1572.
Korotkova, N., L. Nauheimer, H. Ter-Voskanyan, M. Allgaier, and T. Borsch. 2014. Variability among the most rapidly evolving plastid genomic regions is lineage-specific: implications of pairwise genome comparisons in Pyrus (Rosaceae) and other angiosperms for marker choice. PLoS One 9: 1–16.
Langmead, B., and S. Salzberg. 2012. Fast gapped-read alignment with Bowtie 2. Nature Methods 9: 357.
Leebens-Mack, J., L. Raubeson, L. Cui, J. Kuehl, M. Fourcade, T. Chumley, J. Boore, et al., 2005.

Identifying the basal angiosperm node in chloroplast genome phylogenies: sampling one's way out of the Felsenstein zone. Molecular Biology and Evolution 22: 1948–1963.
Lewis, P. 2001. A likelihood approach to estimating phylogeny from discrete morphological character data. Systematic Biology 50: 913–925.
Li, C., R. Wang, and D. Li. 2020. Comparative analysis of plastid genomes within the Campanulaceae and phylogenetic implications. PLoS One 15: 23.
Loehne, C., and T. Borsch. 2005. Molecular evolution and phylogenetic utility of the *petD* group II intron: A case study in basal angiosperms. Molecular Biology and Evolution 22: 317–332.
Lu, L., C. Cox, S. Mathews, W. Wang, J. Wen, and Z. Chen. 2018. Optimal data partitioning, multispecies coalescent and Bayesian concordance analyses resolve early divergences of the grape family. Cladistics 34: 57–77.
Luebert, F., and M. Weigend. 2014. Phylogenetic insights into Andean plant diversification. Frontiers in Ecology and Evolution 2: 27. Lundin, R. 2006. Nordenstamia Lundin (Compositae-Senecioneae), a new genus from the Andes of South America. Compositae Newsletter 44: 14–23.
Ma, P., Y. Zhang, C. Zeng, Z. Guo, and D. Li. 2014. Chloroplast phylogenomic analyses resolve deep-level relationships of an intractable bamboo tribe Arundinarieae (Poaceae). Systematic Biology 63: 933–950.
Marechal, A., and N. Brisson. 2010. Recombination and the maintenance of plant organelle genome stability. New Phytologist 186: 299–317.
Moore, M., P. Soltis, C. Bell, J. Burleigh, and D. Soltis. 2010. Phylogenetic analysis of 83 plastid genes further resolves the early diversification of Eudicots. Proceedings of the National Academy of Sciences, USA 107: 4623–4628.
Morillo, G., and B. Briceno. 2000. Distribución de las Asteraceas de los páramos venezolanos. Acta Botánica Venezuélica 23: 47–67.
Morrison, D. 2006. Multiple sequence alignment for phylogenetic purposes. Australian Systematic Botany 19: 479–539.
Morrison, D. 2015. Is sequence alignment an art or a science? Systematic Botany 40: 14–26.
Morrison, D., and J. Ellis. 1997. Effects of nucleotide sequence alignment on phylogeny estimation: a case study of 18 S rDNAs of Apicomplexa. Molecular Biology and Evolution 14: 428–441.
Morton, B., and M. Clegg. 1995. Neighboring base composition is strongly correlated with base substitution bias in a region of the chloroplast genome. Journal of Molecular Evolution 41: 597–603.
Mower, J., and T. Vickrey. 2018. Structural diversity among plastid genomes of land plants. Advances in Botanical Research 85: 263–292.
Müller, J., K. Müller, C. Neinhuis, and D. Quandt. 2010. PhyDE: Phylogenetic Data Editor. Website: http://www.phyde.de/ [accessed 19 August 2020].
Müller, K. 2005. SeqState: primer design and sequence statistics for phylogenetic DNA datasets. Applied Bioinformatics 4: 65–69.
Müller, K., T. Borsch, and K. Hilu. 2006. Phylogenetic utility of rapidly evolving DNA at high taxonomical levels: contrasting *matK, trnT-F,* and *rbcL* in basal angiosperms. Molecular Phylogenetics and Evolution 41: 99–117.
Nei, M., and S. Kumar. 2000. Molecular evolution and phylogenetics. Oxford University Press, NY, NY, USA.
Nei, M., and W. Li. 1979. Mathematical model for studying genetic variation in terms of restriction endonucleases. Proceedings of the National Academy of Sciences, USA 76: 5269–5273.
Nordenstam, B. 2007. XII. Tribe Senecioneae. In J. Kadereit and C. Jeffrey [eds.], Flowering plants, eudicots: Asterales, 208–241. Springer, NY, NY, USA.
Nordenstam, B., P. Pelser, J. Kadereit, and L. Watson. 2009. Senecioneae. In V. Funk, A. Susanna, T. Stuessy, and R. Bayer [eds.], Systematics, evolution, and biogeography of Compositae, 503–525. International Association for Plant Taxonomy, Vienna, Austria.

Ochoterena, H. 2008. Homology in coding and non-coding DNA sequences: a parsimony perspective. Plant Systematic and Evolution 282: 151–168.

Paradis, E., and K. Schliep. 2018. Ape 5.0: AN environment for modern phylogenetics and evolutionary analyses in R. Bioinformatics 35: 526–528.

Pelser, P., A. Kennedy, E. Tepe, J. Shidler, B. Nordenstam, J. Kadereit, and L. Watson. 2010. Patterns and causes of incongruence between plastid and nuclear Senecioneae (Asteraceae) phylogenies. American Journal of Botany 97: 856–873.

Pelser, P., B. Nordenstam, J. Kadereit, and L. Watson. 2007. An ITS phylogeny of tribe Senecioneae (Asteraceae) and a new delimitation of *Senecio* L. Taxon 56: 1077–1104.

Pervez, M., M. Babar, A. Nadeem, M. Aslam, A. Awan, N. Aslam, T. Hussain, et al., 2014. Evaluating the accuracy and efficiency of multiple sequence alignment methods. Evolutionary Bioinformatics 10: 205–217.

Pouchon, C., A. Fernandez, J. Nassar, F. Boyer, S. Aubert, S. Lavergne, and J. Mavarez. 2018. Phylogenomic analysis of the explosive adaptive radiation of the *Espeletia* complex (Asteraceae) in the tropical Andes. Systematic Biology 67: 1041–1060.

Quedensley, T., M. Gruenstaeudl, and R. Jansen. 2018. Phylogenetic relationships of the Mexican tussilaginoid genera (Asteraceae: Senecioneae). Journal of the Botanical Research Institute of Texas 12: 481–498. 2254

Rambaut, A., A. Drummond, D. Xie, G. Baele, and M. Suchard. 2018. Posterior summarization in Bayesian phylogenetics using Tracer 1.7. Systematic Biology 67: 901–904.

Ronquist, F., and J. Huelsenbeck. 2003. MrBayes 3: Bayesian phylogenetic inference under mixed models. Bioinformatics 19: 1572–1574.

Ross, T., C. Barrett, M. Soto Gomez, V. Lam, C. Henriquez, D. Les, J. Davis, et al., 2015. Plastid phylogenomics and molecular evolution of Alismatales. Cladistics 32: 160–178.

Rozas, J., A. Ferrer-Mata, J. Sánchez-DelBarrio, S. Guirao-Rico, P. Librado, S. Ramos-Onsins, and A. Sánchez-Gracia. 2017. DnaSP 6: DNA sequence polymorphism analysis of large datasets. Molecular Biology and Evolution 34: 3299–3302.

Ruhlman, T., J. Zhang, J. Blazier, J. Sabir, and R. Jansen. 2017. Recombination-dependent replication and gene conversion homogenize repeat sequences and diversify plastid genome structure. American Journal of Botany 104: 559–572.

Schliep, K. 2011. Phangorn: phylogenetic analysis in R. Bioinformatics 27: 592–593. Shaw, J., E. Lickey, E. Schilling, and R. Small. 2007. Comparison of whole chloroplast genome sequence to choose non-coding regions for phylogenetic studies in angiosperms: the tortoise and the hare III. American Journal of Botany 94: 275–288.

Shimodaira, H. 2002. An approximately unbiased test of phylogenetic tree selection. Systematic Biology 51: 492–508. Shimodaira, H., and M. Hasegawa. 2001. CONSEL: for assessing the confidence of phylogenetic tree selection. Bioinformatics 517: 1246–1247.

Simmons, M., K. Mueller, and A. Norton. 2010a. Alignment of, and phylogenetic inference from, random sequences: the susceptibility of alternative alignment methods to creating artifactual resolution and support. Molecular Phylogenetics and Evolution 57: 1004–1016.

Simmons, M., K. Mueller, and C. Webb. 2010b. The deterministic effects of alignment bias in phylogenetic inference. Cladistics 27: 402–416.

Simmons, M., and H. Ochoterena. 2000. Gaps as characters in sequence- based phylogenetic analyses. Systematic Biology 49: 369–381. Smith, D. 2009. Unparalleled GC content in the plastid DNA of Selaginella. Plant Molecular Biology 71: 627–639. Smith, D., and P. Keeling. 2015. Mitochondrial and plastid genome architecture: reoccurring themes, but significant differences at the extremes. Proceedings of the National Academy of Sciences, USA 112: 10177–10184.

Stamatakis, A. 2014. RAxML version 8: a tool for phylogenetic analysis and post-analysis of large phylogenies. Bioinformatics 30: 1312–1313.

Stamatakis, A., J. Hoover, and J. Rougemint. 2008. A rapid boot-strap algorithm for the RAxML web servers. Systematic Biology 57: 758–771.

Tan, G., M. Muffato, C. Ledergerber, J. Herrero, N. Goldman, M. Gil, and C. Dessimoz. 2015. Current methods for automated filtering of multiple sequence alignments frequently worsen single-gene phylogenetic inference. Systematic Biology 64: 778–791.

Team, R. D. C. 2019. R: A language and environment for statistical computing. R Foundation for Statistical Computing, Vienna, Austria. Website: http://www.r-project.org/

Tesfaye, K., T. Borsch, K. Govers, and E. Bekele. 2007. Characterization of *Coffea* chloroplast microsatellites and evidence for the recent divergence of *C. arabica* and *C. eugenioides* chloroplast genomes. Genome 50: 1112–1129.

Thode, V., L. Lohmann, and I. Sanmartin. 2020. Evaluating character partitioning and molecular models in plastid phylogenomics at low taxonomic levels: a case study using *Amphilophium* (Bignonieae, Bignoniaceae). Journal of Systematics and Evolution 58: 1071–1089.

Thompson, J., D. Higgins, and T. Gibson. 1994. CLUSTAL W: improving the sensitivity of progressive multiple sequence alignment through sequence weighting, position-specific gap penalties and weight matrix choice. Nucleic Acids Research 22: 4673–4680.

Tinoco, B., P. Astudillo, S. Latta, D. Strubbe, and C. Graham. 2013. Influence of patch factors and connectivity on the avifauna of fragmented *Polylepis* forest in the Ecuadorian Andes. Biotropica 45: 602–611.

Vargas, O., and S. Madrinan. 2012. Preliminary phylogeny of *Diplostephium* (Asteraceae): speciation rate and character evolution. Lundellia 15: 1–15.

Vargas, O., E. Ortiz, and B. Simpson. 2017. Conflicting phylogenomic signals reveal a pattern of reticulate evolution in a recent high- Andean diversification (Asteraceae: Astereae: Diplostephium). New Phytologist 214: 1736–1750.

Vision, T., and M. Dillon. 1996. Sinopsis de *Senecio* (Senecioneae, Asteraceae) para el Peru. Arnolda 4: 23–46.

Walker, J., N. Walker-Hale, O. Vargas, D. Larson, and G. Stull. 2019. Characterizing gene tree conflict in plastome-inferred phylogenies. PeerJ 7: 1–31.

Wikström, N., B. Bremer, and C. Rydin. 2020. Conflicting phylogenetic signals in genomic data of the coffee family (Rubiaceae). Journal of Systematics and Evolution 58: 440–460.

Wong, K., M. Suchard, and J. Huelsenbeck. 2008. Alignment uncertainty and genomic analysis. Science 319: 473–476.

Wu, M., S. Chatterji, and J. Eisen. 2012. Accounting for alignment uncertainty in phylogenomics. PLoS One 7: 1–10.

Wyman, S., R. Jansen, and J. Boore. 2004. Automatic annotation of organellar genomes with DOGMA. Bioinformatics 20: 3252–3255.

Xi, Z., B. Ruhfel, H. Schaefer, A. Amorim, S. Manickam, K. Wurdack, P. Endress, et al., 2012. Phylogenomics and a posteriori data portioning resolve the Cretaceous angiosperm radiation Malpighiales. Proceedings of the National Academy of Sciences, USA 109: 17519–17524.

Yao, G., J. Jin, H. Li, J. Yang, V. Mandala, M. Croley, R. Mostow, et al., 2019. Plastid phylogenomic insights into the evolution of Caryophyllales. Molecular Phylogenetics and Evolution 134: 74–86.

Zhang, R., Y. Wang, J. Jin, G. Stull, A. Bruneau, D. Cardoso, L. Queiroz, et al., 2020. Exploration of plastid phylogenomic conflict yields new insights into the deep relationships of Leguminosae. Systematic Biology 69: 613–622.

Zhang, S., J. Jin, S. Chen, M. Chase, D. Soltis, H. Li, J. Yang, et al., 2017. Diversification of Rosaceae since the late cretaceous based on plastid phylogenomics. New Phytologist 214: 1355–1367.

Zhang, X., T. Deng, M. Moore, Y. Ji, N. Lin, Z. Huajie, A. Meng, et al., 2019. Plastome phylogenomics of *Saussurea* (Asteraceae: Cardueae). BMC Plant Biology 19: 1–10.

Chapter 3. Genus concepts and species diversity within the Gynoxyoid

3.1 Summary

The Gynoxyoid clade of the Senecioneae (Asteraceae) was considered to be constituted by the five genera *Aequatorium*, *Gynoxys*, *Nordenstamia*, *Paracalia* and *Paragynoxys* that were circumscribed by individual morphological data. In this pre-phylogenetic circumscription the distribution was taken into account specially for the delimitation of four genera. *Aequatorium* and *Paragynoxys* inhabits the northern Andes in compare to *Nordenstamia* and *Paracalia* which are found in the central Andes. The most species-rich genus *Gynoxys* is distributed throughout the Andes. Using our recently inferred molecular trees that comprise representatives of all genera, we reconstructed ancestral character-states of eleven morphological characters. The character-state inferences displayed a high level of homoplasy, including characters hitherto used to diagnose genera i.e., phyllotaxis, flower colours, capitula structure. Nevertheless, a specific combination of characters enabled the monophyletic circumscription of four genera. *Aequatorium*, characterizes by white radiate capitula. *Paracalia* and *Paragynoxys* share floral structure, but differentiate on the habit (scandent vs trees) and by the absence of outer phyllaries in *Paracalia*. Finally the biggest genus *Gynoxys* comprises all species with yellow capitula. The genus *Nordenstamia* with eight species is synonymized under *Gynoxys* since neither molecular nor morphological evidence supported its existence as a specific clade. In addition, we evaluated the character-states on all members of the Gynoxyoids and elaborated a taxonomic treatment for all recognized genera in this study. Newly ETS and ITS sequences were generated for 171 specimens belonging to 49 species. The taxonomic treatment includes the number of species in each genus; emended diagnoses and morphological descriptions of the four genera are provided. Protologue and type information for accepted names and synonyms

Introduction

The Gynoxyoid group is a new world clade of the tribe Senecioneae of the Asteraceae (Escobari et al., 2021) that was estimated to comprise around 150 species in five genera. The group includes woody species growing in the paramo at the Andean tree-line, humid mountain forest, and subalpine forest. Originally, Jeffrey (1992) suggested the existence of this group of putatively related genera on the basis of cylindrical anther-collars, polar endothecial thickening and a basic chromosome number of x = 10 and included the genera *Alciope* DC. ex Lindl, *Paracalia* Cuatrec., *Paragynoxys* Cuatrec. (Cuatrec.), *Gynoxys* (Cass.), *Aequatorium* B. Nord. and *Herodotia* Urb. & Eckm. Subsequently, Robinson et al. (1997) restricted the group to the South American genera (*Aequatorium*, *Gynoxys*, *Paracalia*, and *Paragynoxys*) and pointed out that it is characterized it by an octoploid chromosome number (x=10, 2n=80). The genus *Nordenstamia* Lund. was later described as a segregate accommodating species previously placed in *Aequatorium* and *Gynoxys* (Lundin, 2006)

The first phylogenetic data for the Gynoxyoid group were provided by Pelser et al. (2007) in the context of inferring relationships within the Senecioneae based sequences of the nrITS region. The authors included the genera *Aequatorium*, *Gynoxys*, *Nordenstamia* and *Paragynoxys,* and found *Nordenstamia* nested within *Gynoxys*. Pelser et al. (2010) then extended the taxon sampling by a representative of *Paracalia* and increased the number of molecular markers (nrITS and nrETS, and plastid *ndhF*, *psbA-trnH*, 5′ and 3′ *trnK*, *trnL*, and *trnL-F* regions and *rbcL*). Recently, Escobari et al. (2022) provided a comprehensive plastid phylogenomic framework based on 17 complete plastid genomes representing all five genera and close relatives of the Tussilagiinae. Their results retrieved the Gynoxyoid group as monophyletic with high support. The two species of the genus *Paragynoxys* were retrieved as sisters. The three representatives of the genus *Nordenstamia* as well as one species of *Paracalia* were recovered within the genus *Gynoxys*. The second member of *Paracalia* was retrieved as basal species of the Gynoxyoids. The second diverging clade was comprised by the monophyletic *Paragynoxys* and the only representative of the genus *Aequatorium*. Furthermore, the authors observed and presented evidence for extremely low genetic distances among the species sequences within this clade.

The Gynoxyoid group represents one of the speciose Andean plant lineages and thus contributes significantly to the high species diversity and endemism in the Andes as one of the global biodiversity hotspots (Myers et al., 2000; Padilla-Gonzalez et al., 2021). The uplift of the Andes (Luebert and Weigend, 2014; Bacon et al., 2022) led to shifts in ecosystem barriers and enabled the creation of new habitats (Colwell et al., 2008; Moreira-Munoz et al., 2020; Perez-Escobar et al., 2022) which seem to have triggered rapid speciation of Andean plants (e.g. Madriñán et al., 2013; Zhang et al., 2021; Perez-Escobar et al., 2022). Among the studies focusing on the evolution of Andean plant groups (see Hughes and Atchison, 2015) several dealt with genera of the sunflower family, such as *Diplostephium* Kunth (Vargas et al., 2017), *Espeletia* Mutis ex Bonpl. (Pouchon et al., 2018) and *Loricaria* Wedd. (Kandziora et al., 2022). In all three cases, the authors reported low genetic distances, complicating the study of species relationships and species limits. Moreover, frequent events of reticulate evolution and incomplete linage sorting have been reported from rapidly evolving Andean plant groups (Garcia et al., 2014; Vargas et al., 2017; Schley et al., 2021; Kandziora et al., 2022). Low genetic distances were also observed among plastid genomes in the Gynoxyoid clade in our previous study (Escobari et al., 2021) in which we demonstrated that complete plastid genomes including the information from the more variable intron and spacer partitions were needed to achieve resolution at species and even genus level. The results of Escobari et al. (2021) underscored that in particular *Gynoxys* is not monophyletic as currently circumscribed, and that an evaluation of morphological characters hitherto used to diagnose genera in an evolutionary context would be warranted.

Gynoxys, published by Cassini (1827), was diagnosed by a tree-like habit, opposite leaves, the presence of an indumentum on the lower leaf surface, corymbiform capitula and the apex of style branches protected by papillose hairs. Weddell (1855) subdivided the genus in two sections: one with radiate and the other with discoid capitula, which was lately adopted by Correa (2003). The first taxonomic treatment including a larger number of species was made by Herrera (1980) who dealt with the 30 species distributed in Peru. The author redefined the genus by usually opposite leaves, presence of an indumentum on the lower leaf face, discoid or radiate capitula with up to 32 yellow disc flowers, an inconspicuously sagittate anther base, conical hispid and caudate style-branch apex. The genus is distributed from Bolivia to Venezuela at altitudes between 1600 and 4700 m, and comprises according to the published

checklists (Bernal et al., 2019; Beck and Ibanez, 2014; Brako and Zarucchi, 1993; Jorgensen and Leon-Yanez, 1999) about 180 species.

Paragynoxys was first described by Cuatrecasas (1951) as a section within *Senecio* (*Senecio* sect. *Paragynoxys*) but raised to generic rank shortly after (Cuatrecasas 1955). It is characterized by a tree or shrub-like habit, sub-coriaceous petiolate alternate leaves, a corymbose-paniculate terminal inflorescence, few-flowered discoid capitula, white corollae with the limb divided to its base, conical style-branches and a distribution in Colombia and Venezuela. Since the description of the genus, a single taxonomic revision was made by Correa (2003) who recognized 12 species and extended its diagnosis by having radiate capitula with five or more inner phyllaries and up to 12 flowers

Paracalia was segregated by Cuatrecasas (1960) from *Paragynoxys* by the differing scandent habit, smaller leaves, and the involucre lacking outer phyllaries. The genus comprises two species distributed in Bolivia and Peru (Cuatrecasas, 1960; Nordenstam, 2007; Hind, 2007).

Aequatorium was published by Nordenstam (1978) to accommodate two shrubby species with alternate leaves, a rusty tomentum of stellate hairs with patches, white corollae, sagittate or auriculate anther bases and blunt style-branches apex. Subsequently, several new species were added (i.e., Díaz-Piedrahita and Cuatrecasas, 1990; Díaz-Piedrahita and Cuatrecasas, 1994; Jeffrey, 1992; Nordenstam, 1997), what has led to a still ongoing discussion on morphological features suitable for circumscribing the genus (see Nordenstam, 1997). Based on the presence of stellate hairs and a different involucrum shape, Jeffrey (1992) transferred *Gynoxys* section *Praegynoxys* to *Aequatorium*. Nordenstam (1997) concurred with this hypothesis and divided *Aequatorium* in two subgenera. *Aequatorium* subg. *Aequatorium* included species with (generally) alternate leaves, white flowers, obtuse apex of stylar branches, peltate trichomes forming two layers, and distributed in Ecuador and Colombia. *Aequatorium* subg. *Praegynoxys* included the species with opposite or alternate leaves, irregular branching trichomes, absence of overlying brownish tomentum, yellow flowers, and pointed stylar branches apex, with a distribution in Argentina, Bolivia, Peru, and southern Ecuador. Interestingly, he even suspected that the latter subgenus may actually be closer to *Gynoxys* than to *Aequatorium*. These concerns were taken up by Lundin (2006), who raised *Aequatorium* subg. *Praegynoxys* to a genus of its own, *Nordenstamia,* and proposed 14 new combinations.

Since the establishment of the name-giving genus of the Gynoxyoids almost 200 years ago, new species are constantly being described in this conspicuous Andean group (Beltrán and Baldeón, 2009; Beltrán and Calvo, 2020; Cuatrecasas, 1950; 1951; 1954; 1955; Maffteld, 1921; Robinson and Cuatrecasas, 1992). In contrast, synthesizing work on the gathered data was largely limited to a certain genus (Herrera, 1980; Robinson and Cuatrecasas, 1984; Nordenstam, 1997; Correa, 2003) or geographically limited areas (Bernal et al., 2019; Beck and Ibanez, 2014; Brako and Zarucchi, 1993; Jorgensen and Leon-Yanez, 1999). The considerable species number, the altogether rather shallow morphological differentiation within the clade, and the absence of a taxonomic treatment including all species of the clade added considerable uncertainty and instability for the circumscription of the genera of the Gynoxyoids, which found its expression in the frequent transfer of species between genera. A consistent taxonomic synthesis of the whole Gynoxyoid clade was therefore also needed to evaluate the concepts of its genera.

The availability of electronic sources for names and protologue citations (IPNI www.ipni.org, TROPICOS www.tropicos.org) as well as online access to digitized type specimens (JSTOR Global Plants, https://plants.jstor.org/), but also electronic tools to support the taxonomic workflow (EDIT Platform; Berendsohn, 2010) has facilitated the way taxonomic treatments are undertaken. Names can be imported so that the work can focus on checking validity of names, and testing taxon concepts at species level. At the same time the taxonomic workflows are revolutionized by structured data (Kilian et al., 2015) and evolutionary approaches to investigate species limits (Stuessy and Lack, 2011; Marhold et al., 2013).

For the Gynoxyoid clade a first approach that synthesizes all names and presents a consistent classification at species level for the whole clade using the available data is the first step. This alpha taxonomic approach is largely based on morpho-species but utilizes some phylogenetic data that were generated for specimens representing a part of the species. The goal is an expert-revised taxonomic backbone for a plant group throughout its range of distribution in the sense of the workflow of the World Flora Online (WFO; see Borsch et al., 2020) ideally including all validly published names assigned to a status as accepted name or synonym. Such a taxonomic backbone also serves as which is needed as a reference for conservation status assessments, biodiversity monitoring, etc.

Considering this situation, the aims of this investigation are [1] To revise the generic classification of the Gynoxyoids making use of molecular (plastome and nrDNA) and morphological data, and [2] Elaborate a taxonomic backbone of all species belonging to the Gynoxyoids for their entire range of distribution.

3.2 Materials and Methods

3.2.1 Plant material and sources for specimen data

The study was based on plants observed, collected and photo-documented in the field during three collecting trips in Bolivia and Peru, as well as physical specimens loaned to B from AAU, F, G, K, LPB, MA, MO, NY, and P. Specimens that were physically examined or served as vouchers for DNA isolation are listed in Appendix 3.1. In addition, high resolution digital images of herbarium specimens, in particular types, were consulted online either accessed through JSTOR Global Plants (https://plants.jstor.org/), GBIF (https://www.gbif.org/) or directly through the herbarium websites.

3.2.2 Sources of names and compilation into a checklist of the species of the *Gynoxys* clade

The taxonomic backbone of the species of the Gynoxyoids was elaborated in a database using the EDIT Platform for Cybertaxonomy (Berendsohn, 2010) based on taxon name data imports from the International Plant Names Index (IPNI) (https://www.ipni.org/) supplemented by TROPICOS (https://tropicos.org/home) and the Global Asteraceae Database (https://www.Asteraceae.org/aphia.php?p=stats)

3.2.3 Definition and assessment of morphological characters and states

In a first round of assessing the morphological variation in the Gynoxyoid group including species providing the type of generic names of the genera *Aequatorium*, *Nordenstamia*, *Paracalia* and *Paragynoxys*, and a representative selection in terms of morphological diversity of *Gynoxys* species were morphologically examined. Based on an initial comparative morphological examination including the diagnostic characters stated in the protologues of the five genera and in other studies, a list of characters and their states was developed. A character state was considered taxonomically relevant and selected for further processing if its expression marked morphological discontinuities at supra-specific level. For each such character unordered categorical states were defined following the terminology by Roque et al. (2009) and Beentje (2010). In cases a more detailed homology statement was needed due to conflicting or unclear use of character definitions or terms, a description and illustration was included. For later reconstruction of character evolution, a specimen-based matrix of characters and states suitable for reliable delimitation and characterisation of supra-specific entities was constructed using the specimens included in the plastid phylogenomic analysis of Escobari et al. (2021). For certain characters, e.g., the plant habit, the respective states were recorded from the literature if not given on the specimen label, and if these data were unavailable, they were coded as missing. In a second step, the diagnostic value of the selected characters and states was morphologically investigated for the remaining *Gynoxys* species.

3.2.4 Extraction, amplification, and phylogenetic tree inference on molecular nuclear data

In order to achieve an overview on species-level phylogenetic relationships within the Gynoxyoid clade, and to test if groups of samples identified with the same species name appeared in terminal subclades, 171 samples belonging to 50 species were (Appendix 3.1) included into a molecular analysis. These samples were selected to cover morphological and geographical variation as much as possible and also comprised the samples that were already part of the plastid phylogenomic study. Genomic DNA was extracted using the CTAB method by Doyle and Doyle (1987), with three fractions for each sample as modified by Borsch et al. (2003). The nrITS and nrETS regions were used as they provided at least some variable and informative characters in a short marker that was possible to sequence with little effort per sample, and as they represent the nuclear genome. Plastid regions often applied to assess the tree space of speciose clades (Mansion et al., 2012) were not suitable in the Gynoxyoid clade due to extremely low genetic distances (Escobari et al., 2020). PCR amplification of the ITS followed White et al. (1990), ETS was amplified with the primers AST–1 (f) and 18–S–ETS (r) (Markos and Baldwing, 2001) following Pelser et al. (2010). PCR was performed in a peqSTAR Thermocycler 1107D (PeqLab, Erlangen, Germany). The PCR products were electrophoresed on 1.5% agarose, the bands were cutted out, and cleaned with the GenepHlow Gel/PCR kit (Geneaid, New Taipei, Taiwan). Samples were sequenced by Macrogen Europe (Amsterdam, The Netherlands). Sequence files were aligned using MAFFT v.7.394 (Katoh and Standley, 2013) and manually edited using PhyDE version 0.9971 (Müller et al., 2010) following the rules of Löhne and Borsch (2005). This included the masking of mutational hotspots for those sections of the alignment where positional homology was uncertain. Indels

were coded as binary characters using the simple-indel-coding method (Simmons and Ochoterena, 2000) in SeqState version 1.4.1 (Müller, 2005). Altogether 146 ETS and 166 ITS sequences were newly generated and the sequences were deposited in the European Nucleotide Archive (ENA) using the annonex2embl submission pipeline (Gruenstaudl, 2020) and can be retrieved from ENA under study number PRJEB53579 (https://www.ebi.ac.uk/ena/submit/webin/study/PRJEB53579)

Phylogenetic tree inferences were conducted with Bayesian inference (BI) on the ITS and ETS nuclear markers with MrBayes v.3.2.6 (Ronquist and Huelsenbeck, 2003) using four parallel Markov chain Monte Carlo (MCMC) runs for a total of 50 million generations. The nucleotide substitution model GTR + G + I was selected by default as it is the most parameter-rich model. The convergence of the Markov chains was checked with Tracer v.1.7 (Rambaut et al., 2018); the initial 25% of all trees were discarded as burn-in, and the remaining trees were used to summarize the 50% majority consensus tree. The phylogenetic trees are shown in supplementary material (Appendix 3.2 and 3.3)

3.2.5 Ancestral character-state reconstruction

We used the Bayesian trees obtained from the complete plastome sequences with indels coded and alignments manually corrected as provided Escobari et al. (2021) as hypothesis of the phylogenetic relationships in the Gynoxyoids. The reconstruction of character states at ancestral nodes was performed with a Bayesian approach using BayesTraits version 2.0 (Pagel and Meade, 2006), which uses a selection of post-burn-in trees obtained from the t.files of the Bayesian analysis. This random selection of 800 of the total of 1600 post-burn-in trees taken from Escobari et al. (2021) was obtained through Mesquite version 3.7 (Maddison and Maddison, 2021). The file stating the relevant nodes of the tree to be addressed by the analyses of BayesTraits was generated with TreeGraph v2.14beta (Stoever and Mueller, 2010). The inference of the ancestral character state reconstruction was performed using the reverse jump MCMC approach with 5,050,000 iterations, with a burn-in of 50000, a sample frequency of 1000 and, following the recommendation by Pagel and Meade (2006), a hyper-prior where the mean of the exponential is drawn from a uniform 0–100 distribution. TreeGraph v2.14beta (Stöver and Müller, 2010) was used to plot the results from the BayesTraits output log file with the function Import BayesTraits data on the Bayesian major consensus tree. We excluded the other genera of the Tussilagineae that were present the plastid phylogenomic investigation, considering that the outgroup sampling in their data set is incomplete with respect to the morphological diversity.

3.2.6 Taxonomic revision of the members of the Gynoxyoid clade

Based on the revised taxonomic backbone, all species were assigned to a genus or to an informal infrageneric taxon of *Gynoxys*. The supraspecific taxonomic entities were described and keyed out. Always the protologues were directly consulted for the typification of names. Type specimens of all names with the exception of only few unavailable ones (marked in the checklist) were examined from high resolution digital images provided by JSTOR Global

Plants, GBIF and the herbarium catalogues of individual herbaria. The digital images of types specimens were hyperlinked in the checklist to the type citation. Where necessary, new combinations were made, and species names were lectotypified. As a general principle a morpho-species concept was applied. Type specimens and additional specimens (see Appendix 3.1) were examined to assess the qualitative differences and possible infraspecific variation with the aim to hypothesize a name as accepted or as a synonym. Insights from the densely sampled ITS/ETS trees for the circumscription of species and synonymization of names were taken into account where possible. The citation of authors follows the recommended international standards by Brummitt and Powell (1992); the citation of publications follows BPH (Lawrence et al., 1968) and TL-2 (Stafleu and Cowan, 1976-1986 and supplements 1992-2009), the latter was also consulted for actual publication dates. Accepted names were provided with full synonymies and type citations.

3.3 Results

3.3.1 Morphological characters of taxonomic relevance on supra-specific level

The evaluation of morphological characters with respect to discontinuities at supra-specific level resulted in an initial specimen-based matrix of 48 characters and 65 species. The condensed list of characters evaluated in our comparative morphological investigation as taxonomically relevant on supra-specific level finally comprised eleven characters. These characters and their states are defined in Table 3.1 and, where appropriate, illustrated in Figure 3.1.

3.3.2 Phylogenetic inferences on plastid genomes and nuclear ribosomal markers.

Escobari et al. (2021) proposed the first phylogenetic hypothesis of the Gynoxyoids based on plastid genomes. In this study we additionally infer trees of nuclear ribosomal regions (ETS, ITS) (Appendix 3.2). In contrast to the tree based on the plastid genome, the Bayesian ETS and ITS trees are poorly resolved. In both trees, the members of the *Gynoxys* clade form a single polytomy. The moderately supported sister group relationship between the two *Paragynoxys* members is the only clear congruence between the two nuclear ribosomal trees and is, moreover, in conformity with the plastid genome tree. The phylogenetic inference on plastid genome strongly retrieved the three members of the genus *Nordenstamia* non-monophyletic just as in both nuclear ribosomal trees. Likewise, the plastid genome tree recovered the two *Paracalia* species in separated clades with high support. This was also observed in the ITS tree but with moderate support. In contrast to the plastid genome tree and the ITS tree, the ETS tree resolved *Paracalia* as a moderately supported clade (Appendix 3.2). The phylogenetic inference on the markers ITS, ETS and the concatenated matrix of ITS and ETS tree with additional species retrieved a tree with strongly supported crown nodes and low supported stem nodes. The clustering of closely geographic-distributed species in monophyletic groups is noteworthy in all ribosomic trees. This means that species with a narrower distribution are more likely to form a clade (i.e., *Nordenstamia repanda*), contrary to this, species with a wider range of distribution tend to spread throughout the trees (i.e., *Gynoxys hallii*) (Appendix 3.3).

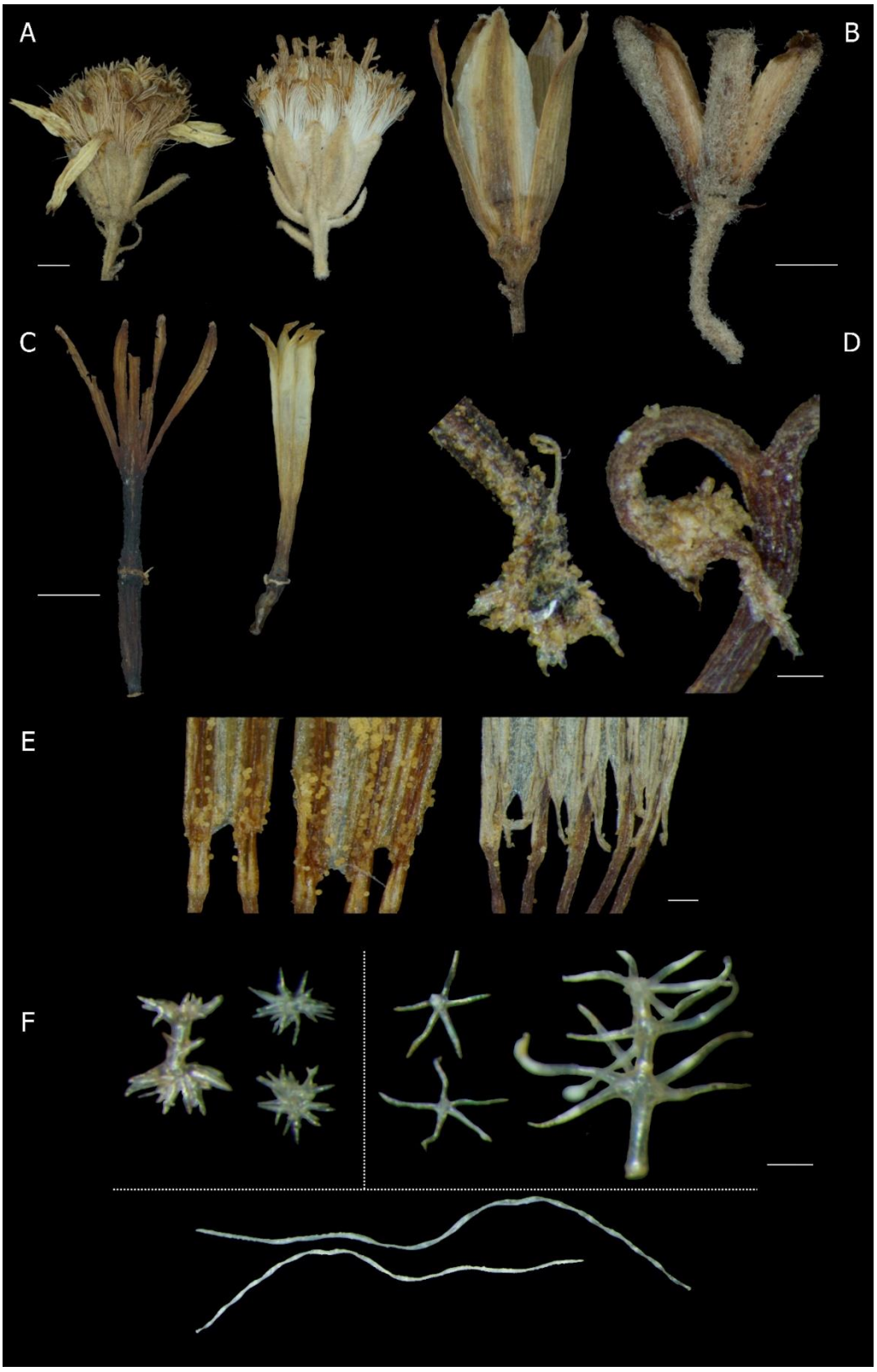

Figure 3.1: Some morphological characters and character states for the Gynoxyoid clade. A) Capitula: radiate (*G. calyculisolvens* left), discoid (*G. longifolia* right); B) Involucral outer phyllaries: absent (*Paracalia pentamera* left), present (*Paragynoxys martingrantii* right); C) Depth of corolla opening (1:2 mm): deeply lobated (*Paragynoxys venezuelae* left), shortly lobated (*G. asterotricha* right); D) Style branches apex shape: rounded (*G. ignaciana* left), acute (*G. baccharoides* right); E) Anther-base shape: obtuse (*Paracalia jungioides* left), sagittate (*G. ignaciana* right); F) Trichomes architecture: multicellular hairs (*A. jamesonii* up left, *N. kingii* up right), unicellular hairs (*G. violacea* down) . – Scale bars a-c = 2 mm, d = 200 µm, e = 500 µm, f-g = 100 µm.

Table 3.1: Morphological characters selected for the ancestral character reconstruction analysis with their respective character abbreviation (Abbr.), and character states with a respective abbreviation and definition when needed.

Character	Abbr.	Character states
Plant habit	H	tree (T), shrub (S), scandent (C)
Phyllotaxis	P	alternate (A), opposite (O)
Trichome architecture	T	absent (G), unicellular hairs (S), multicellular hairs (M) Unicellular hairs: unicellular simple hair. Multicellular hairs: branched or unbranched hairs. Differences between multicellular hairs were avoided since several types of these can be present in a same specimen (Figure. 3.1F).
Corolla colour	CF	white (W), yellow (Y) This character states describe both ray and disc florets since it is always shared by both flowers.
Outer phyllaries	OP	absent (A), present (P) As outer phyllaries were considered all phyllaries attached at the base of the involucrum and not at the peduncle of the capitula
Number of inner phyllaries	InP	≤5 (F), 6-8 (M) The following categories are based on the stability of a defined number of phyllaries for the genera
Number of ray flowers	RF	0 (D), >0 (R) The states implicitly define the architecture of the capitulum. The absence of ray flowers (0=A) represents a discoid capitula (Figure. 3.1A). A number >0 represents a radiate capitula
Number of disc flowers	DF	≤8 (F), >8 (M) The following categories are based on the stability of a defined number for the genera
Ratio lobe/tube length	Rat	≤0.6 (S), >0.6 (D) This character describes the opening depth of the corolla. Length of lobes in relation to the length of the corolla tube (shortly vs deeply lobated corolla) (Figure 3.1C).
Anther-base shape	AB	sagittate (S), obtuse (O) The base of the anthers is defined as obtuse when no appendage can be distinguished (Figure 3.1E). We ignored the difference between acute (small appendages) vs sagittate (large appendages) since both can be present in a same specimen and this may be unstable depending on the state of the specimen
Style branches apex shape	SA	acute (A), rounded (R) The style branches apex is described as acute when the branch tips have a notorious pointed tissue termination (Fig. 3.1D). We use rounded in a wider sense also including an apex described as truncate, the presence of papillose hairs makes the distinction unreliable

3.3.3 Character evolution in the Gynoxyoids

Employing the eleven characters of Table 3.1, a species-based matrix was created for the 17 members of the Gynoxyoid clade represented in the phylogenetic tree by Escobari et al. (2021) (Table 3.2) and used for ancestral character reconstruction. Two character-states for *G. ignaciana* (colour of flowers) and *G. violaceae* (rate lobes/tube) were coded as missing because they were not accessible in the material at hand. The accession *Gynoxys* sp. in Escobari et al. (2021), was identified as *G. calyculisolvens* during this study. The ancestral character reconstruction for the eleven characters in the Gynoxyoid clade are presented in Figures. 3.2, 3.3 and 3.4.

Table 3.2: Evaluation of the characters-states for all species within the Gynoxyoid clade in the phylogeny inferred by Escobari et al. (2021). Character and character states codes same as Table 3.1, (-) missing data.

Species	H	P	T	CF	OP	InP	RF	DF	Rat	AB	SA
Aequatorium jamesonii	S	O	M	W	P	M	R	F	S	O	R
Gynoxys asterotricha	S	O	S	Y	P	M	R	M	S	S	A
Gynoxys baccharoides	S	O	S	Y	P	M	R	M	S	S	A
Gynoxys ignaciana	S	O	S	-	P	M	R	M	S	S	R
Gynoxys longifolia	S	O	S	Y	P	M	D	M	S	S	R
Gynoxys mandonii	T	O	S	Y	P	M	R	M	S	S	A
Gynoxys megacephala	S	O	M	Y	P	M	D	M	S	S	A
Gynoxys calyculisolvens	S	O	S	Y	P	M	R	M	S	S	A
Gynoxys tomentosissima	S	O	S	Y	P	M	R	M	S	S	A
Gynoxys violacea	S	O	S	Y	P	M	R	M	-	S	R
Nordenstamia cajamarcensis	T	O	M	Y	P	M	R	F	S	O	R
Nordenstamia kingii	S	A	M	Y	P	M	R	M	S	S	A
Nordenstamia repanda	T	A	M	Y	P	M	R	F	S	S	A
Paracalia jungioides	C	A	S	W	A	F	D	F	D	O	R
Paracalia pentamera	C	A	G	W	A	F	D	F	D	O	A
Paragynoxys martingrantii	T	A	M	W	P	F	D	F	D	O	R
Paragynoxys venezuelae	T	A	M	W	P	F	D	F	D	O	R

Habit: the shrubby habit was reconstructed as plesiomorphic for the Gynoxyoids. Two independent shifts from shrubby to scandent habit occurred at the two *Paracalia* species. A shift from shrub to tree habit took place at the stem node of *Paragynoxys* and within the *Gynoxys* clade.

Phyllotaxis: opposite phyllotaxis was revealed as the ancestral state for the Gynoxyoids. Shifts to alternate phyllotaxis occurred at *Paracalia pentamera*, the stem node of *Paragynoxys*, in two (out of three) species of *Nordenstamia* and at *Paracalia jungioides.*

Trichome architecture: unicellular trichomes were reconstructed as the ancestral character state for all Gynoxyoids. *Paracalia pentamera* seems to have experienced a loss of this character turning this species to be glabrous. A shift to multicellular hairs took place in the MCRA of *Aequatorium* and *Paragynoxys*, and in species within the *Gynoxys* clade

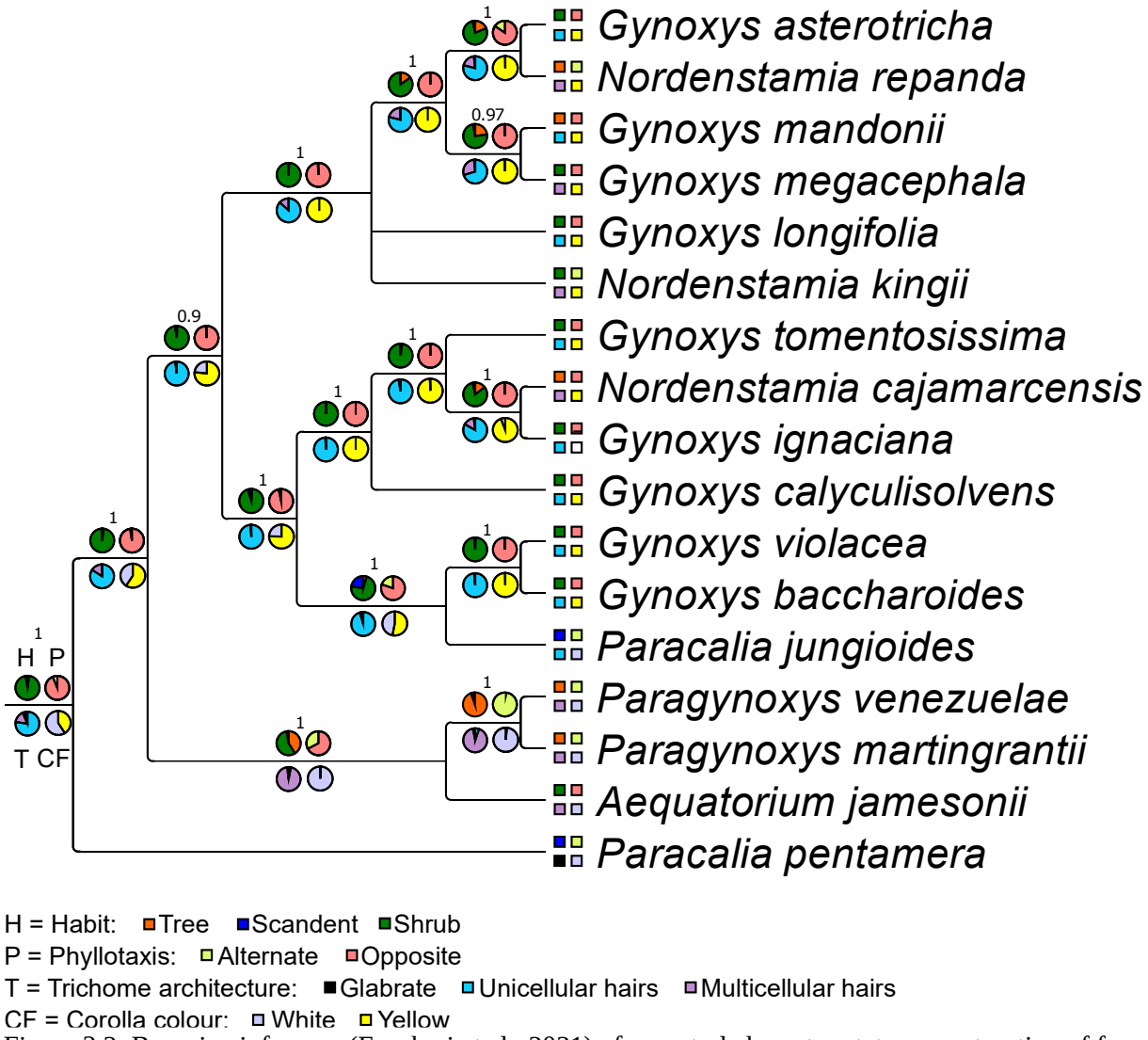

H = Habit: Tree Scandent Shrub
P = Phyllotaxis: Alternate Opposite
T = Trichome architecture: Glabrate Unicellular hairs Multicellular hairs
CF = Corolla colour: White Yellow

Figure 3.2: Bayesian inference (Escobari et al., 2021) of ancestral character-state reconstruction of four morphological characters of the Gynoxyoid clade in the consensus tree of the Bayesian analysis. Each pie chart represents a single character, and each colour represents a character-state which are described in the legend. The actual state of the characters is represented by boxes next to the species names. The pie charts at the stem of the tree show the character abbreviation as mentioned in Table 3.1. Missing data is represented as (-)

Colour of flowers: white flowers were recovered as plesiomorphic for the Gynoxyoid clade and retained by the first diverging clades (i.e., *Aequatorium*, *Paragynoxys* and *Paracalia pentamera*). Yellow flowers were retrieved as apomorphic at the stem node of *Gynoxys* and *Nordenstamia.* A reversal to white flowers is indicated for *Paracalia jungioides*.

Number of outer phyllaries: the presence of outer phyllaries was retrieved as the ancestral character state of the Gynoxyoid clade. Two independent losses seemed to have taken place in both species of *Paracalia.*

Number of inner phyllaries: a higher number of inner phyllaries was reconstructed as the ancestral state for the Gynoxyoids. A decrease of the number is suggested in both *Paracalia* and *Paragynoxys* species.

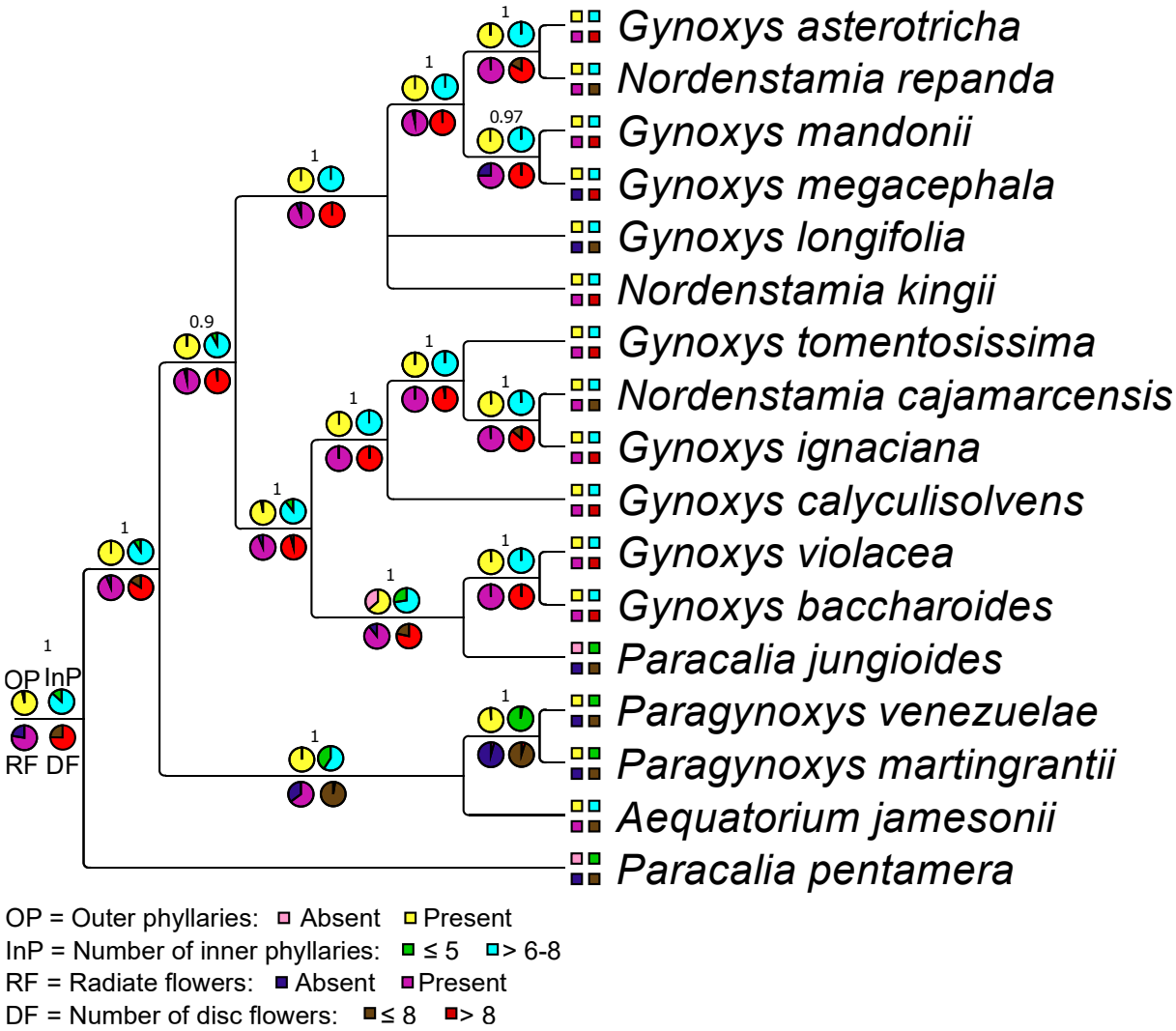

Figure 3.3: Bayesian inference of ancestral character-state reconstruction of four morphological characters of the Gynoxyoid clade in the consensus tree of the Bayesian analysis. Each pie chart represents a single character, and each colour represents a character-state which are described in the legend. The actual state of the characters is represented by boxes next to the species names. The pie charts at the stem of the tree show the character abbreviation as mentioned in Table 3.1.

Number of ray flowers: radiate capitula (presence of ray flowers) were recovered as ancestral for the Gynoxyoids. Shifts to discoid capitula (absence of ray flowers) occurred in all species of *Paracalia* and *Paragynoxys*. Further losses of the ray flowers are indicated to have taken place in certain *Gynoxys* species.

Number of disc flowers: a high number of disc flowers was retrieved as the ancestral state for the Gynoxyoid clade. Our analysis suggests a reduction of disc flower numbers at the stem node of *Aequatorium* and *Paragynoxys*, and several further depletions in all species of *Paracalia* and partially within the *Gynoxys* clade.

Ratio length of lobes/length of corolla tube: a short-lobed disc corolla was revealed as plesiomorphic for the Gynoxys group. An increment of the corolla tube opening (thus an elongation of the corolla lobes) occurred exclusively in *Paracalia* and *Paragynoxys* species. The presence of this state in *Paracalia jungioides* is exceptional within the *Gynoxys* clade.

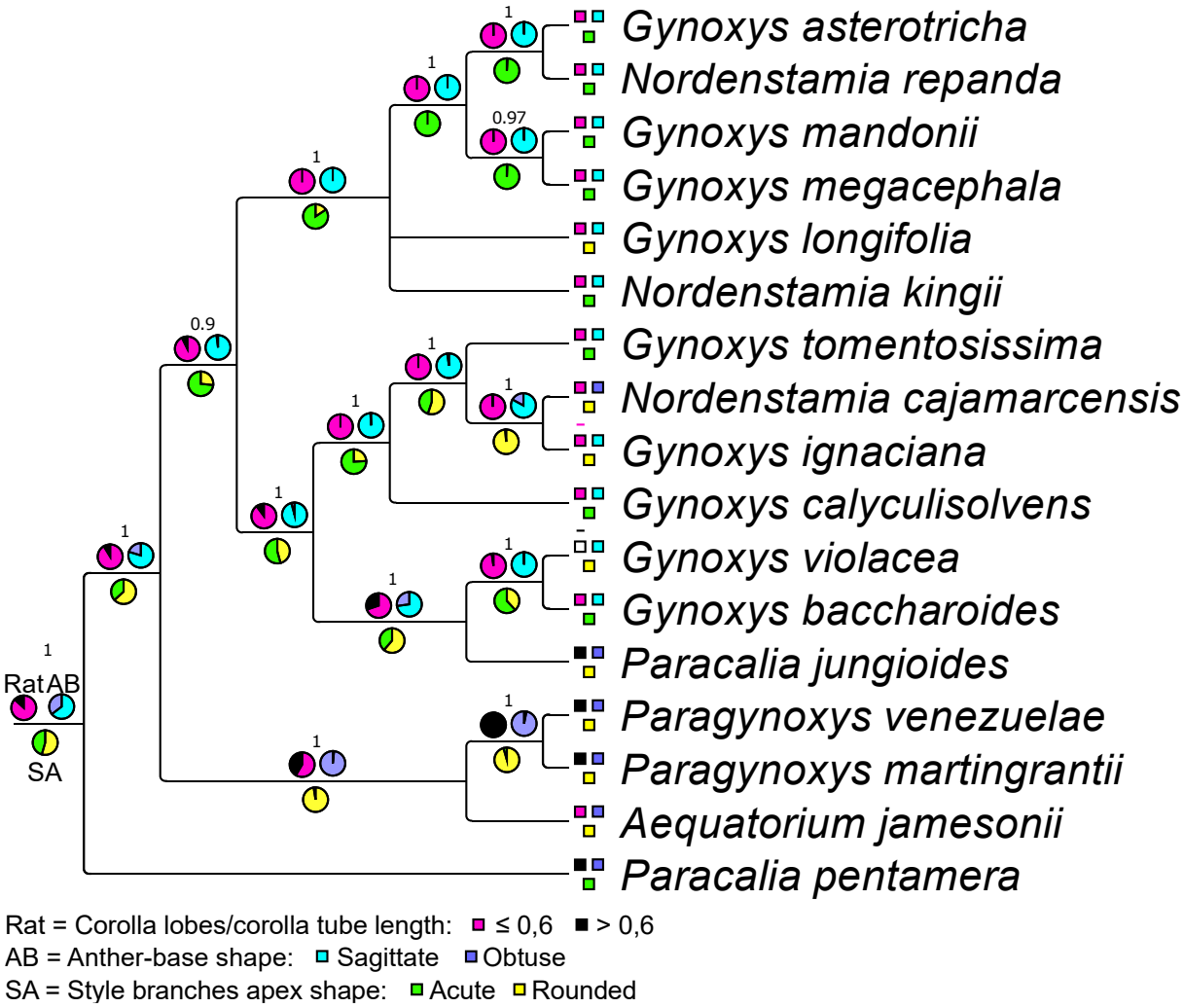

Figure 3.4: Bayesian inference of ancestral character-state reconstruction of four morphological characters of the Gynoxyoid clade in the consensus tree of the Bayesian analysis. Each pie chart represents a single character, and each colour represents a character-state which are described in the legend. The actual state of the characters is represented by boxes next to the species names. The pie charts at the stem of the tree show the character abbreviation as mentioned in Table 3.1. Missing data is represented as (-)

Anther base shape: the sagittate anther base was recovered at stem node of the Gynoxyoid clade. Several independent shifts to obtuse anther bases took place in *Paracalia*, *Aequatorium*, *Paragynoxys* and in one species of *Nordenstamia.*

Shape of style branches apex: the rounded style branch apex was retrieved as plesiomorphic for the Gynoxyoids and was retained in *Aequatorium* and *Paragynoxys* but a shift to an acute apex occurred in the earliest diverging species *Paracalia pentamera*. Several further shifts and frequent reversals occurred in *Gynoxys*, *Nordenstamia* and *Paracalia jungioides*.

A summary of the BayesTraits analysis of all state shifts for each character in Figure 2,3 and 4 is given in Figure 5. The ancestral states for the clade are given at the stem of the tree inference with all shifts represented as white (homoplasies) or black (synapomorphies) boxes and

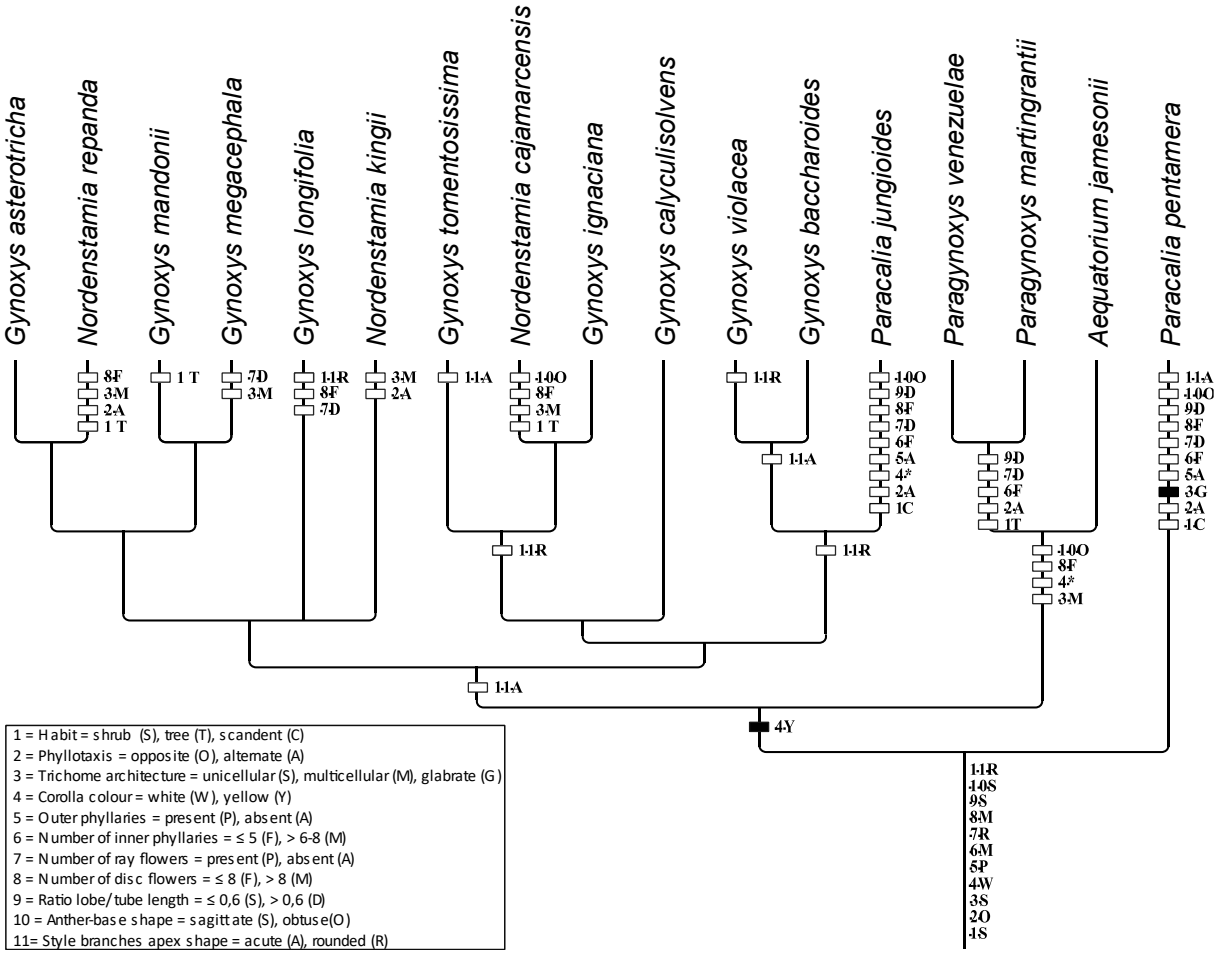

Figure 3.5: Summary tree based on the results of the BayesTraits analysis (Figure. 3.2, 3.3, 3.4) of states shifts in morphological character. Unique shifts (syn)apomorphies are represented with black boxes and characters with multiple states shift (homoplasies) are shown with white boxes. Reversal are indicated by *

reversals as asterisks (*). Characters are represented by numbers and states with the codes given in Table 3.1. A great number of shifts are accumulated in both species of *Paracalia* which are retrieved as non-monophyletic. The clade represented by both *Paragynoxys* species shared all derived characters with *Aequatorium jamesonii* in addition to five derived characters that characterize the clade. A single character (corolla colour) was retrieved as synapomorphic for the clade containing *Aequatorium*, *Gynoxys*, *Paragynoxys*, *Nordenstamia* and *Paracalia jungioides*. This character shows several reversals at the MCRA of *Aequatorium* and *Paragynoxys* and of both species of *Paracalia*. The analysis retrieved most of the morphological characters as highly homoplastic with the style branches being the most variable character throughout the tree in many nodes.

3.3.4 Morphological characterization of the members of the *Gynoxys* clade

We tested the continuity of a set of characters in all species belonging to the Gynoxyoid clade. This morphological examination resulted in the characterization of the genera on diagnostic characters.

All species of *Aequatorium* share the combination of multicellular trichomes, radiate capitula, white flowers, low number of disc flowers (<8) and obtuse shape of the anther base. Diagnostic for this genus is the unique combination of white flowers and radiate capitula.

Species of *Paracalia* and *Paragynoxys* share deep-lobed corolla, white flowers and discoid capitula and differentiates them from the other Gynoxyoid genera. *Paracalia* can be distinguished from *Paragynoxys* by a scandent habit, absence of outer phyllaries and a central Andean distribution. In contrast, *Paragynoxys* has a woody habit, an involucrum with outer phyllaries, and a north-Andean distribution.

The genus *Nordenstamia* is not only revealed as polyphyletic in the phylogenetic reconstruction but also cannot be delimited morphologically. The presence of stellate hairs by which this genus was distinguished from *Gynoxys* is highly variable not only among the *Nordenstamia* species but also shared with many *Gynoxys* species. Merging *Nordenstamia* into *Gynoxys* seems therefore appropriate.

Gynoxys resulted to be the morphologically most diverse taxon within the Gynoxyoid clade. The great number of species (158) hinders the finding of characters states that support the circumscription of this genus. If *Nordenstamia* is included in *Gynoxys*, this genus can be differentiated from all others by the presence of yellow flowers. For pragmatic reasons, we suggest a subdivision of Gynoxys into fours informal morphological groups based on a set of characters, namely phyllotaxis, number of ray flowers, and type of trichomes.

3.3.5 Checklist of the *Gynoxys* clade

The checklist comprises a total of 209 names and 188 of accepted morpho-species. 11 names were newly synonymized, two were lectotypified, eight were newly combined.

3.4 Discussion

3.4.1 Morphology and putative cytonuclear discordance.

In the present study we were able to compare, for the members of the Gynoxyoid clade, tree reconstructions based on the plastid genome, and on the ITS and ETS nuclear ribosomal markers. Genetic variation was extremely low in the plastid genomes (Escobari et al., 2021) as well as in the nuclear ribosomal markers. The nuclear ribosomal trees are, in contrast to the plastid genome tree, even poorly resolved. This indicates that the Gynoxyoids are one of the young, fast evolving groups. The low resolution of the nuclear ribosomal trees allows only very limited conclusion from the comparison of the different gene trees. One is the unequivocal support for the sister group relationship of the two *Paragynoxys* members. A second is the missing support for the monophyly of the three *Nordenstamia* members in all three trees. The most significant result is, however, the gene tree incongruence concerning the two *Paracalia* species. Although the incongruence received only moderate statistical support it is consider significant in the context of our analyses. The plastid tree placed *Paracalia jungioides* within *Gynoxys* and far distant from the second species of *Paracalia* (i.e., *P. pentamera*). This finding

is surprising because *Paracalia jungioides* is morphologically entirely unrelated to *Gynoxys*. *P. jungioides* is scandent (instead of tree or shrub), has white (instead of yellow) flowers, and an involucrum without outer phyllaries (instead of present). Moreover, *P. jungioides* and *P. pentamera* are morphologically very similar, and the plastome phylogeny would suggest that these species have accumulated a high number of independent parallel state shifts (i.e., scandent habit, alternate leaves, absent outer phyllaries, few inner phyllaries, discoid capitula, few number of disc flowers, deep-lobated corolla, obtuse anther base) (Figure 3.5). In contrast, the two species of *Paracalia* are supported as monophyletic in the ETS tree in conformity with morphology, although not in the ITS tree (Appendix 3.1). The strong morphological signals given, we assume that the incongruence between the ETS and plastome tree with respect to the position of the two *Paracalia* species, is best explained by a chloroplast capture event, in which *P. jungioides* has captured after introgression with a *Gynoxys* species, the plastome of a member of the latter genus. Similar incongruent topologies of ITS and ETS trees, (with moderate support in ML and BI) were found for the rapidly radiating Andean *Diplostephium* by Vargas et al. (2012).

Nuclear-cytoplasmic incongruences have been reported in several studies within the Asteraceae family at higher and specific levels (Pelser et al., 2010; Wang et al., 2013; Kilian et al., 2017; Esklual 2017; Lee-Yaw et al., 2018; Lichter-Marck et al., 2020; Stull et al., 2020; Pascual-Díaz et al., 2021; Senderowicz et al., 2021; Yin et al., 2021; Kandziora et al., 2022). It has been shown by Stull et al. (2020) for the asterids that conflicts between nuclear and plastome trees are a relevant issue even at higher evolutionary scales. Phylogenetic inferences on nuclear data recovered different placements for several asterid lineages compared to topologies on plastid data (One Thousand Plant Transcriptomes Initiative 2019). This is of some significance when we consider that current backbones of angiosperm phylogeny are largely based on plastid phylogenies (APG IV 2016). Among the principal reasons for these incongruences, horizontal gene flow among linages, introgression, hybridization, and incomplete linage sorting were suggested (Rieseberg and Soltis, 1991; Maddison, 1997; Vargas et al., 2017). The inclusion of different markers of different origins in a phylogenetic analysis has the capacity to elucidate signals of such events. Pelser et al. (2010) analyzed potential causes for tree incongruences in the tribe Senecioneae comparing two nuclear (ITS/ETS) and six plastid markers. They conclude that hybridization is a much more likely explanation than ILS, long-branch attraction, or sampling error. Lee-Yaw et al. (2018) focused their study on organelle discordances by sequencing whole plastomes and over 1000 nuclear single-nucleotide polymorphisms in *Helianthus* L. The authors showed that incongruences in this genus can be expected at species level and within individuals of the same species. Specifically, the authors analyzed the levels of sequence divergence when changing the species position in chloroplast trees compared to simulated sequences. The low levels of sequences divergences suggested introgression as the best explanation for patterns in tree incongruencies.

Gene tree discordance is expected to be more likely in rapid radiating lineages that can be found in young biodiversity hotspots, such as the Andean region (Madriñán et al., 2013; Kandziora et al., 2022). The fast succession and accumulation of descendant species are prone to inter-breeding before reproductive barriers develop, increasing the probability of incomplete linage sorting (ILS) (Vargas et al., 2017). In addition, young radiating groups have shown whole genome duplication and hybridization events in the tropical high-altitude areas of South America (*Lachemilla*: Morales-Briones et al., 2018; *Lupinus*: Nevado et al., 2018; *Diplostephium*: Vargas et al., 2017; Espeletiinae: Cortés et al., 2018). Hybridization may be a

result of sexual selection, ecological adaptation, pollinator changes (Moreira-Munoz, 2020; Kandziora et al., 2022) or due to the dynamic in this ecosystem with multiple topography changes during the Pleistocene (Flantua et al., 2019) which facilitated the contact between geographically isolated species before exhibiting strong barriers to gene flow (Vargas et al., 2017; Kandziora et al., 2022). Vargas et al. (2017) revealed complex patterns of reticulate evolution at generic and species level of *Diplostephium.* Specifically, the authors recovered four different tree topologies from complete nuclear ribosomal cistron, complete chloroplast genome, a partial mitochondrial genome, and nuclear-ddRAD. The results reported strong signals of ancient hybridization and introgression. Rieseberg and Soltis (1991) suggest that horizontal gene transfer causes tree incongruences since hybridization events could replace strange chloroplast or mitochondrial DNA of a linage. Pouchon et al. (2018) reconstructed a fully resolved phylogeny of Espeletiinae, using whole plastid genomes and ca. 1 million nuclear nucleotides and additionally analyzed the possible impact of incomplete lineage sorting and hybridization on phylogenetic discordances. Their analysis on gene flow between species suggested that hybridization may have played an important role during speciation within species and inter-clade species. This hypothesis is supported by the fact that the phylogenetic analysis retrieved morphological groups as non-monophyletic. Moreover, they suggest that plastids were exchanged between geographically close situated taxa regardless of their morphologic or nuclear phylogenetic distance. Kandziora et al. (2022) studied the discordances in the recent and rapidly radiating Andean *Loricaria* and developed a workflow on how to tackle phylogenetic discordance in recent radiations. The authors reconstructed phylogenetic analysis on plastomes and hundreds of nuclear loci to test ILS and hybridization in this group. Their results suggest that gene tree incongruences are both due to ILS and numerous reticulation events followed by backcrossing, but the presence of paralogous loci also indicated possible multiple whole genome duplication events in this group. Moreover, the results indicate chloroplast capture in a species represented by two specimens of which their position was incongruent in the phylogenies. Chloroplast capture occurs when two species hybridize and go through extensive backcrossing to one of the ancestors (Rieseberg and Soltis, 1991). The hybridization event followed by extensive backcrossing swamp out the nuclear signal, but the captured plastid remains (Kandziora et al., 2022).

In absence of any well-resolved alternative, we have based our analysis of the evolution of morphological characters in the Gynoxyoids on the phylogenetic hypothesis provided by the plastid genome tree. With the striking odd exception of the *Paracalia* case, the plastid genome tree provided a useful guidance for the generic classification of the Gynoxyoid clade and a plausible scenario for the character evolution. Accepting chloroplast capture as a plausible cause for the odd *Paracalia* results and employing the alternative phylogenetic hypothesis of the ETS tree for the taxonomy of the two *Paracalia* members, provides a much more parsimonious scenario for the character evolution within the clade, and a classification in line with morphology.

3.4.2 Evolution and significance of morphological characters in the *Gynoxys* clade

Previous generic classifications of the Gynoxyoid group were based on morphological similarities and discontinuities between species assemblages. In this study we tested such classification hypotheses by optimizing character states on the full plastome phylogeny.

Morphological differentiation among the Gynoxyoids is essentially shallow, as has been confirmed by our analysis, and restricted to comparatively few and often rather subtle characters. Thus, it well corresponds with the shallow genetic differentiation found by Escobari et al. (2021). Repeating and often independent character state shifts moreover caused morphological homoplasies. After a comprehensive morphological revision of all species of the Gynoxyoid, we discuss the morphological characterization of the accepted genera in this study and the importance of morphological characters for these delimitations compared to traditional taxonomic studies.

The genus *Paragynoxys* is the only genus strongly supported by both molecular and morphological data. As already Cuatrecasas (1955) suggested, the length of the lobes relative to the length of the corolla tube, white corollas, and discoid capitula are diagnostic for the genus. Nevertheless, all these states are shared with *Paracalia* (Cuatrecasas, 1960), but the latter can, in addition, be characterized by a scandent habit (instead of tree-like) and absence of outer phyllaries. Additionally, we distinguished *Paragynoxys* as being present in the northern Andean (Colombia and Venezuela) whereas *Paracalia* is restricted to central Andean distribution (Peru and Bolivia).

Aequatorium was represented by one single species in the phylogenetic analysis which preclude any conclusion on phylogenetic relationships of this genus. Nordenstam (1978) compared *Aequatorium* to *Paracalia* and *Nordenstamia* but distinguished it by shrubby habit, shape and consistency of leaves, rusty tomentum of stellate hairs, and radiate capitula, white ray flowers, obtuse or truncate style-branches tips. Lundin (2006) distinguished *Nordenstamia* from *Aequatorium* but did not evaluate the morphological discontinuities between *Nordenstamia* and *Gynoxys*. Based on our morphological revision of its species we conclude that the combination of radiate capitula and white ray flowers and a restricted distribution in the northern Andean (Colombia and Venezuela) are diagnostic for that genus. The rusty tomentum of stellate hairs stated by Nordenstam (1978) may be diagnostic in addition, but with the limited access to material, no conclusion could be reached in this study.

The genus *Gynoxys* was retrieved as non-monophyletic in the plastome and nrITS phylogeny with respect to the representatives of *Nordenstamia*. Comparing, in addition, the species of both genera morphologically, it became clear that the attempt by Lundin (2006) to distinguish *Nordenstamia* from *Gynoxys* by (usually) alternate leaves, yellow capitula, pointed style-branch apex, sub-stellate trichomes and a southern Andean distribution, does not work. Consequently, we broadened the concept of *Gynoxys* including species with opposite or alternate leaves, with single or multicellular trichomes, radiate or discoid capitula and yellow flowers.

3.4.3 Morphological and genetic incongruences in species delimitation in the Gynoxyoids

Incongruences on morphological and molecular data in closely related species within Asteraceae has been previously documented. Pouchon et al. (2018) performed phylogenetic inferences on 41 plastid genomes of the *Espeletia* complex and found a morpho-phylogenetic discordance as none of the genera within the complex was retrieved as monophyletic. Moreover, their results reject monophyly hypothesis on diagnostic characters for these genera. Additionally, the analysis found a significant influence of spatial distribution on the clustering

of species. Cho et al. (2020) sequenced seven plastid genomes of the morphologically high-variable *Dendroseris.* Although the seven sequences displayed 99.8% similarity, the phylogenetic analysis retrieved a well-supported tree contradicting the circumscriptions of previously suggested genera. The Gynoxyoid is a further example of short molecular distances on plastid and ribosomal markers among species. The lack of molecular variability hampers the reconstruction of well-supported clades on this type of data, nevertheless the great morphological variation enables the definition of morpho-species in many cases. On the other hand, the phylogenetic reconstruction, although with moderate support, can give evidence to support the assignment of morphologically similar individuals to same entities (hypothesized species).

3.5 Conclusion

3.5.1 Taxonomic conclusions

Gynoxyoid clade

158 species

Argentina, Bolivia, Colombia, Ecuador, Peru, Venezuela

Trees, shrubs or scandents. Indumentum tomentose of unicellular (simple) or multicellular trichomes (simple, stellate, T-shaped, multibranched), with age becoming rusty or greyish white in petioles, abaxial side of the leaves, and involucres. Leaves alternate, opposite or subopposite, petiolate or subsessil; margin angulate, dentate, denticulate, entire, sinuate or repand, callous-tipped teeth present or absent; base acute, cordate, cuneate, obtuse, oblique, rotund, or truncated; apex acute, acuminate, attenuate, mucronate, obtuse, or rotund; coriaceous or papyraceous; leaves indumentum on abaxial leaf surfaces rusty-brownish or greyish white with age. Inflorescence terminal, subterminal or axillar, thyrsoidiform, paniculiform or corymbiform, peduncles bracteolate. Capitula heterogamous or homogamous, numerous, Receptacle flat to convex. Involucre campanular or tubular; outer phyllaries 0-8; inner phyllaries 5-10 (-13), uni- or biseriate. Ray florets 0-8 (-13), female; tube cylindrical, glabrous; ligule white, cream-coloured, or yellow, almost equalling the tube in length, 3-4-veined, 3 toothed at the apex, with a papillate upper surface. Style bifid, fertile. Disc-florets 5-32 (-36), hermaphrodite; corolla campanulate or funnel-shaped, white, pale greenish-yellow or yellow, shortly, or largely lobated; lobes ovate, triangular, or oblong, straight, recurved to the outside or helically twisted. Anthers exserted; apical appendage oblong-ovate or obtuse; base obtuse, auriculate or sagittate; filament collar narrowly cylindrical, uniform, or thicker than the filament with polar endothecial thickenings (Jeffrey, 1992). Style-base gradually dilated, placed on a nectary; style branches straight or contorted, apically obtuse, truncate, or acute, with papilliform sweeping-hairs. Achenes homomorphic, oblong, glabrate, ribbed. Pappus bristles pluriseriate, persistent, coarse, shortly barbellate, off-white or somewhat brownish-fulvous. n = ca. 40 (Watanabe, 2002)

Key to the genera of the Gynoxyoid clade

1a White flowers……..2

2a Radiate capitula, peltate-stellate hairs……*Aequatorium*

2b Discoid capitula glabrate, single or stellate hairs…….……...3

3a Trees. Outer phyllaries present, stellate hairs. Colombia and Venezuela....*Paragynoxys*

3b Scandent shrublets. Outer phyllaries absent, absent or simple hairs. Bolivia and Peru……...…….……*Paracalia*

1b Yellow flowers……*Gynoxys*

Revised classification of the species of the Gynoxyoid clade

1. *Aequatorium* B. Nord in Opera Bot. 44: 59. 1978 (Figure 3.1f)

Type: *Aequatorium asterotrichum* B. Nord.

12 species

Colombia, Ecuador

Erect shrubs or trees, sometimes with sub scandent branches. Indumentum tomentose of subsessile stellate trichomes (with 1-3-tiered, irregularly star shaped, subtended by a narrow pluricellular uniseriate stalk), with age glabrescent but with persistent greyish white tomentum in petioles, abaxial side of leaves, and sometimes involucres. Leaves alternate or sub-opposite or rarely opposite, petiolate, rounded-elliptic to lanceolate; margin entire, sinuate-dentate or denticulate, with small callous-tipped teeth; base acute, cuneate to rounded-truncate, sub cordate or oblique; apex acute or rotund; coriaceous; leaves indumentum rusty-brownish in the adaxial site with two layers of peltate-stellate hairs, internal layer with sessile hairs and outer layer with subsessile hairs in patches, becoming grey-tomentose with age. Inflorescence terminal rarely subterminal, (thyrsoid-) paniculiform or corymbiform. Capitula heterogamous. Receptacle flat or slightly convex. Involucre campanular; outer phyllaries usually <6; inner phyllaries 5-10, biseriate. Ray florets usually <5 (-8); ligule white or cream-coloured. Disc-florets 5-10; corolla campanulate or funnel-shaped, white, or pale greenish yellow, shortly lobated, ratio lobes/tube < 0.8; lobes narrowly ovate, triangular, or oblong, recurved to the outside or straight. Anthers base sagittate-auriculate; filament collar narrowly cylindrical, uniform, not thicker than the filament. Style branches half contorted, apically obtuse or truncate. Distribution: Colombia, Ecuador

Notes: We exclude *Aequatorium venezuelanum* from this genus based on the presence of yellow flowers and its distribution and transfer it to *Gynoxys*

Aequatorium albiflorum (Wedd.) Cuatrec. & S. Díaz, Revista Acad. Colomb. Ci. Exact. 17(67): 665. 1990 ≡ *Gynoxys albiflora* Wedd., Chlor. Andina 1(3): 78. 1856["1855"]. – Syntypes: Colombia. Mariquita, sur la lisière du volcan de Tolima, 3900 m, Jan 1843, *J. Linden 907* (F: V0076792F V0076793F (photo & fragments), K: K000497659, NY 178788, P: P00711390 P00711391 P02273078).

Aequatorium asterotrichum B. Nord., Opera Bot. 44: 59. 1978. – Holotype: Ecuador. Pichincha, lago Papallacta, thicket, 3300 m, 31 Oct 1955, *E. Asplund 18263* (S: S-R-8297; isotypes: K: K000497658, LD 1821970, MO: MO-3237504, NY not traced, P: P00971087, R not traced, S: S18-7665, UPS not traced, US not traced).

Aequatorium caucanum S. Díaz & Cuatrec., Revista Acab. Colomb. Ci. Exact. 73: 248. 1994. – Holotype: Colombia. Cauca, Macizo Central Colombiano, Páramo de las Papas, El Boquerón, 3200-3510 m, 7-27 Sep 1958, *J. Idrobo et al., 3221* (COL: COL000004758).

= *Aequatorium caucanum* var. *abbreviatum* S. Díaz & Cuatrec., Revista Acab. Colomb. Ci. Exact. 73: 248, f. 2. 1994. – Holotype: Colombia. Cauca, Volcán Puracé, alrededores de la Laguna San Rafael, 3340 m, 6 Jan 1972, *A. M. Cleef & A. Fernandez 526* (COL: COL000004759).

Aequatorium jamesonii (S. F. Blake) C. Jeffrey, Kew Bull. 47(1): 61. 1992 ≡ *Gynoxys jamesonii* S. F. Blake, Acad. Sci. 18: 34. 1928. – Holotype: Ecuador. Pichincha, west side of Mount Pichincha, 3050 m, 2 Aug 1926, *Jameson 227* (K: K000497657; isotype: US 00122911 (fragments & photo)).

= *Senecio simulans* Benoist, Bull. Soc. Bot. France 83: 808. 1937 [non *Senecio simulans* Chiov. 1935] ≡ *Gynoxys simulans* Cuatrec., Brittonia 8: 158. 1955. –Syntype: Ecuador. Pichincha, 12 Jul 1931, *Benoist 4572* (P: P02273075).

Aequatorium latibracteolatum S. Díaz & Cuatrec., Revista Acad. Colomb. Ci. Exact. 17(67): 661, 663, f. 1. 1990. – Holotype: Colombia. Cauca, Municipio de Puracé, Parque Nacional Natural del Puracé, cercanías de la Laguna San Rafael, 3300 m, 6 Oct 1984, *C. G. Lozano 4667* (COL: COL000004762; isotypes: COL: COL000004760 COL000004761).

Aequatorium lepidotum B. Nord., Asteraceae Newslett. 31: 6, f. 3. 6B. 1997. – Holotype: Ecuador. Carchi, El Mirador, 15 km S of San Francisco, 00°37'N, 77°31'W, 3300 m, 2 Aug 1990, *W. Palacios & D. Rubio 5286* (MO: MO-037535; isotype: US 01919680).

Aequatorium polygonoides B. Nord., Opera Bot. 44: 63. 1978 ≡ *Senecio polygonoides* Cuatrec., Notas a la Flora de Colombia 6: 20, f. 14. 1944 [non *Senecio polygonoides* Muschl. 1911]. – Holotype: Colombia. Caldas, Cordillera Central, vertiente occidental, vertiente SE del Nevado del Ruiz, Termales, 3400 m, 4 May 1940, *J. Cuatrecasas 9243* (COL not traced)

Aequatorium palealbum S. Díaz & A. Correa, Revista Acad. Colomb. Ci. Exact. 26(100): 345–346, f. 3. 2002. – Holotype: Colombia. Nariño, Ospina, páramo de Paja Blanca, alrededores de la bocatoma del acueducto, 77°34'W, 1°58'N, 3200 m, 2 Dic 1995, *B. Ramirez-P. et al., 8904* (PSO: PSO0000058; isotype: MO: s.n.).

Aequatorium repandiforme B. Nord., Asteraceae Newslett. 31: 9, f. 4. 1997. – Holotype: Ecuador. Pichincha, over high pass en route to Quito, 92 km E of Quevedo, 3400 m, 19 Sept 1959, *B. Maguire & C. Maguire 44246* (NY 3468431; isotypes: K: K000497656, US 01919679).

Aequatorium sinuatifolium S. Díaz & A. Correa, Revista Acad. Colomb. Ci. Exact. 19(73): 251–252, f. 3. 1994. – Holotype: Colombia. Quindío, Mun. de Salento, arriba de Guayaquil, 3680 m, 10 Jan 1994, *W. G. Vargas 1335* (COL: COL000004764; isotype: COL: COL000004763).

Aequatorium tatamanum S. Díaz & A. Correa, Revista Acad. Colomb. Ci. Exact. 23(88): 332, f. 1. 1999. – Holotype: Colombia. Risaralda, Municipio de Santua Río, Macizo de Tatamá, 200 m arriba del campamento El Reposo, 3700 m, 8 Feb 1983, *J. H. Torres et al., 1720* (COL: COL000004765).

Note: this species is probably a synonym of *A. albiflora*

Aequatorium verrucosum (Wedd.) S. Díaz & Cuatrec., Revista Acad. Colomb. Ci. Exact. 17(67): 659–666. 1990. ≡ *Gynoxys verrucosa* Wedd., Chlor. Andina 1(3): 77. 1856["1855"] [*non Gynoxys verrucosa* V. M. Badillo 1946]. – Lectotype (Diaz & Cuatrecasas, 1990: 663): Colombia. Nueva Granada, Mariquita, Cordillere de Quindiu, a Los Volcancitos, 3200 m, Jan 1843, *Linden 1050* (P: P02273077; isolectotype: F: V0076796F V0076797F V0076798F, K: K000497655).

= *Senecio verrucosus* Klatt, Abh. Naturf. Ges. Halle 15(2): 332. 1881[1882]. –Syntypes: *Triana s.n.* (P not traced; photo: F not traced)

2. *Paracalia* Cuatr. in Brittonia 12: 183. 1960 (Figure 3.1b, e)

Type: *Paracalia pentamera* (Cuatrec.) Cuatrec.

2 species

Bolivia, Peru

Scandent shrublets. Indumentum glabrate to glabrescent of simple hairs, with age glabrate. Leaves alternate, petiolate, ovate; margin entire or angulate, with or without small callous-tipped teeth; base rotund or cordate; apex acuminate or mucronate; coriaceous; leaves indumentum absent or pilose glabrescent in the adaxial site, disappearing with age. Inflorescence terminal or axillar, paniculiform or corymbiform. Capitula homogamous. Receptacle flat. Involucre tubular; outer phyllaries absent; inner phyllaries 5, uniseriated. Ray florets absent. Disc-florets 5; corolla campanulate, white or pale greenish, deeply lobated, ratio lobes/tube ≈ 1; lobes linear, helically twisted. Anthers base auriculate or obtuse; filament collar cylindrical, thicker than the filament. Style branches half contorted, apically obtuse or subtruncate. Distribution: Peru, Bolivia.

Note: although the phylogenetic inferences suggest this genus to be not monophyletic, we kept the circumscription of *Paracalia* including two species. We substantiate this decision based on shared morphological characters such as deeply lobated and white-flowered corolla, and the central Andean distribution beginning from lowlands (800 m). *Paracalia jungioides* which is nested in the *Gynoxys* clade strikingly differs morphologically from the true *Gynoxys* species and its inclusion in this genus would break the continuity of the morphological characters and altitudinal distribution in this group. A possible explanation for the contradiction between morphological/ecological and molecular data may be chloroplast capture and needs to be further

studied and better understood before further nomenclatural decision are made. In this context, we think the best practice is to keep the circumscription of *Paracalia* and avoid suggesting further possibly wrong hypotheses of relationships of these species.

Paracalia jungioides (Hook. & Arn.) Cuatrec., Brittonia 12: 183. 1960 ≡ *Pentanthus jungioides* Hook. & Arn. Companion Bot. Mag. 1: 33. 1835. – Holotype: Perú. Purruchuca, Jun 1833, *Matthews 1016* (K: K000497546; isotypes: E: E00414051 E00414052, K: K000497547).

= *Cacalia mikaniifolia* DC. Prodr. 6: 328. 1837 ≡ *Senecio mikaniifolius* (DC.) Sch. Bip. Flora 28: 498. 1845. – Syntypes: Peru. San Buenaventura, *Nee & Thibaud s.n.* (not traced in G-DC, F: s.n. (photo)).

Paracalia pentamera (Cuatrec.) Cuatrec., Brittonia 12: 183. 1960 ≡ *Senecio pentamerus* Cuatrec. Fieldiana, Bot. 27: 57. 1951. – Holotype: Bolivia. La Paz, Larecaja, Copacabana (ca. 10 km. south of Mapiri), 850-950 m, 08 Oct – 15 Nov 1939, *B. A. Krukoff 11150* (NY 259336; isotypes: A: A00010877, F: V0077069F, K: K000497545, S: S-R-7986, U 0105750, US 00123446).

3. *Paragynoxys* (Cuatrec.) Cuatrec. in Brittonia 8: 153. 1955. (Figure 3.1b, c)

≡ *Senecio* sect. *Paragynoxys* Cuatr. Fieldiana Bot. 27(2): 72. 1951.

Type: *Paragynoxys neodrendoides* (Cuatrec.) Cuatrec.

13 species

Colombia, Venezuela

Erect shrubs or trees. Indumentum tomentose of (always?) stellate T-shaped trichomes, persistent in all age states becoming greyish white in petioles, abaxial side of leaves, and involucres. Leaves alternate or rarely opposite, petiolate, oblong-elliptic, obovate-elliptic, or ovate; margin entire or repand, with or without small callous-tipped teeth; base cordate, obtuse, or rarely cuneate; apex obtuse, attenuate or rarely acute; coriaceous; leaves indumentum shaggy rusty-brownish in the adaxial site, persistent with age. Inflorescence terminal rarely subterminal, (thyrsoid-) paniculiform or corymbiform. Capitula homogamous. Receptacle flat. Involucre campanular; outer phyllaries <6; inner phyllaries 5 or 8, uniseriate. Ray florets absent. Disc-florets 5-11; corolla campanulate, white, deeply lobated, ratio lobes/tube => 1; lobes linear, helically twisted. Anthers base auricular or obtuse; filament collar cylindrical, thicker than the filament. Style branches fully contorted (forming a complete loop or even two), apically obtuse to subacute. Distribution: Colombia, Venezuela

Note: We support the view of Correa 2003 who transferred *Paragynoxys regis* back to *Gynoxys* (as it was originally described) based on the radiate capitula of yellow flowers and its distribution.

Paragynoxys angosturae (Cuatrec.) Cuatrec., Brittonia 8: 154. 1955 ≡ *Senecio angosturae* Cuatrec., Feddes Repert. Spec. Nov. Regni Veg. 55: 132. 1953. – Holotype: Colombia. Antioquia, Angostura, just outside town, 2000 m, 11 Mar 1944, *F. R. Fosberg 21603* (US 00123252; isotypes: US 00123253 00123254).

Paragynoxys corei (Cuatrec.) Cuatrec., Brittonia 8: 154. 1955 ≡ *Senecio corei* Cuatrec., Feddes Repert. Spec. Nov. Regni Veg. 55: 136. 1953. – Holotype: Colombia. Antioquia, Alto El Oso, n. of Yarumal, 2320 m, 4 Mar 1944, *E. L. Core 624* (F: V0051295F; isotype: US 00123277).

Paragynoxys cuatrecasasii Ruiz-Teran & López-Fig., Revista Fac. Farm. Univ. Andes 14: 14, f. 3, 4. 1974. – Holotype: Venezuela. Merida, Rangel, norte de la población Las Piedras, Cuenca del río Aracay, afluente del Santo Domingo, 2550-2700 m, 16 Dic 1972, *Ruiz-Terán et al., 8258* (MERF not traced; isotype: US not traced).

Paragynoxys magnifolia Cuatrec., Brittonia 8(2): 154. 1955. – Holotype: Venezuela. Merida, Culata, 7000 ft., May 1847, *N. Funck & Schlimm 1522* (P: P00711443 + P00711444; isotypes: G: G00301285, P: P00711445 P00711446, US 00811048, VEN: VEN118056 (fragments of holotype)).

Paragynoxys martingrantii (Cuatrec.) Cuatrec., Brittonia 8: 156. 1955 ≡ *Senecio martingrantii* Cuatrec., Feddes Repert. Spec. Nov. Regni Veg. 55: 139. 1953. – Holotype: Colombia. Magdalena, Sierra de Perijá, Casacará Valley 23 km. East of Codazzi, 2 km from the Venezuelan border, 2450, 15 Feb 1945, *M. L. Grant 10949* (F: V0051336F + V0051337F; isotypes: COL: COL000005419, HUA: HUA0000364, NY 259292 259293, US 00123324 00123323, VEN: VEN209193, WIS: WISv0256984WIS WISv0256985WIS).

Paragynoxys meridana (Cuatrec.) Cuatrec., Brittonia 8(2): 156. 1955 ≡ *Senecio steyermarkii* Cuatrec., Fieldiana, Bot. 27: 32–33. Jun 1950 [non *Senecio steyermarkii* Greenm. Apr 1950] ≡ *Senecio meridanus* Cuatrec., Fieldiana Bot. 27(2):38. 1951 ≡ *Gynoxys verrucosa* V. M. Badillo, Bol. Soc. Venez. Ci. Nat. 10: 312. 1946 [*non Gynoxys verrucosa* Wedd. 1855]. – Syntypes: Venezuela. Merida, Paramo de Pozo Negro between San José and Beguilla, 2590-3220 m, 3 May 1944, *A. Steyermark 56268* (NY 259418, US 00123361).

Paragynoxys neodrendoides (Cuatrec.) Cuatrec., Brittonia 8(2): 156, f. 13, 14. 1955 ≡ *Senecio neodendroides* Cuatrec., Notas Fl. Colombia 6: 19, f. 13. 14. 1944. – Holotype: Colombia. Santander, Cordillera Oriental, Páramo de la Rusia, vertiente noroeste, 3300-3500 m, 4 Ago 1940, *J. Cuatrecasas 10435* (COL not traced; isotypes: F: V0051343F V0051344F V0051345F, P: P01816686).

Paragynoxys pileolanata S. Díaz, Caldasia 12(59): 379–381, f. 1. 1979. – Holotype: Colombia. Santander, Municipio de Onzaga, vereda Chaguaz, finca de Oliverio Mesa, en robledal, 2820 m, 29 Mar 1976, *J. H. Torres et al., 500* (COL: COL000005310).

Paragynoxys santurbanensis (Cuatrec.) Cuatrec., Brittonia 8(2): 156. 1955 ≡ *Senecio santurbanensis* Cuatrec., Feddes Repert. Spec. Nov. Regni Veg. 55: 145. 1953. – Holotype: Colombia. Santander, Páramo de Santurbán, vert. W, 3100 m, 27 Jul 1940, *J. Cuatrecasas & H. García Barriga 10326* (F: V0051361F + V0051362F; isotype: P: P01816508).

Paragynoxys steyermarkii Cuatrec., Phytologia 40(1): 34. 1978. – Holotype: Venezuela. Táchira, Between Las Copas de Alto de Fila de Tierra Negra at the ridge dividing headwaters of rivers Quinimarí, Riofrio, Uribante and Talco (Oirá), 2870-2880 m, 16 Jan 1968, *J. A. Steyermark & E. Dunsterville 101014* (US 00115958; isotypes: MA 638740, US 00115959, VEN: VEN74042).

Paragynoxys undatifolia Cuatrec., Proc. Biol. Soc. Washington 74: 15. 1961. – Holotype: Colombia. Magdalena, Sierra Nevada de Santa Marta. Southeastern slope: Hoya del Río

Donachuí, below Sabanita Diricune, 3200 m, 29 Sep 1959, *J. Cuatrecasas & R. Romero-Castañeda 24485* (US 00115961 + 00115962 + 00115963 + 00115964 + 00115965; isotypes: COL: COL000005311 COL000005312 COL000005313 COL000005314, P: P00711449 P00711450, US 00115960 00930968).

Paragynoxys uribei Cuatrec., Phytologia 40(1): 33. 1978. – Holotype: Colombia. Boyaca, Arcabuco, 4 km. NE of town, 08 Jun 1966, *L. U. Uribe 5633* (US 00115966 + 00115967; isotypes: COL: COL000005315 COL000005316).

Paragynoxys venezuelae (V. M. Badillo) Cuatrec., Brittonia 8(2): 156. 1955 ≡ *Cacalia venezuelae* V.M. Badillo. Bol. Soc. Venez. Ci. Nat. 10: 319. 1947 ≡ *Senecio venezuelae* (V.M. Badillo) Cuatrec. Fieldiana, Bot. 27(1): 31. 1950. – Holotype: Venezuela. Merida, Below páramo above San Isidro Alto, 1820 m, 14 May 1944, *J. Steyermark 56560* (VEN: VEN32772; isotypes: F: V0049135F, NY 162855).

4. ***Gynoxys*** Cass. in Cuvier, Dict. Sci. Nat., ed. 2 48: 455. 1827. (Figure 3.1a, c, d, e, f)

Lectotype (Flann et al., 2010:1225): *Gynoxys baccharoides* (Kunth) Cass.

= *Nordenstamia* Lundin Compositae Newslett. 44: 15–16, f. 1. 2006. Type: *Nordenstamia repanda* (Wedd.) Lundin [≡ *Gynoxys repanda* Wedd.]

131 species

Argentina, Bolivia, Colombia, Ecuador, Peru, Venezuela

Erect shrubs or trees. Indumentum glabrate, glabrescent, or tomentose of simple or multicellular simple trichomes, with age glabrescent but with persistent greyish white tomentum in all abaxial side of leaves and involucres. Leaves alternate or opposite, petiolate or subsessile, elliptic, lanceolate, ovate, obovate; margin entire, repand, sinuate, sparsely angular, or denticulate, with small callous-tipped teeth; base acute, attenuate, cordate, cuneate, obtuse, rotund, truncate, or oblique; apex acute, acuminate, obtuse or mucronate; coriaceous or papyraceous; leaves indumentum absent, white or rusty-brownish in the adaxial site, persistent with age. Inflorescence terminal or axillar, paniculiform or corymbiform. Capitula homogamous (Sec 1) or heterogamous. Receptacle flat or convex. Involucre campanular; outer phyllaries 1-8; inner phyllaries usually 5-8(-13), biseriate. Ray florets usually <8 (-10-13); ligule yellow. Disc-florets usually 5-32 (-36); corolla tubular, campanulate or funnel-shaped, yellow, usually shortly lobated, ratio lobes/tube usually <0.5; lobes triangular, oblong, or narrowly ovate, recurved to the outside or straight. Anthers base sagittate, auriculate or rarely obtuse; filament collar narrowly cylindrical, usually thicker than the filament. Style branches straight or half contorted, apically obtuse, truncate, or acute.

Note: *Gynoxys alternifolia* and *G. mandonii* are the only two species described as scandent. In our opinion none of these have this type of habit. In our collection trips we had the chance to trace several specimens of *G. mandonii* as big trees with thick branches. On the other hand, the type specimen of *G. alternifolia* shows thick and erect branches which is atypical for scandent species.

1a Discoid capitula …… *Gynoxys*, discoid group

1b Radiate capitula ……...2

2a Stellate hairs……..*Gynoxys, Praegynoxys* group

2b Simple hairs…….*Gynoxys, Gynoxys s.str.* group

Gynoxys discoid group

Gynoxys campii Cuatrec., Brittonia 8(1): 39. 1954. – Holotype: Ecuador. Cañar, Near El Tambo (ca. 69 km. by railroad south of Sibambe), 9500-10000 ft., 5 Jul 1945, *W. H. Camp E-3970* (F: V0076704F; isotypes: G: G00223899, GH: GH00008575, K: K000497540, NY 178793, P: P00711407, US 00122893, VEN: VEN34418).

Gynoxys dielsiana Domke, Biblioth. Bot. 116: 169. 1937. – Syntype: Ecuador. Chimborazo, Tipococha, untere Rand des Paramo, ca. 3230 m, 20 Aug 1933, *L. Diels 675* (B, destroyed).

Gynoxys hutchisonii H. Rob. & Cuatrec., Novon 2(4): 414. 1992. – Holotype: Perú. Piura, above Huancabamba, road to Piura, 3000 m, 10 Oct 1957, *P. C. Hutchison 1609* (US 00409556; isotype: F: V0076714F).

Gynoxys induta Cuatrec., Fieldiana, Bot. 27: 9. 1950. – Syntypes: Colombia. Valle, Cordillera Central, Hoya del río Bugalagrande, Barragán, Páramo de Bavaya, corrales, 3550-3400 m, 9 Apr 1946, *J. Cuatrecasas 20546* (COL: COL000005215 COL000005216, F: V0076715F V0076716F V0076717F, P: P00711414, US 00122909, WIS: WIS00001047MAD).

Gynoxys leiotheca S. F. Blake, J. Wash. Acad. Sci. 18: 35. 1928. – Holotype: Ecuador. Borma, Sep 1904, *Rivet 671* (P: P00711416; isotypes: US 00122915 (photo & fragments)).

Gynoxys littlei Cuatrec., Revista Acad. Colomb. Ci. Exact. 9: 242. 1954. – Holotype: Colombia. Huila, on foot of Cordillera Oriental, 20 km. SE of gigant, 103000 ft., 15 Sep 1944, *E. L. Little 8658* (F: V0076752F; isotypes: COL: COL000005220, US 00650427).

Note: this species is described as having “pale flowers” in the protologue, nonetheless the label of the type specimen describes the flowers as “pale yellow”.

Gynoxys longifolia Wedd., Chlor. Andina 1(3): 79. 1855. – Syntypes: Perú. Cuzco, Andes de Cuzco, Oct 1839 – Feb 1940, *Gay s.n.* (F: V0076718F, P: P00711417 P00711418 P00711419, US 00122917 (fragments)).

Gynoxys lopezii M. O. Dillon & Sagást., Brittonia 40(2): 223, f. 2. 1988 ≡ *Paragynoxys lopezii* (M.O. Dillon & Sagást.) Cuatrec., Phytologia 69(5): 314. 1990 ≡ *Paracalia lopezii* (M.O. Dillon & Sagást.) A. Correa, Brittonia 55(2): 167. 2003. – Holotype: Perú. La Libertad, Patáz, Yaupa (Llaupa), entre Chagual-Retanas, carretera a Tayabamba, en borde carretera, pedregoso, 2300 m, 24 Jan 1974, *A. López & A. Sagástegui 8160* (HUT not traced; isotypes: F: V0076719F, MO: MO-176388 s.n.).

Note: the nomenclatural definition of this specie was discussed by Cuatrecasas (1990) and Correa (2003). The floral structure resembles the genus *Paracalia*, nevertheless as we mentioned before (see note for the genus *Paracalia*) we agree with Correa (2003) in transferring

this species back to *Gynoxys* based on the presence of yellow flowers and its central Andean distribution.

Gynoxys megacephala Rusby, Bull. New York Bot. Gard. 4: 398. 1907. – Syntypes: Bolivia. *M. Bang 1959* (F: V0076754F (fragments), GH: GH00008597, K: K000497526, MICH: MICH1107432, MO: MO-1183133, NY 178867 178868, PH: PH00013514, US 00122920, WIS: WISv0256704WIS). Bolivia. Huaycani, 11000 ft., May 1866, *Pearce s.n.* (MO: s.n.).

= *Gynoxys foliosa* (Rusby) S. F. Blake, Contr. U.S. Natl. Herb. 24: 86. 1922 ≡ *Diplostephium foliosum* Rusby, Bull. New York Bot. Gard. 8(28): 128–129. 1912. – Syntypes: Bolivia. Cargadira, 8000 ft., 29 Jul 1902, *W. Roberts 1529* (BM: BM001024073, F: V0076745F, K: K000497534, NY 168221).

Gynoxys moritziana Sch. Bip. ex Wedd., Chlor. Andina 1: 79. 1855. – Syntypes: Venezuela. Merida, Sierra Nevada, 1844, *Moritz 1385* (GH: GH00008598 GH00008599 (drawing & fragment), K: K000497525, P: P00711421 P00711422 P00711423, US 00122924 (fragments)).

Gynoxys pendula Sch. Bip. ex Wedd., Chlor. Andina 1(3): 78. 1855. – Syntypes: Colombia. Nouvelle-Grenade, Mariquita, Boqueron, Tolima, Jan 1843, *J. J. Linden 954* (F: V0076760F V0076761F, GH: GH00008601, K: K000497523, NY 178870, P: P00711425 P00711426, US 00122929 (fragments)).

= *Gynoxys pendula* var. *sinuata* Cuatrec. Trab. Mus. Nac. Ci. Nat., Ser. Bot. 29: 38. 1935 – Syntypes: Colombia. Tolima, Andes, Cordillera Central, vert. merid. monte Tolima, loc. dict. Las Mesetas, 3600 m, 13 May 1932, *J. Cuatrecasas 2851* (MA: MA240997 MA240997-2 (fragments))

Gynoxys regis H. Rob. & Cuatrec., Phytologia 56: 370(–371), f. 1984 ≡ *Paragynoxys regis* (H. Rob. & Cuatrec.) H. Rob. & Cuatrec., Novon 2(4): 415. 1992. – Holotype: Ecuador. Azuday, 30 km S of cumbé on the road to Saraguro at an elevation of 9800 ft. 26 Jan 1979. *R. M. King & F. Almeda 7804* (US 00122934; isotypes: K: K000497542, QCA: QCA17841).

Gynoxys soukupii Cuatrec., Bull. Soc. Bot. France 101: 245. 1954. – Holotype: Perú. Amazonas, Chachapoyas, cerro Puma Urco, Jun 1952, *Soukup 4072* (F: V0076774F; isotype: US 00122939).

Gynoxys subhirsuta Cuatrec., Notas Fl. Colombia 6: 35. 1944. – Holotype: Colombia. Santander, Cordillera Oriental, Páramo de Tamá, alrededores ed la Cueva, 3000-3200 m, 28 Oct 1941, *J. Cuatrecasas et al., 12714* (COL: COL000005229; isotypes: BC: BC634998, F: V0076778F, GH: GH00008611, U: U0001284, US 00122942).

Gynoxys, Praegynoxys group

Gynoxys azuayensis Cuatrec., Brittonia 8(1): 39. 1954. – Holotype: Ecuador. Azuay, Eastern Cordillera, 4-6 km N of Sevilla de Oro, 9000-10000 ft., 16 Aug 1945, *Camp E-4724B* (F: V0076733F; isotypes: GH: GH00008572, K: K000497543, NY 178791, P: P00711396, US 00122890).

Gynoxys cajamarcense (H. Rob. & Cuatrec.) Escobari & N. Kilian, comb. nov. ≡ *Aequatorium cajamarcense* H. Rob. & Cuatrec., Novon 2(4): 411. 1992 ≡ *Nordenstamia cajamarcensis* (H. Rob. & Cuatrec.) B. Nord., Asteraceae Newslett. 44: 20. 2006. – Holotype: Perú. Cajamarca, Cutervo, Dist. San Andrés de Cutervo, Parque Nacional de Cutervo, caserío „Pajonal“ camino

hacia Jaén, 2600 m, 10 Aug 1987, *Díaz & Osores 2585* (US 00409567; isotypes: F: V0043642F, MO: MO-2940604).

Gynoxys carpishensis Cuatrec., Brittonia 12: 185. 1960 ≡ *Aequatorium carpishense* (Cuatrec.) H. Rob. & Cuatrec., Novon 2(4): 412. 1992 ≡ *Nordenstamia carpishensis* (Cuatrec.) B. Nord., Asteraceae Newslett. 44: 20. 2006. – Holotype: Perú. Carpish, between Huánuco and Tingo María, 2800 m, 10 Jul 1957, *H. Ellenberg 2211* (U: U.1610531; isotypes: GOET010400 GOET010401).

Gynoxys chingualensis H. Rob. & Cuatrec., Novon 2(4): 414. 1992. – Holotype: Ecuador. Sucumbíos, Paramo mirador SW of Playón de San Francisco, S del Río Chingual headwaters, 3400-3600 m, 15 May 1990, *P. King & Judziewicz 10131* (US 00409557; isotypes: F: V0076702F, K: K000497538, MO not traced, S: S-R-2685).

Gynoxys congestiflora Sagást. & M. O. Dillon, Brittonia 37(1): 8, f. 3. 1985. – Holotype: Perú. Huánuco, ca. 46 Km NNE of Huánuco on road to Tingo María, Carpish Pass, E slope, 14 Jul 1981, *M. Dillon 2608* (F: V0043633F; isotypes: HUT, MO: MO-2940531, NY 178795, TEX00374263, US 00122897, USM: USM000112).

Gynoxys cuatrecasasii B. Herrera, Bol. Soc. Perúana Bot. 8(1–2): 40, f. 30. 1980. – Holotype: Perú. Amazonas, Chachapoyas, Cerros Calla Calla, east side, 19 km. above Leimebamba on road to Balsas, 3100 m, 4 Jun 1964, *P. C. Hutchison & J. Kenneth Wright 5519* (USM: USM000114; isotypes: US 00122898, F: V0076740F, NY 804137).

Gynoxys fabrisii Cabrera, Bol. Soc. Argent. Bot. 15(4): 332, f. 6. 1974. ≡ *Aequatorium fabrisii* (Cabrera) C. Jeffrey, Kew Bulletin 47(1): 61. 1992 ≡ *Nordenstamia fabrisii* (Cabrera) B. Nord., Asteraceae Newslett. 44: 20. 2006. – Holotype: Argentina. Jujuy, Valle Grande, Serranía de Calilegua, senda Alto Calilegua, 2500 m, 18 Feb 1964, *H. A. Fabris et al., 5338* (LP: LP000275).

Note: Jeffrey (1992) and Nordenstam (2006) cite incorrectly a paratype as holotype and isotype.

Gynoxys jaramilloi H. Rob. & Cuatrec., Novon 2(4): 415. 1992. – Holotype: Ecuador. Loja, Loma del Oro, 2800-3200 m, 4 Aug 1986, *Z. Jaramillo & Valencia 8799* (US 00409555; isotypes: MO: MO-1891634, QCA: QCA17836).

Gynoxys juninensis (H. Rob. & Cuatrec.) Escobari & N. Kilian, comb. nov. ≡ *Aequatorium juninensis* H. Rob. & Cuatrec., Novon 2(4): 412. 1992 ≡ *Nordenstamia juninensis* (H. Rob. & Cuatrec.) B. Nord., Asteraceae Newslett. 44: 20. 2006. – Holotype: Perú. Junin, Carpata, above Huacapistana, 2700-3200 m, 7 Jun 1929, *Killip & Smith 24434* (US 00409566).

Gynoxys kingii (H. Rob. & Cuatrec.) Escobari & N. Kilian, comb. nov. ≡ *Aequatorium kingii* H. Rob. & Cuatrec., Novon 2(4): 412. 1992 ≡ *Nordenstamia kingii* (H. Rob. & Cuatrec.) B. Nord., Asteraceae Newslett. 44: 20. 2006. – Holotype: Bolivia. Cochabamba, 15 km from Colomi, on the road to Tunari, 10600 ft., 7 Feb 1978, *King & Bishop 7680* (US 00409565).

Gynoxys limonensis (B. Nord.) Escobari & N. Kilian, comb. nov. ≡ *Aequatorium limonensis* B. Nord., Asteraceae Newslett. 31: 14, f. 7. 1997 ≡ *Nordenstamia limonensis* (B. Nord.) B. Nord., Asteraceae Newslett. 44: 21. 2006. – Holotype: Ecuador. Morona-Santiago, 49 km from Limón on road to Gualaceo, 2300 m, 16 Jul 1996, *Stahl & Knudsen 2882* (S: S18-7653; isotype: QCA: QCA148693) .

Gynoxys pascoensis (H. Beltrán & H. Rob.) Escobari & N. Kilian, comb. nov. ≡ *Aequatorium pascoensis* H. Beltrán & H. Rob., Asteraceae Newslett. 42: 5–7, f. 1. 2005 ≡ *Nordenstamia pascoensis* (H. Beltrán & H. Rob.) B. Nord., Asteraceae Newslett. 44: 22. 2006. – Holotype: Perú. Pasco, Oxapampa, trail to summit of Cordillera Yanachaga via Río San Daniel, 75°27'W, 10°23'S, 2600 m, 18 Jul 1984, *D. N. Smith & H. Botiger 7884* (USM not traced; isotypes: AMAZ not traced, MO: MO-037539, US 00810884).

Gynoxys repanda Wedd., Chlor. Andina 1(3): 77. 1855 ≡ *Aequatorium repandum* (Wedd.) C. Jeffrey, Kew Bull. 47(2): 292. 1992 ≡ *Nordenstamia repanda* (Wedd.) Lundin, Asteraceae Newslett. 44: 16. 2006. – Syntypes: Bolivia. La Paz, Larecaja, Vallée de Tipuani, 1851, *M. Weddell s.n.* (F: V0076768F (fragments), P: P02273082, US 00122936 (fragments))

Note: We consider the locality designation in the protologue "dans les taillis, sur le versant orientale du mont Illampù" to correspond to the (upper) Valle de Tipuani given on the label of the above specimen, because of its location east of Mt. Illampu. No specimen with the locality designation in the protologue could be found.

= *Schistocarpha triangularis* Rusby, Bull. New York Bot. Gard. 4: 392. 1907. – Syntypes: Bolivia. La Paz, Unduavi, Sep 1894, *M. Bang 2477* (F: V0076813F, GH: GH00549665, US 00122819 00955547). = *Gynoxys alternifolia* Sch. Bip. ex Rusby, Mem. Torrey Bot. Club 6(1): 67. 1896 – *Gynoxys alternifolia* Sch. Bip. Linnaea 34: 531. 1865, nom. nud. ≡ *Senecio alternifolius* (Sch. Bip. ex Rusby) Greenm., Ann. Missouri Bot. Gard. 10: 76. 1923. – Syntypes: Bolivia. La Paz, Vic. Mapiri, 8000 ft, Sep 1892, *Bang 1574* (A: A00008569, F: V0076725F, GH: GH00549664, K: K000634163, NDG: NDG62631, NY 114876 114877, PH: PH00013520, PUL: PUL00000344, US 00122884). Bolivia. La Paz, Larecaja, Viciniis Sorata, inter Laripata et tani, in nemoribus, 3000-3200 m, Apr 1858-May 1859, *Mandon 131* (BR: BR0000005318605, GH: GH00012072, K: K000497519, MPU: MPU016063, P: P02273079 P04099622 P00711394 P00711395).

Gynoxys rimachiana Cuatrec., Phytologia 52(3): 164. 1982 ≡ *Aequatorium rimachianum* (Cuatrec.) H. Rob. & Cuatrec., Novon 2(4): 413. 1992 ≡ *Nordenstamia rimachiana* (Cuatrec.) B. Nord., Asteraceae Newsletter 44: 22. 2006. – Holotype: Perú. Huanuco, Carretera de Tingo Maria - Huanuco, El Mirador, near Carpish, 2600-2700 m, 21 Mar 1980, *M. Rimachi 4908* (US 00324004; isotypes: F: V0043643F, US 00324003).

Gynoxys stellatopilosa (Greenm. & Cuatrec.) Escobari & N. Kilian, comb. nov. ≡ *Senecio stellatopilosus* Greenm. & Cuatrec., Collect. Bot. (Barcelona) 3: 264. 1953 ≡ Aequatorium *stellatopilosa* (Greenm. & Cuatrec.) C. Jeffrey, Kew Bull. 47(1): 62.1992 ≡ *Nordenstamia stellatopilosa* (Greenm. & Cuatrec.) B. Nord., Asteraceae Newslett. 44: 22. 2006. – Holotype: Perú. Villcabamba, hacienda on río Chinchao, 6000 ft., 17 Jul 1923, *F. Macbride 4966* (F: V0043600F).

Note: this species is probably a synonym of *G. rimachiana*

Gynoxys tovarii (H. Rob. & Cuatrec.) Escobari & N. Kilian, comb. nov. ≡ Aequatorium *tovarii* H. Rob. & Cuatrec., Novon 2(4): 413. 1992 ≡ *Nordenstamia tovarii* (H. Rob. & Cuatrec.) B. Nord. Asteraceae Newslett. 44: 22. 2006. – Holotype: Perú. Huancavelica, Tayacaja, arriba de Marcavalle, entre Huachocolpa y Tintay, 3300 m, 21 Apr 1964, *O. Tovar 4781* (US 00409564).

Gynoxys tuestae (Cuatrec.) Cuatrec., Brittonia 8: 158. 1955 ≡ *Senecio tuestae* Cuatrec., Fieldiana, Bot. 27: 46. 1951 ≡ *Aequatorium tuestae* (Cuatrec.) H. Rob. & Cuatrec., Novon 2:

413. 1992 ≡ *Nordenstamia tuestae* (Cuatrec.) B. Nord., Asteraceae Newslett. 44: 22. 2006. – Holotype: Perú. Huanuco, Pillao, 2700 m, 17 Feb 1946, *D. Tuesta Díaz & J. Woytkowski 34095* (F: V0043646F).

Note: this species is very likely a synonym of *G. repanda* and will be treated in a following work

Gynoxys valenzuelae (H. Beltrán & J. Calvo) Escobari & N. Kilian, comb. nov. ≡ *Nordenstamia valenzuelae* H. Beltrán & J. Calvo, Phytotaxa 474(3): 294, f. 1 & 2. 2020. – Holotype: Perú. Junín, Jauja, Monobamba, comunidad campesina Marancocha, zona de amortiguamiento del Bosque de Protección PuiPui, 11°18'39''S,75°11'01''W, 3470 m, 25 Oct 2014, L. Valenzuela et al., 28791 (USM: USM306000; isotypes: HOXA68690, MO: MO-2951169).

Gynoxys venezuelana (V. M. Badillo) Escobari & N. Kilian, comb. nov. ≡ *Aequatorium venezuelanum* V.M. Badillo, Ernstia, ser. 2 10(1): 16, f. 9. 2000. – Holotype: Venezuela. Edo, Trujillo. Mun. Carache, Parque Nacional Dinira, arriba de Mesa, debajo del Pico Cendé, 9°53'N, 70°07'W, 3000 m, 1 Apr 1999, *Duno & Riina 783* (MY not traced; isotype: VEN not traced)

Gynoxys s. l.

Gynoxys acostae Cuatrec., Feddes Repert. Spec. Nov. Regni Veg. 55: 129. 1953. – Holotype: Ecuador. Tunguragua, Alta de Pasa, 3500 m, 28 Oct 1944, *M. Acosta Solís 8738* (F: V0076722F).

Gynoxys albifluminis Cuatrec., Fieldiana, Bot. 27(2): 12. 1951. – Holotype: Perú. Lima, Río blanco, 15000 ft, 20 Mar 1923, *J. F. Macbride 3028* (F: V0076723F; isotype: US 00122883).

Gynoxys albivestita Cuatrec., Revista Acad. Colomb. Ci. Exact. 9: 242. 1954. – Holotype: Colombia. Boyacá, Nevada del Cocuy, Las Lagunillas, Pozo Azul, 4300 m, 12 Dic 1938, *J. Cuatrecasas 1434-A* (F: V0076724F; isotype: BC: BC624334).

Gynoxys apollinaris Cuatrec., Fieldiana, Bot. 27(2): 16. 1951. – Holotype: Colombia. Caldas, Salamina, Corregimiento San Félix, Jul 1943, *T. Alberto 1884* (F: V0076726F; isotype: MEDEL: MEDEL000097).

Gynoxys arnicae Cuatrec., Fieldiana, Bot. 27(1): 2–3. 1950. – Syntypes: Colombia. Departamento del Valle, Cordillera Occidental, Los Farallones, vertiente oriental, bajo el filo de la Cordillera en el cerro de La Torre: La Laguna, 3500-3550 m, 1 Aug 1946, *J. Cuatrecasas 21864* (COL: COL000005204 COL000005205 COL000005206, F: V0076728F V0076727F, K: K000497544, P: P00711392, US 00122885).

= *Gynoxys arnicae var. scandens* Cuatrec., Fieldiana, Bot. 27: 3. 1950. – Syntypes: Colombia. Dep. del Valle, Cordillera Occidental, Los Farallones, extremo N. bajando a Las Cascadas, 3100 m, 2 Aug 1946, *J. Cuatrecasas 21923* (F: V0076729F V0076730F, P: P00711393, US 00122886 00122887).

Gynoxys asterotricha Sch. Bip., Linnaea 34: 529. 1865.

Lectotype (designated here): Bolivia. Larecaja, Viciniis Sorata, Lancha de Cochipata in scopulsis montis Illampia, 3300 m, 1 Apr 1859, *G. Mandon 84* (P02273125; isolectotypes: BR: BR0000005318506, F: V0076731F V0076732F, GH: GH00008570 GH00008571, MPU: MPU012549 MPU012550 MPU012570, NY 178790, P: P02273080 P02273126).

Note: The gathering Mandon 84 is a mixed collection of material representing *G. asterotricha* and *G. mandonii*. The above cited specimens in BR, F, GH, MPU, NY & P represent *G. asterotricha*. The specimen in K (K000497527) and P (P04099621) holds material of both species on the same sheet.

Gynoxys baccharoides (Kunth) Cass. in Cuvier, Dict. Sci. Nat. (ed. 2) 48: 455. 1827 ≡ *Senecio baccharoides* Kunth, Nov. Gen. Sp. (folio ed.) 4: 146. 1818 ["1820"]. – Syntypes: Ecuador. Crescit locis frigidis Andium Quitensium, 3240 m, Jul, *F. W. H. A. Humboldt & A. Bonpland s.n.* (P: P00320174 P00320173).

= *Gynoxys lindenii* Sch. Bip. ex Wedd., Chlor. Andina 1: 76. 1856. – Syntypes: Colombia. New Granada, Mariquita, Pic. de Tolima, 4280 m, *Linden 930* (syntypes; G: G00223897 F: V0076720F, NY 468695; US 00122916 (fragment)).

Gynoxys bracteolata Cuatrec., Notas Fl. Colombia 6: 33, f. 26. 1944. – Holotype: Colombia. Caldas, Cordillera Central, vertiente occidental, faldas sudoese del Ruiz, El Aprisco, 3500-3600 m, 5 May 1940, *J. Cuatrecasas 9313* (COL not traced; isotypes: BC: BC-Cuatrecasas-635016 BC-Cuatrecasas-634964, F: V0076735F V0076734F, P: P00711406, US00122891, U: U 0001282).

Gynoxys buxifolia (Kunth) Cass. in Cuvier, Dict. Sci. Nat. 48(2): 455. 1827 ≡ *Senecio buxifolius* Kunth., Nov. Gen. Sp. (folio ed.) 4: 147. 1818 ["1820"]. – Syntypes: Ecuador. Quito, Rucu Pichincha, Crescit cum praecedente: locis frigidis Andium Quitensium., *F. W. H. A. Humboldt & A. Bonpland s.n.*(F: s.n. V0077029F (fragments), HAL: HAL0113451, P: P00320176 P00670367 P00670368).

= *Gynoxys buxifolia* var. *brevifolia* Hieron., Bot. Jahrb. Syst. 19(1): 63. 1895. – Syntypes: Ecuador. Loja, Alsos de Zoghunes, Oña & Zaraguro, 3000-3300 m, 23 Oct 1888, *F. C. Lehmann 4899* (US 00122892 01101244 (fragments), K: K000497541).

Gynoxys callacallana Cuatrec., Ciencia (Mexico) 23: 146. 1964. – Holotype: Perú. Amazonas, Chachapoyas, Middle eastern Calla-Calla slopes, ca. Kms. 411-416 of Leimebamba-Balsas road, 3100-3250 m, 11 Jul 1962, *J. J. Wurdack 1324* (US 00323999; isotypes: GH: GH00008574, LIMA not traced, NY 178792, P not traced, US 00811165).

Gynoxys calyculisolvens Hieron., Bot. Jahrb. Syst. 36: 504. 1905. – Syntypes: Perú. Cajamarca, entre Chota y Cutervo, Jun 1879, *C. von Jelski 611* (not traced), *C. von Jelski 780* (B, destroyed; photo: F: F0BN018153).

Gynoxys capituliparva Cuatrec., Fieldiana, Bot. 27(2): 6. 1951. – Holotype: Perú. Huanuco, Tambo de Vaca, 12000 ft., 10 Jun 1923, *J. F. Macbride 4434* (F: V0076736F; isotype: US 00122894).

Gynoxys caracensis Muschl., Bot. Jahrb. Syst. 50(2/3, Beibl. 111): 85–86. 1913. – Syntypes: Perú. Ancash, in declivibus Cordillerae blancae Supra Caraz, 3200-3700 m, 9 Jun 1903, *A. Weberbauer 3248* (B, destroyed). Perú. Ancash, Formatio aperta, 3600-3700 m, 18 Apr 1903, *A. Weberbauer 2909* (B, destroyed; photo: F: F0BN018154).

Gynoxys cerrateana B. Herrera, Bol. Soc. Perúana Bot. 8(1–2): 37, f. 28. 1980. – Holotype: Perú. Amazonas, Chachapoyas, Cordillera Calla-Calla lado del Maranón, 3400-3600 m, *R. Ferreyra 15578* (USM not traced).

Gynoxys chagalensis Hieron., Bot. Jahrb. Syst. 28: 630. 1901. – Syntypes: Ecuador. Cuenca, chagal W Andens of Cutca, 2200-2800 m, Sep [no year], *F. C. Lehmann 7948* (B, destroyed; photo: F: F0BN018156; F: V0076703F, K: K000497539, US 00122895).

Gynoxys chimborazensis Hieron., Bot. Jahrb. Syst. 29: 66. 1900. – Syntypes: Ecuador. Chimborazo, crescit in declivibus montis Chimborazo, 2600 m, Sep 1881, *A. Sodiro 60/9* (P: P00711408 (fragments), QPLS: QPLS211069).

Gynoxys colanensis M. O. Dillon & Sagást., Brittonia 40(2): 221. 1988. – Holotype: Perú., Bagua, Cordillera Colán, NE of La Peca, 5.350383W, 78.26064N, 2980-3100 m, 8 Sep 1978, *P. Barbour 3409* (F: V0043641F; isotypes: HUT not traced, LSU: LSU00210549, MO: MO-2152935).

Gynoxys columbiana (Klatt) Hieron., Bot. Jahrb. Syst. 28: 631. 1901 ≡ *Liabum columbianum* Klatt, Bot. Jahrb. Syst. 8(1): 47. 1886. – Syntypes: Columbia. Cauca, in silvis densis ad latera montis Páramo de Moras, 2800-3400 m, 16 Mar 1884, *F. C. Lehmann 3783* (GH: GH00008578 (fragment), K: K000497537, US 00122695).

Gynoxys compressissima Cuatrec., Fieldiana, Bot. 27(2): 4. 1951. – Holotype: Perú. Huanuco, Tambo de Vaca, ca. 12000 ft., 10-24 Jun 1923, *J. F. Macbride 4435* (F: V0076738F; isotype US 00122896).

Gynoxys corazonensis Hieron., Bot. Jahrb. Syst. 29: 65. 1900. – Syntype: Ecuador. Pichincha, Monte Corazón, *A. Sodiro 60/8* (P: P00711411 (fragments)).

Gynoxys costihirsuta Cuatrec., Ciencia (Mexico) 23: 146. 1964. – Holotype: Perú. Amazonas, Chachapoyas, upper slopes and summit of Cerro Yama-uma above Taulia, 12-15 km south-southeast (145°) of Molinopampa, 3200-3450 m, 11 Aug 1962, *J. J. Wurdack 1670* (US 00324000; isotypes: GH: GH00008580, K: K000497535, LIMA not traced, LP: LP002068, NY 178796, P, US 00811164, USM: USM000113).

Gynoxys cuicochensis Cuatrec., Fieldiana, Bot. 27: 16. 1951. – Holotype: Ecuador. Imbabura, Lake Cuicocha, 3500 m, 27 May 1939, *C. W. Pendland & R. H. Summer 722* (F: V0076705F).

Gynoxys cusilluyocana Cuatrec., Fieldiana, Bot. 27(2): 8. 1951. – Syntypes: Perú. Cuzco, Paso de tres Cruces, Cerro de Cusilluyoc, 3500-3800 m, 3 May 1925, *F. W. Pennell 13900* (F: V0076741F, GH: GH00008582, PH: PH00013518, US 00122899).

Gynoxys cutervensis Hieron., Bot. Jahrb. Syst. 36: 506. 1905. – Syntypes: Perú. Crescit prope Cutervo, May 1879, *C. von Jelski 632* (B, destroyed; photo: F: F0BN018157).

Gynoxys cuzcoensis Cuatrec., Fieldiana, Bot. 27(2): 9. 1951. – Holotype: Perú. Cuzco, Tres Cruces, Pancartambo, 3600 m, 1 Oct 1941, *C. Vargas 2253* (NY 178797; isotypes: F: V0076742F (fragment), LP: LP002069 LP002070).

Gynoxys cygnata S. Díaz & A. Correa, Revista Acad. Colomb. Ci. Exact. 26(100): 343–344, f. 2. 2002. – Holotype: Colombia. Caldas, Sur del Nevado del Cisne, cerca a Laguna Verde, 04°50’07”N,75°21’38”W, 4600-4800 m, 28 Jan 1986, *V. A. Funk 8082* (COL: COL000005207; isotype: US 01826640).

Gynoxys dilloniana Sagást. & C. Téllez, Brittonia 39(4): 432, f. 1. 1987. – Holotype: Perú. Lambayeque. Ferreñafe, distrito Incahuasi, Laguna Tembladera-Cerro Negro, 3300 m, 12 Sep

1985, *A. Sagástegui et al., 12835* (HUT not traced; isotypes: F: V0043636F, MO: s.n., NY not traced).

Gynoxys fallax Mattf., Repert. Spec. Nov. Regni Veg. 17: 183. 1921. – Syntypes: Perú. Piura, Huancabamba, westhänge der Cordillere östlich von Huancabamba, über der Hacienda Chantaco, 2500 m, 17 Apr 1912, *A. Weberbauer 6319b* (F: V0076706F V0076707F, GH: GH00008584).

Gynoxys ferreyrae B. Herrera, Bol. Soc. Perúana Bot. 8(1–2): 35. 1980. – Holotype: Perú. Cajamarca, Hualgayoc, Jalca, 16 Aug 1952, 3400 m, *R. Ferreyra 8559* (not traced; isotypes USM: USM000115; MO-714138, US 00122903).

Note: The protologue states the holotype specimen to be USM (not traced online), the specimen in USM (USM000115) digitally available in JSTOR is labelled as isotype by Herrera. In case no other specimen exists in USM, USM000115 would actually be the holotype).

Gynoxys flexopedes Cuatrec., Fieldiana, Bot. 27: 13. 1950. – Syntypes: Colombia. Cundinamarca, Paramo de Guasca, 3000-3500 m, 11 Oct 1939, H. *Garcia Barriga 08098* (COL: COL000005209 COL000005208, F: V0076708F V0076709F, US 00122904).

Gynoxys florulenta Cuatrec., Fieldiana, Bot. 27(1): 4–5. 1950. – Syntypes: Colombia. Valle, Cordillera Central, Hoya del río Bugalagrande, Barragán, Páramo de Bavaya, Corrales, 3450-3520 m, 18-20 May 1946, *J. Cuatrecasas 20148* (COL000005210, COL000005211, F: V0076743F V0076744F, P: P00711412, US 00122905, WIS: WIS00001046MAD).

Gynoxys frontinoensis S. Díaz & A. Correa, Revista Acad. Colomb. Ci. Exact. 23(88): 333. 1999. – Holotype: Colombia. Antioquia, Municipio de Urrao, Páramo de Frontino, Llano Grande, 3460 m, 1 Jul 1984, *R. Lodoño et al., 29* (COL: COL000005212; isotype: MEDEL: MEDEL000047).

Gynoxys fuliginosa (Kunth) Cass. in Cuvier, Dict. Sci. Nat. (ed. 2) 48: 455. 1827 ≡ *Senecio fuliginosus* Kunth, Nov. Gen. Sp. (folio ed.) 4: 146. 1818 [“1820”]. – Syntypes: Colombia. Pasto, Inter pagos Ypidales et Guachucal, 2916 m, Dic, *F. W. H. A. Humboldt & A. Bonpland s.n.* (F: V0076822F (fragments), P: P00320175 P00670369).

= *Gynoxys fuliginosa* var. *glabriuscula* Domke, Biblioth. Bot. 116: 170. 1937. – Syntype: Ecuador. Cañar, Tipococha, 3200 m, 16 Aug 1933, *Diels 551* (B, destroyed).

Gynoxys huanucona (Cuatrec.) Cuatrec., Brittonia 8: 158. 1955 ≡ *Senecio huanuconus* Cuatrec., Fieldiana, Bot. 27: 45. 1951 ≡ *Nordenstamia huanucona* (Cuatrec.) B. Nord., Asteraceae Newslett. 44: 20. 2006. – Syntypes: Perú. Huanuco, 1927, *M. Sawada 45* (F: V0076921F, US 00123418).

Gynoxys hallii Hieron., Bot. Jahrb. Syst. 19: 64. 1894. – Syntypes: Ecuador. Quito, crescit in regione suprema silvae Andinum occidentalium 2500-3400 m, Aug 1888, *F. C. Lehmann 4664* (K: K000634159 K000634160); prope Zurucucho et Tambo de Quinua haud procul ab urbe Cuenca, 3000-3500 m, Sep 1888, *F. C. Lehmann 4605* (K: K000497532 K000634158); In monte ignivomo Pichincha, 3400 m, *F. Hall s.n.* (B, destroyed; photo: F: F0BN018158).

Gynoxys henrici Mattf., Repert. Spec. Nov. Regni Veg. 17: 178. 1921. – Syntype: Perú. Amazonas, Östlich von Chachapoyas: zwischen dem steppe mit eizelnen Sträuchern, 3200-3400 m, 29 Jul 1904, *Weberbauer 4413* (B, destroyed).

Gynoxys hirsuta Wedd., Chlor. Andina 1: 79. 1855. – Syntypes: Colombia. Bogotá, Nouvelle-Grenade, *F. W. H. A. Humboldt & A. Bonpland s.n.* (F: V0076746F, P: P00670371), *Goudot s.n.* (GH: GH00008586).

Gynoxys hirsutissima Cuatrec., Notas Fl. Colombia 6: 34, f. 27–29. 1944. – Syntypes: Colombia. Cundinamarca, Cordillera oriental, extremo sudeste de la Sabana de Bogota en San Miguel, 2800-3000 m, 10 Sep 1941, *J. Cuatrecasas & R. Jaramillo 12022* (COL: COL000005213 COL000005214, BC: BC-635006, F: V0076711F V0076712F, K: K000497530, LL: LL00374264, NY 178858, P: P00711413, U: U 0001283, US 00122902).

Gynoxys huasahuasis Cuatrec., Fieldiana, Bot. 27(2): 2. 1951. – Holotype: Perú. Huasahuasu, 2900 m, 29 Apr 1940, *F. Woytkowski 37* (F: V0076713F).

Gynoxys hypoleucophylla Cuatrec., Ciencia (Mexico) 23: 148. 1964. – Holotype: Perú. Amazonas, Chachapoyas, Upper slopes and summit of Cerro Yamauma above Taulia, 12-15 km, south-southeast (145°) of Molinopampa, 3200-3450 m, 11 Aug 1962, *J. J. Wurdack 1671* (US 00324001; isotypes: GH: GH00008587, K: K000497529, LIMA not traced, LP: LP002071, NY 178860, P, US 00811163).

Gynoxys ignaciana Cuatrec., Fieldiana, Bot. 27(2): 14. 1951. – Holotype: Ecuador. Pichincha, San Ignacio, 11200 ft., 14-19 Aug 1923, *H. E. Anthony & G. H. H. Tate 127* (US 00122908; isotype: F: V0076747F).

Gynoxys infralanata Cuatrec., Fieldiana, Bot. 27(2): 6. 1951. – Holotype: Perú. Cusco. Torontoy, Urubamba Valley, 3900 m, 1915, *E. Heller 2181* (US 00122910; isotype: F: V0076748F).

Gynoxys jelskii Hieron., Bot. Jahrb. Syst. 36: 507. 1905. – Syntypes: Perú. Crescit prope Cutervo, May 1879, *C. von Jelski 678* (B, destroyed; photo: F: F0BN018159; F: V0076749F (fragments), US 00122912).

Gynoxys laurata Cuatrec., Fieldiana, Bot. 27: 5. 1950. – Syntypes: Colombia. Valle, Cordillera Central, cabeceras del río Tulu, quebrada de Las Vegas, 3400-3500 m, 23 Mar 1946, *J. Cuatrecasas 20399* (COL: COL000005217 COL000005218 COL000005219, F: V0076750F V0076751F, P: P00711415, US 00122913).

Gynoxys laurifolia (Kunth) Cass. in Cuvier, Dict. Sci. Nat. 48(2): 455. 1827 ≡ *Senecio laurifolius* Kunth, Nov. Gen. Sp. (folio ed.) 4: 146. 1818 [“1820”]. – Syntypes: Ecuador. Loja, Crescit locis subcalidis, umbrosis inter Lucarque et Gonzanama Quitensium, 1908 m, Aug, *F. W. H. A. Humboldt & A. Bonpland s.n.* (B, destroyed; photo: F: F0BN018160).

Gynoxys lehmannii Hieron., Bot. Jahrb. Syst. 28: 629. 1901. – Syntypes: Colombia. Cauca, crescit in fruticetis densis in Páramo de las Delicias in Andibus centralibus papayanensibus, 3200-3600 m, Jan-Feb, *F. C. Lehmann 8501* (B, destroyed; photo: F: F0BN018155; F: V0076721F, PH: PH00013515, S-R-2688, US 00122914 01014476).

Gynoxys longistyla (Greenm. & Cuatrec.) Cuatrec., Chlor. Andina 1(3): 79. 1855 ≡ *Senecio longistylus* Greenm. & Cuatrec., Collect. Bot. (Barcelona) 3: 292. 1953 ≡ *Nordenstamia longistyla* (Greenm. & Cuatrec.) B. Nord., Asteraceae Newslett. 44: 21. 2006. – Holotype: Perú. Moquegua, Saylapa near Carumas, 3600-3700 m, 3 Mar 1925, *Weberbauer 7331a* (F: V0076925F).

Gynoxys macfrancisci Cuatrec., Fieldiana, Bot. 27(2): 3. 1951. – Syntypes: Perú. Pachitea, Yanano, ca 6000 ft., 13-16 May 1923, *J. F. Macbride 3747* (F: V0076753F, US 00122918).

Gynoxys macrophylla Muschl., Bot. Jahrb. Syst. 50(2/3, Beibl. 111): 88–89. 1913. – Syntypes: Perú. Huanuco, Huamalies, Montes prope Monzon, 2000-2500 m, 8 Aug 1903, *Weberbauer 3534* (B, destroyed; photo: F: F0BN018161).

Gynoxys magnifolia (H. Beltrán & J. Campos) Escobari & N. Kilian, comb. nov. ≡ *Nordenstamia magnifolia* H. Beltrán & J. Campos, Arnaldoa 16(1): 37. 2009. – Holotype: Perú. Amazonas, Luya. Camporredondo, Tullanga, Subiendo del campamento o Pascana hacia el Cerro Huicsocunga, 2700-3000 m, 7 Sep 1989, *C. Díaz & J. Campos 3830* (USM not traced; isotypes: MO: MO-1962029 MO-1962030, S: S19-3395 S19-3398).

Gynoxys malcabalensis Cuatrec., Ciencia (Mexico) 23: 149. 1964. – Holotype: Perú. Amazonas, Chachapoyas, Summit of Cerro Malcabal (Cerro Tumbe) 3-6 km. southwest of Molinopampa, 2850-2900 m, 20 Jul 1962, *J. J. Wurdack 1413* (US 00324002; isotypes: GH: GH00008591, LIMA not traced, LP: LP002072, NY 178862, P not traced, USM: USM000117, US 00811161).

Gynoxys mandonii Sch. Bip. ex Rusby, Mem. Torrey Bot. Club 6(1): 67. 1896. – *Gynoxys mandonii* Sch. Bip. Bulletin de la Société Botanique de France 12: 80. 1865, nom. nud. – **Lectotype (designated here):** Bolivia. Cochabamba, Chapare, Espiritu Santo, 1891, *M. Bang 1196* (NY 178865; isolectotypes: BR: BR0000005318933, K: K000634162, NDG: NDG62632, PH: PH00013513). Bolivia. Larecaja, Viciniis Sorata, Lancha de Cochipata in scopulsis montis Illampia, 3300 m, 1 Apr 1859, *G. Mandon 84* (BR: BR0000005317899, P: P00711420, S: S10-31297 S10-31297, US 01117686).

= *Gynoxys hypomalaca* S. F. Blake, Bot. Gaz. 74: 427. 1922. – Holotype: Bolivia. La Paz, Sorata, higher limit of trees, 22 Apr 1920, *E. W. D. Holway & M. M. Holway 567* (US 00122907; isotypes: GH: GH00008588, NY 178861, US 01100708).

= *Gynoxys cochabambensis* Cabrera s.l., Notas Mus. La Plata, Bot. 14: 194. 1949. – Holotype: Bolivia. Cochabamba, Chapare, Yanta-Aduana, 3200 m, 10 Jul 1929, *J. Steinbach 9813* (LP: LP000274; isotypes: E00414368, F: V0076737F, G: G00223898, GH: GH00008576 GH00008577, K: K000634161 K000659419, NY 178794, S: S-R-2686).

= *Gynoxys cruzensis* Cuatrec., Collect. Bot. (Barcelona) 3(3): 295. 1953. – Syntypes: Bolivia. Santa Cruz, Comarapa, Cerro San Mateo, 3400 m, 24 Oct 1928, *J. Steinbach 8515* (E00414367, F: V0076739F, GH: GH00008581, K: K000497536, PH: PH00013519, S: S-R-2687).

Note: The gathering Mandon 84 is a mixed collection of material representing *G. asterotricha* & *G. mandonii*. The above cited specimens in BR, P, S, US represent *G. mandonii*. The specimen in K (K000497527) depicts material of both species on the same sheet.

Note: the species are doubtfully distinct and will be treated in a following work.

Gynoxys marcapatana Cuatrec., Collect. Bot. (Barcelona) 3: 297. 1953. – Holotype: Perú. Cuzco, Quispicanchis, Marcapata, Compi-pampa, on the grade from Huaillai to Huallo-hualla, 4100 m, 11 Dic 1938, *C. Vargas 9717* (GH: GH00008596; isotype: F: V0076835F).

Gynoxys meridana Cuatrec., Bol. Soc. Venez. Ci. Nat. 15(81): 109. 1954. – Holotype: Venezuela. Merida, Laguna Negra, 9 Nov 1952, *L. Aristeguieta 970* (F: s.n.; isotypes: US 00122921 00122922, VEN: VEN282322).

Gynoxys metcalfii Cuatrec., Fieldiana, Bot. 27(2): 2. 1951. – Holotype: Perú. Puno, Sandía. Near Limbani, 3200-3450 m, *R. D. Metfcalf 30529* (US 00122923).

Gynoxys miniphylla Cuatrec., Fieldiana, Bot. 27(1): 11. 1950. – Holotype: Ecuador. Azuay, In vicinity of Toreador, between Molleturo and Quinoas, 3810-3930 m, 15 Jun 1943, *J. A. Steyermark 53175* (F: V0076701F; isotype: NY 178863).

Gynoxys monzonensis Mattf., Repert. Spec. Nov. Regni Veg. 17: 180. 1921. – Syntype: Perú. Huanuco, Huamalies, Berge südwestlich von Monzon, 3400-3500 m, 11 Jul 1903. *Weberbauer 3338* (B, destroyed).

Gynoxys multibracteifera H. Rob. & Cuatrec., Phytologia 56: 369, f. 1984. – Holotype: Ecuador. Azuay, Ridge between El Pan and Guachapala, 7500-9800 ft., 4 Sep 1945, *W. H. Camp E-5244* (US 00122925; isotype: NY 178864).

Gynoxys myrtoides Mattf., Repert. Spec. Nov. Regni Veg. 17: 182. 1921. – Syntype: Perú. Piura, Huancabamba, westhänge der Cordillere östlich von Huancabamba, über der Hacienda Chantaco, 5°10'W,5°20'S, 2500 m, 17 Apr 1912, *Weberbauer 2. Ser., 6319a* (B, destroyed).

Gynoxys neovelutina Cuatrec., Fieldiana, Bot. 27(2): 11. 1951. – Holotype: Bolivia, 3000 m, 1-4 Apr 1892, *O. Kuntze* (NY 178869; isotype: F: V0076755F (fragment)).

= *Gynoxys tablaensis* Cabrera, Blumea 7: 197. 1952. – Syntypes: Bolivia. Cochabamba, Tablas, 3400 m, May 1911, *T. Herzog 2201* (B: B 10 0093559, L: L0001978 L0001979, LP: LP000276, S: S-R-2690, Z: Z-000003473 (fragments)).

Gynoxys nervosa Hieron., Bot. Jahrb. 21: 354. 1895. – Syntypes: Colombia. Boyacá, Crescit prope Muso civitatis Boyacá, Jul 1868, *A. Stuebel 161* (B, destroyed; photo: F: F0BN018162).

Gynoxys nitida Muschl., Bot. Jahrb. Syst. 50(2/3, Beibl. 111): 86–87. 1913. – Syntypes: Perú. Ayacucho, Supra Quinuam prope Ayacucho, 3300-3500 m, 30 May 1910, *Weberbauer 5535* (F: V0076756F, G: G00223896 (fragments), GH: GH00008600, K: K000497524, US 00122927; photo: US 00122926).

Gynoxys oleifolia Muschl., Bot. Jahrb. Syst. 50(2/3, Beibl. 111): 89–90. 1913. – Syntypes: Perú. Ancash, Pichiu, provinsia Huari, 4000–4100 m, 20. Apr 1903, *Weberbauer 2937* (photo F: V0076757F, S: S07-10464 (fragments)).

Gynoxys pachyphylla Mattf., Repert. Spec. Nov. Regni Veg. 17: 184. 1921. – Syntype: Perú. Huancabamba, Cordillera östlich von Huacabamba. 5°10'W,5°20'S, 3400-3500 m, 8 Apr 1912, *Weberbauer 2. Ser. 6082* (B, destroyed).

Gynoxys paramuna Cuatrec., Fieldiana, Bot. 27: 7. 1950. – Syntypes: Colombia. Boyacá, Sierra Nevada del Cocuy, valle de Las Lagunillas, 4110 m, 11 Sep 1938, *J. Cuatrecasas & H. García Barriga 1434* (BC: BC-624335, COL: COL000005221, F: V0076758F, P: P00711424, US 00122928).

Gynoxys parvifolia Cuatrec., Revista Acad. Colomb. Ci. Exact. 6: 59, f. 25. 1944. – Holotype: Colombia. Nariño, Páramo de la Laguna del Cumbal, 3475 m, 7 Feb 1942, *Miguel de Garganta 418* (COL: COL000005222; isotype: F: V0076759F).

Gynoxys perbracteosa Cuatrec., Fieldiana, Bot. 27(1): 1. 1950. – Syntypes: Colombia. Cauca, Cordillera Central, Cabeceras del Río Páez, Páramo alrededor de la Laguna del Páez, 3450 m, 4 Dic 1944, *J. Cuatrecasas 19057* (COL: COL000005223 COL000005224 COL000005225, DUKE10000786, F: V0076762F V0076763F G: G00223895, GH: GH00008602, K: K000497522, MO: MO-714136, NY 178871, P: P00603125 P00711427).

Gynoxys pillahuatensis Cuatrec., Fieldiana, Bot. 27(2): 7. 1951. – Syntypes: Perú. Cuzco, „Pillahuata“, Cerro de Cusilluyoc, 3000-3300 m, 3 May 1925, *F. W. Pennell 14134* (F: V0076764F, GH: GH00008603, K: K000497521, NY 178872, PH: PH00013512, US 00122930).

Gynoxys poggeana Mattf., Repert. Spec. Nov. Regni Veg. 17: 179. 1921. – Syntypes: Perú. Junin, Valle del Río Masamerich, abajo del Tambo de Atac. 11°30’S, 3400-3500 m, 25 Apr 1913, *Weberbauer 2. Ser. 6645* (F: V0077103F, GH: GH00008605, MO: MO-714135 (fragments), MOL: MOL00006552, US 00122931, USM: USM000118).

Gynoxys psilophylla Klatt, Ann. K. K. Naturhist. Hofmus. 9: 367. 1894 ≡ *Gynoxys glabriuscula* Rusby, Mem. Torrey Bot. Club 6(1): 68. 1896, nom. illeg. – Syntypes: Bolivia. Cochabamba, 1 Jul 1891, *M. Bang 1116* (A: A00008585, BR: BR0000005318186 BR0000005318513, E: E00413271, F: V0076765F, GH: GH00008606 GH00008607, US 00122935, WIS: WISv0256703WIS).

= *Gynoxys hoffmannii* Kuntze, Revis. Gen. Pl. 3(3): 156. 1898. – Syntype: Bolivia. Cochabamba, Weg zum Río Juntas, 3000 m, 13-21 Apr 1892. *O. Kuntze s.n.* (NY 178859).

= *Gynoxys boliviana* S. F. Blake, Contr. Gray Herb. 53: 28. 1918 ≡ *Liabum bolivianum* Klatt., Ann. K. K. Naturhist. Hofmus. 9: 362. 1894. – Holotype: Bolivia, *Cuming s.n.* (W: W18890106172; isotype: GH: GH00008573 (fragment with drawing)).

Gynoxys pulchella (Kunth) Cass. in Cuvier, Dict. Sci. Nat. (ed. 2) 48: 455. 1827 ≡ *Senecio pulchellus* Kunth, Nov. Gen. Sp. (folio ed.) 4: 146–147. 1818 [“1820”]. – Syntype: Ecuador. Crescit locis frigidis Andium Quitensium.,3240 m, Jul, *F. W. H. A. Humboldt & A. Bonpland s.n.* (P: P00320177).

Gynoxys reinaldii Cuatrec., Fieldiana, Bot. 27(2): 15.1951. – Holotype: Ecuador. Loja, Cajamuna, 2400 m, 7 May 1946, *R. Espinosa 312* (F: V0076767F).

Gynoxys rimbachii Cuatrec., Fieldiana, Bot. 27: 10. 1950. – Syntypes: Ecuador. Eastern Cordillera, inner slope, 3200 m, Dec [no year], *A. Rimbach 79* (A: A00008608, F: V0076769F).

Gynoxys rugulosa Muschl., Bot. Jahrb. Syst. 50(2/3, Beibl. 111): 87–88. 1913. – Lectotype (Herrera de Loja 1980: 39): Perú. Sandia, 3300 m, 11 Apr 1902, *Weberbauer 747* (F: F0BN018163 (photo)). – Isolectotype: Perú. Cuzco, Supra Picri, via inter Cuzco et Santa Anna, Formatio aperta, 3800-3900 m, 16 Jun 1905, *Weberbauer 4940* (B, destroyed).

Gynoxys rusbyi Cuatrec., Fieldiana, Bot. 27(2): 10. 1951. – Syntypes: Bolivia. La Paz, Vic. Pongo de Queme, 12500 ft., 2 Jul 1921, *H. H. Rusby 3* (F: V0076770F (fragments), MO: MO-1508476, NY 178874, US 00122937).

Gynoxys sancti-antonii Cuatrec., Fieldiana, Bot. 27(1): 9. 1950. – Syntypes: Colombia. Comisaría del Putumayo, Páramo de San Antonio del Bordoncillo, entre el Encano y Sibundoy, 3250 m, 3 Jan 1941, *J. Cuatrecasas 11722* (BC: BC635012, COL: COL000005226, F: V0076771F, P: P00711429, US 00122938). Colombia. Narino, Yacuanquer, 2800-3000 m, 4 Jan 1943, *M de Garganta 504* (not traced).

= *Gynoxys sancti-antonii* var. *latifolia* Cuatrec., Brittonia 12: 186. 1960. – Holotype: Ecuador. Chimborazo. Border to Canar (western escarpment), between Sta. Rosa and Joyagahi, 8000-9000 ft., *W. H. CampE-4049* (F: V0076772F; isotypes: GH: GH00008609, K: K000497518, MO: MO-714134, NY 178875, S: S-R-2689, VEN: VEN34425)

Gynoxys seleriana Muschl., Bot. Jahrb. Syst. 50(2/3, Beibl. 111): 90–91. 1913. – Syntypes: Perú. Cuzco, Cazeo, in dumetis, 28 Jun 1910, *Seler 163* (B, destroyed). Perú. Cuzco, Urubamba, 3400 m, 10 Jun 1905, *Weberbauer 4926* (B, destroyed).

Gynoxys sodiroi Hieron., Bot. Jahrb. Syst. 29: 64. 1900. – Syntypes: Ecuador. In decliv. m. Chimbor. vers. Guaranda, *L. Sodiro 60/3* (B, destroyed; photo: F: F0BN018164; QPLS: QPLS211119)

Gynoxys sorataensis Cuatrec., Fieldiana, Bot. 27(2): 12. 1951. – Syntypes: Bolivia, La Paz, Sorata, 10000 ft, Feb 1886, *H. H. Rusby 1638* (F: V0076773F s.n., MO: s.n., NY 178876).

Gynoxys stuebelii Hieron., Bot. Jahrb. Syst. 21: 355. 1895. – Syntypes: Ecuador. Pichincha, Crescit prope Verdecuchu in monte Pichincha, 4000 m, Jul-Aug, *Stuebel 31* (B, destroyed; photo: F: F0BN018165). Ecuador. Pichincha, Monte Cayambe, 4300 m, *Stuebel 114* (not traced).

Gynoxys subamplectens Cuatrec., Fieldiana, Bot. 27(2): 1. 1951. – Syntypes: Perú. Cuzco, Paso de Tres Cruces, Cerro de Cusilluyoc, 3800-3900 m, 3 May 1925, *F. W. Pennell 13825* (F: V0076775F, GH: GH00008610, US 00122940).

Gynoxys subcinerea Cuatrec., Fieldiana, Bot. 27: 6. 1950. – Syntypes: Colombia. Santander, Cordillera Oriental, Hoya del río Chitagá en Vega Colombia, 2880 m, 28 Nov 1941, *J. Cuatrecasas 13473* (BC: BC634976, COL: COL000005227 COL000005228, LP: LP002075, F: V0076776F V0076777F, P: P00711430, US 00122941).

Gynoxys szyszylowiczii Hieron., Bot. Jahrb. Syst. 36(5): 505. 1905. – Syntypes: Perú. Caldas, Crescit prope Cutervo, May 1879, *Jelski 607* (B, destroyed); ibid., Apr 1879, *Jelski 754* (B, destroyed, photo: F: F0BN018166).

Gynoxys tabaconasensis H. Beltrán & S. Baldeón, Asteraceae Newslett. 47: 14, f. 1. 2009. – Holotype: Perú. Caldas, Province San Ignacio, District Tabaconas, Lagunas Arrebiatadas, Santuario Nacional Tabaconas-Namballe, 3150-3180 m, 9 Apr 2003, *S. Baldeón & L. Adrianzen 5160* (USM not traced; isotypes: MO not traced, S: S09-3275).

Gynoxys tetroici V. A. Funk & H. Rob., Revista Acad. Colomb. Ci. Exact. 17(65): 243–245, f. 1. 1989. – Holotype: Perú. Piura, Bosque de Huamba, 2950 m, 20 Sep 1987, *Valencia 1991* (US 00169692; isotype: USM not traced).

Gynoxys tolimensis Cuatrec., Trab. Mus. Nac. Ci. Nat., Ser. Bot. 29: 37–38. 1935. – Syntypes: Colombia. Tolima, Cordillera Central, vert. merid. monte Tolima, El Salto, 3200 m, 15 May 1932, *J. Cuatrecasas 2850* (F: V0076779F (fragment), MA: MA240999).

Gynoxys tomentosissima Cuatrec., Ciencia (Mexico) 23: 149. 1964. – Holotype: Perú. Amazonas, Chachapoyas, middle eastern Calla-Calla, near Kms. 416-419 of Leimebamba-Balsas road, 3900-3100 m, 9 Jul 1962, *J. J. Wurdack 1254* (US00122943; isotypes: F: V0076780F, GH: GH00008612, K: K000497517, LP: LP002076, NY 178878, US 00811162, USM: USM000119).

Gynoxys trianae Hieron., Bot. Jahrb. Syst. 21: 353. 1895. – Syntypes: Colombia. Nueva Granada, Tuquerres, 3000 m, Jun 1853, *Triana 1444* (B, destroyed; photo: F: F0BN018167; E: E00413269 E00413270, NY 77375, P: P00711431 P00711432, US 00122944). Colombia. Santisimo, haud procul a vico Cumbal, *Stuebel 435a* (not traced).

= *Gynoxys trianae* var. *nemocona* Cuatrec., Fieldiana, Bot. 27(2): 17. 1951. – Holotype: Colombia. Cundinamarca, Nemocón, 2900-3000 m, 23 Oct 1917, *F. W. Pennell 2619* (NY 178879).

Gynoxys vacana Cuatrec., Fieldiana, Bot. 27(2): 5. 1951. – Syntypes: Perú. Pasco, Tambo de Vaca, 13000 ft., 10-24 Jun 1923, J. F. Macbride 4391 (F: V0076782F, US 00122945).

Gynoxys validifolia Cuatrec., Brittonia 8(1): 40. 1954. – Holotype: Ecuador. Azuay, N-NW of the Páramo del Castillo, 6-8 km N-NE of Sevilla de Oro, 10000-11200 ft., 31 Aug 1945, *W. H. Camp E-5156* (F: V0076783F; isotypes: GH: GH00008613, K: K000497516, NY 178880, US 00122946).

Gynoxys vargasiana Cabrera, Revista Univ. (Cuzco) 33(87): 121–122, f. 20. 1944. – Holotype: Perú. Cuzco, Calvca, alrededores de Lares, 3200 m, 30 Aug 1943, *C. Vargas 3598* (LP: LP000277).

Note: Probably not a *Gynoxys.* Too many inner phyllaries for a *Gynoxys*

Gynoxys venulosa Cuatrec., Fieldiana, Bot. 27(1): 8. 1950. – Syntypes: Colombia. Cauca, Cordillera Central, Cabeceras del Río López, Quebrada del Duende, 3400-3450 m, 3 Dic 1944, *J Cuatrecasas 18945* (COL: COL000005230 COL000005231, DUKE: DUKE10000787, F: V0076784F, GH: GH00008614, K: K000497515, NY 178881, P: P00711433).

Gynoxys violacea Sch. Bip. ex Wedd., Chlor. Andina 1(3): 77. 1855. – Syntypes: Venezuela. Merida, Sierra nevada de Merida, 2920 m, 1 Sep 1846, *Funck & Schlim 1159* (F: V0076789F (fragments), GH: GH00008617 (fragments), K: K000497514, LD 1001683, MPU: MPU012551, P: P00711439 P00711440 P00711441 P00711442, US 00122948 (fragments & photo)).

Gynoxys visoensis Cuatrec., Fieldiana, Bot. 27(2): 13. 1951. – Syntypes: Perú. Viso, 9000 ft., 5-14 May 1922, *Macbride & Featherstone 580* (F: V0076788F, US 00122949).

Gynoxys weberbaueri Mattf., Repert. Spec. Nov. Regni Veg. 17: 181. 1921. – Syntype: Perú. Huancabamba, Cordillere östlich von Huancabamba, 3300-3500 m, 5°10‘-5°20’S, 8 Apr 1912, *Weberbauer 2. Ser. 6075* (B destroyed).

Gynoxys woytkowskii (Cuatrec.) Cuatrec., Brittonia 8: 158. 1955 ≡ *Senecio woytkowskii* Cuatrec., Fieldiana, Bot. 27: 49. 1951 ≡ *Nordenstamia woytkowskii* (Cuatrec.) B. Nord., Asteraceae Newslett. 44: 22. 2006. – Holotype: Perú. Huánuco, vicinity of Tambo de Vacas, 3500 m, 4 Nov 1937, *F. Woytkowski 145* (F: V0076790F).

Gynoxys yananoensis Cuatrec., Fieldiana, Bot. 27(2): 10. 1951. – Holotype: Perú. Huanuco, Yanano, 6000 ft., 20 Jun 1923, *J. F. Macbride 4931* (F: V0076791F).

Excluded names

Gynoxys aquifolia Cuatrec ≡ *Scrobicaria aquifolia* (Cuatrec.) B. Nord.

Gynoxys auriculata Turcz. = *Aetheolaena patens* (Kunth) B. Nord.

Gynoxys berlandieri DC. = *Pseudogynoxys chenopodioides* (Kunth) Cabrera

Gynoxys cordifolia Cass. ≡ *Pseudogynoxys cordifolia* (Cass.) Cabrera

Gynoxys cummingii Benth. ≡ *Pseudogynoxys chenopodioides* var. *cummingii* (Benth.) B. L. Turner

Gynoxys discolor Rusby = *Pentacalia marinii* (Cabrera) Cuatrec.

Gynoxys fragrans Hook. ≡ *Pseudogynoxys fragrans* (Hook.) H. Rob. & Cuatrec.

Gynoxys haenkei DC. ≡ *Pseudogynoxys haenkei* (DC.) Cabrera

Gynoxys heterophylla Turcz. ≡ *Aetheolaena heterophylla* (Turcz.) B. Nord.

Gynoxys ilicifolia (L.f.) Wedd. = *Scrobicaria ilicifolia* (L.f.) B. Nord.

Gynoxys incana Less = *Jacmaia incana* (Sw.) B. Nord.

Gynoxys laciniata Less. = *Odontocline laciniata* (Sw.) B. Nord.

Gynoxys lucida Less. = *Dendrophorbium lucidum* (Sw.) C. Jeffrey

Gynoxys oerstedii Benth. ≡ *Pseudogynoxys oerstedii* (Benth.) Cuatrec.

Gynoxys poeppigii DC. ≡ *Pseudogynoxys poeppigii* (DC.) H. Rob. & Cuatrec.

Gynoxys prenanthifolia Turcz. = *Aetheolaena patens* (Kunth) B. Nord.

Gynoxys scabra Benth. ≡ *Pseudogynoxys scabra* (Benth.) Cuatrec.

Gynoxys sinclairii Benth. = *Pseudogynoxys sonchoides* (Kunth) Cuatrec.

3.6 References

APG, IV [Angiosperm Phylogeny Group IV] (2016) An update of the Angiosperm Phylogeny Group classification for the orders and families of flowering plants: APG IV. Botanical Journal of the Linnean Society 181: 1–20. Available from: https://doi.org/10.1111/boj.12385

Beck S, Ibáñez D (2014) Asteraceae. In: Jorgensen PM, Nee N, Beck SG (Eds) Catálogo de las plantas vasculares de Bolivia. Monographs in Systematic Botany from the Missouri Botanical Garden 127: 290–382.

Bacon CD, Gutiérrez-Pinto N, Flantua S, Castellanos Suárez D, Jaramillo C, Pennington RT, Antonelli A (2022) The seasonally dry tropical forest species *Cavanillesia chicamochae* has a middle Quaternary origin. Biotropica 54(1): 91–99. https://doi.org/10.1111/btp.13031

Beentje H (2010) The Kew Plant Glossary: An illustrated dictionary of plant terms. Kew Publishing, Surrey, 184 pp.

BGBM 2011+: EDIT Platform for Cybertaxonomy. – Published at http://www.cybertaxonomy.org [accessed May 2022].

Beltrán H, Baldeón S (2009) A new species of *Gynoxys* (Asteraceae: Senecioneae) from Peru. Compositae Newsletter 47: 13–18. Available from: https://www.biodiversitylibrary.org/page/15548133.

Beltrán H, Calvo J (2020) A new species of *Nordenstamia* (Compositae, Senecioneae) from central Peru. Phytotaxa 474(3): 293–297. https://doi.org/10.11646/phytotaxa.474.3.8

Berendsohn WG (2010) Devising the EDIT Platform for Cybertaxonomy. In: Nimis PL, Vignes-Lebbe R (Eds) Proceedings of the international Congress on tools for identifying Biodiversity: Progress and Problems. Muséum national d'Histoire naturelle – Grand Amphithéâtre, Paris, 1–6. Available from: http://www.openstarts.units.it/dspace/bitstream/10077/3737/1/Berendsohn, bioidentify.pdf.

Bergh NG, Verboom GA (2011) Anomalous capitulum structure and monoecy may confer flexibility in sex allocation and life history evolution in the *Ifloga* lineage of paper daisies (Compositae: Gnaphalieae). American Journal of Botany 98(7): 1113–1127. https://doi.org/10.3732/ajb.1000457

Bernal R, Gradstein S., Celis M (Eds) (2016) Catálogo de plantas y líquenes de Colombia. Universidad Nacional de Colombia, Facultad de Ciencias, Instituto de Ciencias Naturales, Bogotá.

Borsch T, Berendsohn W, Dalcin E, Delmas M, Demissew S, Elliott A, Fritsch P, Fuchs A, Geltman D, Güner A, Haevermans T, Knapp S, le Roux MM, Loizeau PA, Miller C, Miller J, Miller JT, Palese R, Paton A, Parnell J, Pendry C, Qin HN, Sosa V, Sosef M, von Raab-Straube E, Ranwashe F, Raz L, Salimov R, Smets E, Thiers B, Thomas W, Tulig M, Ulate W, Ung V, Watson M, Jackson PW, Zamora N (2020) World Flora Online: Placing taxonomists at the heart of a definitive and comprehensive global resource on the world's plants. Taxon 69(6): 1311–1341. https://doi.org/10.1002/tax.12373

Borsch T, Hilu K, Quandt D, Wilde V, Neinhuis C, Barthlott W. (2003) Noncoding plastid trnT-trnF sequences reveal a well resolved phylogeny of basal angiosperms. Journal of Evolutionary Biology 16: 558-576.

Brako L, Zarucchi J. (Eds) (1993) 49 Kew Bulletin Catalogue of the flowering plants and Gymnosperms of Peru. Monographs in Systematic Botany from the Missouri Botanical Garden, St. Louis.

Brummitt RK, Powell CE (1992) Authors of Plant Names. Royal Botanic Gardens, Kew, 736 pp.

Cassini AHG (1827) Sénécionées, Senecioneae. In: Cuvier F. (Eds) Dictionnaire des sciences naturelles, dans lequel on traite méthodiquement des différens êtres de la nature. F.G. Levrault, Strasbourg & Le Normant, Paris, 48(2): 446–466.

Colwell RK, Brehm G, Cardelús CL, Gilman AC, Longino JT, Cardelus CL, Gilman AC, Longino JT (2008) Global warming, elevational range shifts, and lowland biotic attrition in the Wet Tropics. Science 322: 258–261. https://doi.org/10.1126/science.1162547

Correa A (2003) Revision of the genus *Paragynoxys* (Asteraceae, Senecioneae-Tussilagininae). Brittonia 55(2): 157–168. Available from: https://www.jstor.org/stable/3218456.

Cuatrecasas J (1950) Contributions to the flora of South America: Studies on Andean Compositae - I. Studies in South American plants - II. Fieldiana 27(1). https://doi.org/10.5962/bhl.title.2414
Cuatrecasas J (1951) Contributions to the Flora of South America. Studies on Andean Compositae - II. Fieldiana 27(2): 1–74. Available from: https://www.biodiversitylibrary.org/page/2457150.
Cuatrecasas J (1954) Notas a la Flora de Colombia, XIII. Revista Academia Colombiana de Ciencias Exactas, Físiicas y Naturales 9(35): 233.
Cuatrecasas J (1955) A new genus and other novelties in Compositae. Brittonia 8(2): 151–163. Available from: https://www.jstor.org/stable/2804857.
Cuatrecasas J (1960) Studies on Andean Compositae-IV. Brittonia 12: 182–195. https://doi.org/https://doi.org/10.2307/2805052
Cuatrecasas J (1990) Miscelllaneous notes on neotropical flora. XIX. Combinations in Senecioneae, Compositae. Phytologia 69(5): 313–315. https://doi.org/10.1002/fedr.19530550203
Díaz-Piedrahita S, Cuatrecasas J (1990) El género Aequatorium Nord. (Senecioneae–Asteraceae) en Colombia. Rev. Acad. Colomb. Cienc. 17(67): 659–666.
Díaz-Piedrahita S, Cuatrecasas J (1994) Novedades colombianas en el género Aequatorium Nord. (Asteraceae, Senecioneae). Rev. Acad. Colomb. Cienc. 19(73): 247–252.
Dorr LJ and Nicolson DH (2009) Taxonomic literature, Suppl. 7-8. – Regnum Veg. 149, 150
Doyle JJ and Doyle JL (1987) A rapid DNA isolation procedure for small quantities of fresh leaf tissue. Phytochemical Bulletin 19(1): 11–15. https://webpages.uncc.edu/~jweller2/pages/BINF8350f2011/BINF8350_Readings/Doyle_plantDNAextractCTAB_1987.pdf
Dušková E, Sklenář P, Kolář F, Vásquez DLA, Romoleroux K, Fér T, Marhold K (2017) Growth form evolution and hybridization in *Senecio* (Asteraceae) from the high equatorial Andes. Ecology and Evolution 7(16): 6455–6468. https://doi.org/10.1002/ece3.3206
Erbar C, Leins P (2021) Style diversity in Asteraceae morphology, anatomy, phylogeny, and function. Schweizerbart Science Publishers, Stuttgart, Germany, 260 pp. Available from: http://www.schweizerbart.de//publications/detail/isbn/9783510480340/Bibliotheca%5C_Botanica%5C_Vol%5C_163%5C_Erbar%5C_Le.
Escobari B, Borsch T, Quedensley TS, Gruenstaeudl M (2021) Plastid phylogenomics of the Gynoxoid group (Senecioneae, Asteraceae) highlights the importance of motif-based sequence alignment amid low genetic distances. American Journal of Botany 108(11): 2235–2256. https://doi.org/10.1002/ajb2.1775
Esklual G (2017) A phylogenetic study of *Crepis* L. species sect. Barkhausia (Asteraceae) using low-copy nuclear genes (*gsh1*, *sqs*) and plastid genes (*rps16*, *matK1*). Justus-Liebig-University Giessen
Ezcurra C (2002) Phylogeny, morphology, and biogeography of *Chuquiraga*, an Andean-Patagonian genus of Asteraceae-Barnadesioideae. The Botanical Review 68(1): 153–170. https://doi.org/https://doi.org/10.1663/0006-8101(2002)068[0153:PMABOC]2.0.CO;2
Flantua SGA, O'Dea A, Onstein RE, Giraldo C, Hooghiemstra H (2019) The flickering connectivity system of the north Andean páramos. Journal of Biogeography 46(8): 1808–1825. https://doi.org/10.1111/jbi.13607
Frable BW, Melo BF, Fontenelle JP, Oliveira C, Sidlauskas BL (2022) Biogeographic reconstruction of the migratory Neotropical fish family Prochilodontidae (Teleostei: Characiformes). Zoologica Scripta 51: 348–364. https://doi.org/10.1111/zsc.12531
Funk V, Susanna A, Stuessy T, Robinson H (2009a). Classification of Compositae. In: Funk V, Susanna A, Stuessy T, Bayer RJ (Eds) Systematics, evolution, and biogeography of Compositae, Vienna: International Association for Plant Taxonomy, Vienna, 171-176.
Garcia N, Meerow AW, Soltis DE, Soltis PS (2014) Testing deep reticulate evolution in Amaryllidaceae tribe Hippeastreae (Asparagales) with its and chloroplast sequence data. Systematic Botany 39(1): 75–89. https://doi.org/10.1600/036364414X678099
GBIF (2022) GBIF.org. Global Biodiversity Information Facility. Available from: https://www.gbif.org/ [accessed: 21.04.2022]
Global Compositae Database (2022). Available from: https://www.compositae.org/aphia.php?p=stats [accessed: 20 Februar 2022]
Global Plants JSTOR (2022) JSTOR Global Plants. Available from: http://plants.jstor.org/

[accessed: 20 Februar 2022]
Gruenstaeudl M (2020) Annonex2embl: Automatic preparation of annotated DNA sequences for bulk submissions to ENA. Bioinformatics *36*(12): 3841–3848. https://doi.org/10.1093/bioinformatics/btaa209
Herrera B (1980) Revision de las especies peruanas del género *Gynoxys* (Compositae). Boletin de la Sociedad Peruana de Botanica 8(1): 3–74.
Hilliard M, Burtt B (1981) Some generic concepts in Compositae - Gnaphaliinae. Botanical Journal of the Linnean Society 82: 181–232. https://doi.org/https://doi.org/10.1111/j.1095-8339.1981.tb00958.x
Hind N (2007) An annotated preliminary checklist of the Compositae of Bolivia, version 2. Available from: https://www.kew.org/sites/default/files/ 2019-01/Bolivian%20compositae%20checklist.pdf [accessed: 05 November 2021].
Horton BK (2018) Sedimentary record of Andean mountain building. Earth-Science Reviews 178: 279–309. https://doi.org/10.1016/j.earscirev.2017.11.025
Hughes CE, Atchison GW (2015) The ubiquity of alpine plant radiations: From the Andes to the Hengduan Mountains. New Phytologist 207: 275–282. https://doi.org/10.1111/nph.13230
IPNI (2022) IPNI.org. International Plant Names Index. Available from: https://www.ipni.org/ [accessed: 20 Februar 2022]
Jeffrey C (1992) The Tribe Senecioneae (Compositae) in the Mascarene Islands with an Annotated World Check-List of the Genera of the Tribe: Notes on Compositae: VI. Kew Bulletin 47(1): 49–109. https://doi.org/10.2307/4110768
Jorgensen P, Leon-Yanez S (Eds) (1999) Catalogue of the Vascular Plants of Ecuador. Monographs in Systematic Botany from the Missouri Botanical Garden, Quito.
Kadereit J, Jeffrey C (1996) A preliminary analysis of cpDNA variation in the tribe Senecioneae (Compositae). In: Hind D, Beentje H (Eds) Compositae: Systematics. Proceedings of the International Compositae Conference, UK, 349–360.
Kandziora M, Sklenář P, Kolář F, Schmickl R (2022) How to tackle phylogenetic discordance in recent and rapidly radiating groups? Developing a workflow using *Loricaria* (Asteraceae) as an example. Frontiers in Plant Science 12: 1–16. https://doi.org/10.3389/fpls.2021.765719
Karis PO (1993) Morphological phylogenetics of the Asteraceae-Asteroideae, with notes on character evolution. Plant Systematics and Evolution 186: 69–93. https://doi.org/10.1007/BF00937714
Katoh K, Standley DM (2013) MAFFT multiple sequence alignment software version 7: Improvements in performance and usability. Molecular Biology and Evolution 30(4): 772–780. https://doi.org/10.1093/molbev/mst010
Kilian N, Henning T, Plitzner P, Müller A, Güntsch A, Stöver BC, Müller KF, Berendsohn WG, Borsch T (2015) Sample data processing in an additive and reproducible taxonomic workflow by using character data persistently linked to preserved individual specimens. Database 2015(v): 1–19. https://doi.org/10.1093/database/bav094
Kilian N, Sennikov A, Wang ZH, Gemeinholzer B, Zhang JW (2017) Sub-paratethyan origin and middle to late miocene principal diversification of the lactucinae (Compositae: Cichorieae) inferred from molecular phylogenetics, divergence-dating and biogeographic analysis. Taxon 66(3): 675–703. https://doi.org/10.12705/663.9
Lawrence GHM, Buchheim AFG, Daniels GS, Dolezal H (Eds) (1968) B-P-H, Botanico-Periodicum-Huntianum. Hunt Botanical Library, Pittsburgh.
Lee-Yaw JA, Grassa CJ, Joly S, Andrew RL, Rieseberg LH (2018) An evaluation of alternative explanations for widespread cytonuclear discordance in annual sunflowers (*Helianthus*). New Phytologist 221(1): 515–526
Lichter-Marck IH, Freyman WA, Siniscalchi CM, Mandel JR, Castro-Castro A, Johnson G, Baldwin BG (2020) Phylogenomics of Perityleae (Compositae) provides new insights into morphological and chromosomal evolution of the rock daisies. Journal of Systematics and Evolution 58(6): 853–880. https://doi.org/10.1111/jse.12711
Löhne C, Borsch T (2005) Molecular evolution and phylogenetic utility of the petD group II intron: A case study in basal angiosperms. Molecular Biology and Evolution 22(2): 317–332. https://doi.org/10.1093/molbev/msi019
Luebert F, Weigend M (2014) Phylogenetic insights into Andean plant diversification. Frontiers in

Ecology and Evolution 2: 1–17. https://doi.org/10.3389/fevo.2014.00027
Lundin R (2006) *Nordenstamia* Lundin (Compositae-Senecioneae), a new genus from the Andes of South America. Compositae Newsletter 44(44): 14–23. Available from: https://www.biodiversitylibrary.org/page/13749318.
Maddison WP (1997) Gene trees in species trees. Systematic Biology 46(3): 523–536. https://doi.org/10.1093/sysbio/46.3.523
Maddison W, Maddison D (2021) Mesquite: a modular system for evolutionary analysis. Available from: http://www.mesquiteproject.org.
Madriñán S, Cortés AJ, Richardson JE (2013) Páramo is the world's fastest evolving and coolest biodiversity hotspot. Frontiers in Genetics 4: 1–7. https://doi.org/10.3389/fgene.2013.00192
Mafftfeld J (1921) Compositae novae Austro-Americaneae. I. In: Fedde F (Ed.), Repertorium specierum novarum regni vegetabilis. Berlin, Selbstverlag des Herausgebers, Berlin, 178–185. Available from: https://www.biodiversitylibrary.org/item/7042.
Mansion G, Parolly G, Crowl AA, Mavrodiev E, Cellinese N, Oganesian M, Fraunhofer K, Kamari G, Phitos D, Haberle R, Akaydin G, Ikinci N, Raus T, Borsch T (2012) How to Handle Speciose Clades? Mass Taxon-Sampling as a Strategy towards Illuminating the Natural History of Campanula (Campanuloideae). PLoS ONE 7(11). https://doi.org/10.1371/journal.pone.0050076
Marhold K, Stuessy T, Agababian M, Agosti D, Alford MH, Crespo A, Crisci J V., Dorr LJ, Ferencová Z, Frodin D, Geltman D V., Kilian N, Peter Linder H, Lohmann LG, Oberprieler C, Penev L, Smith GF, Thomas W, Tulig M, Turland N, Zhang XC (2013) The future of botanical monography: Report from an international workshop, 12-16 March 2012, Smolenice, Slovak Republic. Taxon 62(1): 4–20. https://doi.org/10.1002/tax.621003
Markos S, Baldwin BG (2001) Higher-level relationships and major lineages of Lessingia (Compositae, Astereae) based on nuclear rDNA internal and external transcribed spacer (ITS and ETS) sequences. Systematic Botany 26(1): 168–183.
Morales-Briones DF, Liston A, Tank DC (2018) Phylogenomic analyses reveal a deep history of hybridization and polyploidy in the Neotropical genus *Lachemilla* (Rosaceae). New Phytologist 218(4): 1668–1684. https://doi.org/10.1111/nph.15099
Moreira-Muñoz A, Scherson RA, Luebert F, Román MJ, Monge M, Diazgranados M, Silva H (2020) Biogeography, phylogenetic relationships, and morphological analyses of the South American genus *Mutisia* L.f. (Asteraceae) shows early connections of two disjunct biodiversity hotspots. Organisms Diversity and Evolution 20(4): 639–656. https://doi.org/10.1007/s13127-020-00454-z
Müller K (2005) SeqState: primer design and sequence statistics for phylogenetic DNA datasets. Applied Bioinformatics 4: 65–69.
Müller J, Müller K, Neinhuis C, Quandt D (2010) PhyDE: Phylogenetic Data Editor. Available from: http://www.phyde.de/ [accessed: 20 Februar 2022].
Myers N, Mittermeier R, Mittermeier C, da Fonseca G, Kent J (2000) Biodiversity hotspots for conservation priorities. Nature 403: 853–858. https://doi.org/10.1038/468895a
NCBI (2022) National Center for Biotechnology Information. Available from: https://www.ncbi.nlm.nih.gov/ [accessed: Januar 2022]
Nevado B, Contreras-Ortiz N, Hughes C, Filatov DA (2018) Pleistocene glacial cycles drive isolation, gene flow and speciation in the high-elevation Andes. New Phytologist 219(2): 779–793. https://doi.org/10.1111/nph.15243
Nordenstam B (1978) Taxonomic studies in the tribe Senecioneae (Compositae). Opera Botanica 44: 1–83.
Nordenstam B (1997) The genus *Aequatorium* B. Nord. (Compositae-Senecioneae) in Ecuador. Compositae Newsletter 31(31): 1–16. Available from: https://www.biodiversitylibrary.org/page/13152227.
Nordenstam B (2007) XII. Tribe Senecioneae. In: Kadereit JW, Jeffrey C (Eds) The families and genera of vascular plants. Springer Berlin Heidelberg, Berlin, 208–241. https://doi.org/10.1007/978-3-642-39417-1
One Thousand Plant Transcriptomes Initiative Green (2019) One thousand plant transcriptomes and

the phylogenomics of green plants. Nature 574: 679–685. https://doi.org/10.1038/s41586-019-1693-2
Padilla-González GF, Diazgranados M, Da Costa FB (2021) Effect of the Andean geography and climate on the specialized metabolism of its vegetation: The subtribe Espeletiinae (Asteraceae) as a case example. Metabolites 11: 220–221. https://doi.org/10.3390/metabo11040220
Pagel M, Meade A (2006) Bayesian analysis of correlated evolution of discrete characters by reversible-jump Markov chain Monte Carlo. American Naturalist 167(6): 808–825. https://doi.org/10.1086/503444
Pascual-Díaz JP, Garcia S, Vitales D (2021) Plastome diversity and phylogenomic relationships in Asteraceae. Plants 10(12): 1–16. https://doi.org/10.3390/plants10122699
Pelser PB, Nordenstam B, Kadereit JW, Watson LE (2007) An ITS phylogeny of tribe Senecioneae (Asteraceae) and a new delimitation of *Senecio* L. Taxon 56(4): 1077–1104. https://doi.org/10.2307/25065905
Pelser PB, Kennedy AH, Tepe EJ, Shidler JB, Nordenstam B, Kadereit JW, Watson LE (2010) Patterns and causes of incongruence between plastid and nuclear Senecioneae (Asteraceae) phylogenies. American Journal of Botany 97(5): 856–873. https://doi.org/10.3732/ajb.0900287
Pérez-Escobar OA, Zizka A, Bermúdez MA, Meseguer AS, Condamine FL, Hoorn C, Hooghiemstra H, Pu Y, Bogarín D, Boschman LM, Pennington RT, Antonelli A, Chomicki G (2022) The Andes through time: evolution and distribution of Andean floras. Trends in Plant Science 27(4): 364–378. https://doi.org/10.1016/j.tplants.2021.09.010
Pouchon C, Fernández A, Nassar JM, Boyer F, Aubert S, Lavergne S, Mavárez J (2018) Phylogenomic analysis of the explosive adaptive radiation of the *Espeletia* complex (Asteraceae) in the tropical Andes. Systematic Biology 67: 1041–1060. https://doi.org/10.1093/sysbio/syy022
Pruski J (2018) Compositae of Central America-VII. *Digitacalia*, *Dresslerothamnus*, *Pentacalia*, *Zemisia*, their microcharacters, and some other Senecioneae. Phytoneuron 53: 1–112.
Rieseberg LH, Soltis DE (1991) Phylogenetic consequences of cytoplasmic gene flow in plants. Evolutionary Trends in Plants 5(1): 65–84. Available from: https://www.cabdirect.org/cabdirect/abstract/19911624824.
Rambaut A (2012) FigTree v1.4. Molecular evolution, phylogenetics and epidemiology. University of Edinburgh, Institute of Evolutionary Biology. Edinburgh. UK.
Robinson H, Cuatrecasas J (1984) Observations of the genus *Gynoxys* in Ecuador (Senecioneae, Asteraceae). Phytologia 56: 368–375. Available from: https://www.biodiversitylibrary.org/item/47412#page/383/mode/1up.
Robinson H, Cuatrecasas J (1992) Additions to *Aequatorium* and *Gynoxys* (Asteraceae: Senecioneae) in Bolivia, Ecuador, and Peru. Novon 2(4): 411–416. https://doi.org/10.2307/3391502
Robinson H, Carr GD, King RM, Powell AM, Robinson H, Carr GD, King RM, Powella AM (1997) Chromosome Numbers in Compositae, XVII: Senecioneae III. Annals of the Missouri Botanical Garden 84(4): 893–906.
Robinson H. (2009). An introduction to micro-characters of Compositae. In: Funk V, Susanna A, Stuessy T, Bayer R (Eds) Systematics, evolution, and biogeography of Compositae. Vienna: International Association for Plant Taxonomy, Vienna, 89-99
Ronquist F and Huelsenbeck JP (2003) MrBayes 3: Bayesian phylogenetic inference under mixed models. Bioinformatics 19: 1572-1574
Roque N, Keil DJ, Susanna A (2009) Illustrated glossary of Compositae. In: Funk V, Susanna A, Stuessy T, Bayer R (Eds) Systematics, evolution, and biogeography of Compositae. International Association for Plant Taxonomy, Vienna, 781–806.
Senderowicz M, Nowak T, Rojek-Jelonek M, Bisaga M, Papp L, Weiss-Schneeweiss H, Kolano B (2021) Descending dysploidy and bidirectional changes in genome size accompanied *Crepis* (Asteraceae) evolution. Genes 12(9): 1436. https://doi.org/10.3390/genes12091436
Simmons MP, Ochoterena H (2000) Gaps as characters in sequence-based phylogenetic analyses. Systematic Biology 49(2): 369–381. https://doi.org/10.1093/sysbio/49.2.369
Stafleu FA and Cowan RS (1976, 1979, 1981, 1983, 1985, 1986, 1986) Taxonomic literature, ed. 2, vol. 1-7. - Regnum Veg. 94, 98, 105, 110, 112, 115, 116.

Stafleu F and Mennega EA (1992, 1993, 1995, 1997, 1998, 2000) Taxonomic literature, Suppl. 1-6. – Regnum Veg. 125, 130, 132, 134, 135, 137.
Stöver BC, Müller KF (2010) TreeGraph2: Combining and visualizing evidence from different phylogenetic analyses. BMC Bioinformatics 11: 7. Available from: https://doi.org/10.1186/1471-2105-11-7.
Stuessy T, Lack HW (Eds) (2011) 153 Monographic Plant Systematics. Fundamental Assessment of Plant Biodiversity. Koeltz, Königstein, Viena, 222 pp.
Stull GW, Schori M, Soltis DE, Soltis PS (2018) Character evolution and missing (morphological) data across Asteridae. American Journal of Botany 105(3): 470–479. https://doi.org/10.1002/ajb2.1050
Stull GW, Soltis PS, Soltis DE, Gitzendanner MA, Smith SA (2020) Nuclear phylogenomic analyses of asterids conflict with plastome trees and support novel relationships among major lineages. American Journal of Botany 107(5): 790–805. https://doi.org/10.1002/ajb2.1468
Testo WL, Sessa E, Barrington DS (2019) The rise of the Andes promoted rapid diversification in Neotropical *Phlegmariurus* (Lycopodiaceae). New Phytologist 222: 604–613. https://doi.org/10.1111/nph.15544
Tropicos (2022) Tropicos.org. Missouri Botanical Garden. Available from: http://www.tropicos.org/ [accessed: 20 Februar 2022]
Van Der Hammen T, Hooghiemstra H (2000) Neogene and Quaternary history of vegetation, climate, and plant diversity in Amazonia. Quaternary Science Reviews 19: 725–742. https://doi.org/10.1016/S0277-3791(99)00024-4
Vargas OM, Madriñán S (2012) Preliminary phylogeny of *Diplostephium* (Asteraceae): Speciation rate and character evolution. Lundellia 15(1): 1–15. https://doi.org/10.25224/1097-993x-15.1.1
Vargas OM, Ortiz EM, Simpson BB (2017) Conflicting phylogenomic signals reveal a pattern of reticulate evolution in a recent high-Andean diversification (Asteraceae: Astereae: *Diplostephium*). New Phytologist 214(4): 1736–1750. https://doi.org/10.1111/nph.14530
Wang ZH, Peng H, Kilian N (2013) Molecular phylogeny of the *Lactuca* alliance (Cichorieae subtribe Lactucinae, Asteraceae) with focus on their Chinese center of diversity detects potential events of reticulation and chloroplast capture. PLoS ONE 8(12). https://doi.org/10.1371/journal.pone.0082692
Watanabe K (2002) Index to chromosome numbers in Asteraceae. Available from: http://www.lib.kobe-u.ac.jp/infolib/meta_pub/G0000003asteraceae_e [accessed: 21 February 2022].
Weddell HA (1855) Chloris Andina. Essai d'une flore de la région alpine des Cordilléres de l'Amerique du Sud, vol. 1, part 1. Bertrand, Paris.
White TJ, Bruns T, Lee S, Taylor J (1990) Amplification and Direct Sequencing of Fungal Ribosomal RNA Genes for Phylogenetics. PCR Protocols: 315–322. https://doi.org/10.1016/b978-0-12-372180-8.50042-1
Yin ZJ, Wang ZH, Kilian N, Liu Y, Peng H, Zhao MX (2022) Mojiangia oreophila (Crepidinae, Cichorieae, Asteraceae), a new species and genus from Mojiang County, SW Yunnan, China, and putative successor of the maternal Faberia ancestor. Plant Diversity 44(1): 83–93. https://doi.org/10.1016/j.pld.2021.06.007
Zhang T, Elomaa P (2021) Don't be fooled: false flowers in Asteraceae. Current Opinion in Plant Biology 59: 101972. https://doi.org/10.1016/j.pbi.2020.09.006
Zhang X (2021) Insights into the drivers of radiating diversification in biodiversity. bioRxiv: 2021.03.15.435394. Available from: https://doi.org/10.1101/2021.03.15.435394.

Chapter 4. Taxonomic revision for Bolivian species of the Gynoxyoid clade

4.1 Summary

Gynoxyoid is a large clade comprising four genera: *Aequatorium*, *Gynoxys*, *Paracalia* and *Paragynoxys* and ca 160 species distributed in the Andean region from Venezuela to Argentina.. The Bolivian checklist reports 12 species distributed in the country, nevertheless, no morphological revision was made for this group. In this study we aim to elaborate the first taxonomic treatment of all accepted species of the Gynoxyoid clade present in Bolivia. In that sense morphological and phylogenetic data was analyzed. To cover the greatest variation for both type of data, a representative number of specimens were included. A set of potential diagnostic characters were listed and its state was evaluated on each specimen. Based on morphological discontinuities morpho-species were defined and parallel to this evaluation the phylogenetic inference retrieved well defined clades. The definition of the morpho-species and the clades retrieved on the phylogenetic trees were tested based on a principal component analysis. The molecular and morphological analysis congruently supported the circumscription of three species. All remaining species were characterized on morphological data retrieved from the PCA analysis until further molecular analyses can be performed and the species limits on phylogenetic data can be better understood. The taxonomic treatment includes 13 *Gynoxys* species and one species of *Paracalia*. It includes a taxonomic key, species description including type specimens and nomenclatural information, habitat characterization and distribution maps. Additionally, when available the conservation status is mentioned. One species is treated as doubtful as it is not supported on any type of data and three new species are suggested.

4.2 Introduction

The Gynoxyoid group was originally defined by Jeffrey (1992) based on the combination of cylindrical anther-collars, polar endothecial thickening and a basic chromosome number = 10, including six genera. Later Robinson et al. (1997) restricted the group to the South American Andean genera (*Aequatorium, Gynoxys, Paracalia,* and *Paragynoxys*) and characterized it by a chromosome number of n = 40. The genus *Nordenstamia* Lund. was later added as a segregate

accommodating species previously placed in *Aequatorium* and *Gynoxys* (Lundin, 2006). The monophyly of the group in this circumscription was confirmed through molecular phylogenetics by Pelser et al. (2007; 2010), and through plastome phylogenomics by Escobari et al. (2021). The number of species in this group has increased drastically over time and currently amounts to ca. 158 species (see Escobari chapter 3). That last study also provided a revised generic classification of the group, again recognizing only the four genera *Aequatorium, Gynoxys, Paracalia* and *Paragynoxys,* based on morphological and molecular data.

The first checklist for Bolivia including members of the Gynoxyoid clade was published by Foster (1985), who listed 19 species, all belonging to the largest genus *Gynoxys*. Later Hind (2009; 2011) reported 20 species, of which 17 belong to *Gynoxys,* two species to *Nordenstamia* and one species to *Paracalia*. Hind's checklists represented so far, the first and most complete taxonomic revision of the Bolivian Gynoxyoids, including significant notes both on nomenclature, potential misidentifications and synonyms. Beck and Ibanez (2014) published the last updated checklist of Asteraceae as part of the Flora of Bolivia and recognized 22 Gynoxyoid species (18 in *Gynoxys,* three in *Nordenstamia* and one in *Paracalia*), of which eight are endemic to Bolivia.

The Gynoxyoids are a predominantly high Andean group, only the genus *Paracalia* with its two scandent shrubby species makes an exception, being distributed in moist forests at elevations between 900 and 2100 m (Cuatrecasas, 1951). Following the ecoregion classification for Bolivia by Ibisch and Mérida (2003), the genus *Gynoxys* in Bolivia is distributed mainly in the following ecoregions: Yungas (subtype Paramo yungueno and Ceja de Monte), Dry Inter-Andean Forest and in the Northern Puna (Semihumid and Humid Puna) from 2000 to 4500 m. The species are mainly shrubs (Beck and Ibanez, 2014) or more rarely trees and flower all year round (Beck and Ibanez, 2014; Killeen et al., 1993). Some *Gynoxys* species (i.e., *G. psilophylla*) are closely associated with *Polylepis* forests and represent an important habitat for a great number of birds species (Aucca et al., 2015) as they glean sugary secretions and aphids from the underside of the leaves of the bushes (Fjeldsa, 1993).

Knowledge of the Gynoxyoid species is still very limited. More in-depth studies at species level are largely missing, and only a small number of specimens is available for many species. Beck and Ibanez (2014), e.g., report five of the 24 Bolivian species being known only from the type collection. The ranges of distribution, ecology and infraspecific morphological variation are therefore usually badly known. At the same time, the morphological differentiation between many species, in particular of the large genus *Gynoxys*, is rather shallow. Information on the

thread status of Gynoxyoid species is equally scarce, only four Bolivian species were evaluated and are included in the IUCN Red List of Threatened Species (https://www.iucnredlist.org/).

Using our revised generic classification and checklist of all members of the Gynoxyoids given in chapter 3 as the basis, the aim of this study is to provide the first taxonomic treatment for the Gynoxyoids in Bolivia, based on morphological investigation and supplemented by molecular phylogenetic analysis of nuclear ribosomal ETS and ITS sequences.

4.3 Materials and Methods

4.3.1 Plant material

Herbarium specimens of the Gynoxyoid clade in Bolivia were collected during field work in 2016 and 2018 and deposited in the National Herbarium in La Paz (LPB) with duplicates in the herbarium of the Botanic Garden and Botanical Museum Berlin (B). In addition, specimens received on loan from the herbaria G, K, LPB, MO, NY, and P were examined. Altogether 165 specimens from Bolivia were studies physically. In addition, high resolution digital images of herbarium specimens from Bolivia and adjacent counties, in particular types, were consulted from the herbaria A, B, BM, BR, E, F, G, GH, K, L, LP, MICH, MO, MPU, NDG, NY, P, PH, PUL, S, US, W, WIS and Z either accessed through JSTOR Global Plants (https://plants.jstor.org/), GBIF (https://www.gbif.org/) or directly through the herbarium catalogues. All type specimens studied are listed under the corresponding taxon names in the taxonomy part. The other revised specimens are listed under each taxon in the section "Additional examined specimens". Specimens marked with * after the collection number were included in the phylogenetic analysis

4.3.2 Sources of names and checklist compilation

A checklist with synonymies of all species of the Gynoxyoids also including country occurrence records was elaborated (chapter 3) in a database on the EDIT Platform for Cybertaxonomy (Berendsohn, 2010) based on taxon name data imports from the International Plant Names Index (IPNI) (https://www.ipni.org/), supplemented by TROPICOS (https://tropicos.org/home) and checked against the Global Compositae Database (https://www.compositae.org/aphia.php?p=stats) and the Bolivian Compositae checklists by

Foster (1958), Hind (2011), and Beck and Ibanez (2014). This served as taxon name basis for the present study.

4.3.3 DNA Extraction, amplification, sequencing and phylogenetic tree inference

Nuclear ribosomal ETS and ITS sequences of 101 samples were selected to represent as much of the diversity of the Gynoxyoid clade in Bolivia as was available. 43 specimens were newly generated as described in chapter 3 and submitted to ENA following the submission pipeline of Gruenstaudl (2020) and can be retrieved under study number PRJEB56182. Sequences of further 58 specimens were sequenced and published in chapter 3 (ID number PRJEB53579) . Specimens also included in the PCA analysis are marked with an asterisk (*). A phylogenetic tree was constructed using MrBayes (Ronquist and Huelsenbeck, 2003) with the same parameters as given in chapter 3. Due to low quality of the isolates from the specimen, *Gynoxys sorataensis* could not be sequenced and hence it was excluded from the phylogenetic analysis.

4.3.4 Morphological examination

The herbarium material of all species of the Gynoxyoids reported for Bolivia was morphologically examined, including an assessment of the diagnostic characters stated in the protologues of the species. The morphological examination of the specimens was summarized in a specimen-based matrix of characters and states. The terminology of the character and state definitions followed Roque et al. (2009) and Beentje (2010). All specimens of rarely collected species and a representative selection (with respect to morphological and distributional diversity) of frequently collected species were examined.

In a first step, a set of character states was identified as diagnostic through visual comparison of the material and, using them, morpho-species were delimited by morphological discontinuities and by applying, based on protologues and type material, the concepts of the species described. An identification key was constructed and also used to test the reliability of the morphological character states identified as diagnostic for the morpho-species.

In a second step principal component analysis was performed using PC-ORD v 7.08 (McCune and Mefford, 2018) to determine the most significant variables contributing to the variation, and to assess the variability explained by each principal component. For this analysis, the original matrix was adjusted and two matrices for vegetative and reproductive characters were

generated. In each matrix the character states were encoded as showed in Appendix 4.4. Separate analyses were conducted for each matrix. The results are represented in two different ways: OTU´s colours [1] according to their corresponding morpho-species affiliation based on visual delimitation, and [2] according to the clade affiliation on the ETS-ITS phylogeny.

4.3.5 Distribution maps

Distribution maps were constructed based on the examined specimens after georeferencing, if necessary. The georeferenced maps were generated with DIVA-GIS (Hijmans, 2012) using an adaptation of the SRTM 90 m digital elevation data (CGIAR-CSI, 2022)

4.4 Results

4.4.1 Morphological examination

The morphological examination of the specimens resulted in a specimen-based matrix of 71 characters of which 22 are vegetative and 49 reproductive. A total of 99 accessions were included in the vegetative matrix (Appendix 4.2) and 62 accessions in the reproductive matrix (Appendix 4.3). The available specimens of *G. longifolia* and *G. sorataensis* were sterile and hence not represented in the reproductive matrix. The codes for the characters and their states are given in the Appendix 4.4

Based on visual comparison of the material, 13 morpho-species and one putative hybrid were recognized by morphological discontinuities. Seven names were found to represent synonyms of already published species. The occurrence of one species was excluded from Bolivia. Three of the morpho-species identified, could not be identified with any of the published species and found to be still undescribed. The status of one species, *Gynoxys rusbyi*, remained uncertain.

4.4.2 Phylogenetic analysis

The ETS-ITS alignment shows a low genetic diversity, with 98 parsimony informative out of a total of 1117 sites. Bayesian inference resolved ten strongly supported clades (Figure 4.1). The first diverging clade comprises the single member of *Paracalia* in Bolivia with the two accessions of *Gynoxys megacephala* as sister group. The second diverging clade includes the

single accession of *G. longifolia*. Four further clades form consecutive sister groups to a polytomy of other three clades. Apart from the clade of the single accession of *G. kingii*, all these clades are not congruent with the morpho-species: The samples of *G. repanda* were resolved in two independent clades (rep 1 & rep 2). *G. asterotricha* was resolved in a clade together with *G. rusbyi* and *G. psilophylla* (ast-rus-psi). Also, the samples of *G. mandonii* form two clades, the first clade (man 1) contains samples of *G. mandonii* and a putative hybrid of *G. asterotricha* and *G. mandonii*, here named as *G. asterotricha* × *mandonii*. The second clade (man 2) comprises the putative hybrid *G. asterotricha* × *mandonii, G. compressissima* and a sample of *G. asterotricha*. Finally, *G. neovelutina* forms a clade with a sample of *G.* cf. *asterotricha*. Because the physical specimens were not at hand of all samples, it was not possible to identify all specimens in the phylogenetic tree to the morphospecies.

4.4.3 Principal component analyses of morphological characters

The results of the principal component analyses are provided in Figure 4.2 and 4.3. The samples in Figure 4.2 are designated according to their visual morpho-species classification, the samples in Figure 4.3 are designated according to their clade affiliation in the ETS-ITS phylogeny.

Vegetative characters: The first three principal components of the analysis of vegetative characters (Figure 4.2) explained 33.8% of the variation. The principal component 1 (PC1) contributed 17.1% to the total variation and was positively correlated with phyllotaxis, trichomes characteristics such as structure and architecture, and leaf margin shape. This component mainly divided the specimens into two main groups (a) all specimens corresponding to the morpho-species *G. repanda, G. kingii* and *G.* sp. nov. B, with alternate leaves and multicellular stellate trichomes forming a cluster on the left side of the diagram, and (b) specimens with opposite leaves and different trichomes architecture, clustering on the opposite site. The PC2 accounted for 8.9% of the variation and its principal related characters were habit, trichomes characteristics, leaves length and petiole length. On this axis *G. megacephala* could be clearly distinguished from the rest by the presence of mixed multicellular branched and unicellular simple hairs. PC3 contributed 7.9% and comprised leaf shape, leaf margin characteristics and trichome architecture. *Gynoxys* sp. nov. A was particular well distinguished on this axis based on the presence of a revolute white leaves margin. PC1 against PC2 classified the specimens belonging to *Gynoxys* sp. nov. A, *G. megacephala, G. psilophylla* and *G.*

asterotricha (Figure 4.2). The PC1 vs PC3 and PC2 vs PC3 resolved *G.* sp. nov. B and *G. kingii* in nearby different clusters.

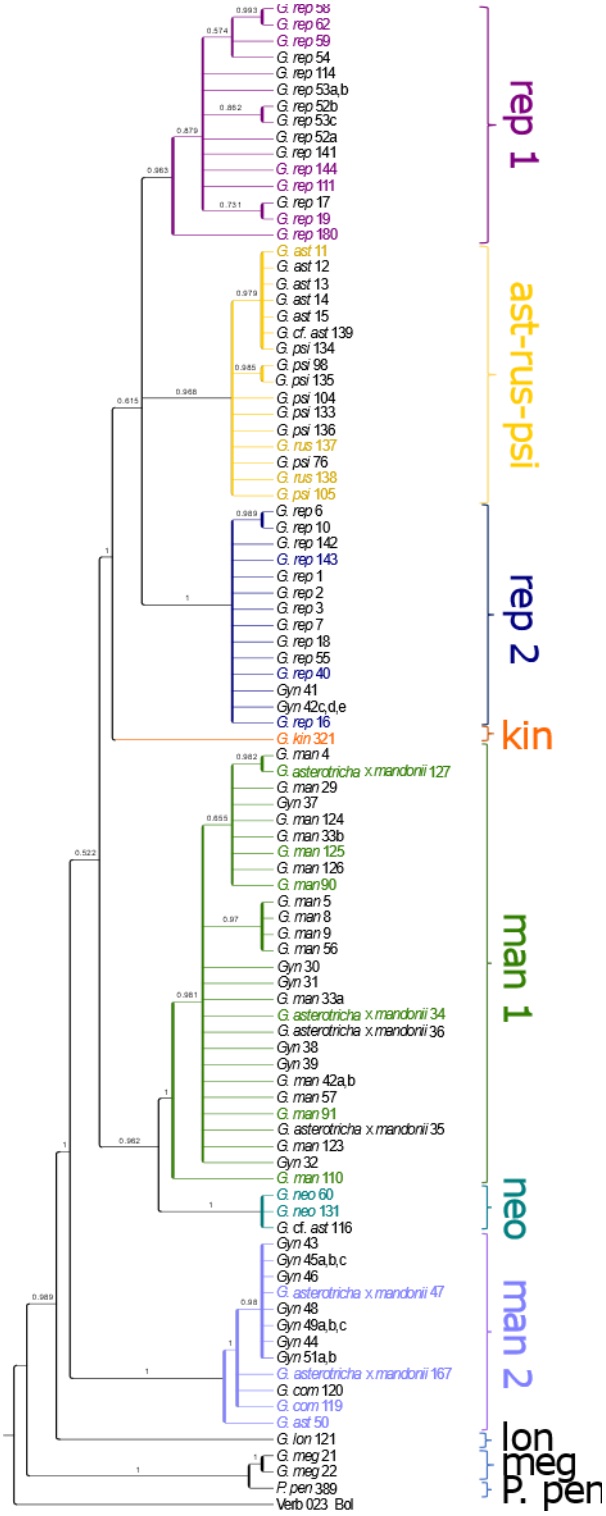

Figure 4.1: 50% majority consensus tree on ITS & ETS under Bayesian inference topology. Posterior probabilities are above branches. The coloured accessions correspond to specimens included in the PCA analysis. For metadata check Appendix 4.1.

The PCA analyses of the vegetative characters using the clade affiliation (Figure 4.3) classified the clade “man 1” and “rep 1” as individual clusters only on PC1 vs PC3. Further axis grouped “rep 1” with “rep 2” and “man 1” with the clades “ast-rus-psi”, “neo” and “man 2”. *G. kingii* (kin) was represented by a single specimen, nevertheless this clade was grouped out on all axis. All remaining clades proposed by the Bayesian analysis were not distinguished by the principal component analysis (Figure 4.3).

Reproductive characters: The first three principal components of the analysis of the reproductive characters accounted for 34% of the total variability. PC1 contributed 16.8% and was positively correlated with the anther length, corolla length and limb length of the disc flowers, and negatively correlated with the outer phyllaries shape and anthers base shape. Consequently, two clusters can be differentiated (Figure 4.2) (a) all accessions belonging to the morpho-species *G. repanda*, *G.* sp. nov. B and *G. mandonii* on the left side of the diagram, and *G. psilophylla*, *G. rusbyi*, *G. compressissima* and *G. neovelutina* on the right side. PC2 accounted for 10.2% of the variation and was positively determined by the style branch length and corolla tube length of the disc flowers, and negatively by the type of capitula, ray flower veins and receptacle shape. On the PC2 axis *G. megacephala* is clearly segregated due to the absence of ray flowers (discoid capitula), additionally, *G.* sp. nov. B is differentiated from *G. kingii* by involucrum shape (tubular vs campanulate). Finally, *G. compressissima* is segregated from *G. psilophylla*, *G. rusbyi* based mainly by its long style branches. PC3 contributed 7% and comprised the style apex shape, inner phyllaries length with a negative influence, and synflorescence type, disc flower width base and receptacle shape with a positive influence. This component classified the specimens in two groups, species with rounded style apex including *G. repanda*, *G. kingii*, *G.* sp. nov. *B* and *G. compressissima*, in contrast to those with an acute style apex including *G. neovelutina* and *G. mandonii*. The combination of PC1 and PC2 resulted in a clear segregation of *G. compressissima*, *G. megacephala*, and partially *G. psilophylla* in a mixed group with *G. rusbyi*, and *G. repanda*. The PC1 vs PC3 diagram partially clustered specimens of *G. repanda*, *G.* sp. nov. B, *G. compressissima*, and *G. mandonii* (Figure 4.2).

The PCA analyses on reproductive characters using clade affiliation (Figure 4.3) classified “ast-rus-psi”, “man 1” and “neo” as independently clusters on all axis. The clade “rep 1” was clustered on PC1 vs PC3 and PC2 vs PC3. Finally, “rep 2”, “kin” and “man 2” were represented by one specimen and hence no conclusion can be achieved.

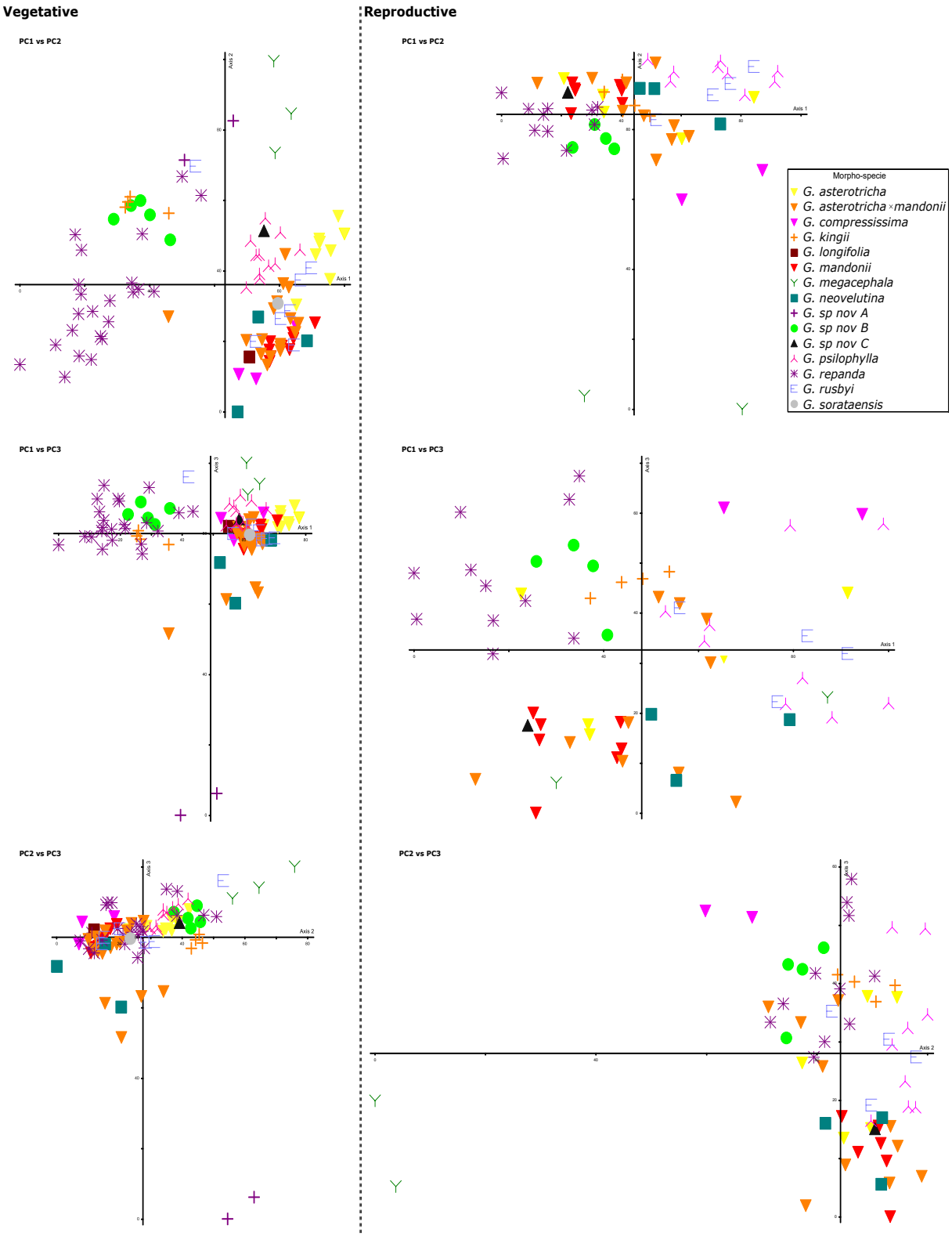

Figure 4.2: Principal component analysis on vegetative and reproductive characters, with the samples designated according to their morpho-species classification

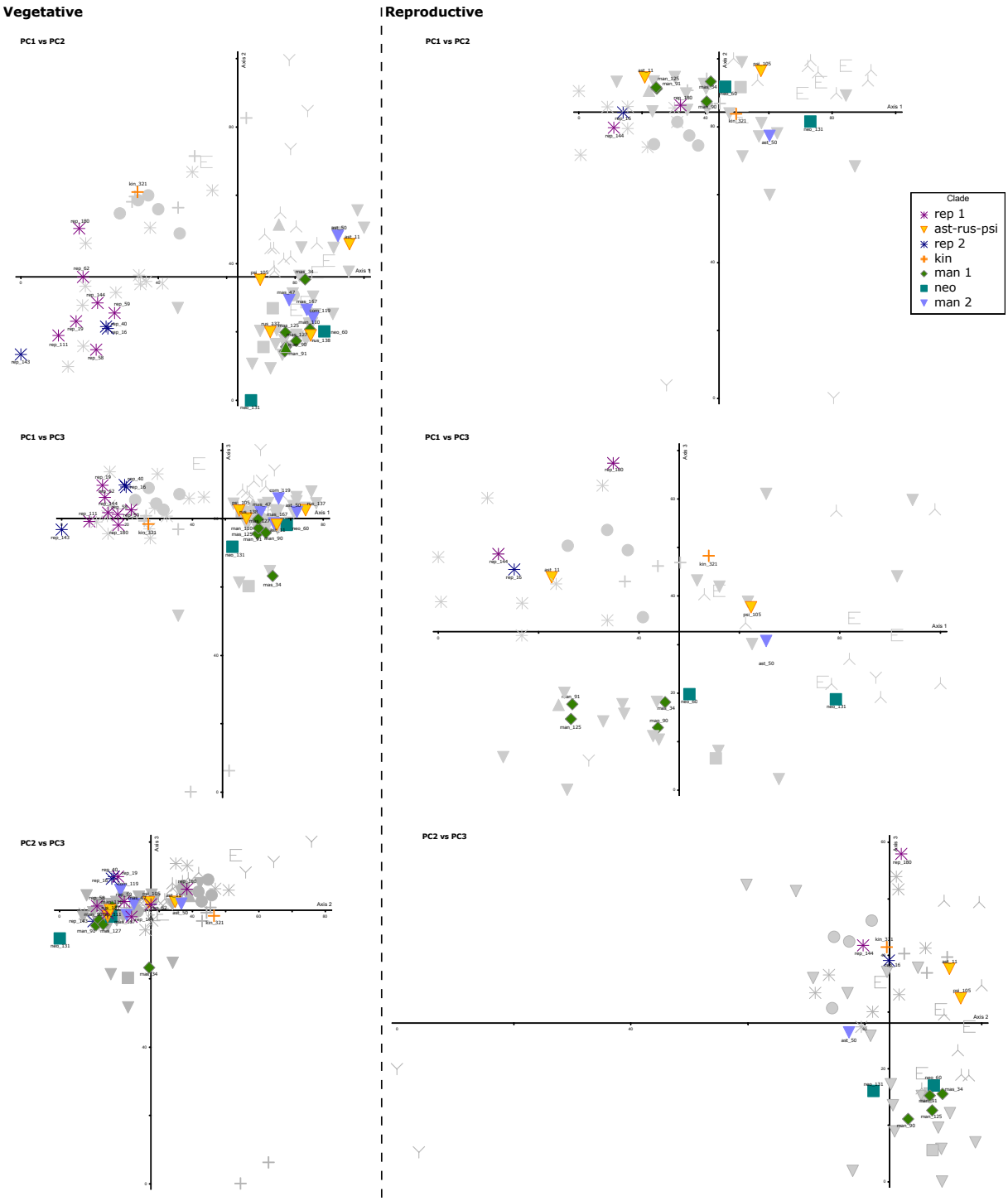

Figure 4.3: Principal component analysis of vegetative and reproductive characters with the samples of the molecular phylogenetic analysis (Figure 4.1) highlighted and designated according to their clade affiliation.

4.5 Discussion

4.5.1 Morpho-species classification and species delimitation Gynoxyoids

Our study is the first presenting a comparative morphological investigation of the Gynoxyoids of Bolivia. The morpho-species classification based on the visual delimitation of the available material by morphological discontinuities corresponding to concepts of the published species was largely corroborated by the principal component analyses. *G. kingii*, *G. repanda*, *G.* sp. nov. B, *G.* sp. nov. A, *G. psilophylla*, *G. megacephala*, *G. asterotricha* and *G. mandonii* were differentiated by vegetative characters and *G. compressissima*, *G. kingii* and *G.* sp. nov. B were differentiated by reproductive characters. *G. longifolia* was not supported for sampling reasons because the only available physical specimen was sterile. *G. neovelutina* is not separated in the PCA because its ovate leaves and constant number of 7 outer phyllaries (versus 1–4 in all other species) as single diagnostic character states in the vegetative and reproductive matrix respectively did not contribute to the first three principal components which are only considered by PC ORD.

Remarkable is the presence of outlier samples in several cases of otherwise fairly well delimited species, see e.g., one specimen of *G. neovelutina* or two specimens of *G. repanda* (Figure 4.2). These blur the delimitation of the clouds and thus of the morpho-species. Revision of the specimens in question nevertheless confirmed their placement in the respective morpho-species in accordance with the set of diagnostic characters defining them. A possible explanation may be introgression between sympatric or adjacently distributed species.

Stronger evidences for the assumption of introgression and hybridization between two species are available in the case of *G. asterotricha* and *G. mandonii*. The PCA separated *G. mandonii* from *G. asterotricha* but a considerable number of specimens is found scattered in between the clouds of both species. These specimens show a greater resemblance to *G. mandonii,* and also in the ETS-ITS tree they are nested with *G. mandonii* which was resolved as biphyletic (Figure 4.1, and see below). The distribution map of these species (Figure 4.7) confirms that *G. asterotricha*, *G. mandonii* and the putative hybrid *G. asterotricha* × *mandonii* are largely sympatric. Moreover, they occupy the same ecological niches. Further molecular and morphological studies on a greater number of specimens should be performed to test this hypothesis. For the time being we treat the three taxa as members of a *G. asterotricha* complex.

A particular case is *G. rusbyi;* it was retrieved in the PCA nested with the specimens of the *G. asterotricha* complex based on vegetative characters and nested in *G. psilophylla* based on reproductive characters. In the ETS-ITS phylogeny the *G. rusbyi* samples are nested in a well-supported polytomy together with *G. asterotricha* and *G. psilophylla*. The morphological differences of *G. rusbyi* to both, *G. asterotricha* and *G. psilophylla,* preclude its placement in

either species. The available evidences instead support the assumption that *G. rusbyi* may be a hybrid between *G. asterotricha* and *G. psilophylla*, which seems also plausible from their distribution areas (Figure 4.5 and 4.7).

4.5.2 Phylogenetic Inference

As it was discussed by Escobari et al. (2021), the study of the Gynoxyoid clade is challenging due to the low genetic distance among the species, which is particularly evident by the extremely low molecular variation in plastid genomes even at genus level. Variation in nuclear ribosomal markers (ITS and ETS) is also low but resolved the Bolivian specimens in ten well supported clades. However, only three morpho-species (*G. megacephala. G. longifolia* and *G. kingii*), were resolved as separate clades. All other morpho-species follow one of two patterns or a combination of both: either multiple morpho-species are nested in the same clade, or a single morpho-species is resolved in separated clades. As mentioned above, *G. asterotricha*, *G. rusbyi* and *G. psilophylla* follow the first pattern, being nested in one polytomous clade, and the apparent morphological differences between the three taxa have no correspondence in the ETS-ITS sequences. The puzzling finding of *G. megacephala* and *Paracalia pentamera* as sister groups in the same early diverging clade may be considered as another example of this pattern. The second pattern is represented by *G. repanda* and *G. mandonii* which both were resolved in strongly supported clades as biphyletic. The two *G. repanda* clades form a trichotomy together with the *G. asterotricha-rusbyi-psilophylla* clade, therefore nothing can be said about their relationships. The relationship of the two *G. mandonii* clades, in contrast, is well-resolved. The *G. mandonii*2 clade and the *G. mandonii*1 together with the *G. neovelutina* clade are consecutive sisters to all other *Gynoxys* clades except for the two earlier diverging ones with *G. longifolia* and *G. megacephala*, respectively. Thus, the two clades are not immediately related. Interestingly, in both *G. mandonii* clades the putative hybrid *G. asterotricha* × *mandonii* (see above) is nested, the *G. mandoni*i clades thus at the same time represent the combined pattern of splitting and uniting morpho-species.

Lacking correlation between morphological delimitation and phylogenetic lineages is not unusual in plant groups of mountain ecosystems. Reasons are the often relatively young age of mountain systems or their ecosystems and a rapid diversification of their taxa by adaptive radiation (Pouchon et al., 2018). Such differences can be caused by incomplete linage sorting, hybridization, reticulate evolution and chloroplast capture (Garcia et al., 2014; Vargas et al.,

2017; Kandziora et al., 2022). Escobari et al. (2021) provided first evidence that also the Gynoxyoids are a young and rapidly evolving group. During this study it was found indications that chloroplast capture may have caused incongruences between plastome phylogeny, nuclear ribosomal phylogenies and morphology.

Altitudinal shifts of ecosystem zonations and expansion-contraction oscillations of distribution areas caused by glaciation cycles can have further effects on the evolution of high mountainous plant groups (Kolar et al., 2016). Introgression and hybridization are likely, when formerly geographically isolated lineages come into contact (Pouchon et al., 2018). This is even more likely in the case of groups such as the Gynoxyoids, where whole genome duplication with some certainty plays an import role in their evolution. The few *Gynoxys* species for which chromosome numbers are known, indicate a basic number of 10 and a somatic number of 80 chromosome, thus octoploidy (Tuner et al., 1967; Powell and Cuatrecasas, 1970; Robinson et al., 1997). The results of our study actually point at the likeliness of ongoing processes of hybridization and introgression among *Gynoxys* species, which should be taken into consideration for the design of further studies on the Gynoxyoids. Chromosome counting in the Gynoxyoids seem in this context an urgent desideratum. Hybridization or, more precisely, recurrent hybridization with different parents may also be a working hypothesis for future studies with respect to the two species *G. mandonii* and *G. repanda* resolved as biphyletic.

4.6 Taxonomic treatment

The taxonomic treatment of the Bolivian Gynoxyoid species was based on the generic revision of the group given in chapter 3. The final morpho-species concept is based the synthesis of the evidences provided by the various analyses of the present study. The initial morpho-species was tested and, in most cases, validated by the PCA. Additional diagnostic morphological characters found by the PCA were incorporated in the taxon characterization. Last but not least, the ETS-ITS phylogeny was especially useful for species delimitation on which the morphological characters were insufficient for a properly classification (i.e., *G. longifolia*, *G. neovelutina*). The taxonomic treatment resulted in the recognition of 14 species of the Gynoxyoid in Bolivia. This represents a reduction of the 24 species reported in Beck and Ibanez (2014). Four species were based on wrong identifications (*G. baccharoides*, *G. hallii*, *G. laurifolia* and *Nordenstamia fabrisii*), seven species were newly synonymized (see checklist), one doubtful (*G. rusbyi*), and twelve were accepted additionally, three species suggested as new for science.

The genus *Paracalia* is represented by a single species and within *Gynoxys* a total of 13 species are recognized.

The taxonomic treatment includes for each accepted species the taxon name, publication, type (! = physical specimen seen, [!] = digital specimen seen) and synonymy information, and the description of the taxon listing the relevant morphological character for its delimitation. Distribution and habitat information including a map, ecoregions and altitudinal records are also provided. The threat status was checked with the IUCN Red List of Threatened Species.

4.6.1 The Gynoxyoid clade in Bolivia

Trees or shrubs (*Gynoxys*) 0.4–12 m high, or scandent (*Paracalia*). Stems always woody, branches woody or herbaceous when young, striated or terete, with or without indumentum. Leaves opposite or alternate, always petiolate; lamina mainly elliptic or ovate; upper face glabrate, lower face pubescent or tomentose of unicellular or multicellular and simple or multibranched trichomes; margin entire or dentate or lobate, with or without small callous-tipped teeth (= mucros); base obtuse, cordate, or irregular; apex acute. Synflorescences axillar or terminal. Involucrum campanulate without or with 1–7 outer phyllaries, inner phyllaries 5 to 10, elliptic with scariose margins. Capitula discoid or radiate, with white or yellow flowers. Ray flowers 3 to 10, pistillate, corolla with 3 terminal teeth; disc flowers 5 to 35, perfect, actinomorphic, cup-shaped, 5–lobed. Anthers with obtuse, auriculate or sagittate base. Style branches with acute or rounded apex and always provided with collecting hairs on the outside of the style arms expanding from the lateral sides upwards forming an arrow-like tip. Pappus of scabrid, white to light brown bristles, dilatated or not at the apex. Achene cylindric, in cross section roundish to striate, surface glabrate, rough, brown. Pappus 1–2 series of barbellate, white to brown bristles.

4.6.2 Key to the genera of the Gynoxyoid clade

Scandent shrub, leaf margin without mucros, capitula white-flowered..... *Paracalia* (1 sp.)

Trees erect, or rarely scandent, shrubs, leaf margin with mucros, capitula yellow-flowered..... *Gynoxys* (14 sp.)

Paracalia Cuatr.

Type: *Paracalia pentamera* (Cuatrec.) Cuatrec.

1 species

La Paz

Scandent shrub; glabrate. Leaves alternate; petiole 1.8–2.3 × 0.2 mm; lamina 9.6–12.6 × 3.2–7 cm, subcoriaceous, ovate, with 11 secondary-veins; upper and lower face always glabrate; margin entire, without mucros, edge brown. Synflorescence axillar, paniculiform. Capitula discoid, white. Involucre 10–17 × 6–8 mm, tubular; outer phyllaries absent; inner phyllaries 5, 10–12 × 2–3 mm long, uniseriate, subcoriaceous, with obtuse apex. Disc flowers 5, 7.5 × 8 mm, corolla tube 3.5 mm, corolla limb absent. Anthers base obtuse to auriculate. Style branches apically obtuse or subtruncate. Achenes 4–5 × 0.8–1 mm, cylindrical. Pappus 8–10 mm, with 1 series of barbellate, white to brown bristles, with broaden tips.

Paracalia pentamera (Cuatrec.) Cuatrec., Brittonia 12: 183. 1960 ≡ *Senecio pentamerus* Cuatrec., Fieldiana, Bot. 27: 57. 1951. – Holotype: La Paz, Larecaja, Copacabana (ca. 10 km. south of Mapiri), 850–950 m, 08 Oct – 15 Nov 1939, *B. A. Krukoff 11150* (NY 259336!; isotypes: A: A00010877[!], F: V0077069F[!], K: K000497545[!], S: S-R-7986[!], U 0105750[!], US 00123446[!]).

Distribution: La Paz. Habitat: Humid Mountain Forest. Altitude: 900–2130 m. (Figure 4.4)

Threat status: Not evaluated

Additional examined specimens: La Paz: Sud Yungas, Municipio de Chulumani, localidad Río Blanco, [-16,267878], [-67,488315], 2130 m, 23 Nov 2011. S. Gallegos 3850* (LPB).

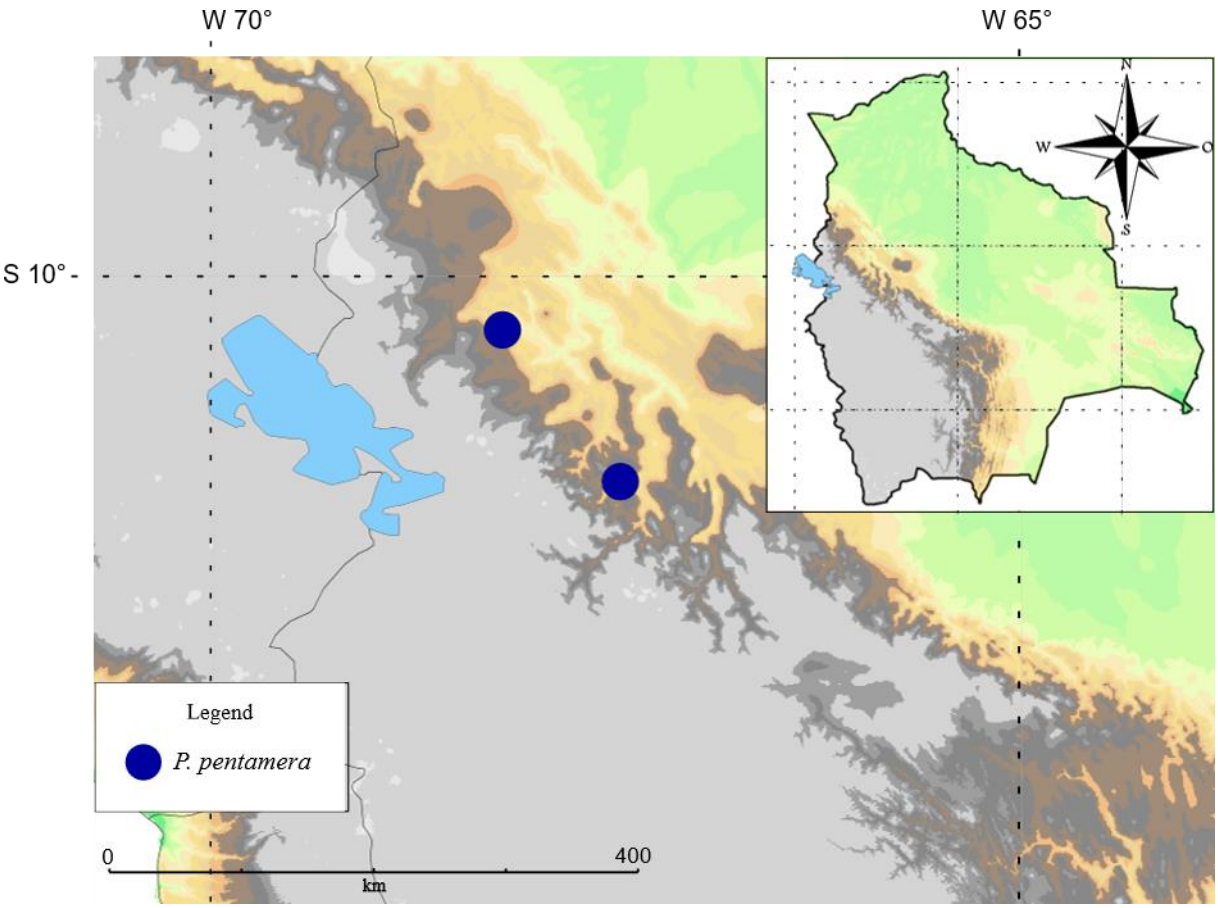

Figure 4.4: Distribution map of *Paracalia pentamera*.

Gynoxys Cass.

Lectotype (Flann et al., 2010:1225): *Gynoxys baccharoides* (Kunth) Cass.

= *Nordenstamia* Lundin, Compositae Newslett. 44: 15–16, f. 1. 2006. Type: *Nordenstamia repanda* (Wedd.) Lundin [≡ *Gynoxys repanda* Wedd.]

13 (14) species

Chuquisaca, Cochabamba, La Paz, Potosí, Santa Cruz, Sucre

Erect or exceptionally scandent shrubs, trees, 0.4–12 m high. Indumentum glabrate to tomentose. Leaves alternate or opposite; petiole 2–72 × 0.8–3.4 mm; lamina 2.2–20 × 1–11 cm, papyraceous to coriaceous, from elliptic to suborbicular, with 4–30 secondary veins; upper face always glabrate; lower face glabrate to tomentose with uni- or multicellular, simple, stellate or T-shaped trichomes; leaf margin entire, dentate, dentate-lobate, angulate-lobate, repand involute or revolute, with mucros. Synflorescence axillar or terminal, paniculiform or corymbiform to cymbiform. Capitula discoid or radiate, yellow. Involucre 5–10 mm; tubular or campanulate; outer phyllaries 1–7, filiform to obovate; inner phyllaries 5–10, 4.5–9.3 mm long,

uni or biseriated, membranaceous or (sub)coriaceous, with acute or obtuse apex. Ray flowers 3–9, limb with 3–5 veins. Disc flowers 5–26, 4.6–12.2 mm, corolla tube 1.4–6.4 mm, corolla limb 2.2–5.7 mm. Anthers with obtuse to sagittate base. Style branches apically obtuse to acute. Achenes 0.9–4.4 × 0.3–1.1 mm. Pappus 3.85–9.8 mm, with 1–2 series of barbellate, white or yellow bristles, with or without broaden tips.

Key to *Gynoxys* species

1 Capitula discoid …….2

1’ Capitula radiate……...3

2 Synflorescence axillar; leaf lamina with length/width ratio > 5, secondary veins 29–30 ……...*G. longifolia*

2’ Synflorescence terminal; leaf lamina with length/width ratio < 1.5, secondary veins <6…….*G. megacephala*

3 Leaves glabrate……*G. psilophylla*

3' Leaves with indumentum…….4

4 Leaf trichomes multicellular……5

4’ Leaf trichomes unicellular……...9

5 Leaf trichomes stellate, leaves normally alternate……6

5’ Leaf trichomes simple or T-shaped, leaves opposite……8

6 Leaves ovate and 6–7.5 × 4.2–4.5 cm, margin with angular lobes…….…*G. kingii*

6' Leaves of other shapes and 5.6–23.4 × 2.5–11.2 cm, margin of various shapes..……7

7 Leaves oblong, length/width ratio of lamina ca 3…….*G.* sp. nov. B

7’ Leaves elliptic, length/width ratio of lamina >4……...*G. repanda*

8 Leaf trichomes T-shaped, petiole > 1.25 cm; leaf margin involute, lamina with white edge……..*G.* sp. nov. A

8’ Leaf trichomes simple, petiole < 1 cm, leaf margin revolute, with brown edge……...*G.* sp. nov. C

9 Twigs with petiole scares very prominent, petiole 2.5 mm wide…….….10

9' Twigs with petiole scares not prominent, petiole < 2.5 mm wide……11

10 Leaves ovate; involucre with outer phyllaries always 7……..*G. neovelutina*

10' Leaves oblong; involucre with outer phyllaries 3–4……*G. sorataensis*

11 Leaves papyraceous to membranaceous, indumentum arachnoid; involucre 0.8–0.9 cm; disc flowers with tube up to 5 mm……..*G. compressissima*

11' Leaves coriaceous or subcoriaceous, indumentum pubescent or tomentose; involucre < 0.8 cm; disc flowers with tube up to 4.5 mm……*G. asterotricha* complex

NB: Attention should be paid to the occurrence of putative hybrids with intermediate morphology, see also *G. rusbyi* (p. 25).

Gynoxys longifolia Wedd., Chlor. Andina 1(3): 79. 1855. – Syntypes: Perú. Cuzco, Andes de Cuzco, Oct 1839 – Feb 1940, *Gay s.n.* (F: V0076718F[!], P: P00711417[!] P00711418[!] P00711419[!], US 00122917 (fragments) [!]).

Shrub, 2 m high. Twigs lacking prominent petiole scares. Leaves opposite; petiole 12.5 × 2 mm; lamina 11–14 × 1.9–2.5 cm, membranaceous, oblong, with 29–30 secondary veins; lower face tomentose of unicellular simple hairs; margin entire, revolute, with brown edge. Synflorescence axilar, cymbiform. Capitula discoid. Involucre 4.7–6.7 mm long, campanulate; outer phyllaries 3–4, oblong; inner phyllaries 4.7–5.4 mm long, coriaceous, with acute apex. Disc flowers 6.3 mm long; tube 3.4 mm, limb 2.6 mm long; tube 0.8 mm wide at base. Anthers 3 mm long, with sagittate base. Style branches 2.3 mm long, with rounded apex.

Distribution: La Paz. Habitat: Pajonal. Altitude: 3115 m. (Figure 4.5)

Threat status: Not evaluated

Additional examined specimens: La Paz: José M Camacho, Jachacirca, -15.4833, -68.45317, 3115 m, 13 Jun 2006, T. Ortuño 639* (LPB).

Gynoxys megacephala Rusby, Bull. New York Bot. Gard. 4: 398. 1907. – Syntypes: *M. Bang 1959* (F: V0076754F (fragments) [!], GH: GH00008597[!], K: K000497526[!], MICH: MICH1107432[!], MO: MO-1183133[!], NY 178867[!] 178868[!], PH: PH00013514[!], US 00122920[!], WIS: WISv0256704WIS[!]); Huaycani, 11000 ft., May 1866, *Pearce s.n.* (MO: s.n.).

= *Gynoxys foliosa* (Rusby) S. F. Blake, Contr. U.S. Natl. Herb. 24: 86. 1922, **syn. nov.** ≡ *Diplostephium foliosum* Rusby, Bull. New York Bot. Gard. 8(28): 128–129. 1912. – Syntypes: Cargadira, 8000 ft., 29 Jul 1902, *W. Roberts 1529* (BM: BM001024073[!], F: V0076745F[!], K: K000497534[!], NY 168221[!]).

Shrub, 1.3–3 m high. Twigs lacking prominent petiole scares. Leaves 3-verticillate, (sub)opposite; petiole 4–5 × 1.5–2 mm; lamina 2.2–4.3 × 1.3–2.4 cm, (sub)coriaceous, elliptic or obovate, with 5–6 secondary veins; lower face tomentose of multicellular simple hairs; margin entire, revolute, with brown edge. Synflorescence terminal, corymbiform, cymbiform or paniculiform. Capitula discoid. Involucre 7–9 mm long, tubular; outer phyllaries 1–4, filiform or obovate; inner phyllaries 7.2–8.3 mm long, (sub)coriaceous, with acute or obtuse apex. Disc flowers 8.4–12.2 mm long; tube 4.4–6.4 mm, limb 2.4–4.5 mm long; tube 0.9–1 mm wide at base. Anthers 2–3.4 mm long, with auriculate or sagittate base. Style branches 2.2–3.9 mm long, with acute apex.

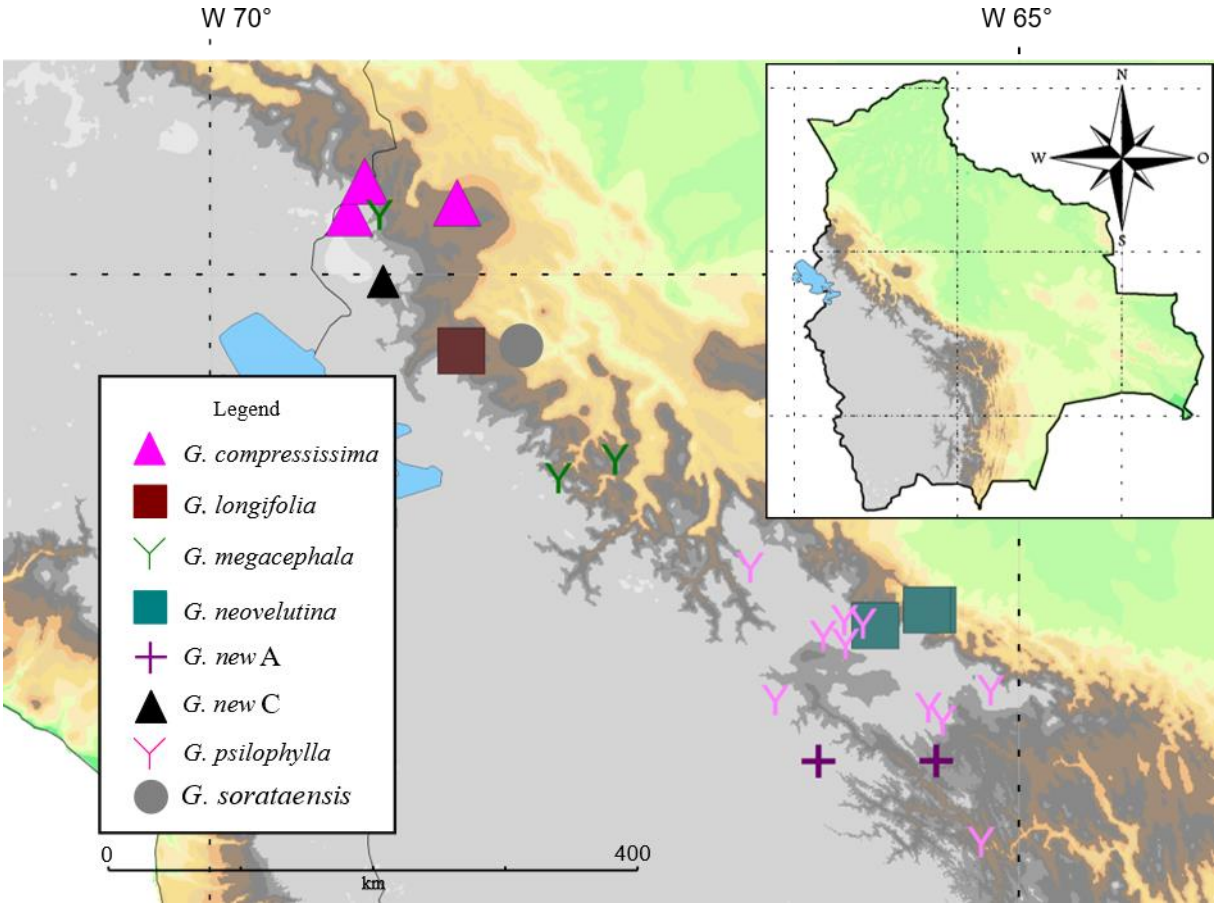

Figure 4.5: Distribution map of *Gynoxys compressissima*, *G. longifolia*, *G. megacephala*, *G. neovelutina*, *G.* sp. nov. A, *G.* sp. nov. C, *G. psilophylla* and *G. sorataensis.*

Distribution: La Paz. Habitat: Humid Mountain Forest to Ceja de monte. Altitude: 2500–3850 m. (Figure 4.5).

Threat status: Not evaluated

Additional examined specimens: La Paz: Franz Tamayo, Parque Nacional Madidi, entre Tocoaque y Chucani, entre Keara y Mojos, -14.62528, -68.95944, 2500 m, 4 Oct 2009, A. Fuentes 15602 (B 10 0720919). La Paz: Nor Yungas, 29,5 km bajando de la cumbre hacia Coroico, -16.28615, -67.85000, 3180 m, 1 Aug 2010, S. Beck 32686 (B 10 0720255). La Paz: Nor Yungas, La Paz - Coroico ca 1 km W Cotapata, -16.17, -67.5, 3200 m, 22 Aug 1999, J. Müller 7454 (LPB).

Gynoxys psilophylla Klatt, Ann. K. K. Naturhist. Hofmus. 9: 367. 1894 ≡ *Gynoxys glabriuscula* Rusby, Mem. Torrey Bot. Club 6(1): 68. 1896, nom. illeg. – Syntypes: Cochabamba, 1 Jul 1891, *M. Bang 1116* (A: A00008585[!], BR: BR0000005318186[!] BR0000005318513[!], E: E00413271[!], F: V0076765F[!], GH: GH00008606[!] GH00008607[!], US 00122935[!], WIS: WISv0256703WIS[!]).

= *Gynoxys hoffmannii* Kuntze, Revis. Gen. Pl. 3(3): 156. 1898, **syn. nov.** – Syntype: Cochabamba, Weg zum Río Juntas, 3000 m, 13–21 Apr 1892. *O. Kuntze s.n.* (NY 178859[!]).

= *Gynoxys boliviana* (Klatt) S. F. Blake, Contr. Gray Herb. 53: 28. 1918, **syn. nov.** ≡ *Liabum bolivianum* Klatt., Ann. K. K. Naturhist. Hofmus. 9: 362. 1894. – Holotype: Bolivia, *Cuming s.n.* (W: W18890106172[!]; isotype: GH: GH00008573 (fragment with drawing)[!]).

Shrub, 0.4–2.5 m high. Twigs lacking prominent petiole scares. Leaves opposite; petiole 12–35 × 1.4–1.7 mm; lamina 3.6–11 × 1.6–4.5 cm, membranaceous to subcoriaceous, elliptic or oblate, with 8–14 secondary veins; lower face glabrescent; margin entire, revolute, with brown edge. Synflorescence terminal, corymbiform, cymbiform or paniculiform. Capitula radiate. Involucre 6–9 mm long, campanulate; outer phyllaries 2–4, obovate; inner phyllaries 5.4–8 mm long, (sub)coriaceous, with acute or obtuse apex. Ray flowers with 4–5 limb veins. Disc flowers 7.6–10.6 mm long; tube 2.4–4.2 mm, limb 3–5.2 mm long; tube 0.7–1.2 mm wide at base. Anthers 2.2–3.4 mm long, with sagittate base. Style branches 1.4–2.3 mm long, with acute to rounded apex.

Distribution: Chuquisaca, Cochabamba, La Paz, Potosi. Habitat: Humid Mountain Forest, Ceja de monte, Dry valley and Puna. Altitude: 2800–4120 m. (Figure 4.5)

Threat status: Not evaluated

Additional examined specimens: Cochabamba: Laguna Wara Wara, -17.1829, -66.0804, 4125 m, 30 Jul 2007, C. Aedo 14429 (LPB). Cochabamba: Arani, desviando hacia Chaupiloma alto, pasando Totota, -65.17278, -17.62500, 3600 m, 24 Jul 2017, B. Escobari, N. Kilian, H. Villca & B. Nieto 299 (B 10 0763248). Cochabamba: Arque, carretera de vuelta CBBA-Oruro, Sayari, -66.50722, -17.68667, 4100 m, 25 Jul 2017, B. Escobari, N. Kilian 313 (B 10 0763265; B 10 0763266). Cochabamba: Chapare, Colomi, camino entre Colomi - Candelaria, -65.96472, -17.20583, 3400 m, 17 Jul 2017, B. Escobari, N. Kilian & H. Villca 176 (B 10 0763097). Cochabamba: Chapare, Colomi, camino a Sapanani, -66.07306, -17.33250, 3900 m, 19 Jul 2017, B. Escobari, N. Kilian & H. Villca 208 (B 10 0763133; B 10 0763134). Cochabamba: Ayopaya, Cocapata, desvío hacia la Rinconada, -66.66194, -16.85167, 3600 m, 22 Jul 2017, B. Escobari, N. Kilian, H. Villca & B. Nieto 247 (B 10 0763187). Cochabamba: Ayopaya, Cocapata, camino de ida a Tiquipaya, -66.21056, -17.28306, 4000 m, 22 Jul 2017, B. Escobari, N. Kilian, H. Villca & B. Nieto 277 (B 10 0763221). Cochabamba: Ayopaya, Cocapata, camino de ida a Tiquipaya, -66.21056, -17.28306, 4000 m, 22 Jul 2017, B. Escobari, N. Kilian, H. Villca & B. Nieto 279 (B 10 0763223). Cochabamba: Arani, Vacas, camino de bajada pasando el santuario de las Puyas, -65.56000, -17.73694, 3800 m, 23 Jul 2017, B. Escobari, N. Kilian, H. Villca & B. Nieto 289 (B 10 0763235; B 10 0763236). Cochabamba: Arani, Vacas, camino asfaltado a Mizque, -65.47000, -17.81722, 3100 m, 23 Jul 2017, B. Escobari, N. Kilian, H. Villca & B. Nieto 292* (B 10 0763239; B 10 0763240). Chuquisaca: Oropeza, Cerro Chataquila, c 15 km past El Bramadero towards Cajamarca, -18.5826, -65.2331, 3380 m, 28 Mar 2007, J.R.I. Wood 23288 (LPB).

Gynoxys kingii (H. Rob. & Cuatrec.) Escobari & N. Kilian, **comb. nov.** ≡ *Aequatorium kingii* H. Rob. & Cuatrec., Novon 2(4): 412. 1992 ≡ *Nordenstamia kingii* (H. Rob. & Cuatrec.) B. Nord., Compositae Newslett. 44: 20. 2006. – Holotype: Cochabamba, 15 km from Colomi, on the road to Tunari, 10600 ft., 7 Feb 1978, *King & Bishop 7680* (US 00409565[!]).

Shrub, 1–4 m high. Twigs lacking prominent petiole scares. Leaves alternate; petiole 15–33 × 1.8–2 mm; lamina 6–9 × 2.6–5.5 cm, membranaceous, ovate, with 6–9 secondary veins; lower face pubescent of multicellular stellate hairs; margin dentate or rarely entire, revolute, with brown edge. Synflorescence terminal, cymbiform. Capitula radiate. Involucre 6.5–9 mm long, campanulate; outer phyllaries 2–4, oblong; inner phyllaries 6.8–8.8 mm long, (sub)coriaceous, with acute or obtuse apex. Ray flowers with 4 limb veins. Disc flowers 6.4–7.9 mm long; tube 1.9–3.6 mm, limb 3.3–4.7 mm long; tube 0.6–1 mm wide at base. Anthers 2–2.5 mm long, with auriculate or sagittate base. Style branches 1.6–2.2 mm long, with acute to rounded apex.

Distribution: Cochabamba, Santa Cruz. Habitat: Humid Mountain Forest. Altitude: 2700–3000 m. (Figure 4.6)

Threat status: Not evaluated

Additional examined specimens: Cochabamba: Carrasco, Montepunco road to Sehuenas, -65.28000, -17.56889, 2788 m, 21 Dic 2003, L. Rico, T. Windsor-Shaw, McRobb & L. Alvarez 1303 (K000295050). Cochabamba: Carrasco, 5 km al NE de Monte Punco por el camino a Sihuenca, -17.34, -65.15, 2700 m, 10 Mar 1988, J. Solomon 18067* (LPB). Cochabamba: Carrasco, ca 4km from Monte Puncu towards Sehuencas, [-17.576118], [-65.28245], 3000 m, 5 Feb 1995, J.R.I. Wood 9342 (K000374292). Santa Cruz: Caballero, c 15 km east of Siberia along road to Comarapa, -17.5011, -64.4409, 2989 m, 6 Mar 2007, J.R.I. Wood 22990 (LPB).

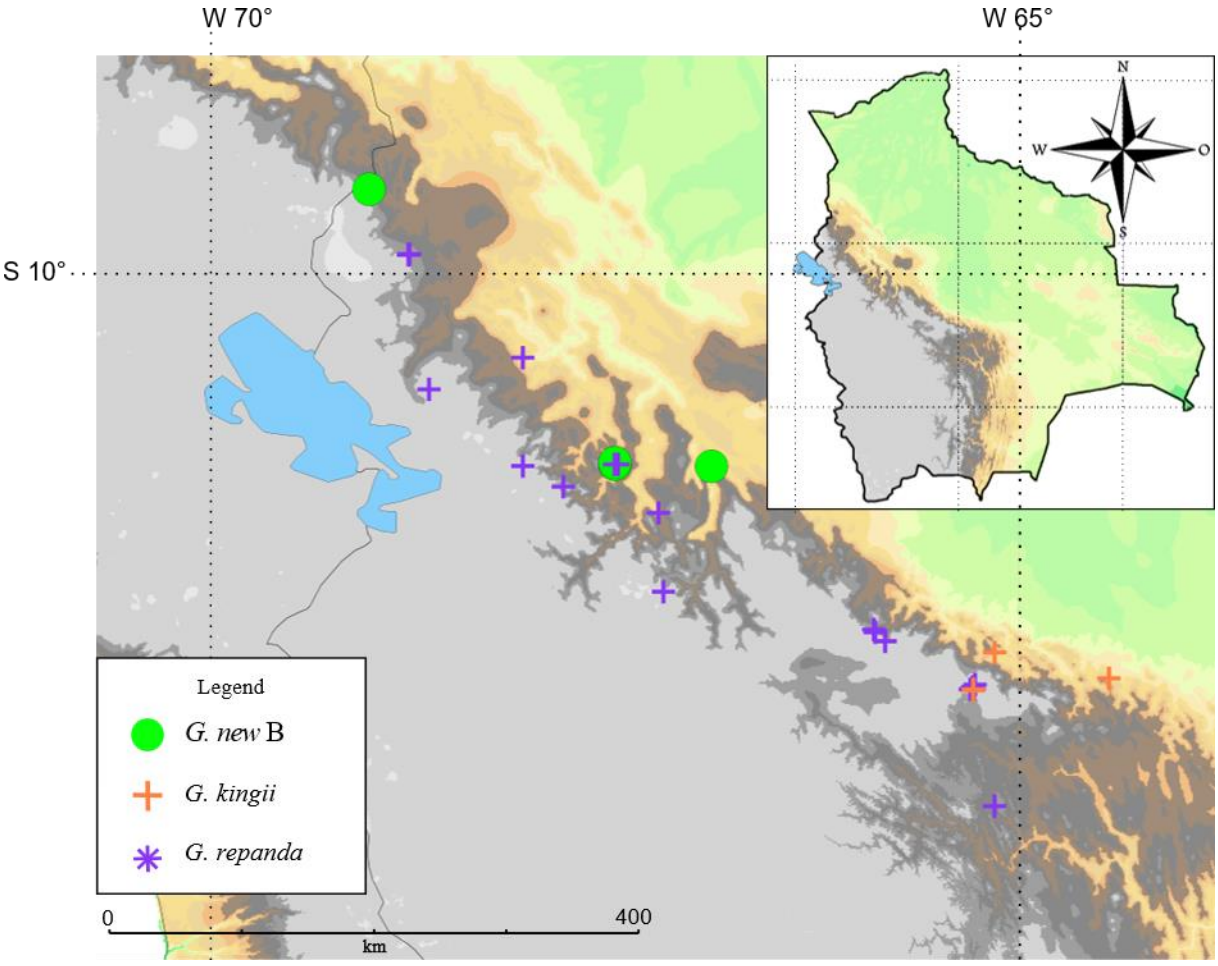

Figure 4.6: Distribution map of *Gynoxys kingii*, *G. repanda* and *G.* sp. nov. B.

***Gynoxys* sp. nov. B**

Diagnosis: This species resembles *Gynoxys repanda* but differs from that by its oblong leaves with a length/width ratio of ca 3 (versus length/width ca 2) and the rusty (versus whitish) indumentum on the lower leaf face.

Shrub, 2–2.5 m high. Twigs lacking prominent petiole scares. Leaves alternate; petiole 11–33 × 1.8–2.5 mm; lamina 9.2–12.7 × 2.5–4.5 cm, subcoriaceous, elliptic or ovate, with 8–14 secondary veins.; lower face pubescent of multicellular stellate hairs; margin entire or sinuate, revolute, with brown edge. Synflorescence terminal, corymbiform, cymbiform or paniculiform. Capitula radiate. Involucre 5.4–8.8 mm long, tubular; outer phyllaries 1–3, filiform or oblong; inner phyllaries 5.7–8 mm long, (sub)coriaceous, with acute or obtuse apex. Ray flowers with 3–4 limb veins. Disc flowers 6.4–8.2 mm long; tube 3.2–4.1 mm, limb 2.6–4.5 mm long; tube 0.7–0.8 mm wide at base. Anthers 2.2–2.9 mm long, with rounded, auriculate or sagittate base. Style branches 1.9–2.7 mm long, with rounded apex.

Distribution: La Paz. Habitat: Humid Mountain Forest. Altitude: 3100 m. (Figure 4.6)

Threat status: Not evaluated yet.

Examined specimens: La Paz: Nor Yungas, Hornuni Alto, 15 m al costado de la 3° estación metereológica, -16.19194, -66.90250, 3140 m, 7 Aug 2003, S. Beck 28794 (B 10 0720277). La Paz: Nor Yungas, Hornuni Alto, 15 m al costado de la 3° estación metereológica, -16.19194, -66.90250, 3140 m, 7 Aug 2003, S. Beck 28794A (B 10 0720279).

La Paz: Nor Yungas, La Paz - Coroico ca 05 km E Cotapata, -16.17, -67.5, 3150 m, 22 Aug 1999, J. Müller 7464 (LPB). La Paz: ANMI Apolobamba Sector Manzana, por el antiguo camino Pelechuco-Apolo, -14.4811, -69.0235, 3142 m, 30 Jun 2009, A. Fuentes 15049 (LPB). La Paz: Nor Yungas, pasando Unduavi, fin del asfalto, Cotapata, -16.18, -67.5, 3100 m, 29 May 1994, S. Beck 21376 (LPB).

Gynoxys repanda Wedd., Chlor. Andina 1(3): 77. 1855 ≡ *Aequatorium repandum* (Wedd.) C. Jeffrey, Kew Bull. 47(2): 292. 1992 ≡ *Nordenstamia repanda* (Wedd.) Lundin, Compositae Newslett. 44: 16. 2006. – Syntypes: La Paz, Larecaja, Vallée de Tipuani, 1851, *M. Weddell s.n.* (F: V0076768F (fragments) [!], P: P02273082[!], US 00122936 (fragments)[!])

Note: We consider the locality designation in the protologue “dans les taillis, sur le versant orientale du mont Illampù” to correspond to the (upper) Valle de Tipuani given on the label of the above specimen, because of its location east of Mt. Illampu. No specimen with the locality designation in the protologue could be found.

= *Schistocarpha triangularis* Rusby, Bull. New York Bot. Gard. 4: 392. 1907. – Syntypes: La Paz, Unduavi, Sep 1894, *M. Bang 2477* (F: V0076813F[!], GH: GH00549665[!], US 00122819[!] 00955547[!]).

= *Gynoxys alternifolia* Sch. Bip. ex Rusby, Mem. Torrey Bot. Club 6(1): 67. 1896 [– *Gynoxys alternifolia* Sch. Bip. Linnaea 34: 531. 1865, nom. nud.] ≡ *Senecio alternifolius* (Sch. Bip. ex Rusby) Greenm., Ann. Missouri Bot. Gard. 10: 76. 1923. – Syntypes: La Paz, Vic. Mapiri, 8000 ft, Sep 1892, *Bang 1574* (A: A00008569[!], F: V0076725F[!], GH: GH00549664[!], K: K000634163[!], NDG: NDG62631[!], NY 114876[!] 114877[!], PH: PH00013520[!], PUL: PUL00000344[!], US 00122884[!]). La Paz, Larecaja, Viciniis Sorata, inter Laripata et tani, in nemoribus, 3000–3200 m, Apr 1858–May 1859, *Mandon 131* (BR: BR0000005318605[!], GH: GH00012072[!], K: K000497519[!], MPU: MPU016063[!], P: P02273079[!] P04099622[!] P00711394[!] P00711395[!]).

Shrub or tree, 1.5–7 m high. Twigs lacking prominent petiole scares. Leaves alternate; petiole 11–72 × 1.4–3.3(4) mm; lamina 6–23.4 × 2.5–11.2 cm, papyraceous to coriaceous, elliptic, obovate, ovate, oblong or suborbicular, with 7–16 secondary veins; lower face pubescent rarely glabrescent of multicellular stellate hairs; margin entire, dentate or lobate, revolute, with brown edge. Synflorescence terminal, corymbiform, cymbiform or paniculiform. Capitula radiate. Involucre 6–9 mm long, tubular or campanulate; outer phyllaries 1–4, filiform, oblong or triangular; inner phyllaries 4.8–7.9 mm long, (sub)coriaceous, with acute or obtuse apex. Ray flowers with 3–5 limb veins. Disc flowers 5.3–7.6 mm long; tube 1.4–3.9 mm, limb 2.5–3.9 mm long; tube 0.4–1.2 mm wide at base. Anthers 1.6–2.5 mm long, with rounded or auriculate base. Style branches 1.2–2.2 mm long, with acute to rounded apex.

Distribution: Cochabamba, La Paz. Habitat: Humid Mountain Forest to Ceja de monte. Altitude: 2200–3300 m. (Figure 4.6)

Threat status: Not evaluated

Additional examined specimens: Cochabamba: Carrasco, c 6 km below Sehuencas, -18.29, -65.15, 2200 m, 30 Jul 1995, J.R.I. Wood 10093* (LPB). Cochabamba: Carrasco, Monte Punco, camino a Sehuencas, -65.28500, -17.55556, 3000 m, 5 Oct 2016, B. Escobari, S. Beck, & C. Beck 87 (B 10 0720939). Cochabamba: Carrasco, Monte Punco, camino a Sehuencas, -65.29889, -17.56889, 3000 m, 5 Oct 2016, B. Escobari, S. Beck, & C. Beck 86 (B 10 0720938). Cochabamba: Carrasco, Monte Punku, entrando hacia Yungas, -65.27056, -17.54056, 2700 m, 24 Jul 2017, B. Escobari, N. Kilian & H. Villca 308* (B 10 0763259). Cochabamba: Carrasco, Monte Punku, entrando hacia Yungas, -65.27694, -17.56722, 2800 m, 24 Jul 2017, B. Escobari, N. Kilian & H. Villca 305 (B 10 0763255). Cochabamba: Chapare, camino Cochabamba - Villa Tunari, [-17.2], [-65.8972222222], [3100] m, 23 Sep 1982, A. Cabrera 33718 (LPB).

Cochabamba: Chapare, Inka Chaka, camino subiendo a hidroelectrica, -65.82667, -17.27306, 3100 m, 16 Jul 2017, B. Escobari, N. Kilian & H. Villca 132* (B 10 0763052; B 10 0763053). Cochabamba: Chapare, Inka Chaka, camino subiendo a hidroelectrica, -65.82778, -17.27167, 3100 m, 16 Jul 2017, B. Escobari, N. Kilian & H. Villca 129* (B 10 0763045). Cochabamba: Chapare, Inka Chaka, camino subiendo a hidroelectrica, -65.88833, -17.21694, 3300 m, 16 Jul 2017, B. Escobari, N. Kilian & H. Villca 147* (B 10 0763069; B 10 0763070). La Paz: ANMI Apolobamba, Chaka, 1,8 km al SE del campamento hacia el Codo, -14.88472, -68.77750, 3281 m, 15 Aug 2009, M. Cornejo 717 (MO-3000641). La Paz: ANMI Apolobamba, Chaka, 300 m al NE del campamento minero, parcela temporal de muestreo (0,1 ha), -14.88428, -68.77728, 3200 m, 23 Aug 2009, M. Cornejo 915 (MO-3000665). La Paz: ANMI Apolobamba, Chaka, campamento minero, sendero Apacheta - El Codo, -14.88497, -68.77825, 3315 m, 21 Aug 2009, M. Cornejo 931 (MO-3000637). La Paz: ANMI Apolobamba, Laji Sorapata, Chaka, El Codo, 2,6 km al E del campamento Chaka, al NE de El Codo, -14.88100, -68.77033, 3162 m, 16 Aug 2009, M. Cornejo 772 (MO-3000644). La Paz: ANMI Apolobamba, Laji Sorapata, Chaka, El Codo, 2,6 km al E del campamento Chaka, al NE de El Codo, parcela temporal de muestreo (0,1 ha), -14.88100, -68.77033, 3162 m, 16 Aug 2009, M. Cornejo 774 (MO-3000664). La Paz: Inquisivi, Camillaya arriba del pueblo, -16.96667, -67.20000, 3000 m, 29 Sep 1997, S. Beck 24375* (B 10 0720276). La Paz: Inquisivi, Choquetanga-Aguas Calientes-Calachaca, cuenca del río Calachaca-Jahura, -16.48, -67.23, 3300 m, 17 Jul 1991, M. Lewis 39262 (LPB). La Paz: Larecaja, pasando Laripata, camino hacia Pacuni-Chinchaya, -68.65000, -15.71667, 3330 m, 7 Aug 2016, B. Escobari, S. Beck, & C. Beck 66* (B 10 0720934). La Paz: Murillo, 245 km N of (below) the pass at the head of the Zongo Valley, -16.19, -68.07, 3100 m, 16 Sep 1984, J. Solomon 12372 (LPB). La Paz: Nor Yungas, entrando a la Ecovia, 36 km desde la cumbre bajando a Unduavi, -67.81964, -16.31736, 3000 m, 5 Jul 2016, B. Escobari, S. Beck, & C. Beck 41* (B 10 0720927). La Paz: Nor Yungas, entrando a la Ecovia, 36 km desde la cumbre bajando a Unduavi, -67.81964, -16.31736, 3000 m, 5 Jul 2016, B. Escobari, S. Beck, & C. Beck 44* (B 10 0720928). La Paz: Nor Yungas, entre Cotapata y Chuspipata, -16.18, -67.5, 3100 m, 1 May 1989, D. Smith 13051 (LPB). La Paz: Nor Yungas, pasando Chuspipata, por elcamino viejo, -16.18, -67.48, 3250 m, 10 Aug 1981, J. Solomon 6024 (LPB). La Paz: Sud Yungas, Cantón Yanacachi Mina Chojlla, Kacapi, -15.52, -68.07, 2182 m, 28 Jul 2000, R. Siñani 264* (LPB).

***Gynoxys* sp. nov. A**

Diagnosis: The combination of a lower leaf face indumentum of T-shaped hairs and a revolute leaf margin with a white edge makes this species unique in the whole genus.

Shrub, 1–2 m high. Twigs lacking prominent petiole scares. Leaves opposite; petiole 14–31 × 2–3 mm; lamina 3.6–10.20 × 2–5.4 cm, papyraceous to subcoriaceous, ovate or oblong, with 8–10 secondary veins; lower face pubescent of multicellular T-shaped hairs; margin entire, involute, with white edge. Synflorescence terminal, cymbiform or paniculiform. Involucre 6–7 mm long, campanulate; outer phyllaries 2–4, obovate; inner phyllaries 5–5.4 mm long, (sub)coriaceous, with acute or obtuse apex. Flowers and fruits not seen.

Distribution: Cochabamba, Potosi. Habitat: Humid Mountain Forest. Altitude: 3200–3300 m. (Figure 4.5)

Threat status: Not evaluated

Examined specimens: Cochabamba: Quillacollo, Wakaplaya, [-18.072956], [-66.238824], 3600 m, 13 Oct 1989, I. Hensen 249 (LPB). Potosí: Charcas, Toro Toro, Quebrada Mula Wacana en el Cerro Manka Paki, -18.07, -65.5109, 3315 m, 27 Feb 2003, J.R.I. Wood 19248 (LPB).

***Gynoxys* sp. nov. C**

Diagnosis: This species resembles *G. marcapatana* from Peru but clearly differs from the latter by the wavy papyraceous leaves with sinuated leaf margin provided by very prominent mucros (versus coriaceous leaves with entire margin and unnoticeable mucros) and its corymbiform synflorescence (versus paniculiform).

Scandent shrub. Twigs supplied by prominent petiole scares. Leaves opposite; petiole 6–9 × 0.2 mm; lamina 3.7–5.4 × 1.7–2.1 cm, subcoriaceous, ovate or oblong, with 9–11 secondary veins; lower face tomentose of multicellular simple hairs; margin weakly sinuate, revolute, with brown edge. Synflorescence terminal, corymbiform. Capitula radiate. Involucre 6–7 mm long, campanulate; outer phyllaries 3, filiform; inner phyllaries 5.5 mm long, (sub)coriaceous, with acute apex. Ray flowers with 4–5 limb veins. Disc flowers 7–7.33 mm long; tube 2.5–2.6 mm, limb 3.2–3.4 mm long; tube 0.4 mm wide at base. Anthers 2.4–2.5 mm long, with rounded or auriculate base. Style branches 1.3–1.8 mm long, with acute apex.

Distribution: La Paz. Habitat: Ceja de monte. Altitude: 3500 m. (Figure 4.5)

Threat status: Not evaluated

Examined specimens: La Paz: ANMI Apolobamba, Pajan, Cerro Machu Layuj, -15.11222, -68.89500, 3487 m, 28 May 2010, L. Cayola 3873 (B 10 0720263).

Gynoxys neovelutina Cuatrec., Fieldiana, Bot. 27(2): 11. 1951. – Holotype: Bolivia, 3000 m, 1–4 Apr 1892, *O. Kuntze* (NY 178869[!]; isotype: F: V0076755F (fragment)[!]).

= *Gynoxys tablaensis* Cabrera, Blumea 7: 197. 1952, **syn. nov.** – Syntypes: Cochabamba, Tablas, 3400 m, May 1911, *T. Herzog 2201* (B: B 10 0093559!, L: L0001978[!] L0001979[!], LP: LP000276[!], S: S-R-2690[!], Z: Z-000003473 (fragments)[!]).

Shrub or tree, 3–5 m high. Twigs supplied by prominent petiole scares. Leaves opposite; petiole 18–37 × (2)3–3.4 mm; lamina 8.1–19.9 × 3.6–5.6 cm, (sub)coriaceous, ovate, with 11–15 secondary veins; lower face tomentose of unicellular simple hairs; margin entire, revolute, with brown edge. Synflorescence terminal, paniculiform. Capitula radiate. Involucre 7–10 mm long, campanulate; outer phyllaries 7, filiform, triangular or oblong; inner phyllaries 6.7–8.2 mm long, coriaceous, with obtuse apex. Ray flowers with 3–4 limb veins. Disc flowers 8–9.2 mm long; tube 2.5–3.8 mm, limb 3.9–5.5 mm long; tube 0.7–0.9 mm wide at base. Anthers 2.3–2.7 mm long, with auriculate base. Style branches 1.4–1.7 mm long, with acute to rounded apex.

Distribution: Cochabamba. Habitat: Humid Mountain Forest to Ceja de monte. Altitude: 3200–3500 m. (Figure 4.5)

Threat status: Data deficient (*Gynoxys tablaensis*). Endangered (*Gynoxys neovelutina*).

Additional examined specimens: Cochabamba: Chapare, Inka Chaka, camino subiendo a hidroelectrica, -65.88833, -17.21694, 3300 m, 16 Jul 2017, B. Escobari, N. Kilian & H. Villca 133* (B 10 0763054; B 10 0763055). Cochabamba: Chapare, below Embalse to Corani along from Cochabamba to Villa Tunari, -17.12, -65.535, 3268 m, 12 Mar 2007, J.R.I. Wood 23092 (LPB). Cochabamba: Chapare, ca 8 km N Maycamayu, -17.12, -65.57, 3550 m, 12 Aug 1991, M. Kessler 2905* (LPB).

Gynoxys sorataensis Cuatrec., Fieldiana, Bot. 27(2): 12. 1951. – Syntypes: Bolivia, La Paz, Sorata, 10000 ft, Feb 1886, *H. H. Rusby 1638* (F: V0076773F[!] s.n., MO: s.n., NY 178876[!]).

Shrub, 1.5 m high. Twigs supplied by prominent petiole scares. Leaves opposite; petiole 8–40 × 2.5 mm; lamina 11–12 × 3.1–3.4 cm, subcoriaceous, oblong, with 13–15 secondary veins; lower face tomentose of unicellular simple hairs; margin entire, revolute, with brown edge. Synflorescence terminal, cymbiform or paniculiform. Capitula radiate. Involucre 8 mm long,

campanulate; outer phyllaries 4–6, filiform; inner phyllaries 6.5 mm long, coriaceous, with obtuse apex. Flowers and fruits not seen.

Distribution: La Paz. Habitat: Ceja de monte. Altitude: 3800 m. (Figure 4.5)

Threat status: Not evaluated

Additional examined specimens: La Paz: Larecaja, localidad de Hirola, pasando Lipichi, -15.44480, -68.18238, 3881 m, 5 Nov 2008, A. Palabral 703 (B 10 0720253).

Gynoxys compressissima Cuatrec., Fieldiana, Bot. 27(2): 4. 1951. – Holotype: Perú. Huanuco, Tambo de Vaca, ca. 12000 ft., 10–24 Jun 1923, *J. F. Macbride 4435* (F: V0076738F[!]; isotype US 00122896[!]).

Tree, 5 m high. Twigs lacking prominent petiole scares. Leaves opposite; petiole 22–41 × 1.5–2 mm; lamina 4.1–12.9 × 2–5.5 cm, papyraceous to membranaceous, elliptic or ovate, with 8–11 secondary veins; lower face arachnoid of unicellular simple hairs; margin entire, revolute, with brown edge. Synflorescence terminal, corymbiform. Capitula radiate. Involucre 8–10 mm long, tubular; outer phyllaries 2–3, obovate; inner phyllaries 7.8–9.3 mm long, (sub)coriaceous, with obtuse apex. Ray flowers with 3–4 limb veins. Disc flowers 8–10.8 mm long; tube 4–5.4 mm, limb 2.3–4.5 mm long; tube 0.8–2 mm wide at base. Anthers 2.6–3.4 mm long, with rounded or auriculate base. Style branches 2–2.5 mm long, with rounded apex.

Distribution: La Paz. Habitat: Ceja de monte. Altitude: 3800–4265 m. (Figure 4.5)

Threat status: Vulnerable (IUCN accessed on 03 Aug 2022)

Additional examined specimens: La Paz: ANMI Apolobamba, Hilo Hilo, Juchuy Queñua, Laji Sorapata, -14.5452, -68.4808, 3879 m, 16 Apr 2009, I. Loza 754 (LPB). La Paz: ANMI Apolobamba, Queara nuevo, Toilcacocha, -14.4112, -69.0517, 3930 m, 11 Apr 2008, P. Paco 78 (LPB). La Paz: J Bautista Saavedra M, Puina, bosque de Queñuapata, -14.61050, -69.14747, 4265 m, 22 Aug 2006, G. Aguirre 83* (LPB).

Gynoxys rusbyi Cuatrec., Fieldiana, Bot. 27(2): 10. 1951. – Syntypes: La Paz, Vic. Pongo de Queme, 12500 ft., 2 Jul 1921, *H. H. Rusby 3* (F: V0076770F (fragments)[!], MO: MO-1508476, NY 178874[!], US 00122937[!]).

Shrub or tree, 1.3–8 m high. Twigs lacking prominent petiole scares. Leaves opposite; petiole 14–22 × 0.8–1 mm; lamina 4.8–9.50 × 1.5–4.2 cm, papyraceous to subcoriaceous, elliptic or ovate, with 7–11 secondary veins; lower face pubescent of unicellular simple hairs; margin

entire, revolute, with brown edge. Synflorescence terminal, corymbiform, cymbiform or paniculiform. Capitula radiate. Involucre 6–8 mm long, campanulate; outer phyllaries 2–4, filiform, elliptic, oblong or obovate; inner phyllaries 6.4–8 mm long, membranaceous, with acute or obtuse apex. Ray flowers with 4 limb veins. Disc flowers 6.7–10.9 mm long; tube 2.7–3.8 mm, limb 3.1–5.7 mm long; tube 0.6–1.1 mm wide at base. Anthers 2.2–3.3 mm long, with sagittate base. Style branches 1.6–2.2 mm long, with acute to rounded apex.

Distribution: Cochabamba, La Paz, Santa Cruz. Habitat: Humid Mountain Forest to Ceja de Monte. Altitude: 3550–3700 m. (Figure 4.7)

Threat status: not evaluated

Additional examined specimens: La Paz: Inquisivi, Rio Mina Jahuira, -16.5, -67.19, 3450 m, 15 Jul 1991, M. Lewis 39240* (LPB). La Paz: Inquisivi, fumarole of the Huichincani Thermal Springs, 10 km S of Choquetanga, -16.93333, -67.28333, 3550 m, 18 Jun 1991, M. Lewis 38940 (B 10 0720289). La Paz: Loayza, Viloco - Aguas Calientes, Choquetanga, [-16.8], [-67.3166666667], 3550 m, 16 Aug 1994, N. Salinas 3315* (LPB). Cochabamba: Chapare, Colomi, camino entre Colomi - Candelaria, -65.95056, -17.21833, 3500 m, 17 Jul 2017, B. Escobari, N. Kilian & H. Villca 178 (B 10 0763099). La Paz: Inquisivi, "Río Condor Khala", 9 km WNW of Choquetanga, -16.48, -67.25, 3700 m, 19 Jul 1991, M. Lewis 39352 (LPB). La Paz: Inquisivi, between Pongo Chico and Laguna Naranjani, ca 3 km W of Quime, -16.59, -67.15, 3600 m, 26 Jan 1989, M. Lewis 35153 (LPB). La Paz: Inquisivi, between Pongo Chico and Laguna Naranjani, [-16.9833333333], [-67.25], [4000] m, 8 Jul 1988, M. Lewis 881017 (LPB).

Gynoxys asterotricha complex

Shrub or tree, 0.4–9 m high. Twigs lacking prominent petiole scares. Leaves opposite; petiole 7–35 × 1.3–2.3 mm; lamina 3.2–12.4 × 1.4–5.6 cm, papyraceous to coriaceous, with 4–14 secondary veins; lower face pubescent to tomentose of unicellular simple hairs; margin entire, revolute, with brown edge. Synflorescence terminal, paniculiform or corymbiform to cymbiform. Capitula radiate. Involucre 5–9 mm long, tubular or campanulate; outer phyllaries 2–4, filiform to obovate; inner phyllaries 4.5–9 mm long, sub- to coriaceous, with acute or obtuse apex. Ray flowers with 3-4 limb veins. Disc flowers 4.6–11.2 mm long; tube 1.9–5 mm, limb 2–5 mm long; tube 0.5-0.9 mm wide at base. Anthers 1.7–3.4 mm long, with rounded or auriculate to sagittate base. Style branches 1.1–2.8 mm long, with acute to rounded apex.

Key to the taxa of the G. asterotricha complex

1 Leaves with white-yellowish indumentum at lower face, tertiary veins prominent on the lower face, 8–9 secondary veins forming a pseudomargin……*G. asterotricha*

1' Leaves with pale orange indumentum at lower face, tertiary veins not prominent on the lower face, > 9 secondary veins not forming a pseudomargin……*G. mandonii*

1`` Intermediate with respect to the above characters……*G. asterotricha* × *mandonii*

Gynoxys asterotricha Sch. Bip., Linnaea 34: 529. 1865.

Lectotype (designated here): Larecaja, Viciniis Sorata, Lancha de Cochipata in scopulsis montis Illampia, 3300 m, 1 Apr 1859, *G. Mandon 84* (P02273125!; isolectotypes: BR: BR0000005318506[!], F: V0076731F[!] V0076732F[!], G: G00426451!, GH: GH00008570[!] GH00008571[!], MPU: MPU012549[!] MPU012550[!] MPU012570[!], NY 178790[!], P: P02273080[!] P02273126[!]).

Distribution: La Paz. Habitat: Ceja de monte. Altitude: 3400–4120 m. (Figure 4.7)

Threat status: not evaluated

Additional examined specimens: Chuquisaca: Oropeza, Cerro Chataquila (Punilla-Chanauca), [-18.9738888889], [-65.3919444444], 3700 m, 27 Feb 1994, J.R.I. Wood 8047 (LPB). La Paz: ANMI Apolobamba Hilo Hilo, Juchuy Queñua, Laji Sorapata, -14.5506, -68.4748, 3765 m, 16 Apr 2009, I. Loza 883 (LPB). La Paz: J Bautista Saavedra M, Charazani-Tal, oberhalb Chullina am Weg Richtung Wayrapata, [-15.339082], [-68.79297], 3700 m, 26 Apr 1982, T. Feuerer 11398 (LPB). La Paz: ANMI Apolobamba, sector Chaka, camino Sorapata-Apolo, -14.89222, -68.78667, 3461 m, 30 Mar 2009, A. Fuentes 13625 (B 10 0720286). La Paz: J Bautista Saavedra M, ANMI Apolobamba, Pajan, sector Cochapata, -15.07, -68.5347, 3401 m, 19 Apr 2010, A. Fuentes 16193 (LPB). La Paz: Nor Yungas, bajando a Unduavi, 16 km desde la cumbre, -67.94686, -16.32872, 3570 m, 5 Jul 2016, B. Escobari, S. Beck, & C. Beck 36* (B 10 0720926). La Paz: ANMI Apolobamba, Pajan, Cerro Machu Layuj, -15.11222, -68.89500, 3487 m, 28 May 2010, L. Cayola 3880 (B 10 0720264). La Paz: J Bautista Saavedra M, Charazani, Al este de Chullina, [-15.141025], [-68.911009], 3400 m, 18 Apr 1933, P. Gutte 424 (LPB). La Paz: Nor Yungas, arriba de Unduavi, en bosques de *Polylepis pepei*, -67.93333, -16.30000, 4120 m, 13 Sep 2016, B. Escobari, S. Beck, & C. Beck 79 (B 10 0720937).

Gynoxys mandonii Sch. Bip. ex Rusby, Mem. Torrey Bot. Club 6(1): 67. 1896. – *Gynoxys mandonii* Sch. Bip. Bulletin de la Société Botanique de France 12: 80. 1865, nom. nud. –

Lectotype (designated here): Cochabamba, Chapare, Espiritu Santo, 1891, *M. Bang 1196* (NY 178865[!]; isolectotypes: BR: BR0000005318933[!], K: K000634162[!], NDG: NDG62632[!], PH: PH00013513[!]). Larecaja, Viciniis Sorata, Lancha de Cochipata in scopulsis montis Illampia, 3300 m, 1 Apr 1859, *G. Mandon 84* (BR: BR0000005317899[!], P: P00711420[!], S: S10–31297[!] S10–31297[!], US 01117686[!]).

= *Gynoxys hypomalaca* S. F. Blake, Bot. Gaz. 74: 427. 1922, **syn. nov.** – Holotype: La Paz, Sorata, higher limit of trees, 22 Apr 1920, *E. W. D. Holway & M. M. Holway 567* (US 00122907[!]; isotypes: GH: GH00008588[!], NY 178861[!], US 01100708[!]).

= *Gynoxys cochabambensis* Cabrera s.l., Notas Mus. La Plata, Bot. 14: 194. 1949, **syn. nov.** – Holotype: Cochabamba, Chapare, Yanta-Aduana, 3200 m, 10 Jul 1929, *J. Steinbach 9813* (LP: LP000274[!]; isotypes: E00414368[!]; F: V0076737F[!], G: G00223898[!] G00426400!, GH: GH00008576[!] GH00008577[!], K: K000634161[!] K000659419[!], NY 178794[!], S: S-R-2686[!]).

= *Gynoxys cruzensis* Cuatrec., Collect. Bot. (Barcelona) 3(3): 295. 1953, **syn. nov.** – Syntypes: Santa Cruz, Comarapa, Cerro San Mateo, 3400 m, 24 Oct 1928, *J. Steinbach 8515* (E00414367[!], F: V0076739F[!], GH: GH00008581[!], K: K000497536[!], PH: PH00013519[!], S: S-R-2687[!]).

Distribution: Cochabamba, La Paz, Santa Cruz. Habitat: Humid Mountain Forest to Puna. Altitude: 2800–4286 m. (Figure 4.7)

Threat status: data deficient (*Gynoxys cochabambensis*).

Additional examined specimens: Cochabamba: Ayopaya, Cocapata, encima de Tiquipaya, -66.66472, -16.85361, 3500 m, 22 Jul 2017, B. Escobari, N. Kilian, H. Villca & B. Nieto 273* (B 10 0763216; B 10 0763217). Cochabamba: Ayopaya, Cocapata, encima de Tiquipaya, -66.66417, -16.85000, 3600 m, 22 Jul 2017, B. Escobari, N. Kilian, H. Villca & B. Nieto 272 *(B 10 0763214; B 10 0763215). Cochabamba: Carrasco, Monte Punku, entrando hacia Yungas, -65.27694, -17.56722, 2800 m, 24 Jul 2017, B. Escobari, N. Kilian & H. Villca 307* (B 10 0763257; B 10 0763258). La Paz: Nor Yungas, bajando a los Yungas, antes del tunel y de Unduavi, -16.30000, -67.83333, [2370] m, 10 Jun 2006, S. Beck 31967 (B 10 0720259). La Paz: ANMI Apolobamba, Hilo Hilo, Chaka, senda hacia Amantala, -14.88750, -68.78750, 3576 m, 21 Aug 2009, L. Cayola 3528 (B 10 0720281). La Paz: ANMI Apolobamba, Laji Sorapata, Kañupata, -14.88917, -68.86139, 3324 m, 24 Jun 2010, L. Samo 41 (B 10 0720280). La Paz: Larecaja, 9 km pasando el desvío de Laripata-Lipichi Camino hacia Pacuni, -68.63333, -

15.73333, 3600 m, 7 Aug 2016, B. Escobari, S. Beck, & C. Beck 58 (B 10 0720930). La Paz: Larecaja, pasando Laripata, camino hacia Pacuni-Chinchaya, -68.65000, -15.71667, 3330 m, 7 Aug 2016, B. Escobari, S. Beck, & C. Beck 68 (B 10 0720935). La Paz: Nor Yungas, Parque Nal Cotapata, Unduavi, sendero Sillutincara, -16.1728, -67.5328, 3300 m, 30 May 2007, A. Fuentes 11933* (LPB).

Gynoxys asterotricha × mandonii

Specimens belonging to this taxon share characteristics of *G. asterotricha* and *G. mandonii.* Among the main similarities between the putative hybrid with *G. asterotricha* are the coriaceous leaves with prominent tertiary ribbing on the shiny upper face of the leaves, and the >9 secondary veins and a pale yellow-orange involucrum with *G. mandonii*. Nevertheless, the inclusion of a large number of specimens precludes their identification into one of the formerly described taxa as they exhibit a vast morphological gradient.

Additional examined specimens: BOLIVIA: Cochabamba: Carrasco, Parque Nacional Carrasco, Monte Punco, -17.56528, -65.29056, 3100 m, 18 Sep 2000, M. Zarate 621 (B 10 0720261). La Paz: Nor Yungas, arriba de Unduavi, en bosques de Polylepis pepei, -67.95000, -16.26667, 4000 m, 13 Sep 2016, B. Escobari, S. Beck, & C. Beck 73* (B 10 0720936). La Paz: Larecaja, Escalerani, -15.50459, -68.16988, 4110 m, 8 Nov 2008, A. Palabral 732* (B 10 0720294). La Paz: J Bautista Saavedra M, ANMI Apolobamba Laji-Larisani, sector Chiata, -14.86028, -68.92056, 3629 m, 1 Jul 2010, A. Fuentes 16905 (B 10 0720292). La Paz: ANMI Apolobamba, Queara viejo, -14.70694, -69.08472, 3245 m, 16 Sep 2009, A. Fuentes 15094 (B 10 0720266). La Paz: Franz Tamayo, -14.68129, -69.10174, 4161 m, 17 Jul 2006, A. Palabral 285 (B 10 0720283). La Paz: ANMI Apolobamba, Keara bajo, -14.71194, -69.08417, 3500 m, 18 Jun 2005, A. Fuentes 8392 (B 10 0720265). La Paz: Franz Tamayo, Apolobamba, Palomani, -14.3458, -69.0738, 4286 m, 12 Apr 2008, J. Quisbert 843 (LPB). La Paz: Murillo, laguna Marimarini, sobre el camino precolombino La Reconquistada, casi 23 km al Norte de Ventilla, -16.41583, -67.89917, 4145 m, 23 Apr 2006, C. Aldana 510 (B 10 0720293). La Paz: Murillo, Valle del Río Zongo, 148 km al N de la Cumbre, -16.20000, -68.11667, 3900 m, 11 Apr 1987, J. Solomon 16497 (B 10 0720284). La Paz: Franz Tamayo, Parque Nacional Madidi, Queara nuevo, Chuñuña, -14.68444, -69.09333, 4100 m, 9 Apr 2008, P. Paco 19 (B 10 0720288). La Paz: J Bautista Saavedra M, PN Madidi, Laji-Sorapata, Sector Cañupata, pasando el río Laji, -14.88583, -68.86167, 3310 m, 23 Jun 2010, A. Fuentes 16781 (B 10 0720291). La Paz: ANMI Apolobamba, entre la comunidad de Puina y cerro k`akepununa, -14.61167, -69.14694, 4200 m, 11 Apr 2008, J. Quisbert 822 (B 10 0720287). La Paz: Larecaja, Sorata, 64 km hacia Consata

(20 km despues de Quiabaya) km 226, -15.63361, -68.65389, 3590 m, 6 Aug 2004, S. Beck 29440 (B 10 0720254). La Paz: Franz Tamayo, Senda Pelechuco-Mojo, sector Tambo Quemado, -14.4103, -68.5822, 3455 m, 1 Mar 2003, N. Paniagua 5716* (LPB). La Paz: Larecaja, Lipichi, 5 km pasando el cruce Lakatya-Lipichi Camino a Anilea, -68.60000, -15.70000, 4000 m, 7 Aug 2016, B. Escobari, S. Beck, & C. Beck 59* (B 10 0720931). Santa Cruz: Caballero, 2–3 km al N de Siberia sobre el camino a Waichal, -17.49, -64.45, 3000 m, 26 Jul 1996, M. Saldias 4632 (LPB).

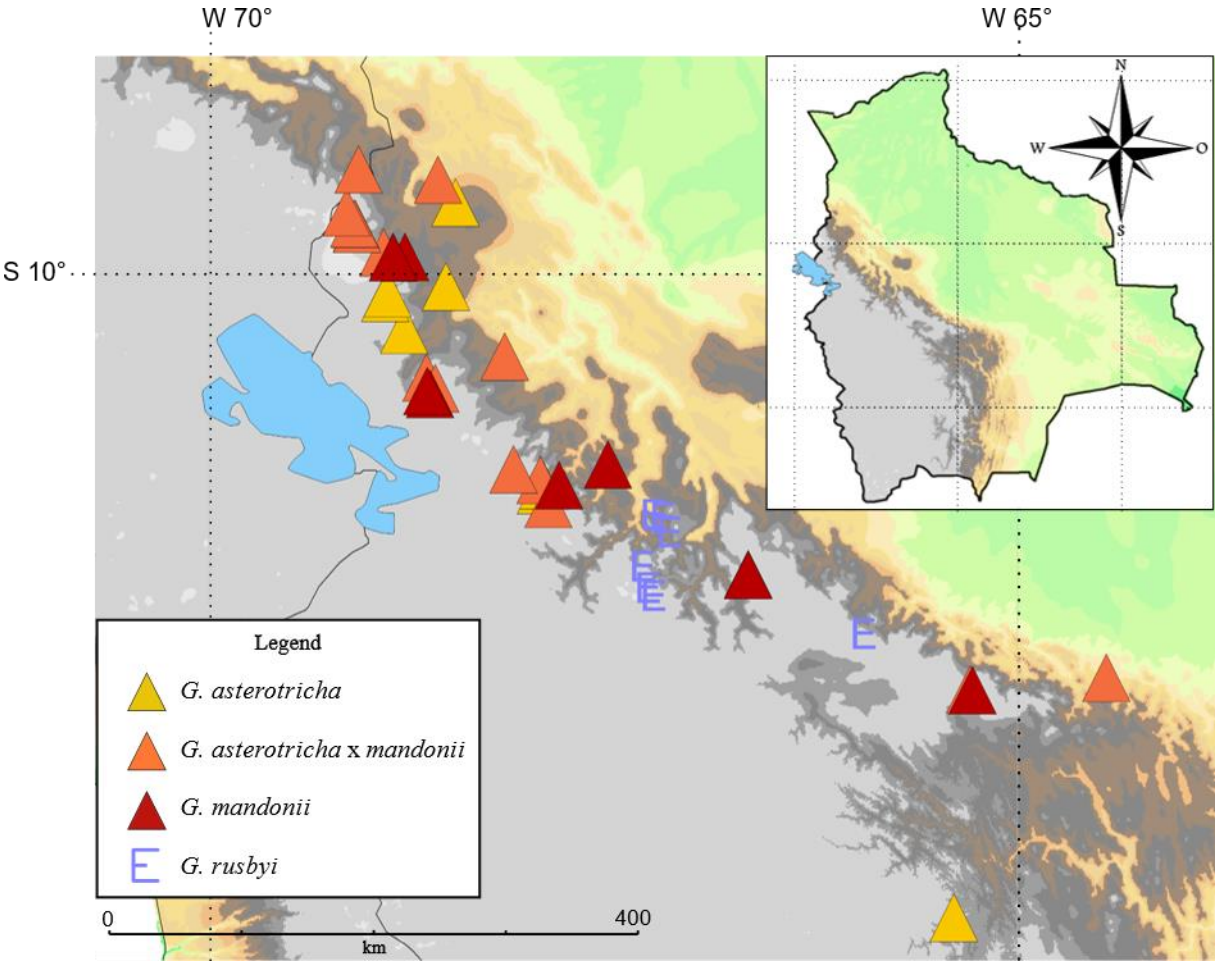

Figure 4.7: Distribution map of *Gynoxys asterotricha*, *G. mandonii*, *G. asterotricha* × *mandonii* and *G. rusbyi*

Specimens of uncertain placement

Two specimens could neither be placed in any of the above species nor distinguished from them with certainty although morphologically perceptible. More material is needed to assess their status successfully.

(1) BOLIVIA: La Paz, J. Bautista Saavedra, PN Madidi, Laji-Sorapata, Sector Cosñímayu, pasando el río Laji, -14.89, -68.861111, 3272 m, 02 Jun 2010, A. Fuentes 16732 (B 10 0720290).

This specimen depicts a set of exclusive morphological characters such as very short petioles (2-5 mm), glabrescent leaves with not branched multicellular trichomes unique in the genus *Gynoxys*.

(2) BOLIVIA: Cochabamba, Tiraque, El Ronco, cordillera el Ronco, -17.00138889, 65.65555556, [3700 m], 2008, A. Barracos 277 (B 10 0720262).

This specimen resembles *Gynoxys psilophylla* but differs by the shaggy arachnoid instead of glabrate indumentum of the lower leaf face. It also resembles *G. jelskii* Hieron. a species distributed in Peru with respect to the peculiar irregular midrib which is thicker at the leaves base and thinner at the apex and is a distinct character of that species.

Excluded taxa

Gynoxys fabrisii Cabrera, Bol. Soc. Argent. Bot. 15(4): 332, f. 6. 1974. Described from Argentina.

The record of this species for Bolivia is based on a misidentified specimen of Altamirano #648. In this study we revised this specimen as *Gynoxys kingii* and hence exclude *G. fabrisii* from Bolivia.

4.7 References

Aucca C, Olmos F, Santander OJ, Chamorro A (2015) Range extension and new habitat for the Critically Endangered Royal Cinclodes Cinclodes aricomae. Cotinga 37: 12–17.

Beck S, Ibáñez D (2014) Asteraceae. In: Jorgensen PM, Nee N, Beck SG (Eds) Catálogo de las plantas vasculares de Bolivia. Monographs in Systematic Botany from the Missouri Botanical Garden 127: 290–382.

Beentje H (2010) The Kew Plant Glossary: An illustrated dictionary of plant terms. Kew Publishing, Surrey, 184 pp.

Berendsohn WG (2010) Devising the EDIT Platform for Cybertaxonomy. In: Nimis PL, Vignes-Lebbe R (Eds) Proceedings of the international Congress on tools for identifying Biodiversity: Progress and Problems. Muséum national d'Histoire naturelle – Grand Amphithéâtre, Paris, 1–6. Available from: http://www.openstarts.units.it/dspace/bitstream/10077/3737/1/Berendsohn, bioidentify.pdf.

CGIAR-CSI (2022) CGIAR-CSI. Consortium for Spatial Information. Available from: https://srtm.csi.cgiar.org/srtmdata/

Cuatrecasas J (1951) Contributions to the Flora of South America. Studies on Andean Compositae - II. Fieldiana 27(2): 1–74. Available from: https://www.biodiversitylibrary.org/page/2457150.

Escobari B, Borsch T, Quedensley TS, Gruenstaeudl M (2021) Plastid phylogenomics of the Gynoxoid group (Senecioneae, Asteraceae) highlights the importance of motif-based sequence alignment amid low genetic distances. American Journal of Botany 108(11): 2235–2256. https://doi.org/10.1002/ajb2.1775

Fjeldså J (1993) The avifauna of the *Polylepis* woodlands of the Andean highlands: The efficiency of basing conservation priorities on patterns of endemism. Bird Conservation International 3(1): 37–55. https://doi.org/10.1017/S0959270900000770

Foster R (1958) A catalogue of ferns and flowering plants of Bolivia (Vol. 184). Harvard University Herbaria.

Garcia N, Meerow AW, Soltis DE, Soltis PS (2014) Testing deep reticulate evolution in Amaryllidaceae tribe Hippeastreae (Asparagales) with its and chloroplast sequence data. Systematic Botany 39(1): 75–89. https://doi.org/10.1600/036364414X678099

GBIF (2022) GBIF.org. Global Biodiversity Information Facility. Available from: https://www.gbif.org/ [accessed: 21 Apr 2022]

Global Compositae Database (2022) Compositae.org. Global Compositae Database. Available from: https://www.compositae.org/aphia.php?p=stats [accessed: 04. September 2022]

Gruenstaeudl M (2020) Annonex2embl: Automatic preparation of annotated DNA sequences for bulk submissions to ENA. Bioinformatics 36(12): 3841–3848. https://doi.org/10.1093/bioinformatics/btaa209

Hijmans RJ, Guarino L, Mathur P (2012) DIVA-GIS Version 7.5, Manual. Available from: https://www.diva-gis.org/

Hind N (2009) An annotated preliminary checklist of the Compositae of Bolivia.

Hind N (2011) An annotated preliminary checklist of the Compositae of Bolivia, version 2. Available from: https://www.kew.org/sites/default/files/ 2019-01/Bolivian%20compositae%20checklist.pdf [accessed: 05 November 2021].

Ibisch PL, Mérida G (eds.) (2003) Biodiversidad: La riqueza de Bolivia. Estado de conocimiento y conservación. Ministerio de Desarrollo Sostenible. Editorial FAN, Santa Cruz de la Sierra - Bolivia

IPNI (2022) IPNI.org. International Plant Names Index. Available from: https://www.ipni.org/ [accessed: 20 Februar 2022].

IUCN (2022) The IUCN Red List of Threatened Species. Version 2022-1. https://www.iucnredlist.org. Accessed on [accessed: 12 Aug 2022].

Jeffrey C (1992) The Tribe Senecioneae (Compositae) in the Mascarene Islands with an Annotated

World Check-List of the Genera of the Tribe: Notes on Compositae: VI. Kew Bulletin 47(1): 49–109. https://doi.org/10.2307/4110768
JSTOR (2022) JSTOR.org. JSTOR Global Plants. Available from: https://plants.jstor.org/ [accessed: 12 Aug 2022]
Kandziora M, Sklenář P, Kolář F, Schmickl R (2022) How to tackle phylogenetic discordance in recent and rapidly radiating groups? Developing a workflow using *Loricaria* (Asteraceae) as an example. Frontiers in Plant Science 12: 1–16. https://doi.org/10.3389/fpls.2021.765719
Killeen TJ, García E, Beck SG (1993) Guía de Arboles de Bolivia. Herbario Nacional de Bolivia & Missouri Botanical Garden. 996. http://pdf.usaid.gov/pdf_docs/pnaca189.pdf
Kolář F, Dušková E, Sklenář P (2016) Niche shifts and range expansions along cordilleras drove diversification in a high-elevation endemic plant genus in the tropical Andes. Molecular Ecology 25(18): 4593–4610. https://doi.org/10.1111/mec.13788
Lundin R (2006) *Nordenstamia* Lundin (Compositae-Senecioneae), a new genus from the Andes of South America. Compositae Newsletter 44(44): 14–23. Available from: https://www.biodiversitylibrary.org/page/13749318.
McCune B, Mefford MJ (2018) PC-ORD. Multivariate Analysis of Ecological Data. Version 7.08
Pelser PB, Nordenstam B, Kadereit JW, Watson LE (2007) An ITS phylogeny of tribe Senecioneae (Asteraceae) and a new delimitation of *Senecio* L. Taxon 56(4): 1077–1104. https://doi.org/10.2307/25065905
Pelser PB, Kennedy AH, Tepe EJ, Shidler JB, Nordenstam B, Kadereit JW, Watson LE (2010) Patterns and causes of incongruence between plastid and nuclear Senecioneae (Asteraceae) phylogenies. American Journal of Botany 97(5): 856–873. https://doi.org/10.3732/ajb.0900287
Pouchon C, Fernández A, Nassar JM, Boyer F, Aubert S, Lavergne S, Mavárez J (2018) Phylogenomic analysis of the explosive adaptive radiation of the Espeletia complex (Asteraceae) in the tropical Andes. Systematic Biology 67(6): 1041–1060. https://doi.org/10.1093/sysbio/syy022
Powell C, Cuatrecasas J (1970) Chromosome number in Compositae. Taxon 57(1), 374–379. https://doi.org/10.2307/1221588
Robinson H, Carr GD, King RM, Powell AM, Robinson H, Carr GD, King RM, Powella AM (1997) Chromosome Numbers in Compositae, XVII: Senecioneae III. Annals of the Missouri Botanical Garden 84(4): 893–906.
Ronquist F, Huelsenbeck JP (2003) MrBayes 3: Bayesian phylogenetic inference under mixed models. Bioinformatics 19: 1572-1574
Roque N, Keil DJ, Susanna A (2009) Illustrated glossary of Compositae. In: Funk V, Susanna A, Stuessy T, Bayer R (Eds) Systematics, evolution, and biogeography of Compositae. International Association for Plant Taxonomy, Vienna, 781–806.
Tropicos (2022) Tropicos.org. Missouri Botanical Garden. Available from: http://www.tropicos.org/ [accessed: 20 Februar 2022]
Tuner BL, Powell AM, Cuatrecasas J (1967) Chromosome Numbers in Compositae. XI. Peruvian Species. Annals of the Missouri Botanical Garden 54(2): 172–177.
Vargas OM, Ortiz EM, Simpson BB (2017) Conflicting phylogenomic signals reveal a pattern of reticulate evolution in a recent high-Andean diversification (Asteraceae: Astereae: *Diplostephium*). New Phytologist 214(4): 1736–1750. https://doi.org/10.1111/nph.14530

Chapter 5. General conclusion

The present investigation represents the first comprehensive study on the Gynoxyoid clade and contributes to a better understanding of high Andean Asteraceae. The study was based on a representative set of taxa that aimed to encompass the molecular, morphological and distributional diversity of the clade. The molecular analysis at genera level was based on whole plastid genome complemented by two nuclear markers (ETS and ITS). The study of plastid whole genomes helped to a better understanding of plastid evolution and independency of plastid partitions. The molecular analysis at species level was based on nuclear markers ETS and ITS. The study on morphology included analyses on morphological characters both at genera and species level resulting in a taxonomic treatment for genera and for a reduced set of species.

5.1 Phylogeny on the Gynoxyoid clade

The first conclusion that was reached still during the development of this study was that the Gynoxyoid group is formed by very closely related genera as the preliminary results on plastid individual markers depicted extremely low nucleotide diversity among genera. The low molecular variation gives insights into very closely species and a young evolutionary history as it was reported within other members of the Asteraceae family (Loeuille et al., 2021; Kelchner 2002; Shaw et al., 2007; Androsiuk et al., 2020). Complete plastid genomes potentially increase the phylogenetic signal that can be used for reconstructing robust phylogenetic trees(Goncalvez et al. (2019). The present study enlarged the molecular input data by using plastid genomes of 17 species belonging to the Gynoxyoid. Although the plastid size exceeded the 120,000 bp, only 698 sites (0.58%) were parsimony informative.

The phylogenetic inference under maximum likelihood and Bayesian inference on both plastid and nuclear data retrieved the Gynoxyoid group as monophyletic. These results supported Pelser et al. (2007; 2010) hypotheses which was built on a reduced number of species as well as few molecular markers. Although the plastid and nuclear inference recovered the Gynoxyoid group as monophyletic, tree topologies among nuclear and plastid data were highly incongruent. Furthermore, incongruences were found among nuclear markers (ETS vs ITS). Incongruences on phylogenetic inferences on plastid against nuclear data was reported at higher levels (Goncalvez et al., 2019) and for closely related taxa (Lui et al, 2021; Favre et al., 2022). Among the most probable explanation for such incongruences among datasets are hybridization, introgression, rapid radiations, reticulate evolution or incomplete lineage sorting (Knope et al., 2020; Loeuille et al., 2021; Lui et al., 2021).

The five initial genera that were included in the molecular analysis (i.e., *Aequatorium*, *Gynoxys*, *Nordenstamia*, *Paracalia* and *Paragynoxys*) were recovered within the Gynoxyoid clade.

Nevertheless, our analyses on plastid and nuclear data could not support the current circumscription of most of the genera (*Gynoxys*, *Nordenstamia* and *Paracalia*).

5.2 Morphology of the Gynoxyoid clade

Analyses on morphological characters helped to understand the morphological evolution in this group. One single genus retrieved as monophyletic in the phylogenetic inference could be supported on morphological characters (i.e., *Paragynoxys*), but for most cases the characterization of genera was based on morphological data. This was due to the existence of alternative hypotheses retrieved on the molecular data which needs further studies in order to make any conclusion based on this data.

The results of the morphological analysis under character ancestral reconstruction suggested a set of putative diagnostic characters for genera delimitation. The evaluation of this character list was extended to all species within the Gynoxyoid clade in order to check their usability as diagnostic characters. Based on this evaluation four genera were characterized.

5.3 Nomenclatural changes within the Gynoxyoid clade

Based on the results of the molecular and morphological data nomenclatural and taxonomic changes needed to be considered.

The circumscription of *Aequatorium* was kept as it was characterized based on morphological characters. Unfortunately, a single specimen of this genera was included in the phylogenetic analysis, hence the monophyly of the genera could not be confirmed. Nevertheless, the single specimen included in the analyses was retrieved as one of the basal clades of the tree. Furthermore, the phylogenetic inference reconstructed by Pelser et al. (2007) on the ITS nuclear markers retrieved two members of this genus forming a clade.

The genus *Nordenstamia* was synonymized under *Gynoxys*. This decision was taken as no phylogenetic result supported this genus as monophyletic but within *Gynoxys.* These results were also obtained by Pelser et al. (2007; 2010). Furthermore, the morphological characters on which the genus is characterized were equally found in *Gynoxys*. In that sense, the genus *Gynoxys* was enlarged in order to include all members of *Nordenstamia.*

Paracalia was retrieved as non-monophyletic in most of the phylogenetic inferences, nevertheless, the alternative hypothesis retrieved by the ETS nuclear marker supports the circumscription of this genus. Nevertheless, the analysis on morphological characters suggested a great number of characters for supporting the circumscription of this genus. In that sense and from a practical point of view the circumscription of *Paracalia* was kept until further investigation focuses on this genera.

Finally the circumscription of *Paragynoxys* was confirmed and its characterization was supported on molecular and morphological data.

The checklist of all species within the Gynoxyoid clade includes a total of 158 species nested in the four previously mentioned genera. *Gynoxys* represents the biggest and most important genus of the clade comprising 131 species, *Aequatorium* includes 12 species, *Paracalia* 2 and *Paragynoxys* 13.

5.4 Taxonomic treatment of Bolivian species belonging to the Gynoxyoid clade.

A deeper study of all members of the Gynoxyoid clade distributed in Bolivia based on molecular and morphological data was performed. Phylogenetic trees were build on nuclear markers (ETS and ITS). Morphological analyses included an exhaustive revision of characters which were used for the performance of principal component analyses. Results of both analyses were used for species delimitation. The phylogenetic analyses supported the circumscription of some species, but at the same time two scenarios were presented: [1] monophyletic groups containing more than one species, and [2] members of one single species retrieved in more than one clade. The principal component analysis was primordial to make decisions on species circumscriptions and to define species delimitations.

In that sense, the species supported in this study are delimited on either molecular, morphological or both type of data. In cases where the species delimitation was not supported in any type of data, the circumscription of the species was not kept. In that sense seven species were newly synonymized in this study. This study resulted in the recognition of 14 species of the Gynoxyoid clade for Bolivia representing a reduction of the latest checklist of Beck and Ibanez (2014), additionally three new species are suggested in this investigation.

The results of the molecular and morphological analysis suggested furthermore, the existence of a putative hybrid among two closely distributed species which need further analyses to confirm this hypothesis.

The results of this chapter achieved the aims of contributing to the Flora of Bolivia.

5.5 Suggestions on future studies for the Gynoxyoid clade

The results of this investigation contribute to a better understanding of a rapid evolving Andean clade, nevertheless, as more questions were answered as more questions arose.

Further studies on the evolution of this clade are suggested here. In the molecular field wider studies on chromosome counts combined with flow cytometry are needed to elucidate the ploidy level(s) within the members of the Gynoxyoid clade. On the other hand, phylogenomic inferences using the Hyb-Seq approach would give insights into phylogenetic relationships among closely related species depicting extremely low genetic variations as it was shown by Hatami et al. (2022). This phylogenetic reconstructions and its comparison with phylogenetic inferences on plastid data is needed to test the existence of evolutionary processes such as hybridization or introgression. Further morphological analysis would give insights into

morphological plasticity of this clade and their relationship with their environment. Regardless the type of analysis to be performed, the collection of fresh specimens is primordial in this group to answer these and more questions.

Additionally, a taxonomic treatment including all species of the Gynoxyoid clade is essential to clarify species limits and define nomenclatural arrangements.

Likely, the inclusion of nuclear data for the newly suggested species for Bolivia would confirm or reject our hypotheses but, as mentioned before, more specimens need to be collected to accomplish this.

References

Androsiuk PJ, Jastrzebski L, Paukszto K, Makowczenko A, Okorski A, Pszczolkowska K Chwedorzewska, et al. (2020) Evolutionary dynamics of the chloroplast genome sequences of six *Colobanthus* species. Scientific Reports 10: 11522

Beck S, Ibáñez D (2014) Asteraceae. In: Jorgensen PM, Nee N, Beck SG (Eds) Catálogo de las plantas vasculares de Bolivia. Monographs in Systematic Botany from the Missouri Botanical Garden 127: 290–382.

Bremer K (1994) Asteraceae: Cladistics and classification. Timber Press, Portland, Oregon, USA.

Correa A (2003) Revision of the genus Paragynoxys (Asteraceae, Senecioneae-Tussilagininae). Brittonia 55(2): 157–168. Available from: https://www.jstor.org/stable/3218456.

Cuatrecasas J (1951) Contributions to the Flora of South America. Studies on Andean Compositae – II. Fieldiana 27(2): 1–74. Available from: https://www.biodiversitylibrary.org/page/2457150.

Cuatrecasas J (1955) A new genus and other novelties in Compositae. Brittonia 8(2): 151–163. Available from: https://www.jstor.org/stable/2804857.

Cuatrecasas J. (1960) Studies on Andean Compositae-IV. Brittonia 12: 182–195. https://doi.org/https://doi.org/10.2307/2805052

Cuatrecasas J. (1990) Miscellaneous notes on neotropical flora, XIX. Combinations in Senecioneae, Compositae. Phytologia 69(5).

Díaz-Piedrahita S, Cuatrecasas J (1990) El género Aequatorium Nord. (Senecioneae–Asteraceae) en Colombia. Rev. Acad. Colomb. Cienc. 17(67): 659–666.

Favre A, Paule J, Ebersbach J (2022) Incongruences between nuclear and plastid phylogenies challenge the identification of correlates of diversification in Gentiana in the European Alpine System. Alpine Botany 132(1): 29–50. https://doi.org/10.1007/s00035-021-00267-6.

Funk VA, Susanna A, Stuessy TF, Bayer RJ (2009) Systematics, Evolution, and Biogeography of Compositae. 1001 pp.

García-Mendoza AJ, Sándoval-Gutiérrez D, Redonda-Martínez R (2020) Erratum: Mixtecalia, a new monotypic genus of the subtribe Tussilagininae (Senecioneae, Asteraceae) from the state of Oaxaca, Mexico. Phytotaxa, 439(1), 107. https://doi.org/10.11646/PHYTOTAXA.439.1.9

Gonçalves DJP, Simpson BB, Shimizu GH, Jansen RK, Ortiz EM (2019) Genome assembly and phylogenomic data analyses using plastid data: Contrasting species tree estimation methods. Data in Brief 25: 104271. https://doi.org/10.1016/j.dib.2019.104271 Herrera B (1980) Revision de las especies peruanas del género Gynoxys (Compositae). Boletin de la Sociedad Peruana de Botanica 8(1): 3–74.

Jeffrey C (1992) The Tribe Senecioneae (Compositae) in the Mascarene Islands with an Annotated World Check-List of the Genera of the Tribe: Notes on Compositae: VI. Kew Bulletin 47(1): 49–109. https://doi.org/10.2307/4110768

Jeffrey AC, Yi-ling C, Jeffrey C, Yi-lings C (1984) Taxonomic Studies on the Tribe Senecioneae (Compositae) of Eastern Asia Published by : Springer on behalf of Royal Botanic Gardens , Kew Stable URL : https://www.jstor.org/stable/4110124 REFERENCES Linked references are available on JSTOR for this artic. 39(2), 205–446.

Kadereit J, Jeffrey C (1996) A preliminary analysis of cpDNA variation in the tribe Senecioneae (Compositae). In D. Hind and H. Beentje [eds.], Compositae: Systematics. Proceedings of the International Compositae Conference, vol. 1, 349–360. Royal Botanic Gardens, Kew, UK.

Kelchner S (2002) Group II introns as phylogenetic tools: structure, function, and evolutionary constraints. American Journal of Botany 89: 1651–1669

Knope ML, Bellinger MR, Datlof EM, Gallaher TJ, Johnson MA (2020) Insights into the Evolutionary

History of the Hawaiian *Bidens* (Asteraceae) Adaptive Radiation Revealed Through Phylogenomics. Journal of Heredity 111(1): 119–137. https://doi.org/10.1093/jhered/esz066

Liu ZF, Ma H, Ci XQ, Li L, Song Y, Liu B, Li HW, Wang SL, Qu XJ, Hu JL, Zhang XY, Conran JG, Twyford AD, Yang JB, Hollingsworth PM, Li J (2021) Can plastid genome sequencing be used for species identification in Lauraceae? Botanical Journal of the Linnean Society 197(1): 1–14. https://doi.org/10.1093/botlinnean/boab018

Loeuille B, Thode V, Siniscalchi C, Andrade S, Rossi M, Pirani JR. (2021) Extremely low nucleotide diversity among thirty-six new chloroplast genome sequences from *Aldama* (Heliantheae, Asteraceae) and comparative chloroplast genomics analyses with closely related genera. PeerJ. 9:e10886. doi: 10.7717/peerj.10886.

Lundin R (2006) Nordenstamia Lundin (Compositae-Senecioneae), a new genus from the Andes of South America. Compositae Newsletter 44(44): 14–23. Available from: https://www.biodiversitylibrary.org/page/13749318.

Nordenstam B (1978) Taxonomic studies in the tribe Senecioneae (Compositae). Opera Botanica 44: 1–83.

Nordenstam B (1997) The genus Aequatorium B. Nord. (Compositae-Senecioneae) in Ecuador. Compositae Newsletter 31(31): 1–16. Available from: https://www.biodiversitylibrary.org/page/13152227.

Pelser PB, Nordenstam B, Kadereit JW, Watson LE (2007) An ITS phylogeny of tribe Senecioneae (Asteraceae) and a new delimitation of *Senecio* L. Taxon, 56(4), 1077–1104. https://doi.org/10.2307/25065905

Pelser PB, Kennedy, AH, Tepe EJ, Shidler JB, Nordenstam B, Kadereit JW, Watson LE (2010) Patterns and causes of incongruence between plastid and nuclear Senecioneae (Asteraceae) phylogenies. American Journal of Botany, 97(5), 856–873. https://doi.org/10.3732/ajb.0900287

Robinson H, King GD, Powell RM (1997) Chromosome numbers in Compositae, XVII: Senecioneae III. Annals of the Missouri Botanical Garden 84(4): 893–906.

Shaw JE, Lickey E, Small R (2007) Comparison of whole chloroplast genome sequence to choose non-coding regions for phylogenetic studies in angiosperms: the tortoise and the hare III. American Journal of Botany 94: 275–288.

List of publications and contributions

Chapter 2

Escobari B, Borsch T, Quedensley TS, Gruenstaeudl M (2021) Plastid phylogenomics of the Gynoxoid group (Senecioneae, Asteraceae) highlights the importance of motif-based sequence alignment amid low genetic distances. American Journal of Botany 108(11): 2235–2256. https://doi.org/10.1002/ajb2.1775

Contributions: B.E. and T.S.Q. conducted the fieldwork, generated herbarium vouchers, and extracted DNA. B.E. and M.G. conducted the lab work and assembled and annotated the plastid genomes. B.E. and T.B. conducted the visual inspection and adjustment of sequence alignments. B.E. and M.G. conducted the phylogenetic analyses and generated all figures and tables. B.E. and M.G. led the writing of the manuscript, with additional contributions by T.B. and T.S.Q. All authors approved the final version of the manuscript.

Appendices

Appendix 2: Supplementary material for Chapter 2

Appendix 2.1: Summary of the position and length of the microsatellites and small sequence inversions in the multiple sequence alignments (MSAs) that were masked during alignment adjustment. By default, the listed regions represent microsatellites with a DNA motif comprising an A and/or T, unless marked otherwise. Notes: a = sequence inversions with length <50 bp; b = microsatellites with a DNA motif comprising a G and/or C.

Class	Marker	Masked sequence regions
CDS	rbcL	1345-1415[a]
	psaA	1292-1299[a]
	rpl23	148-153[a]
	ycf1	2673-2703, 3699-3710
	ycf2	6067-6080[a]
INT	atpF intron	436-443
	clpP intron 1	328-338, 370-380
	clpP intron 2	86-102, 196-222, 427-441, 686-696[b]
	ndhA intron	72-82, 614-651
	rpoC1 intron	245-262, 671-685[b]
	rps16 intron	249-259[a], 284-297[b], 721-730
	trnG intron	127-138, 407-428
	trnI intron	432-444
	trnK intron 1	219-230
	trnK intron 2	211-225
	trnL intron	132-142
	ycf3 intron 2	617-625, 683-693
IGS	atpB–rbcL	395-436, 522-536
	atpF–atpA	40-55
	atpH–atpF	274-288[a]
	atpI–atpH	19-27, 127-138, 171-191, 1112-1122
	ccsA–trnL-TAG	8-20
	clpP–psbB	110-119
	ndhC–trnV-TAC	317-326, 136-143[b], 727-732[a]
	petA–psbJ	217-225, 639-652
	petD–rpoA	175-193
	petN–psbM	300-318
	psaA–ycf3	450-473

Class	Marker	Masked sequence regions
IGS	psaI–ycf4	26-36
	psaJ–rpl33	52-68[b]
	psbA–trnK-TTT	175-186
	psbB–psbT	88-97
	psbC–trnS-TGA	73-111
	psbE–petL	81-88, 279-289, 467-500, 763-776, 908-921
	psbI–trnS-GCT	61-64[a]
	psbM–trnD-GTC	444-448[a], 210-222[a]
	rpl14–rpl16	64-86
	rpl16–rps3	62-70
	rpl32–ndhF	88-132, 1043-1040
	rpl36–infA	76-89[a]
	rpoC2–rps2	188-202
	rps16–trnQ-TTG	875-888
	rps18–rpl20	115-139
	rps4–trnT-TGT	310-322
	rps8–rpl14	49-89
	rrn5–trnR-ACG	46-58
	trnC-GCA–petN	377-423
	trnE-TTC–rpoB	735-751
	trnF-GAA–ndhJ	241-249[a]
	trnK-TTT–rps16	75-98, 102-112
	trnL-TAG–rpl32	249-259, 637-673
	trnM-CAT–atpE	2-40[a]
	trnR-TCT–trnG-TCC	44-63, 95-110
	trnS-GGA–rps4	291-312
	trnS-TGA–psbZ	141-151
	trnT-GGT–psbD	917-924[b]
	trnT-TGT–trnL-TAA	262-355
	ycf1–rps15	53-66
	ycf3–trnS-GGA	403-422
	ycf4–cemA	196-219, 264-270[b]

Appendix 2.2: Overview of the total and regional lengths of the plastid genomes of the Gynoxyoid group. All lengths are given in bp.

Species	Total	LSC	SSC	IR
Aequatorium jamesonii	151,015	83,176	18,193	24,823
Arnoglossum atriplicifolium	150,837	83,036	18,149	24,826
Gynoxys asterotricha	151,022	83,213	18,195	24,807
Gynoxys baccharoides	151,071	83,215	18,150	24,853
Gynoxys ignaciana	150,979	83,140	18,191	24,824
Gynoxys longifolia	150,998	83,180	18,172	24,823
Gynoxys mandonii	151,004	83,169	18,189	24,823
Gynoxys megacephala	151,014	83,178	18,192	24,822
Gynoxys sp. SEN301	151,013	83,316	18,193	24,752
Gynoxys tomentosissima	155,060	79,946	18,194	28,460
Gynoxys violaceae	151,006	83,159	18,141	24,853
Nordenstamia cajamarcensis	150,907	83,111	18,122	24,837
Nordenstamia kingii	150,891	83,049	18,196	24,823
Nordenstamia repanda	151,031	83,192	18,193	24,823
Paracalia jungioides	151,014	83,183	18,183	24,824
Paracalia pentamera	151,640	83,095	18,551	24,997
Paragynoxys martingrantii	150,996	83,168	18,180	24,824
Paragynoxys venezuelae	150,927	83,100	18,181	24,823
Roldana aschenborniana	151,018	83,195	18,147	24,838
Roldana barba-johannis	151,016	83,230	18,127	24,829
Telanthophora grandifolia	151,093	83,255	18,148	24,845

Appendix 2.3: Plastome map of *Gynoxys tomentosissima*, the longest of the sequenced plastid genomes of the Gynoyxoid group.

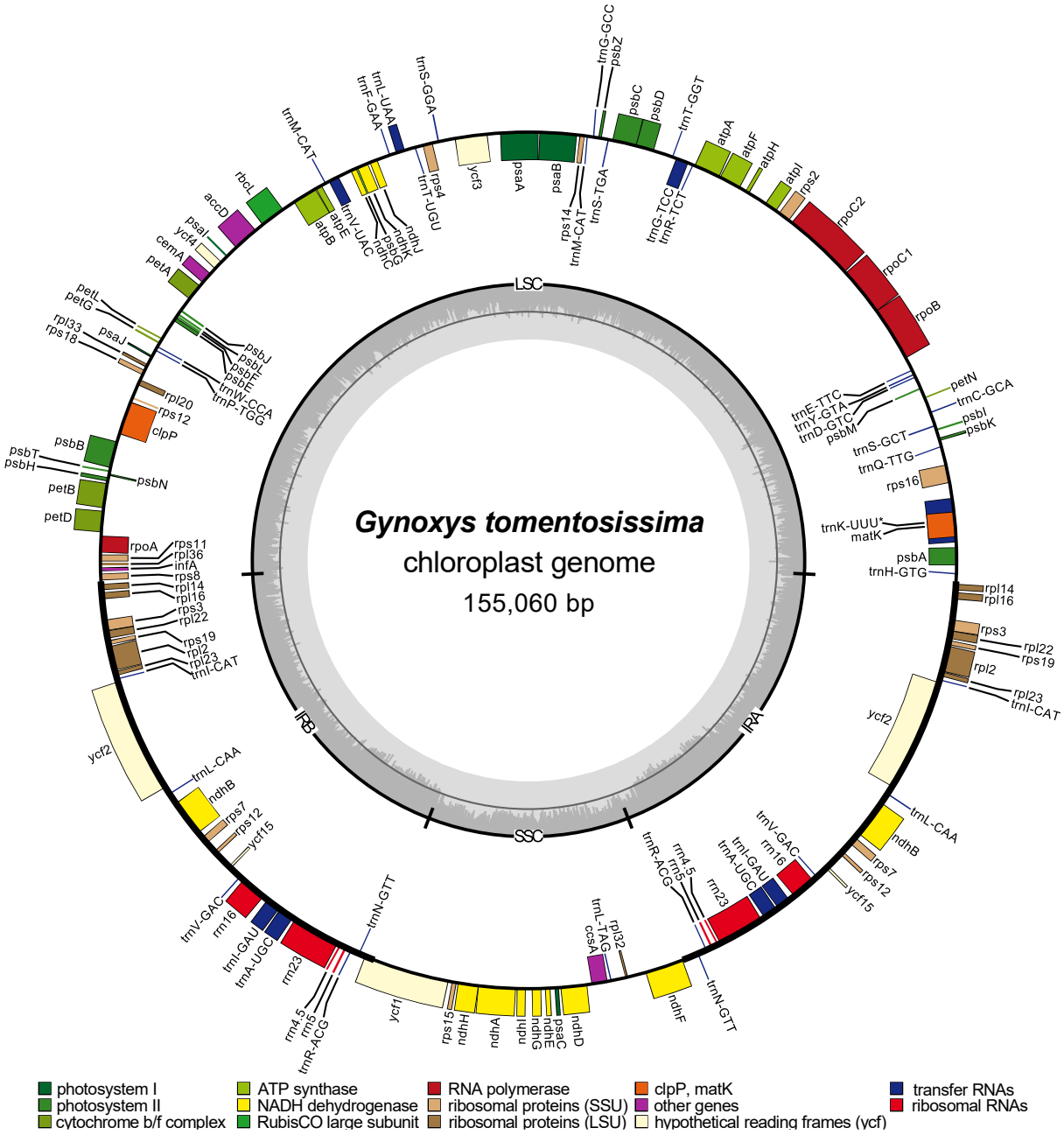

Appendix 2.4: Alignment metrics and homoplasy indices of the MSAs of the coding regions before and after alignment adjustment. The columns are: alignment length, GC content, fraction of polymorphic sites, fraction of parsimony informative sites, ensemble consistency index (CI), ensemble retention index (RI), ensemble rescaled consistency index (RC), and the maximum uncorrected p-distance. The table is ordered by the RC value, but the concatenated dataset of all markers is always on top. Fractions refer to the full alignment length.

	Alignm. (bp)		GC content		Polymorph. sites		Pars. inform. sites		CI		RI		RC		Uncorr. p-dist.	
Region	Before	After	Before	After	Before	After	Before	After	Before	After	Before	After	Before	After	Before	After
81 CDS	68,118	68,076	0.38	0.38	0.02	0.03	0.00	0.00	0.92	0.92	0.87	0.87	0.80	0.80	0.09	0.09
atpA	1524	1524	0.41	0.41	0.01	0.01	0.00	0.00	1.00	1.00	1.00	1.00	1.00	1.00	0.09	0.09
atpB	1494	1494	0.42	0.42	0.01	0.01	0.00	0.00	1.00	1.00	1.00	1.00	1.00	1.00	0.08	0.08
atpF	594	594	0.37	0.37	0.01	0.01	0.00	0.00	1.00	1.00	1.00	1.00	1.00	1.00	0.08	0.08
atpI	741	741	0.38	0.38	0.02	0.02	0.00	0.00	1.00	1.00	1.00	1.00	1.00	1.00	0.12	0.12
ccsA	966	966	0.32	0.32	0.02	0.02	0.00	0.00	1.00	1.00	1.00	1.00	1.00	1.00	0.11	0.11
cemA	687	687	0.33	0.33	0.02	0.02	0.00	0.00	1.00	1.00	1.00	1.00	1.00	1.00	0.10	0.10
clpP	585	585	0.43	0.43	0.01	0.01	0.00	0.00	1.00	1.00	1.00	1.00	1.00	1.00	0.10	0.10
ndhA	1101	1101	0.34	0.34	0.01	0.01	0.00	0.00	1.00	1.00	1.00	1.00	1.00	1.00	0.10	0.10
ndhD	1503	1503	0.36	0.36	0.02	0.02	0.00	0.00	1.00	1.00	1.00	1.00	1.00	1.00	0.11	0.11
ndhE	303	303	0.32	0.32	0.01	0.01	0.00	0.00	1.00	1.00	1.00	1.00	1.00	1.00	0.12	0.12
ndhG	528	528	0.35	0.35	0.02	0.02	0.01	0.01	1.00	1.00	1.00	1.00	1.00	1.00	0.12	0.12
ndhH	1176	1176	0.38	0.38	0.02	0.02	0.00	0.00	1.00	1.00	1.00	1.00	1.00	1.00	0.11	0.11
ndhI	498	498	0.35	0.35	0.01	0.01	0.00	0.00	1.00	1.00	1.00	1.00	1.00	1.00	0.09	0.09
ndhJ	474	474	0.40	0.40	0.02	0.02	0.00	0.00	1.00	1.00	1.00	1.00	1.00	1.00	0.14	0.14
petA	960	960	0.41	0.41	0.01	0.01	0.00	0.00	1.00	1.00	1.00	1.00	1.00	1.00	0.07	0.07
petB	645	645	0.40	0.40	0.01	0.01	0.01	0.01	1.00	1.00	1.00	1.00	1.00	1.00	0.10	0.10
petD	531	531	0.40	0.40	0.02	0.02	0.01	0.01	1.00	1.00	1.00	1.00	1.00	1.00	0.11	0.11
petG	111	111	0.37	0.37	0.03	0.03	0.01	0.01	1.00	1.00	1.00	1.00	1.00	1.00	0.16	0.16
psaC	243	243	0.44	0.44	0.01	0.01	0.00	0.00	1.00	1.00	1.00	1.00	1.00	1.00	0.11	0.11
psbA	1059	1059	0.42	0.42	0.01	0.01	0.00	0.00	1.00	1.00	1.00	1.00	1.00	1.00	0.07	0.07
psbB	1524	1524	0.44	0.44	0.01	0.01	0.00	0.00	1.00	1.00	1.00	1.00	1.00	1.00	0.09	0.09
psbC	1419	1419	0.43	0.43	0.01	0.01	0.00	0.00	1.00	1.00	1.00	1.00	1.00	1.00	0.07	0.07

	Alignm. (bp)		GC content		Polymorph. sites		Pars. inform. sites		CI		RI		RC		Uncorr. p-dist.	
Region	Before	After	Before	After	Before	After	Before	After	Before	After	Before	After	Before	After	Before	After
psbD	1059	1059	0.43	0.43	0.01	0.01	0.00	0.00	1.00	1.00	1.00	1.00	1.00	1.00	0.07	0.07
psbE	249	249	0.41	0.41	0.00	0.00	0.00	0.00	1.00	1.00	1.00	1.00	1.00	1.00	0.06	0.06
rpl2	825	825	0.44	0.44	0.01	0.01	0.00	0.00	1.00	1.00	1.00	1.00	1.00	1.00	0.08	0.08
rpl20	360	360	0.36	0.36	0.01	0.01	0.00	0.00	1.00	1.00	1.00	1.00	1.00	1.00	0.07	0.07
rpl22	468	468	0.35	0.35	0.02	0.02	0.01	0.01	1.00	1.00	1.00	1.00	1.00	1.00	0.09	0.09
rpl23	279	285	0.40	0.40	0.01	0.03	0.01	0.00	1.00	1.00	1.00	1.00	1.00	1.00	0.10	0.06
rpl33	198	198	0.41	0.41	0.02	0.02	0.01	0.01	1.00	1.00	1.00	1.00	1.00	1.00	0.14	0.14
rpoA	1005	1005	0.35	0.35	0.03	0.03	0.01	0.01	1.00	1.00	1.00	1.00	1.00	1.00	0.12	0.12
rps15	276	276	0.33	0.33	0.02	0.02	0.00	0.00	1.00	1.00	1.00	1.00	1.00	1.00	0.10	0.10
rps16	261	261	0.39	0.39	0.03	0.03	0.02	0.02	1.00	1.00	1.00	1.00	1.00	1.00	0.17	0.17
rps2	708	708	0.37	0.37	0.02	0.02	0.00	0.00	1.00	1.00	1.00	1.00	1.00	1.00	0.09	0.09
rps4	603	603	0.40	0.40	0.02	0.02	0.00	0.00	1.00	1.00	1.00	1.00	1.00	1.00	0.11	0.11
ycf3	504	504	0.39	0.39	0.01	0.01	0.01	0.01	1.00	1.00	1.00	1.00	1.00	1.00	0.06	0.06
ndhF	2232	2232	0.32	0.32	0.03	0.03	0.01	0.01	0.97	0.97	0.94	0.94	0.91	0.91	0.12	0.12
rpoB	318	3198	0.39	0.39	0.02	0.02	0.00	0.00	0.97	0.96	0.93	0.93	0.90	0.90	0.10	0.10
matK	1509	1509	0.34	0.34	0.03	0.03	0.01	0.01	0.96	0.96	0.93	0.93	0.90	0.90	0.12	0.12
ycf4	552	552	0.39	0.39	0.03	0.03	0.01	0.01	0.94	0.94	0.95	0.95	0.89	0.89	0.13	0.13
rpoC2	4146	4146	0.38	0.38	0.02	0.02	0.00	0.00	0.96	0.96	0.92	0.92	0.89	0.88	0.10	0.10
psaA	2250	2250	0.43	0.43	0.01	0.01	0.00	0.00	0.97	1.00	0.88	1.00	0.85	1.00	0.09	0.08
ndhK	675	675	0.38	0.38	0.01	0.01	0.00	0.00	0.91	0.91	0.90	0.90	0.82	0.82	0.11	0.11
ycf2	6675	6689	0.38	0.38	0.01	0.01	0.00	0.00	0.93	0.95	0.88	0.89	0.82	0.84	0.06	0.06
rpoC1	2088	2088	0.38	0.38	0.02	0.02	0.01	0.01	0.92	0.92	0.89	0.89	0.81	0.81	0.10	0.10
accD	1494	1494	0.36	0.36	0.02	0.02	0.01	0.01	0.94	0.94	0.83	0.83	0.78	0.78	0.09	0.09
psaB	2202	2202	0.40	0.40	0.01	0.01	0.00	0.00	0.93	0.93	0.83	0.83	0.77	0.77	0.06	0.06
rps3	654	654	0.34	0.34	0.02	0.02	0.01	0.01	0.88	0.88	0.82	0.82	0.72	0.72	0.10	0.10
rbcL	1455	1455	0.44	0.44	0.01	0.06	0.01	0.01	0.79	0.76	0.87	0.85	0.69	0.64	0.09	0.09
ycf1	5151	5074	0.29	0.29	0.08	0.07	0.01	0.01	0.84	0.84	0.82	0.81	0.69	0.68	0.14	0.13
atpE	399	399	0.41	0.41	0.01	0.01	0.00	0.00	1.00	1.00	n.a.	n.a.	n.a.	n.a.	0.07	0.07
atpH	243	243	0.45	0.45	0.01	0.01	0.00	0.00	1.00	1.00	n.a.	n.a.	n.a.	n.a.	0.09	0.09
infA	231	231	0.37	0.37	0.01	0.01	0.00	0.00	1.00	1.00	n.a.	n.a.	n.a.	n.a.	0.09	0.09
ndhB	1530	1530	0.37	0.37	0.00	0.00	0.00	0.00	1.00	1.00	n.a.	n.a.	n.a.	n.a.	0.05	0.05

Continued on next page

	Alignm. (bp)		GC content		Polymorph. sites		Pars. inform. sites		CI		RI		RC		Uncorr. p-dist.	
Region	Before	After	Before	After	Before	After	Before	After	Before	After	Before	After	Before	After	Before	After
ndhC	360	360	0.35	0.35	0.00	0.00	0.00	0.00	n.a.	n.a.	n.a.	n.a.	n.a.	n.a.	0.00	0.00
petL	93	93	0.34	0.34	0.01	0.01	0.00	0.00	1.00	1.00	n.a.	n.a.	n.a.	n.a.	0.10	0.10
petN	87	87	0.41	0.41	0.01	0.01	0.00	0.00	1.00	1.00	n.a.	n.a.	n.a.	n.a.	0.11	0.11
psaI	108	108	0.37	0.37	0.02	0.02	0.00	0.00	1.00	1.00	n.a.	n.a.	n.a.	n.a.	0.14	0.14
psaJ	132	132	0.40	0.40	0.00	0.00	0.00	0.00	n.a.	n.a.	n.a.	n.a.	n.a.	n.a.	0.00	0.00
psbF	117	117	0.44	0.44	0.00	0.00	0.00	0.00	n.a.	n.a.	n.a.	n.a.	n.a.	n.a.	0.00	0.00
psbG	57	57	0.28	0.28	0.05	0.02	0.00	0.00	1.00	n.a.	n.a.	n.a.	n.a.	n.a.	0.24	0.00
psbH	237	237	0.38	0.38	0.01	0.01	0.00	0.00	1.00	1.00	n.a.	n.a.	n.a.	n.a.	0.09	0.09
psbI	108	108	0.37	0.37	0.02	0.02	0.00	0.00	1.00	1.00	n.a.	n.a.	n.a.	n.a.	0.14	0.14
psbJ	120	120	0.42	0.42	0.00	0.00	0.00	0.00	n.a.	n.a.	n.a.	n.a.	n.a.	n.a.	0.00	0.00
psbK	177	177	0.38	0.38	0.01	0.01	0.00	0.00	1.00	1.00	n.a.	n.a.	n.a.	n.a.	0.11	0.11
psbL	114	114	0.34	0.34	0.00	0.00	0.00	0.00	n.a.	n.a.	n.a.	n.a.	n.a.	n.a.	0.00	0.00
psbM	102	102	0.28	0.28	0.00	0.00	0.00	0.00	n.a.	n.a.	n.a.	n.a.	n.a.	n.a.	0.00	0.00
psbN	138	138	0.43	0.43	0.00	0.00	0.00	0.00	n.a.	n.a.	n.a.	n.a.	n.a.	n.a.	0.00	0.00
psbT	99	99	0.33	0.33	0.01	0.01	0.00	0.00	1.00	1.00	n.a.	n.a.	n.a.	n.a.	0.10	0.10
psbZ	186	186	0.36	0.36	0.01	0.01	0.00	0.00	1.00	1.00	n.a.	n.a.	n.a.	n.a.	0.07	0.07
rpl14	366	366	0.40	0.40	0.01	0.01	0.00	0.00	1.00	1.00	n.a.	n.a.	n.a.	n.a.	0.07	0.07
rpl16	420	417	0.43	0.43	0.01	0.01	0.00	0.00	1.00	1.00	n.a.	n.a.	n.a.	n.a.	0.10	0.10
rpl32	162	162	0.34	0.34	0.01	0.01	0.00	0.00	1.00	1.00	n.a.	n.a.	n.a.	n.a.	0.08	0.08
rpl36	111	111	0.36	0.36	0.00	0.00	0.00	0.00	n.a.	n.a.	n.a.	n.a.	n.a.	n.a.	0.00	0.00
rps11	408	408	0.46	0.46	0.06	0.57	0.00	0.00	1.00	1.00	n.a.	n.a.	n.a.	n.a.	0.23	0.10
rps12	354	354	0.45	0.45	0.00	0.00	0.00	0.00	1.00	1.00	n.a.	n.a.	n.a.	n.a.	0.05	0.05
rps14	300	300	0.41	0.41	0.02	0.02	0.00	0.00	1.00	1.00	n.a.	n.a.	n.a.	n.a.	0.12	0.12
rps18	303	303	0.35	0.35	0.00	0.00	0.00	0.00	1.00	1.00	n.a.	n.a.	n.a.	n.a.	0.06	0.06
rps19	276	276	0.34	0.34	0.01	0.01	0.00	0.00	1.00	1.00	n.a.	n.a.	n.a.	n.a.	0.09	0.09
rps7	465	465	0.41	0.41	0.03	0.37	0.00	0.00	1.00	1.00	n.a.	n.a.	n.a.	n.a.	0.17	0.07
rps8	402	402	0.36	0.36	0.01	0.01	0.00	0.00	1.00	1.00	n.a.	n.a.	n.a.	n.a.	0.09	0.09
ycf15	189	189	0.49	0.49	0.00	0.00	0.00	0.00	n.a.	n.a.	n.a.	n.a.	n.a.	n.a.	0.00	0.00

Appendix 2.5: Alignment metrics and homoplasy indices of the MSAs of the intergenic spacers before and after alignment adjustment. The columns are: alignment length, GC content, fraction of polymorphic sites, fraction of parsimony informative sites, ensemble consistency index (CI), ensemble retention index (RI), ensemble rescaled consistency index (RC), and the maximum uncorrected p-distance. The table is ordered by the RC value, but the concatenated dataset of all markers is always on top. Fractions refer to the full alignment length.

	Alignm. (bp)		GC content		Polymorph. sites		Pars. inform. sites		CI		RI		RC		Uncorr. p-dist.	
Region	Before	After	Before	After	Before	After	Before	After	Before	After	Before	After	Before	After	Before	After
103 IGS	38,752	37,051	0.31	0.32	0.10	0.10	0.01	0.01	0.88	0.92	0.79	0.86	0.69	0.79	0.15	0.14
atpA–trnR-TCT	116	116	0.19	0.19	0.07	0.07	0.01	0.01	1.00	1.00	1.00	1.00	1.00	1.00	0.21	0.21
atpH–atpF	392	407	0.30	0.30	0.08	0.11	0.02	0.00	1.00	1.00	1.00	1.00	1.00	1.00	0.22	0.16
atpI–atpH	1139	1086	0.31	0.32	0.09	0.07	0.00	0.00	1.00	1.00	1.00	1.00	1.00	1.00	0.14	0.13
ndhD–ccsA	282	282	0.30	0.30	0.08	0.08	0.01	0.01	1.00	1.00	1.00	1.00	1.00	1.00	0.17	0.17
ndhE–psaC	247	247	0.26	0.26	0.05	0.09	0.00	0.00	1.00	1.00	1.00	1.00	1.00	1.00	0.20	0.18
ndhG–ndhE	228	228	0.28	0.28	0.07	0.07	0.00	0.00	1.00	1.00	1.00	1.00	1.00	1.00	0.19	0.19
petB–petD	195	195	0.28	0.28	0.05	0.05	0.01	0.01	1.00	1.00	1.00	1.00	1.00	1.00	0.19	0.19
petD–rpoA	202	203	0.31	0.31	0.13	0.11	0.01	0.01	1.00	1.00	1.00	1.00	1.00	1.00	0.21	0.13
petG–trnW-CCA	117	117	0.35	0.35	0.03	0.03	0.01	0.01	1.00	1.00	1.00	1.00	1.00	1.00	0.18	0.18
petL–petG	153	153	0.31	0.31	0.03	0.03	0.01	0.01	1.00	1.00	1.00	1.00	1.00	1.00	0.16	0.16
psaC–ndhD	115	114	0.39	0.39	0.09	0.13	0.02	0.01	1.00	1.00	1.00	1.00	1.00	1.00	0.23	0.13
psaI–ycf4	391	380	0.35	0.36	0.04	0.03	0.00	0.00	1.00	1.00	1.00	1.00	1.00	1.00	0.09	0.09
psbB–psbT	196	186	0.31	0.32	0.20	0.18	0.01	0.01	1.00	1.00	1.00	1.00	1.00	1.00	0.20	0.16
psbH–petB	124	124	0.35	0.35	0.05	0.05	0.03	0.03	1.00	1.00	1.00	1.00	1.00	1.00	0.22	0.22
psbI–trnS-GCT	142	146	0.25	0.25	0.17	0.16	0.01	0.01	1.00	1.00	1.00	1.00	1.00	1.00	0.27	0.21
psbK–psbI	453	453	0.29	0.29	0.15	0.15	0.00	0.00	1.00	1.00	1.00	1.00	1.00	1.00	0.16	0.16
psbZ–trnG-GCC	316	316	0.33	0.33	0.09	0.09	0.02	0.02	1.00	1.00	1.00	1.00	1.00	1.00	0.15	0.15
rbcL–accD	525	525	0.31	0.31	0.06	0.06	0.01	0.01	1.00	1.00	1.00	1.00	1.00	1.00	0.15	0.14
rpl33–rps18	188	188	0.29	0.29	0.01	0.01	0.01	0.01	1.00	1.00	1.00	1.00	1.00	1.00	0.07	0.07
rpoC1–rpoC2	101	101	0.37	0.37	0.03	0.10	0.03	0.01	1.00	1.00	1.00	1.00	1.00	1.00	0.18	0.10
rpoC2–rps2	229	214	0.38	0.40	0.08	0.04	0.00	0.01	1.00	1.00	1.00	1.00	1.00	1.00	0.18	0.14
rps12–ycf15	955	955	0.37	0.37	0.02	0.02	0.00	0.00	1.00	1.00	1.00	1.00	1.00	1.00	0.07	0.07

	Alignm. (bp)		GC content		Polymorph. sites		Pars. inform. sites		CI		RI		RC		Uncorr. p-dist.	
Region	Before	After	Before	After	Before	After	Before	After	Before	After	Before	After	Before	After	Before	After
accD–psaI	696	708	0.23	0.23	0.15	0.17	0.03	0.02	0.97	0.98	0.95	0.97	0.92	0.95	0.20	0.17
trnE-TTC–rpoB	802	785	0.31	0.32	0.17	0.15	0.01	0.01	0.96	0.98	0.93	0.96	0.89	0.94	0.18	0.17
ycf3–trnS-GGA	891	871	0.29	0.30	0.11	0.09	0.01	0.01	0.91	0.97	0.83	0.94	0.76	0.92	0.17	0.15
trnS-GCT–trnC-GCA	764	763	0.29	0.29	0.20	0.20	0.02	0.08	0.92	0.95	0.90	0.95	0.83	0.90	0.19	0.18
clpP–psbB	466	456	0.30	0.31	0.11	0.10	0.01	0.01	0.95	0.95	0.93	0.93	0.89	0.89	0.17	0.17
petA–psbJ	764	741	0.31	0.32	0.09	0.08	0.01	0.01	0.94	0.94	0.94	0.94	0.88	0.88	0.17	0.17
rpl32–ndhF	1098	1047	0.22	0.23	0.19	0.18	0.04	0.03	0.93	0.93	0.94	0.94	0.88	0.88	0.21	0.18
rps16–trnQ-TTG	984	970	0.28	0.28	0.11	0.10	0.02	0.02	0.91	0.94	0.90	0.94	0.82	0.88	0.15	0.15
trnT-TGT–trnL-TAA	635	572	0.26	0.27	0.19	0.12	0.02	0.01	0.88	0.95	0.81	0.92	0.71	0.88	0.18	0.13
rps18–rpl20	344	321	0.30	0.32	0.28	0.25	0.02	0.02	0.96	0.95	0.94	0.91	0.90	0.87	0.23	0.20
trnT-GGT–psbD	1283	1275	0.31	0.30	0.20	0.20	0.01	0.01	0.95	0.94	0.91	0.91	0.87	0.86	0.14	0.13
ndhC–trnV-TAC	765	771	0.31	0.31	0.07	0.07	0.02	0.01	0.87	0.95	0.73	0.91	0.63	0.86	0.19	0.17
psaA–ycf3	734	710	0.30	0.31	0.14	0.13	0.01	0.01	0.86	0.97	0.73	0.88	0.63	0.85	0.16	0.15
trnK-TTT–rps16	877	850	0.25	0.26	0.17	0.20	0.03	0.03	0.94	0.92	0.95	0.92	0.89	0.84	0.20	0.16
psbA–trnK-TTT	295	255	0.30	0.30	0.12	0.12	0.02	0.01	0.90	0.93	0.85	0.90	0.76	0.84	0.23	0.22
petN–psbM	509	499	0.28	0.28	0.08	0.12	0.02	0.02	0.84	0.91	0.83	0.93	0.70	0.84	0.20	0.15
cemA–petA	244	245	0.32	0.32	0.05	0.04	0.03	0.01	0.93	0.90	0.96	0.91	0.89	0.82	0.19	0.16
ndhI–ndhG	376	377	0.22	0.22	0.14	0.17	0.02	0.02	0.95	0.93	0.88	0.88	0.83	0.81	0.24	0.21
trnG-TCC–trnT-GGT	188	188	0.31	0.31	0.20	0.20	0.02	0.02	0.92	0.92	0.88	0.88	0.81	0.81	0.18	0.18
trnL-TAG–rpl32	818	775	0.24	0.25	0.13	0.10	0.02	0.02	0.86	0.93	0.71	0.86	0.61	0.80	0.20	0.20
trnQ-TTG–psbK	368	368	0.26	0.26	0.09	0.10	0.01	0.01	0.96	0.94	0.83	0.83	0.80	0.78	0.18	0.12
trnY-GTA–trnE-TTC	203	203	0.33	0.33	0.04	0.04	0.02	0.02	0.86	0.86	0.91	0.91	0.78	0.78	0.14	0.14
psbE–petL	1268	1187	0.29	0.30	0.12	0.08	0.01	0.01	0.86	0.82	0.84	0.82	0.72	0.68	0.13	0.13
rps14–psaB	133	133	0.33	0.33	0.04	0.04	0.03	0.03	0.83	0.83	0.80	0.80	0.67	0.67	0.17	0.17
rpl16–rps3	145	145	0.23	0.23	0.09	0.09	0.03	0.03	0.81	0.81	0.70	0.70	0.57	0.57	0.20	0.20
rpl14–rpl16	120	98	0.25	0.28	0.24	0.22	0.01	0.00	1.00	1.00	1.00	n.a.	1.00	n.a.	0.35	0.23
rpl36–infA	115	129	0.32	0.33	0.08	0.15	0.04	0.00	1.00	1.00	1.00	n.a.	1.00	n.a.	0.21	0.13
rps8–rpl14	211	170	0.23	0.26	0.19	0.06	0.04	0.00	1.00	1.00	1.00	n.a.	1.00	n.a.	0.24	0.16
trnR-TCT–trnG-TCC	221	185	0.20	0.22	0.14	0.06	0.01	0.00	1.00	1.00	1.00	n.a.	1.00	n.a.	0.24	0.17
trnS-TGA–psbZ	340	329	0.36	0.36	0.17	0.15	0.00	0.00	1.00	1.00	1.00	n.a.	1.00	n.a.	0.12	0.12
atpF–atpA	78	62	0.21	0.24	0.15	0.08	0.00	0.00	1.00	1.00	n.a.	n.a.	n.a.	n.a.	0.23	0.25

Continued on next page

	Alignm. (bp)		GC content		Polymorph. sites		Pars. inform. sites		CI		RI		RC		Uncorr. p-dist.	
Region	Before	After	Before	After	Before	After	Before	After	Before	After	Before	After	Before	After	Before	After
accD–psaI	696	708	0.23	0.23	0.15	0.17	0.03	0.02	0.97	0.98	0.95	0.97	0.92	0.95	0.20	0.17
trnE-TTC–rpoB	802	785	0.31	0.32	0.17	0.15	0.01	0.01	0.96	0.98	0.93	0.96	0.89	0.94	0.18	0.17
ycf3–trnS-GGA	891	871	0.29	0.30	0.11	0.09	0.01	0.01	0.91	0.97	0.83	0.94	0.76	0.92	0.17	0.15
trnS-GCT–trnC-GCA	764	763	0.29	0.29	0.20	0.20	0.02	0.08	0.92	0.95	0.90	0.95	0.83	0.90	0.19	0.18
clpP–psbB	466	456	0.30	0.31	0.11	0.10	0.01	0.01	0.95	0.95	0.93	0.93	0.89	0.89	0.17	0.17
petA–psbJ	764	741	0.31	0.32	0.09	0.08	0.01	0.01	0.94	0.94	0.94	0.94	0.88	0.88	0.17	0.17
rpl32–ndhF	1098	1047	0.22	0.23	0.19	0.18	0.04	0.03	0.93	0.93	0.94	0.94	0.88	0.88	0.21	0.18
rps16–trnQ-TTG	984	970	0.28	0.28	0.11	0.10	0.02	0.02	0.91	0.94	0.90	0.94	0.82	0.88	0.15	0.15
trnT-TGT–trnL-TAA	635	572	0.26	0.27	0.19	0.12	0.02	0.01	0.88	0.95	0.81	0.92	0.71	0.88	0.18	0.13
rps18–rpl20	344	321	0.30	0.32	0.28	0.25	0.02	0.02	0.96	0.95	0.94	0.91	0.90	0.87	0.23	0.20
trnT-GGT–psbD	1283	1275	0.31	0.30	0.20	0.20	0.01	0.01	0.95	0.94	0.91	0.91	0.87	0.86	0.14	0.13
ndhC–trnV-TAC	765	771	0.31	0.31	0.07	0.07	0.02	0.01	0.87	0.95	0.73	0.91	0.63	0.86	0.19	0.17
psaA–ycf3	734	710	0.30	0.31	0.14	0.13	0.01	0.01	0.86	0.97	0.73	0.88	0.63	0.85	0.16	0.15
trnK-TTT–rps16	877	850	0.25	0.26	0.17	0.20	0.03	0.03	0.94	0.92	0.95	0.92	0.89	0.84	0.20	0.16
psbA–trnK-TTT	295	255	0.30	0.30	0.12	0.12	0.02	0.01	0.90	0.93	0.85	0.90	0.76	0.84	0.23	0.22
petN–psbM	509	499	0.28	0.28	0.08	0.12	0.02	0.02	0.84	0.91	0.83	0.93	0.70	0.84	0.20	0.15
cemA–petA	244	245	0.32	0.32	0.05	0.04	0.03	0.01	0.93	0.90	0.96	0.91	0.89	0.82	0.19	0.16
ndhI–ndhG	376	377	0.22	0.22	0.14	0.17	0.02	0.02	0.95	0.93	0.88	0.88	0.83	0.81	0.24	0.21
trnG-TCC–trnT-GGT	188	188	0.31	0.31	0.20	0.20	0.02	0.02	0.92	0.92	0.88	0.88	0.81	0.81	0.18	0.18
trnL-TAG–rpl32	818	775	0.24	0.25	0.13	0.10	0.02	0.02	0.86	0.93	0.71	0.86	0.61	0.80	0.20	0.20
trnQ-TTG–psbK	368	368	0.26	0.26	0.09	0.10	0.01	0.01	0.96	0.94	0.83	0.83	0.80	0.78	0.18	0.12
trnY-GTA–trnE-TTC	203	203	0.33	0.33	0.04	0.04	0.02	0.02	0.86	0.86	0.91	0.91	0.78	0.78	0.14	0.14
psbE–petL	1268	1187	0.29	0.30	0.12	0.08	0.01	0.01	0.86	0.82	0.84	0.82	0.72	0.68	0.13	0.13
rps14–psaB	133	133	0.33	0.33	0.04	0.04	0.03	0.03	0.83	0.83	0.80	0.80	0.67	0.67	0.17	0.17
rpl16–rps3	145	145	0.23	0.23	0.09	0.09	0.03	0.03	0.81	0.81	0.70	0.70	0.57	0.57	0.20	0.20
rpl14–rpl16	120	98	0.25	0.28	0.24	0.22	0.01	0.00	1.00	1.00	1.00	n.a.	1.00	n.a.	0.35	0.23
rpl36–infA	115	129	0.32	0.33	0.08	0.15	0.04	0.00	1.00	1.00	1.00	n.a.	1.00	n.a.	0.21	0.13
rps8–rpl14	211	170	0.23	0.26	0.19	0.06	0.04	0.00	1.00	1.00	1.00	n.a.	1.00	n.a.	0.24	0.16
trnR-TCT–trnG-TCC	221	185	0.20	0.22	0.14	0.06	0.01	0.00	1.00	1.00	1.00	n.a.	1.00	n.a.	0.24	0.17
trnS-TGA–psbZ	340	329	0.36	0.36	0.17	0.15	0.00	0.00	1.00	1.00	1.00	n.a.	1.00	n.a.	0.12	0.12
atpF–atpA	78	62	0.21	0.24	0.15	0.08	0.00	0.00	1.00	1.00	n.a.	n.a.	n.a.	n.a.	0.23	0.25

	Alignm. (bp)		GC content		Polymorph. sites		Pars. inform. sites		CI		RI		RC		Uncorr. p-dist.	
Region	Before	After	Before	After	Before	After	Before	After	Before	After	Before	After	Before	After	Before	After
infA–rps8	121	121	0.36	0.36	0.02	0.02	0.00	0.00	1.00	1.00	n.a.	n.a.	n.a.	n.a.	0.13	0.13
ndhA–ndhI	78	78	0.26	0.26	0.06	0.06	0.00	0.00	1.00	1.00	n.a.	n.a.	n.a.	n.a.	0.23	0.23
ndhB–rps7	289	289	0.33	0.33	0.02	0.02	0.00	0.00	1.00	1.00	n.a.	n.a.	n.a.	n.a.	0.12	0.12
ndhJ–ndhK	105	105	0.31	0.31	0.01	0.01	0.00	0.00	1.00	1.00	n.a.	n.a.	n.a.	n.a.	0.10	0.10
psbJ–psbL	148	148	0.39	0.39	0.05	0.05	0.00	0.00	1.00	1.00	n.a.	n.a.	n.a.	n.a.	0.14	0.14
rpl22–rps19	105	77	0.17	0.22	0.16	0.10	0.00	0.00	1.00	1.00	n.a.	n.a.	n.a.	n.a.	0.17	0.12
rpl23–trnI-CAT	165	165	0.33	0.33	0.01	0.01	0.00	0.00	1.00	1.00	n.a.	n.a.	n.a.	n.a.	0.08	0.08
rpoA–rps11	89	89	0.23	0.23	0.11	0.11	0.00	0.00	1.00	1.00	n.a.	n.a.	n.a.	n.a.	0.11	0.11
rps11–rpl36	105	105	0.32	0.32	0.02	0.02	0.00	0.00	1.00	1.00	n.a.	n.a.	n.a.	n.a.	0.14	0.14
rps15–ndhH	97	97	0.31	0.31	0.07	0.07	0.00	0.00	1.00	1.00	n.a.	n.a.	n.a.	n.a.	0.10	0.10
rrn23–rrn45	99	99	0.56	0.56	0.01	0.01	0.00	0.00	1.00	1.00	n.a.	n.a.	n.a.	n.a.	0.10	0.10
rrn45–rrn5	251	251	0.45	0.45	0.02	0.02	0.00	0.00	1.00	1.00	n.a.	n.a.	n.a.	n.a.	0.06	0.06
trnI-CAT–ycf2	111	111	0.32	0.32	0.01	0.01	0.00	0.00	1.00	1.00	n.a.	n.a.	n.a.	n.a.	0.10	0.10
trnL-CAA–ndhB	576	587	0.36	0.36	0.03	0.05	0.00	0.00	1.00	1.00	n.a.	n.a.	n.a.	n.a.	0.14	0.09
psaB–psaA	25	25	0.44	0.44	0.00	0.00	0.00	0.00	n.a.	n.a.	n.a.	n.a.	n.a.	n.a.	0.00	0.00
psbL–psbF	22	22	0.36	0.36	0.00	0.00	0.00	0.00	n.a.	n.a.	n.a.	n.a.	n.a.	n.a.	0.00	0.00
psbN–psbH	84	84	0.27	0.27	0.00	0.00	0.00	0.00	n.a.	n.a.	n.a.	n.a.	n.a.	n.a.	0.00	0.00
rpl2–rpl23	18	18	0.22	0.22	0.00	0.00	0.00	0.00	n.a.	n.a.	n.a.	n.a.	n.a.	n.a.	0.00	0.00
trnD-GTC–trnY-GTA	92	92	0.36	0.36	0.00	0.00	0.00	0.00	n.a.	n.a.	n.a.	n.a.	n.a.	n.a.	0.00	0.00
trnI-GAT–trnA-TGC	64	64	0.55	0.55	0.00	0.00	0.00	0.00	n.a.	n.a.	n.a.	n.a.	n.a.	n.a.	0.00	0.00

Appendix 2.6: Alignment metrics and homoplasy indices of the MSAs of the introns before and after alignment adjustment. The columns are: alignment length, GC content, fraction of polymorphic sites, fraction of parsimony informative sites, ensemble consistency index (CI), ensemble retention index (RI), ensemble rescaled consistency index (RC), and the maximum uncorrected p-distance. The table is ordered by the RC value, but the concatenated dataset of all markers is always on top. Fractions refer to the full alignment length.

	Alignm. (bp)		GC content		Polymorph. sites		Pars. inform. sites		CI		RI		RC		Uncorr. p-dist.	
Region	Before	After	Before	After	Before	After	Before	After	Before	After	Before	After	Before	After	Before	After
infA–rps8	121	121	0.36	0.36	0.02	0.02	0.00	0.00	1.00	1.00	n.a.	n.a.	n.a.	n.a.	0.13	0.13
ndhA–ndhI	78	78	0.26	0.26	0.06	0.06	0.00	0.00	1.00	1.00	n.a.	n.a.	n.a.	n.a.	0.23	0.23
ndhB–rps7	289	289	0.33	0.33	0.02	0.02	0.00	0.00	1.00	1.00	n.a.	n.a.	n.a.	n.a.	0.12	0.12
ndhJ–ndhK	105	105	0.31	0.31	0.01	0.01	0.00	0.00	1.00	1.00	n.a.	n.a.	n.a.	n.a.	0.10	0.10
psbJ–psbL	148	148	0.39	0.39	0.05	0.05	0.00	0.00	1.00	1.00	n.a.	n.a.	n.a.	n.a.	0.14	0.14
rpl22–rps19	105	77	0.17	0.22	0.16	0.10	0.00	0.00	1.00	1.00	n.a.	n.a.	n.a.	n.a.	0.17	0.12
rpl23–trnI-CAT	165	165	0.33	0.33	0.01	0.01	0.00	0.00	1.00	1.00	n.a.	n.a.	n.a.	n.a.	0.08	0.08
rpoA–rps11	89	89	0.23	0.23	0.11	0.11	0.00	0.00	1.00	1.00	n.a.	n.a.	n.a.	n.a.	0.11	0.11
rps11–rpl36	105	105	0.32	0.32	0.02	0.02	0.00	0.00	1.00	1.00	n.a.	n.a.	n.a.	n.a.	0.14	0.14
rps15–ndhH	97	97	0.31	0.31	0.07	0.07	0.00	0.00	1.00	1.00	n.a.	n.a.	n.a.	n.a.	0.10	0.10
rrn23–rrn45	99	99	0.56	0.56	0.01	0.01	0.00	0.00	1.00	1.00	n.a.	n.a.	n.a.	n.a.	0.10	0.10
rrn45–rrn5	251	251	0.45	0.45	0.02	0.02	0.00	0.00	1.00	1.00	n.a.	n.a.	n.a.	n.a.	0.06	0.06
trnI-CAT–ycf2	111	111	0.32	0.32	0.01	0.01	0.00	0.00	1.00	1.00	n.a.	n.a.	n.a.	n.a.	0.10	0.10
trnL-CAA–ndhB	576	587	0.36	0.36	0.03	0.05	0.00	0.00	1.00	1.00	n.a.	n.a.	n.a.	n.a.	0.14	0.09
psaB–psaA	25	25	0.44	0.44	0.00	0.00	0.00	0.00	n.a.	n.a.	n.a.	n.a.	n.a.	n.a.	0.00	0.00
psbL–psbF	22	22	0.36	0.36	0.00	0.00	0.00	0.00	n.a.	n.a.	n.a.	n.a.	n.a.	n.a.	0.00	0.00
psbN–psbH	84	84	0.27	0.27	0.00	0.00	0.00	0.00	n.a.	n.a.	n.a.	n.a.	n.a.	n.a.	0.00	0.00
rpl2–rpl23	18	18	0.22	0.22	0.00	0.00	0.00	0.00	n.a.	n.a.	n.a.	n.a.	n.a.	n.a.	0.00	0.00
trnD-GTC–trnY-GTA	92	92	0.36	0.36	0.00	0.00	0.00	0.00	n.a.	n.a.	n.a.	n.a.	n.a.	n.a.	0.00	0.00
trnI-GAT–trnA-TGC	64	64	0.55	0.55	0.00	0.00	0.00	0.00	n.a.	n.a.	n.a.	n.a.	n.a.	n.a.	0.00	0.00

Appendix 2.7: Comparison of the CI and the RC values across each MSA under study before (dashed lines) and after (solid lines) the alignment adjustment.

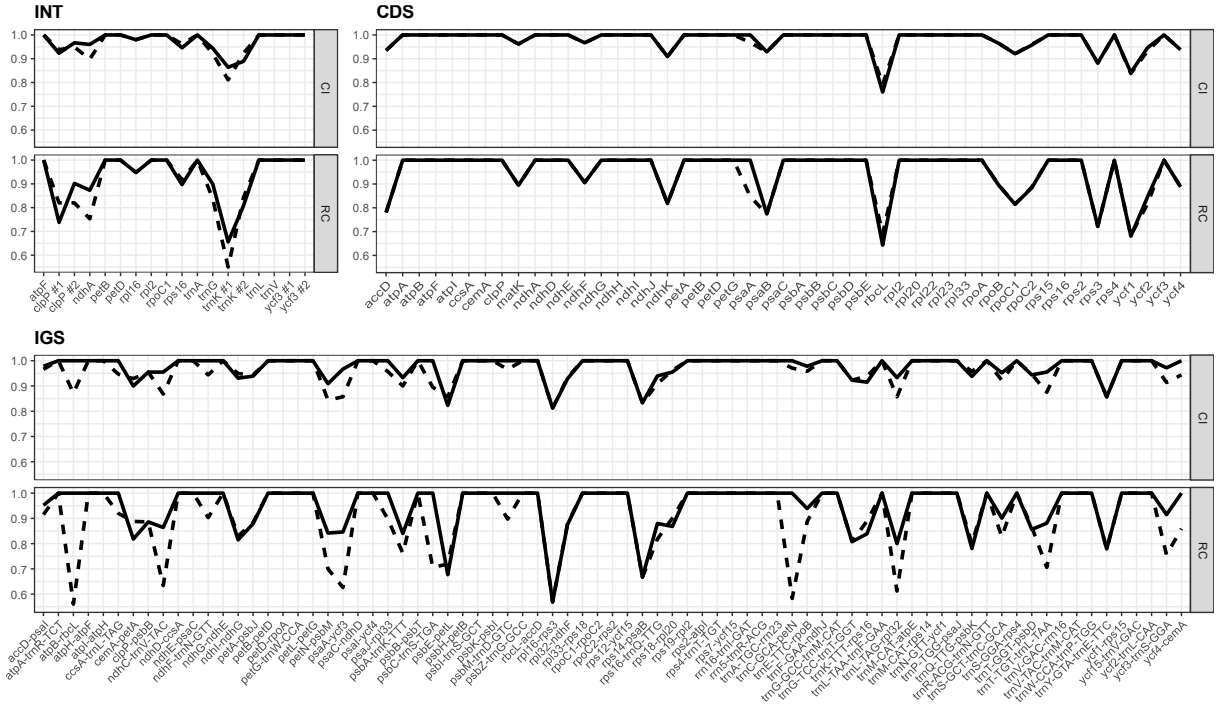

Appendix 2.8: Results of phylogenetic tree inference via ML on the concatenated MSAs of all coding regions before and after alignment adjustment as well as with and without the coding of indels. The tree displayed for each category represents the tree with the highest likelihood score and is visualized as a cladogram with statistical node support (left) and a corresponding phylogram with exact branch lengths (right). Bootstrap support values greater than 50% are given above the branches of each cladogram. All trees were rooted with using *Ligularia fischeri* as outgroup.

Alignment adjust-ment	Indel coding	Tree with the highest likelihood score
before	without	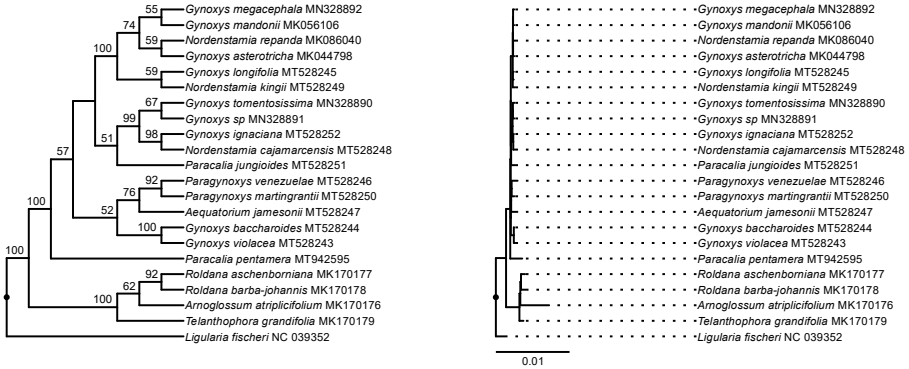
before	with	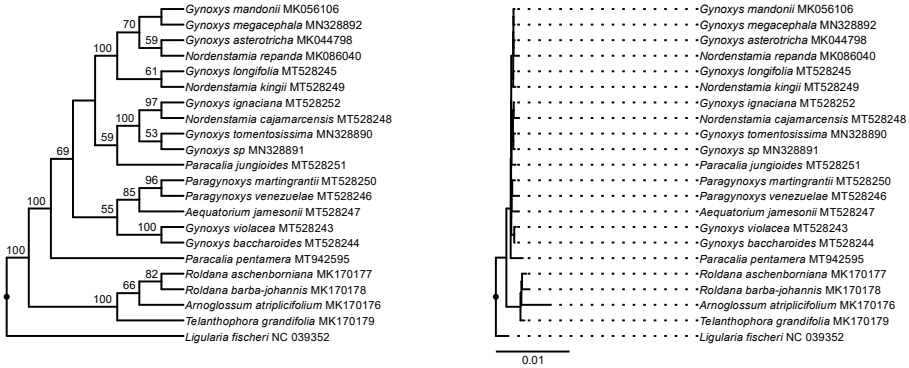
after	without	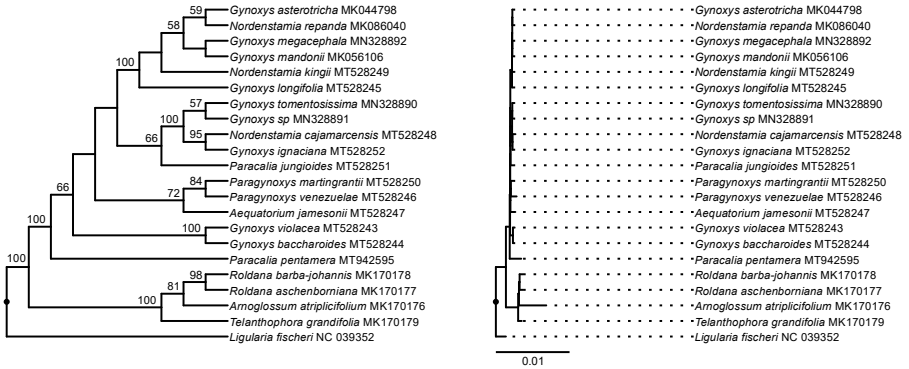
after	with	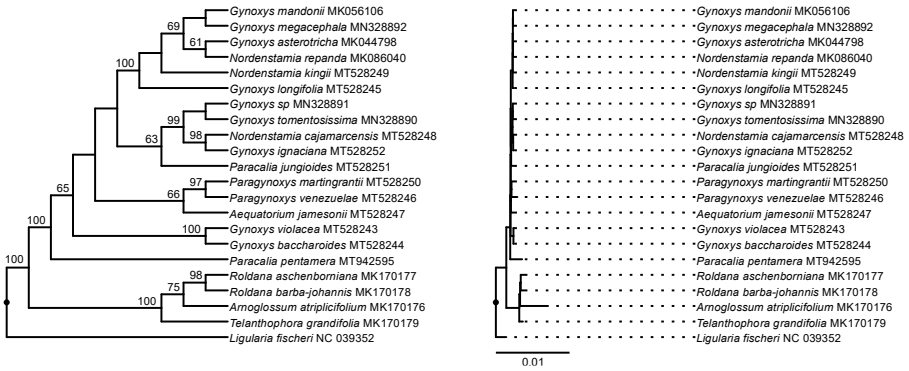

Appendix 2.9: Results of phylogenetic tree inference via ML on the concatenated MSAs of all introns before and after alignment adjustment as well as with and without the coding of indels. The tree displayed for each category represents the tree with the highest likelihood score and is visualized as a cladogram with statistical node support (left) and a corresponding phylogram with exact branch lengths (right). Bootstrap support values greater than 50% are given above the branches of each cladogram. All trees were rooted with using *Ligularia fischeri* as outgroup.

Alignment adjust-ment	Indel coding	Tree with the highest likelihood score
before	without	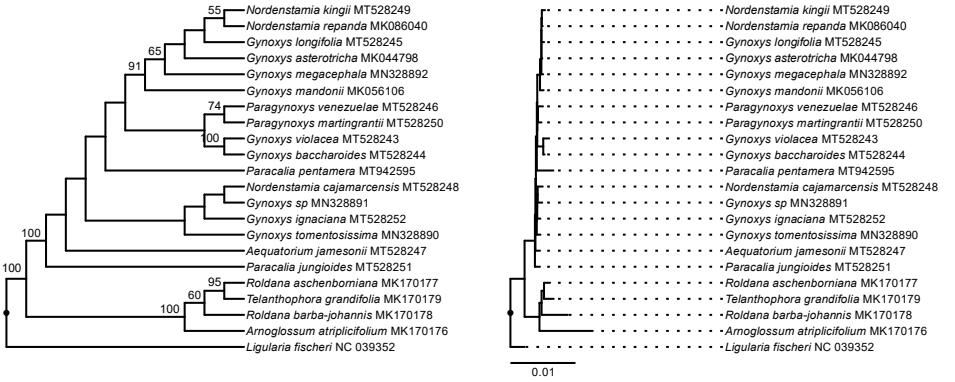
before	with	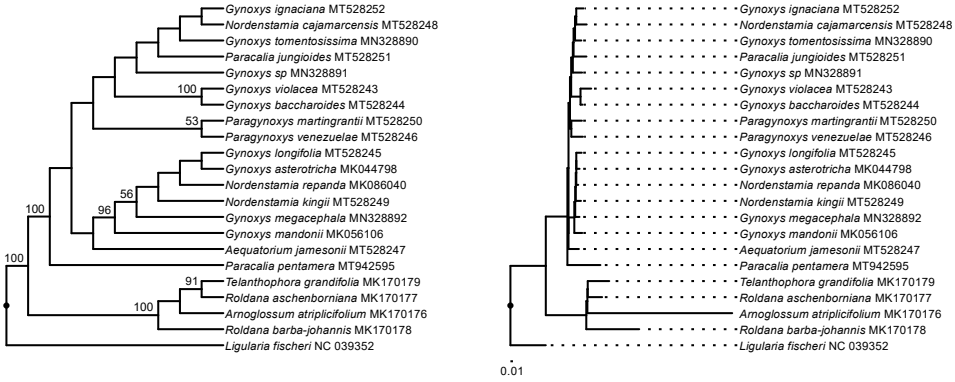
after	without	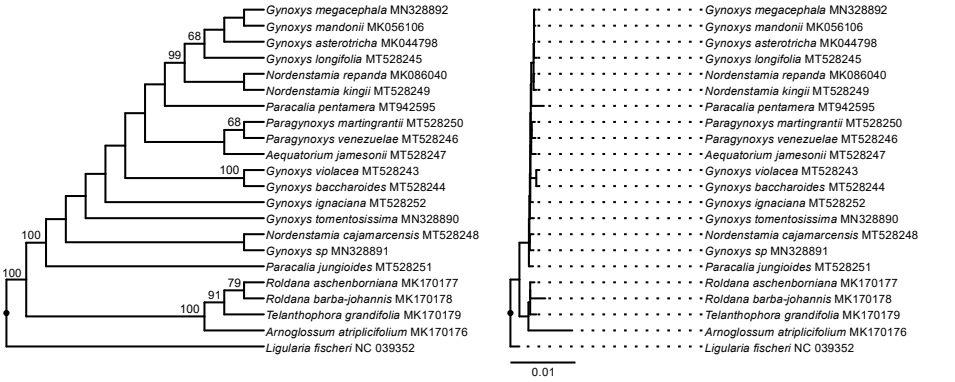
after	with	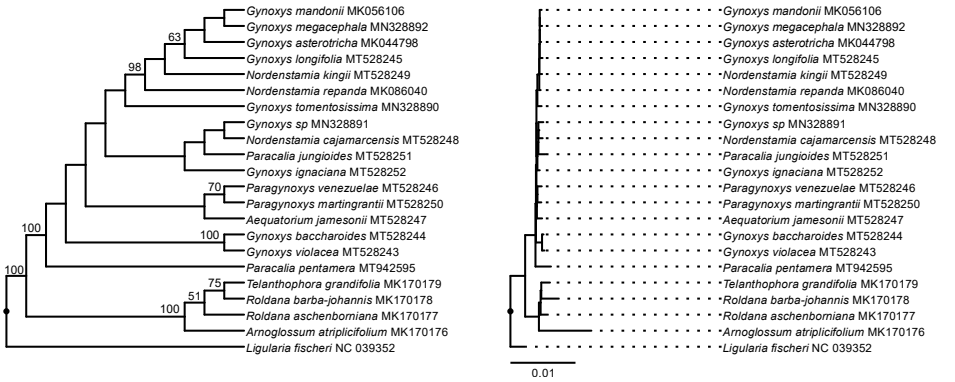

Appendix 2.10: Results of phylogenetic tree inference via ML on the concatenated MSAs of all intergenic spacers before and after alignment adjustment as well as with and without the coding of indels. The tree displayed for each category represents the tree with the highest likelihood score and is visualized as a cladogram with statistical node support (left) and a corresponding phylogram with exact branch lengths (right). Bootstrap support values greater than 50% are given above the branches of each cladogram. All trees were rooted with using *Ligularia fischeri* as outgroup.

Alignment adjust-ment	Indel coding	Tree with the highest likelihood score
before	without	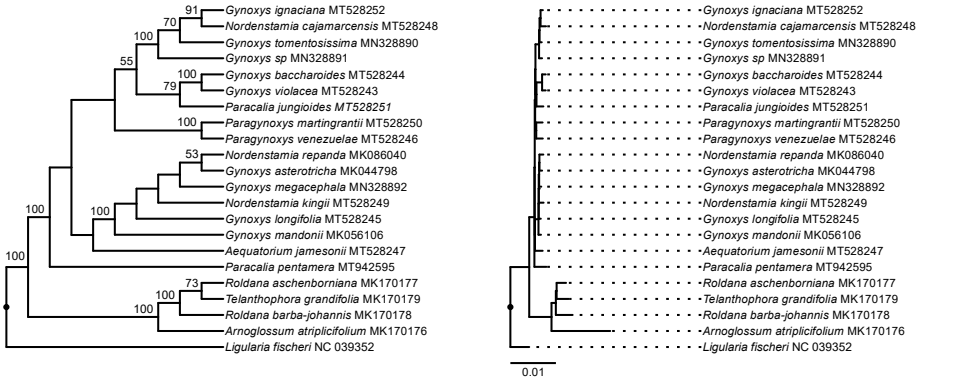
before	with	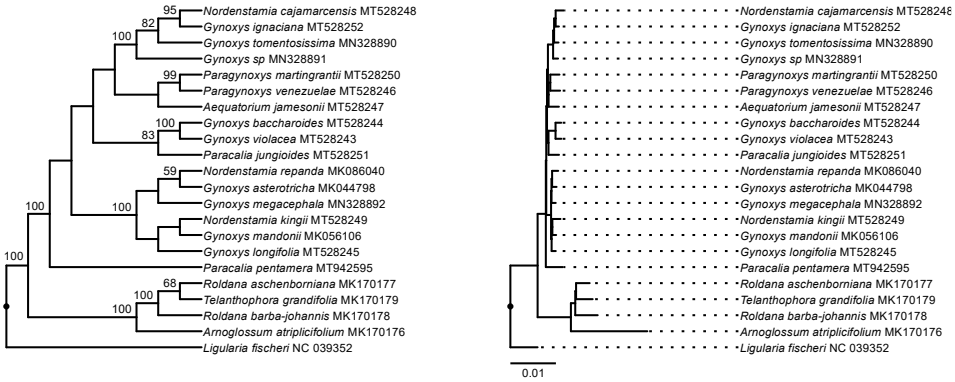
after	without	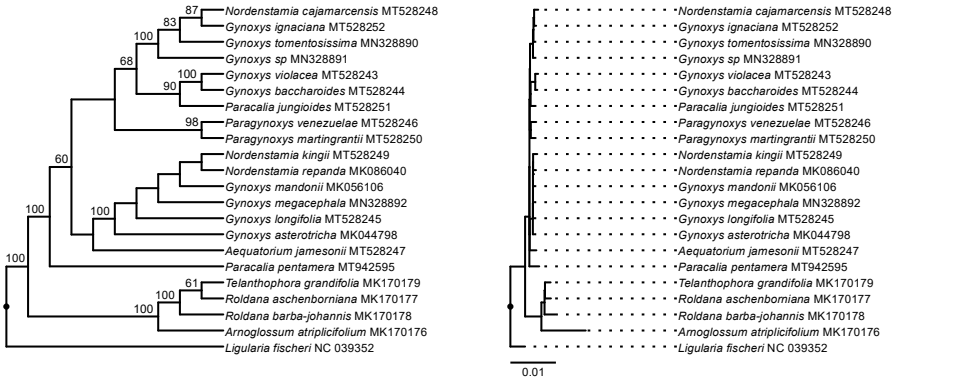
after	with	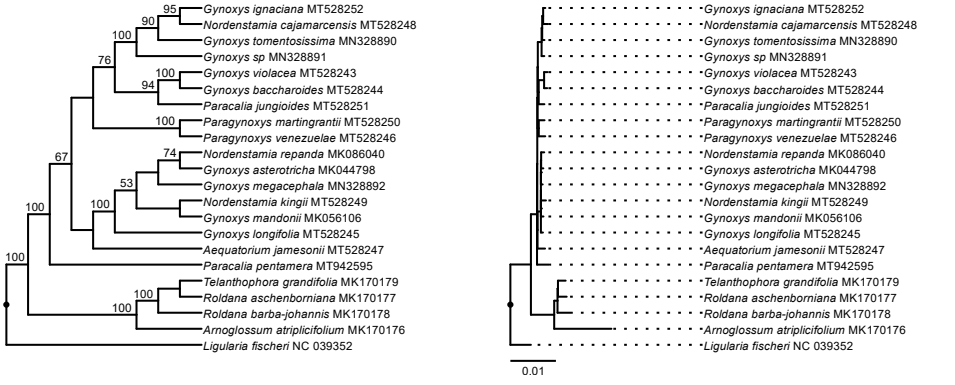

Appendix 2.11: Comparison of phylogenetic trees of the Gynoxyoid group inferred before and after the coding of indels and under different tree inference methods. The tree displayed on the left is held constant across both comparisons and constitutes the tree with the highest likelihood score inferred on the concatenated MSAs of all three plastid genome partitions upon the coding of indels and after alignment adjustment. Three clades (i.e., ”A”, ”B”, and ”C”) are highlighted on this tree by red letters located next to the most recent common ancestor of each clade. (A) Comparison of the best tree against its equivalent inferred without the coding of indels; and (B) comparison of the best tree against its equivalent inferred under BI.

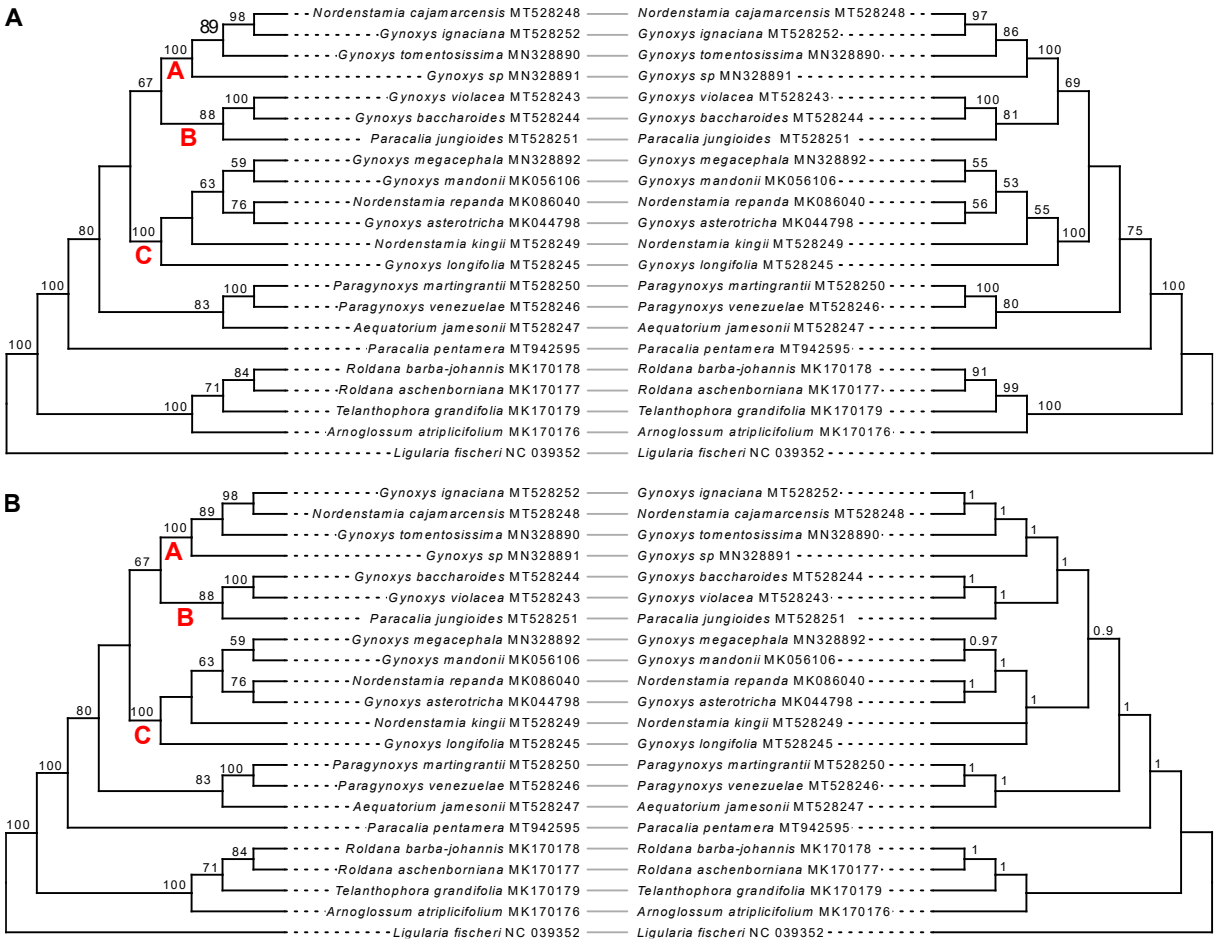

Appendix 2.12: Results of phylogenetic tree inference via ML on the concatenated MSAs of all three plastid genome partitions before and after alignment adjustment as well as with and without the coding of indels. Tree visualization and rooting are as in Appendix 2.8.

Alignment adjust-ment	Indel coding	Tree with the highest likelihood score	
before	without	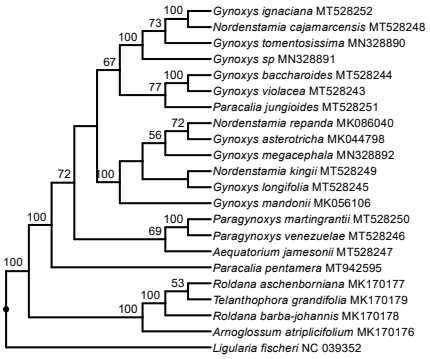	
before	with	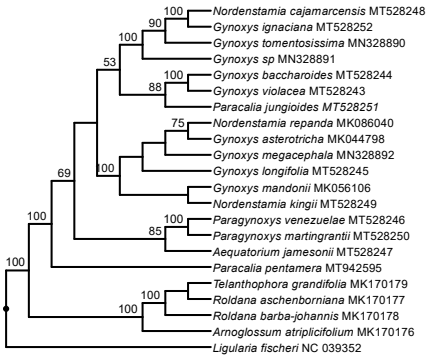	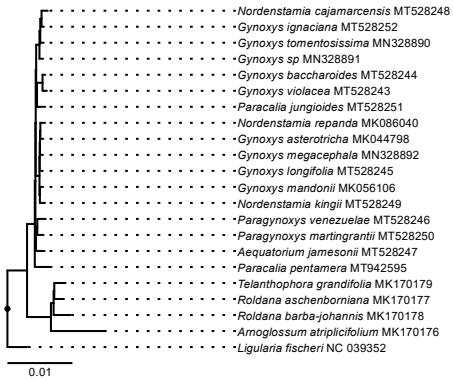
after	without	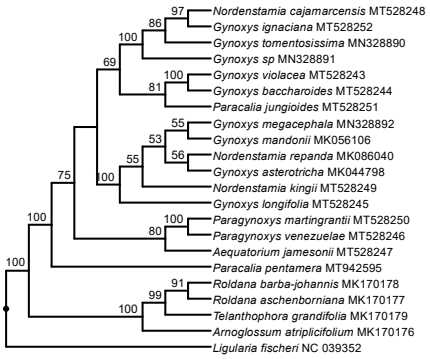	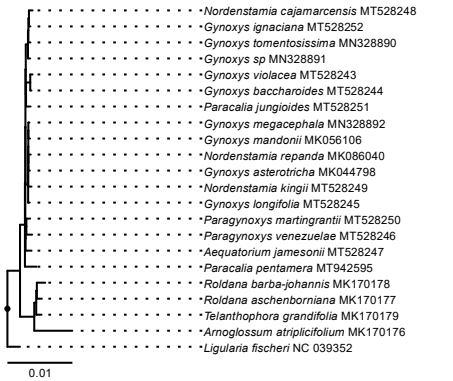
after	with	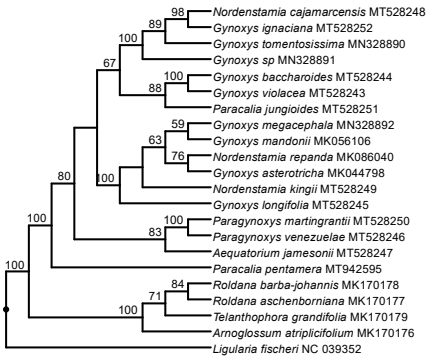	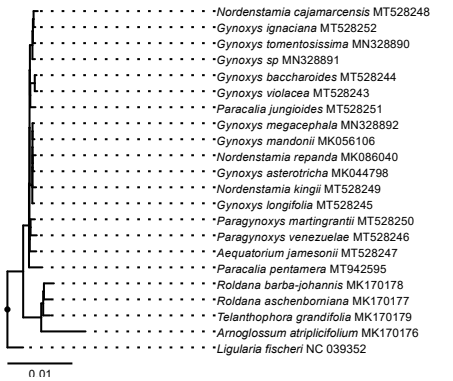

Appendix 2.13: Results of the phylogenetic tree inference via BI on the concatenated MSAs of all three plastid genome partitions before and after alignment adjustment as well as with and without the coding of indels. The tree displayed for each category represents the 50% majority-rule consensus tree of the posterior tree distribution, visualized as a cladogram with posterior probability values greater than 0.5 (left) and a corresponding phylogram with exact branch lengths (right). All trees were rooted with using *Ligularia fischeri* as outgroup.

Alignment adjust-ment	Indel coding	Tree with the highest likelihood score
before	without	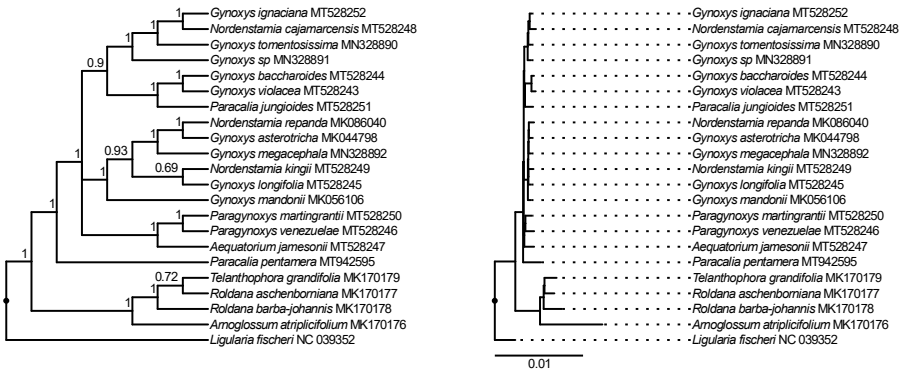
before	with	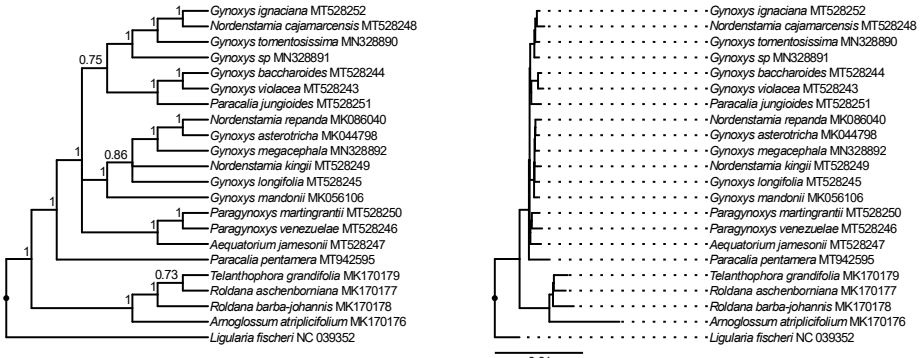
after	without	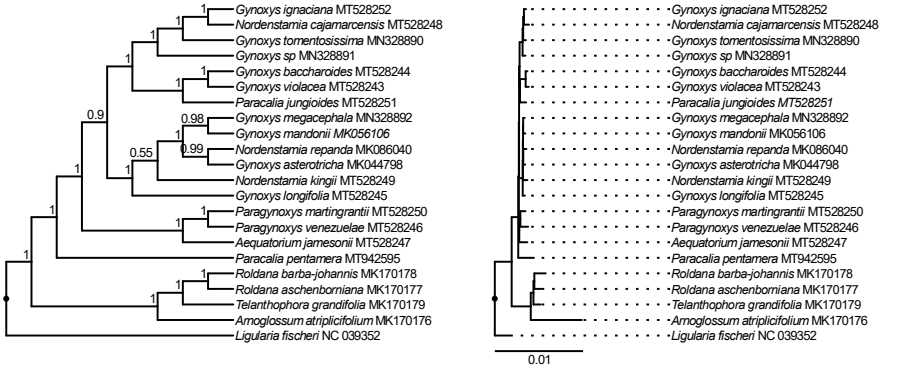
after	with	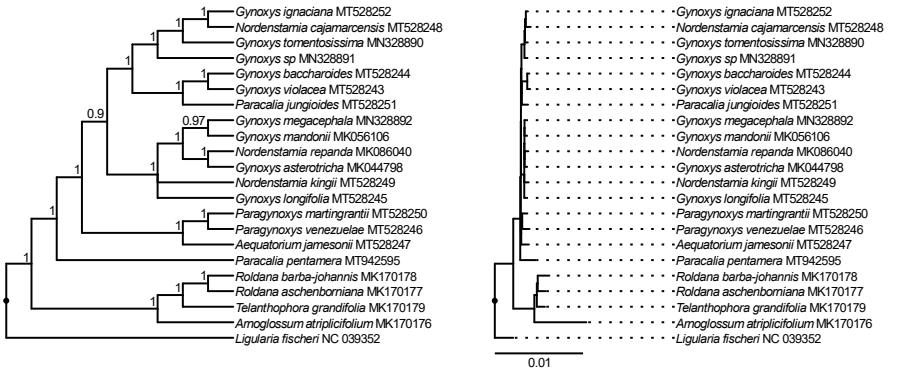

Appendix 3: Supplementary material for Chapter 3

Appendix 3.1. Physical specimens examined

Bolivia. Cochabamba: Chapare, Colomi, camino entre Colomi - Candelaria, 3400 m, 17 Jul 2017, *B. Escobari, N. Kilian & H. Villca 176* (B 10 0763097, LPB); Cochabamba: Ayopaya, Cocapata, encima de Tiquipaya, 3600 m, 22 Jul 2017, *B. Escobari, N. Kilian, H. Villca & B. Nieto 272* (B 10 0763214; B 10 0763215, LPB); Cochabamba: Arani, Vacas, camino de bajada pasando el santuario de las Puyas, 3800 m, 23 Jul 2017, *B. Escobari, N. Kilian, H. Villca & B. Nieto 289* (B 10 0763235; B 10 0763236, LPB); Cochabamba: José Carrasco Torrico, c. 6 km below Sehuencas, 2200 m, 30 Jul 1995, *J.R.I. Wood 10093* (LPB); Cochabamba: Chapare, 3268 m, 12 Mar 2007, *J. Wood 23092* (LPB); Cochabamba: Chapare, camino Cochabamba - Villa Tunari, 23 Sep 1982, *A.L. Cabrera & M. Gutierrez 33718* (LPB); La Paz: Bajando a Unduavi, 16 km desde la cumbre, subiendo ladera a la izquierda de la carretera, 3570 m, 05 Jul 2016, *B. Escobari, S. Beck, & C. Beck 36* (B 10 0720926, LPB); La Paz: Franz Tamayo: Area Natural de Manejo Integrado Apolobamba, Queara nuevo Toilcacocha, 3930 m, 11 Apr 2008, *P. Paco, A. Fuentes, R. Canaza & P. Madriaga 78* (LPB); La Paz: Larecaja, viciniis Sorata, via ad Lacatia, ad rivum Aparasi, in nemoribus, 3300-3600 m, 1 Apr 1859, *G. Mandon 84* (P02714010); La Paz: Bautista Saavedra M., Charazani, al este de Chullina, 3400 m, 18 Apr *1933, P. Gutte & B. Herzog 424* (LPB); La Paz: Larecaja, bosque de la localidad de Hirola, pasando Lipichi, 3881 m, 5 Nov 2008, *A. Palabral 703* (B 10 0720253, LPB); La Paz: Nor Yungas, pasando Chuspipata, por el camino viejo, 3250 m, 21 Aug 1999, *J.C. Solomon 6024* (LPB); La Paz: Nor Yungas, below road La Paz - Coroico ca 0.5 km E Cotapata, 3150 m, 22 Aug 1999, *J. Müller 7464* (LPB); La Paz: Murillo, 24.5 km N of (below) the pass at the head of the Zongo Valley, 3100 m, 16 Sep 1984, *J.C. Solomon 12372* (LPB); La Paz: Nor Yungas, entre Cotapata y Chuspipata, 3100 m, 1 May 1989, *D.N. Smith & J. Smith 13051* (LPB); La Paz: Franz Tamayo, Parque Nacional Madidi entre Tocoaque y Chucani, entre Keara y Mojos, 2500 m, 4 Oct 2009, *A. Fuentes 15602* (B 10 0720919, LPB); La Paz: Nor Yungas, pasando Unduavi, fin del asfalto, Cotapata, bajando sobre la senda (1 hora), 3100 m, 29 May 1994, *S. Beck 21376* (LPB); La Paz: Larecaja, Sorata, 64 km hacia Consata (20 km después de Quiabaya) Kilómetro 226, 3590 m, 6 Ago 2004, *S. Beck 29440* (B 10 0720254, LPB); La Paz: Inquisivi, comunidad Choquetanga-Aguas Calientes-Calachaca, cuenca del río Calachaca-Jahura, pequeno valle, 9 Km de Choquetanga, 3300 m, 17 Jul 1991, *M. Lewis 39262* (LPB); Santa Cruz: Caballero c. 1.5 km east of Siberia along road to Comarapa, 2989 m, 6 Mar 2007, *J.R.I. Wood, D. Hind & J. Gutierrez 22990* (LPB); Colombia. Boyaca: Valle de El Cocuy, La Cueva, Chinchilla, 3800 m, 17 Sep 1969, *J. Cuatrecasas & L. Rodriguez 27823* (P00062656); Boyaca: Santander, cerro Berlín, entre Arcabuco y La Palma, 2800 m, 28 Mar 1973, *J. Cuatrecasas 28675* (MA-01-00897035); Cesar: Sabana Rubia, top of Serrania de Perija, E of Manaure; forest just below paramo (Transect 1), 2940 m, 10 Mar 1993, *A. Gentry & H. Cuadros 79156* (MO-1962013); Magdalena: Sierra Nevada de Santa Maria, 1 km al NW de la quebrada de la Laguna Rio Frio, en direccion al Pico Jose Hilario, 3400 m, 25 May 1905, *E. Forero & J.H. Kirkbride, Jr. 627* (MO-1962022); Magdalena: Cerro Kennedy, near top of highest peak in N massif of sierra Nevada de Santa Marta, 2600 m, 23 Aug 1986, *A. Gentry & H. Cuadros 55536* (MA-01-00551486); Santander: Cordillera Oriental, páramo de Santurban, entre Bucaramanga y Berlín, large open stretch, mostly under cultivation, 3175 m, 3 Jan 1960, *G. Harriet & P. Juajibioy 10418* (MO-1962019); Valle del Cauca: Cordillera Central, vertiente occidental cabeceras del

río Tuluá, quebrada de Las Vegas, 3400 m, 23 Mar 1946, *J. Cuatrecasas 20365* (MA-01-00845320); Ecuador. Azuay: Parque Nacional Cajas, Road Cuena-Sayausí-Molleturo, km 30.2, at the entrance to trail leading to Laguna Mamamag, 3810 m, 5 Jan 2000, *P. Jorgensen 1616* (MO-1892361); Ecuador. Azuay: Km 30 S of Cumbe on the road to Sraguro, 3000 m, 26 Jan 1979, *R.M. King & F. Almeda 7804* (G00426439 383188/1); Ecuador. Azuay: Area de recreación Las Cajas, 2 km W of pass on Cuenca-Molleturo road, 4000 m, 16 Aug 1987, *P. Jorgensen 61856* (MO-1879910); Ecuador. Loja: Guararas (1 km de Matilan), 2580 m, 11 Sep 1982, *L. Emperaire 1318* (P03833291); Ecuador. Loja: Km 67 de Saraguro, localidad entre Susudel y El Progreso, *J.L. Jaramillo, Z. Vlastimil & R. Valencia 8822* (MO-1891653); Ecuador. Morona Santiago: Santiago-Zamora ("Oriente") Eastern slopes of the cordillera, valley of the Rio Negro, down the Rio Pailas (on the trail to Mendez), between Tambo Cerro Negro and the Paramo del Castillo, 3000 m, 20 Aug 1945, *W.H. Camp 4976* (K000374296); Ecuador. Napo: Tena, Parque Nacional Llanganates, via Salcedo-Tena, km 45-55, cabecera del Río Anatenorio, Siete Vueltas, 2720 m, 15 Oct 2006, *J.H. Vargas López* (MO-2940234); Ecuador. Zamora-Chinchipe: Limite provincial entre Loja y Zamora, 2900 m, 9 Oct 2004, *J. Caranqui, M. Melampy & J. Lara 1252* (MO-1891627); Peru. Amazonas: Road from Leymebamba to Balsas, crossing Cerro de Calle Cale, 3150 m, 2 Jun 2018, *B. Escobari, N. Kilian, & T. Henning 590* (B 10 1098697); Amazonas: Road from Leymebamba to Balsas, crossing Cerro de Calle Cale, 3500 m, 2 Jun 2018, *B. Escobari, N. Kilian, & T. Henning 594* (B 10 1098699); Ancash: Huaraz. Pampas Grande, camino entre San Juan y Huiñapajatum , 2600 m, 28 Nov 1985, *C. Díaz 1975* (MO-3030471); Cajamarca: San Ignacio, distrito Huarango, cordillera Huarango, El Romerillo, 2370 m, 18 Jul 2005, *E. Rodriguez, E. Alvitez & A. Arroyo 2900* (MA-01-00916039); Cusco: Machu Picchu, on the hillside of Condortucllana on the flanks of Mt. Veronica, S slope 66%, in a mid-slope that experiences grazing, 3345 m, 15 Aug 1982, *B. Peyton & S.T. Peyton 1023* (MO-1879936); Cusco: Quisicanchis, Chetacuchu, Marcapata, 4150 m, 11 Dec 1938, *C. Vargas 1363* (LPB); Cusco: Cusipata, Chilliwani, 4700 m, 2 May 2005, *A. Tupayachi 6462* (MO-2439104); Moquegua: Mariscal Nieto, Carumas, road from Chilligua to Carumas, 4283 m, 15 Mar 2017, *D. Montesinos 5110* (B 10 0843129); Pasco: Oxapampa, Parque Nacional Yanachaga-Chemillén, sector San Alberto, Abra Esperanza a 30 minutos en dirección al Valle del Palcazú, 2720 m, 15 Oct 2006, *G. Castillo 460* (MO-2940516); Venezuela. Merida: Páramo de San José, Zanjón del Cupís, 3100 m, 1 Feb 1973, *L. Ruiz-Teran 28454* (MA-01-00884485); Merida: Pueblos del Sur, páramo de San José, Monte El Cupís, 3050 m, 14 Nov 1978, *J. Cuatrecasas & L. Ruiz-Teran 28802* (MA-01-00896832); Mérida: Páramo de Las Coloradas, entre La Capilla y El Aserrucho (Santa Cruz de Mora-El Molino), 2700 m, 27 May 1980, *J. Cuatrecasas 28996* (MA-01-00896838)

Appendix 3.2: 50% majority consensus tree on a) ETS and b) ITS under Bayesian inference topology. Posterior probability values are given.

a)

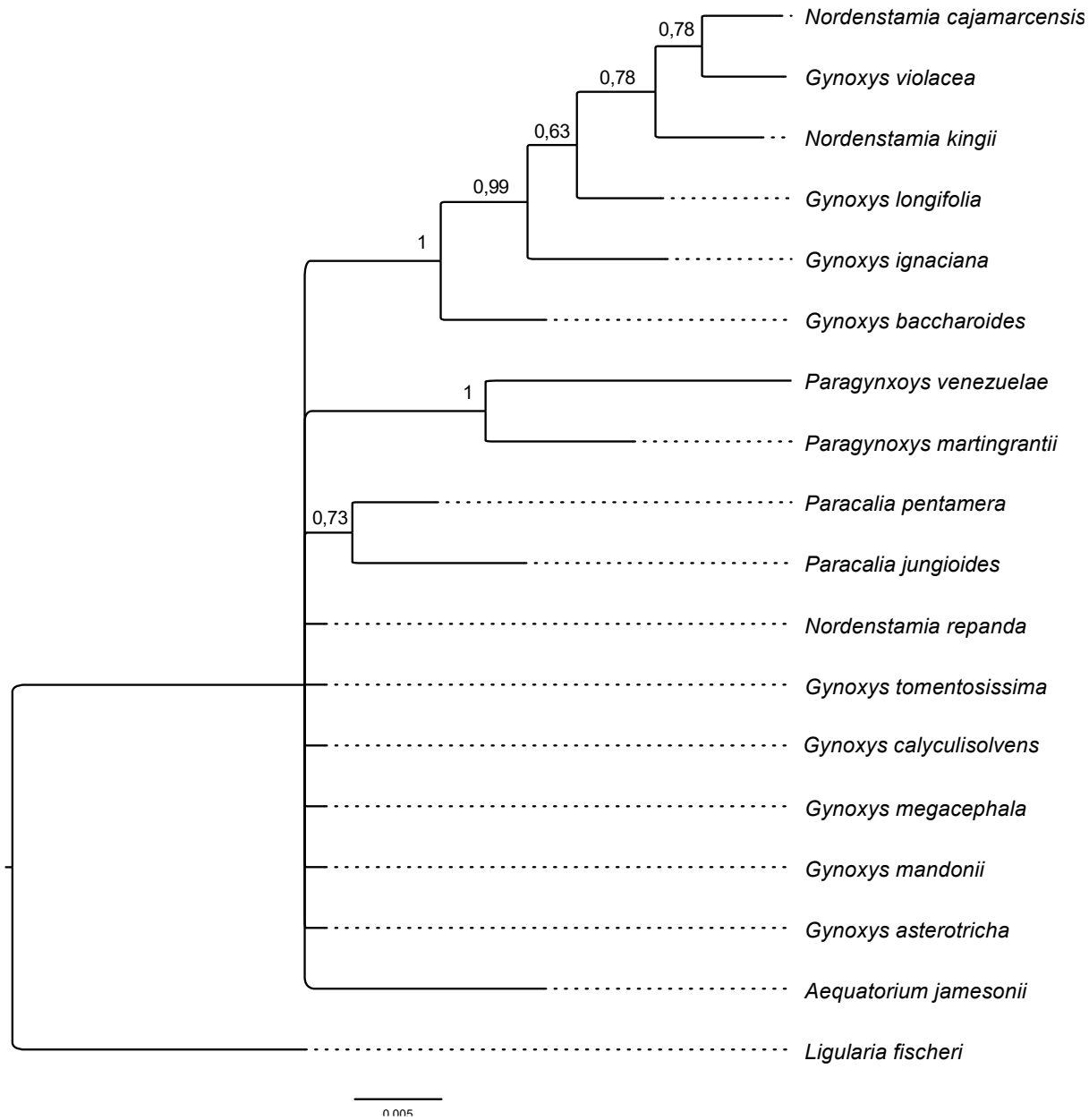

b)

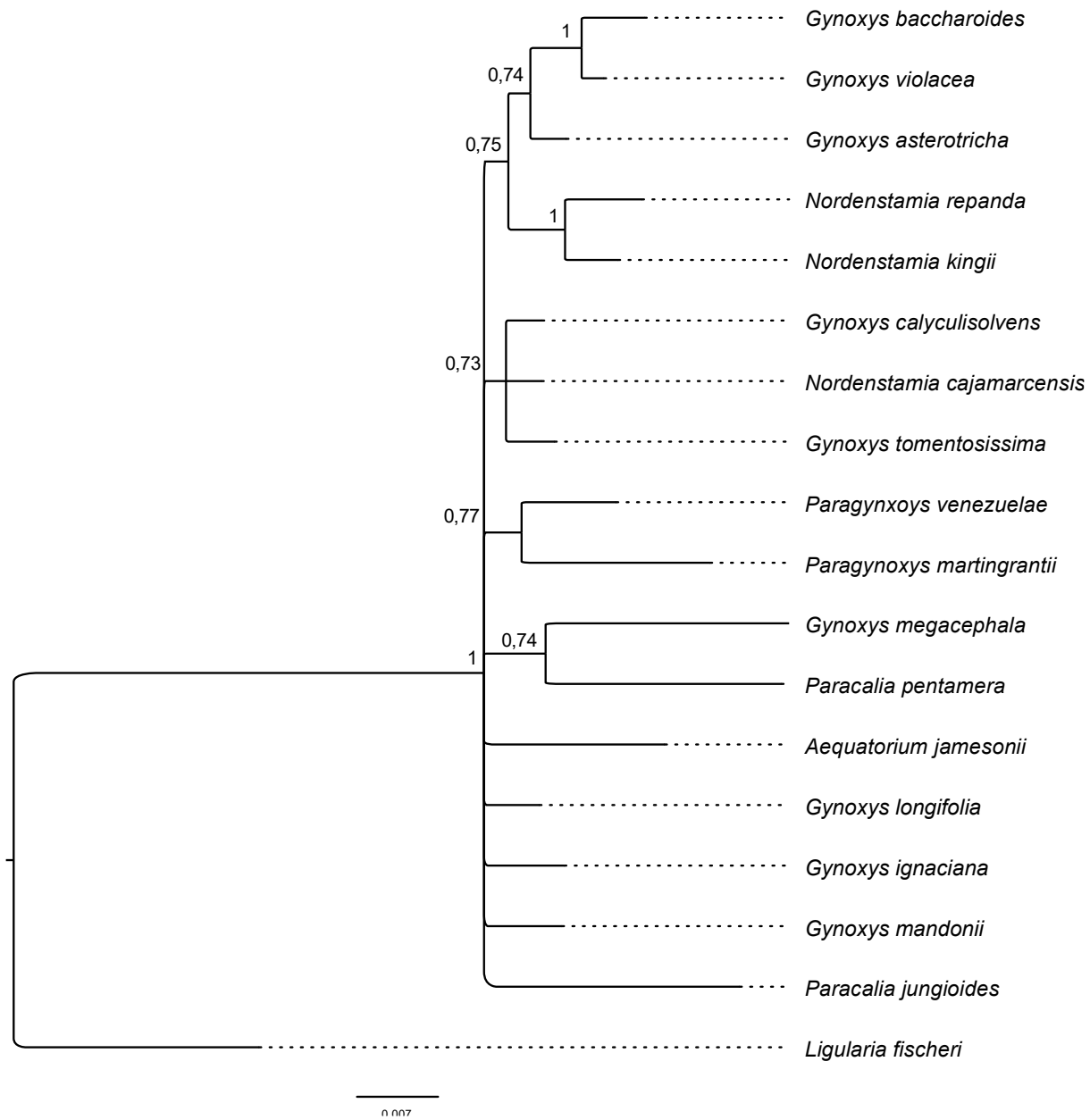
Gynoxys baccharoides
Gynoxys violacea
Gynoxys asterotricha
Nordenstamia repanda
Nordenstamia kingii
Gynoxys calyculisolvens
Nordenstamia cajamarcensis
Gynoxys tomentosissima
Paragynxoys venezuelae
Paragynoxys martingrantii
Gynoxys megacephala
Paracalia pentamera
Aequatorium jamesonii
Gynoxys longifolia
Gynoxys ignaciana
Gynoxys mandonii
Paracalia jungioides
Ligularia fischeri
1
0,74
0,75
1
0,73
0,77
0,74
1

Appendix 3.3: Majority consensus tree on a) ETS and b) ITS and c) ITS & ETS under Bayesian inference topology. Posterior probability values are given. (*) specimens not seen

a)

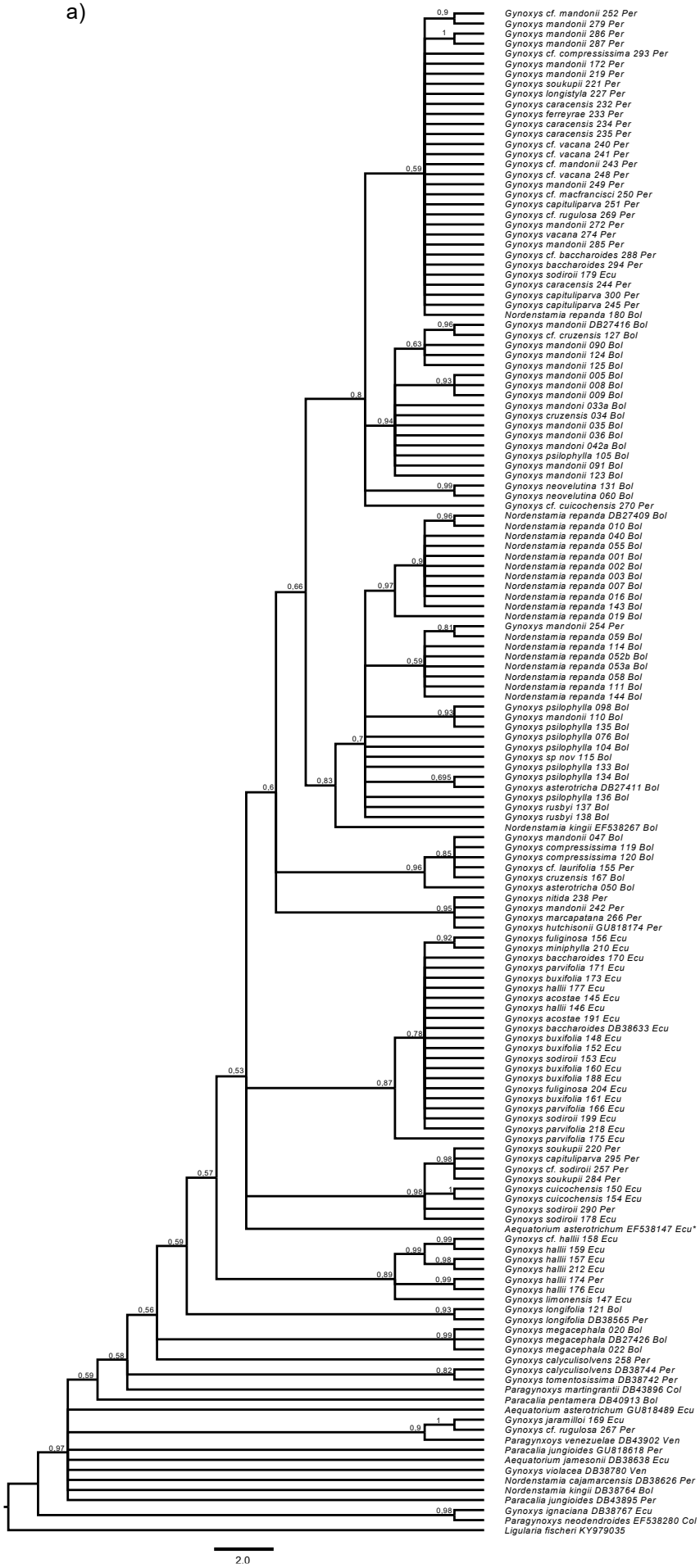
Gynoxys cf. mandonii 252 Per
Gynoxys mandonii 279 Per
Gynoxys mandonii 286 Per
Gynoxys mandonii 287 Per
Gynoxys cf. compressissima 293 Per
Gynoxys mandonii 172 Per
Gynoxys mandonii 219 Per
Gynoxys soukupii 221 Per
Gynoxys longistyla 227 Per
Gynoxys caracensis 232 Per
Gynoxys ferreyrae 233 Per
Gynoxys caracensis 234 Per
Gynoxys caracensis 235 Per
Gynoxys cf. vacana 240 Per
Gynoxys cf. vacana 241 Per
Gynoxys cf. mandonii 243 Per
Gynoxys cf. vacana 248 Per
Gynoxys mandonii 249 Per
Gynoxys cf. macfrancisci 250 Per
Gynoxys capituliparva 251 Per
Gynoxys cf. rugulosa 269 Per
Gynoxys mandonii 272 Per
Gynoxys vacana 274 Per
Gynoxys mandonii 285 Per
Gynoxys cf. baccharoides 288 Per
Gynoxys baccharoides 294 Per
Gynoxys sodiroii 179 Ecu
Gynoxys caracensis 244 Per
Gynoxys capituliparva 300 Per
Gynoxys capituliparva 245 Per
Nordenstamia repanda 180 Bol
Gynoxys mandonii DB27416 Bol
Gynoxys cf. cruzensis 127 Bol
Gynoxys mandonii 090 Bol
Gynoxys mandonii 124 Bol
Gynoxys mandonii 125 Bol
Gynoxys mandonii 005 Bol
Gynoxys mandonii 008 Bol
Gynoxys mandonii 009 Bol
Gynoxys mandoni 033a Bol
Gynoxys cruzensis 034 Bol
Gynoxys mandonii 035 Bol
Gynoxys mandonii 036 Bol
Gynoxys mandoni 042a Bol
Gynoxys psilophylla 105 Bol
Gynoxys mandonii 091 Bol
Gynoxys mandonii 123 Bol
Gynoxys neovelutina 131 Bol
Gynoxys neovelutina 060 Bol
Gynoxys cf. cuicochensis 270 Per
Nordenstamia repanda DB27409 Bol
Nordenstamia repanda 010 Bol
Nordenstamia repanda 040 Bol
Nordenstamia repanda 055 Bol
Nordenstamia repanda 001 Bol
Nordenstamia repanda 002 Bol
Nordenstamia repanda 003 Bol
Nordenstamia repanda 007 Bol
Nordenstamia repanda 016 Bol
Nordenstamia repanda 143 Bol
Nordenstamia repanda 019 Bol
Gynoxys mandonii 254 Per
Nordenstamia repanda 059 Bol
Nordenstamia repanda 114 Bol
Nordenstamia repanda 052b Bol
Nordenstamia repanda 053a Bol
Nordenstamia repanda 058 Bol
Nordenstamia repanda 111 Bol
Nordenstamia repanda 144 Bol
Gynoxys psilophylla 098 Bol
Gynoxys mandonii 110 Bol
Gynoxys psilophylla 135 Bol
Gynoxys psilophylla 076 Bol
Gynoxys psilophylla 104 Bol
Gynoxys sp nov 115 Bol
Gynoxys psilophylla 133 Bol
Gynoxys psilophylla 134 Bol
Gynoxys asterotricha DB27411 Bol
Gynoxys psilophylla 136 Bol
Gynoxys rusbyi 137 Bol
Gynoxys rusbyi 138 Bol
Nordenstamia kingii EF538267 Bol
Gynoxys mandonii 047 Bol
Gynoxys compressissima 119 Bol
Gynoxys compressissima 120 Bol
Gynoxys cf. laurifolia 155 Per
Gynoxys cruzensis 167 Bol
Gynoxys asterotricha 050 Bol
Gynoxys nitida 238 Per
Gynoxys mandonii 242 Per
Gynoxys marcapatana 266 Per
Gynoxys hutchisonii GU818174 Per
Gynoxys fuliginosa 156 Ecu
Gynoxys miniphylla 210 Ecu
Gynoxys baccharoides 170 Ecu
Gynoxys parvifolia 171 Ecu
Gynoxys buxifolia 173 Ecu
Gynoxys hallii 177 Ecu
Gynoxys acostae 145 Ecu
Gynoxys hallii 146 Ecu
Gynoxys acostae 191 Ecu
Gynoxys baccharoides DB38633 Ecu
Gynoxys buxifolia 148 Ecu
Gynoxys buxifolia 152 Ecu
Gynoxys sodiroii 153 Ecu
Gynoxys buxifolia 160 Ecu
Gynoxys buxifolia 188 Ecu
Gynoxys fuliginosa 204 Ecu
Gynoxys buxifolia 161 Ecu
Gynoxys parvifolia 166 Ecu
Gynoxys sodiroii 199 Ecu
Gynoxys parvifolia 218 Ecu
Gynoxys parvifolia 175 Ecu
Gynoxys soukupii 220 Per
Gynoxys capituliparva 295 Per
Gynoxys cf. sodiroii 257 Per
Gynoxys soukupii 284 Per
Gynoxys cuicochensis 150 Ecu
Gynoxys cuicochensis 154 Ecu
Gynoxys sodiroii 290 Per
Gynoxys sodiroii 178 Ecu
Aequatorium asterotrichum EF538147 Ecu*
Gynoxys cf. hallii 158 Ecu
Gynoxys hallii 159 Ecu
Gynoxys hallii 157 Ecu
Gynoxys hallii 212 Ecu
Gynoxys hallii 174 Per
Gynoxys hallii 176 Ecu
Gynoxys limonensis 147 Ecu
Gynoxys longifolia 121 Bol
Gynoxys longifolia DB38565 Per
Gynoxys megacephala 020 Bol
Gynoxys megacephala DB27426 Bol
Gynoxys megacephala 022 Bol
Gynoxys calyculisolvens 258 Per
Gynoxys calyculisolvens DB38744 Per
Gynoxys tomentosissima DB38742 Per
Paragynoxys martingrantii DB43896 Col
Paracalia pentamera DB40913 Bol
Aequatorium asterotrichum GU818489 Ecu
Gynoxys jaramilloi 169 Ecu
Gynoxys cf. rugulosa 267 Per
Paragynoxys venezuelae DB43902 Ven
Paracalia jungioides GU818618 Per
Aequatorium jamesonii DB38638 Ecu
Gynoxys violacea DB38780 Ven
Nordenstamia cajamarcensis DB38626 Per
Nordenstamia kingii DB38764 Bol
Paracalia jungioides DB43895 Per
Gynoxys ignaciana DB38767 Ecu
Paragynoxys neodendroides EF538280 Col
Ligularia fischeri KY979035
2.0

b)

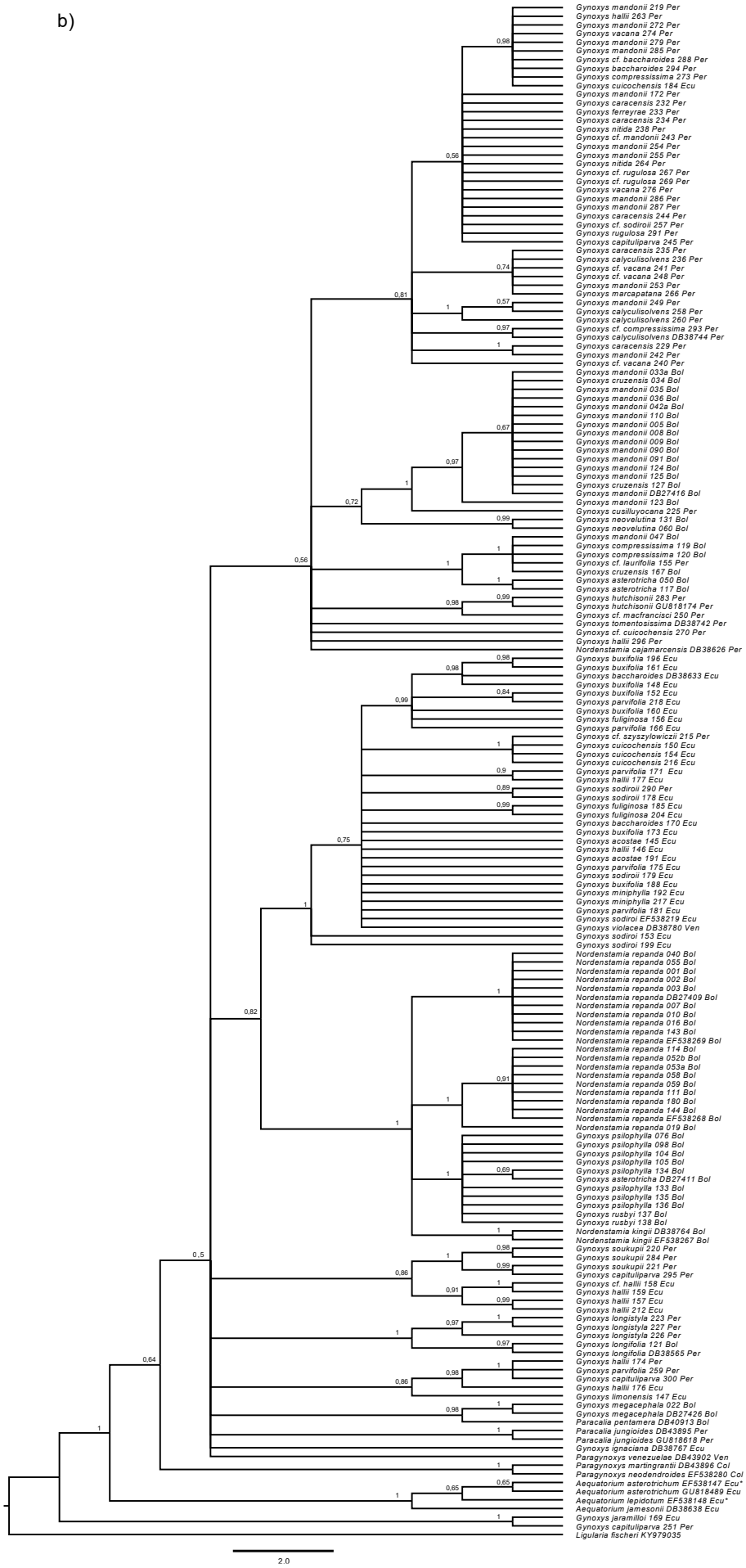
Gynoxys mandonii 219 Per
Gynoxys hallii 263 Per
Gynoxys mandonii 272 Per
Gynoxys vacana 274 Per
Gynoxys mandonii 279 Per
Gynoxys mandonii 285 Per
Gynoxys cf. baccharoides 288 Per
Gynoxys baccharoides 294 Per
Gynoxys compressissima 273 Per
Gynoxys cuicochensis 184 Ecu
Gynoxys mandonii 172 Per
Gynoxys caracensis 232 Per
Gynoxys ferreyrae 233 Per
Gynoxys caracensis 234 Per
Gynoxys nitida 238 Per
Gynoxys cf. mandonii 243 Per
Gynoxys mandonii 254 Per
Gynoxys mandonii 255 Per
Gynoxys nitida 264 Per
Gynoxys cf. rugulosa 267 Per
Gynoxys cf. rugulosa 269 Per
Gynoxys vacana 276 Per
Gynoxys mandonii 286 Per
Gynoxys mandonii 287 Per
Gynoxys caracensis 244 Per
Gynoxys cf. sodiroii 257 Per
Gynoxys rugulosa 291 Per
Gynoxys capituliparva 245 Per
Gynoxys caracensis 235 Per
Gynoxys calyculisolvens 236 Per
Gynoxys cf. vacana 241 Per
Gynoxys cf. vacana 248 Per
Gynoxys mandonii 253 Per
Gynoxys marcapatana 266 Per
Gynoxys mandonii 249 Per
Gynoxys calyculisolvens 258 Per
Gynoxys calyculisolvens 260 Per
Gynoxys cf. compressissima 293 Per
Gynoxys calyculisolvens DB38744 Per
Gynoxys caracensis 229 Per
Gynoxys mandonii 242 Per
Gynoxys cf. vacana 240 Per
Gynoxys mandonii 033a Bol
Gynoxys cruzensis 034 Bol
Gynoxys mandonii 035 Bol
Gynoxys mandonii 036 Bol
Gynoxys mandonii 042a Bol
Gynoxys mandonii 110 Bol
Gynoxys mandonii 005 Bol
Gynoxys mandonii 008 Bol
Gynoxys mandonii 009 Bol
Gynoxys mandonii 090 Bol
Gynoxys mandonii 091 Bol
Gynoxys mandonii 124 Bol
Gynoxys mandonii 125 Bol
Gynoxys cruzensis 127 Bol
Gynoxys mandonii DB27416 Bol
Gynoxys mandonii 123 Bol
Gynoxys cusilluyocana 225 Per
Gynoxys neovelutina 131 Bol
Gynoxys neovelutina 060 Bol
Gynoxys mandonii 047 Bol
Gynoxys compressissima 119 Bol
Gynoxys compressissima 120 Bol
Gynoxys cf. laurifolia 155 Per
Gynoxys cruzensis 167 Bol
Gynoxys asterotricha 050 Bol
Gynoxys asterotricha 117 Bol
Gynoxys hutchisonii 283 Per
Gynoxys hutchisonii GU818174 Per
Gynoxys cf. macfrancisci 250 Per
Gynoxys tomentosissima DB38742 Per
Gynoxys cf. cuicochensis 270 Per
Gynoxys hallii 296 Per
Nordenstamia cajamarcensis DB38626 Per
Gynoxys buxifolia 196 Ecu
Gynoxys buxifolia 161 Ecu
Gynoxys baccharoides DB38633 Ecu
Gynoxys buxifolia 148 Ecu
Gynoxys buxifolia 152 Ecu
Gynoxys parvifolia 218 Ecu
Gynoxys buxifolia 160 Ecu
Gynoxys fuliginosa 156 Ecu
Gynoxys parvifolia 166 Ecu
Gynoxys cf. szyszylowiczii 215 Per
Gynoxys cuicochensis 150 Ecu
Gynoxys cuicochensis 154 Ecu
Gynoxys cuicochensis 216 Ecu
Gynoxys parvifolia 171 Ecu
Gynoxys hallii 177 Ecu
Gynoxys sodiroii 290 Per
Gynoxys sodiroii 178 Ecu
Gynoxys fuliginosa 185 Ecu
Gynoxys fuliginosa 204 Ecu
Gynoxys baccharoides 170 Ecu
Gynoxys buxifolia 173 Ecu
Gynoxys acostae 145 Ecu
Gynoxys hallii 146 Ecu
Gynoxys acostae 191 Ecu
Gynoxys parvifolia 175 Ecu
Gynoxys sodiroii 179 Ecu
Gynoxys buxifolia 188 Ecu
Gynoxys miniphylla 192 Ecu
Gynoxys miniphylla 217 Ecu
Gynoxys parvifolia 181 Ecu
Gynoxys sodiroi EF538219 Ecu
Gynoxys violacea DB38780 Ven
Gynoxys sodiroi 153 Ecu
Gynoxys sodiroi 199 Ecu
Nordenstamia repanda 040 Bol
Nordenstamia repanda 055 Bol
Nordenstamia repanda 001 Bol
Nordenstamia repanda 002 Bol
Nordenstamia repanda 003 Bol
Nordenstamia repanda DB27409 Bol
Nordenstamia repanda 007 Bol
Nordenstamia repanda 010 Bol
Nordenstamia repanda 016 Bol
Nordenstamia repanda 143 Bol
Nordenstamia repanda EF538269 Bol
Nordenstamia repanda 114 Bol
Nordenstamia repanda 052b Bol
Nordenstamia repanda 053a Bol
Nordenstamia repanda 058 Bol
Nordenstamia repanda 059 Bol
Nordenstamia repanda 111 Bol
Nordenstamia repanda 180 Bol
Nordenstamia repanda 144 Bol
Nordenstamia repanda EF538268 Bol
Nordenstamia repanda 019 Bol
Gynoxys psilophylla 076 Bol
Gynoxys psilophylla 098 Bol
Gynoxys psilophylla 104 Bol
Gynoxys psilophylla 105 Bol
Gynoxys psilophylla 134 Bol
Gynoxys asterotricha DB27411 Bol
Gynoxys psilophylla 133 Bol
Gynoxys psilophylla 135 Bol
Gynoxys psilophylla 136 Bol
Gynoxys rusbyi 137 Bol
Gynoxys rusbyi 138 Bol
Nordenstamia kingii DB38764 Bol
Nordenstamia kingii EF538267 Bol
Gynoxys soukupii 220 Per
Gynoxys soukupii 284 Per
Gynoxys soukupii 221 Per
Gynoxys capituliparva 295 Per
Gynoxys cf. hallii 158 Ecu
Gynoxys hallii 159 Ecu
Gynoxys hallii 157 Ecu
Gynoxys hallii 212 Ecu
Gynoxys longistyla 223 Per
Gynoxys longistyla 227 Per
Gynoxys longistyla 226 Per
Gynoxys longifolia 121 Bol
Gynoxys longifolia DB38565 Per
Gynoxys hallii 174 Per
Gynoxys parvifolia 259 Per
Gynoxys capituliparva 300 Per
Gynoxys hallii 176 Ecu
Gynoxys limonensis 147 Ecu
Gynoxys megacephala 022 Bol
Gynoxys megacephala DB27426 Bol
Paracalia pentamera DB40913 Bol
Paracalia jungioides DB43895 Per
Paracalia jungioides GU818618 Per
Gynoxys ignaciana DB38767 Ecu
Paragynoxys venezuelae DB43902 Ven
Paragynoxys martingrantii DB43896 Col
Paragynoxys neodendroides EF538280 Col
Aequatorium asterotrichum EF538147 Ecu*
Aequatorium asterotrichum GU818489 Ecu
Aequatorium lepidotum EF538148 Ecu*
Aequatorium jamesonii DB38638 Ecu
Gynoxys jaramilloi 169 Ecu
Gynoxys capituliparva 251 Per
Ligularia fischeri KY979035
2.0

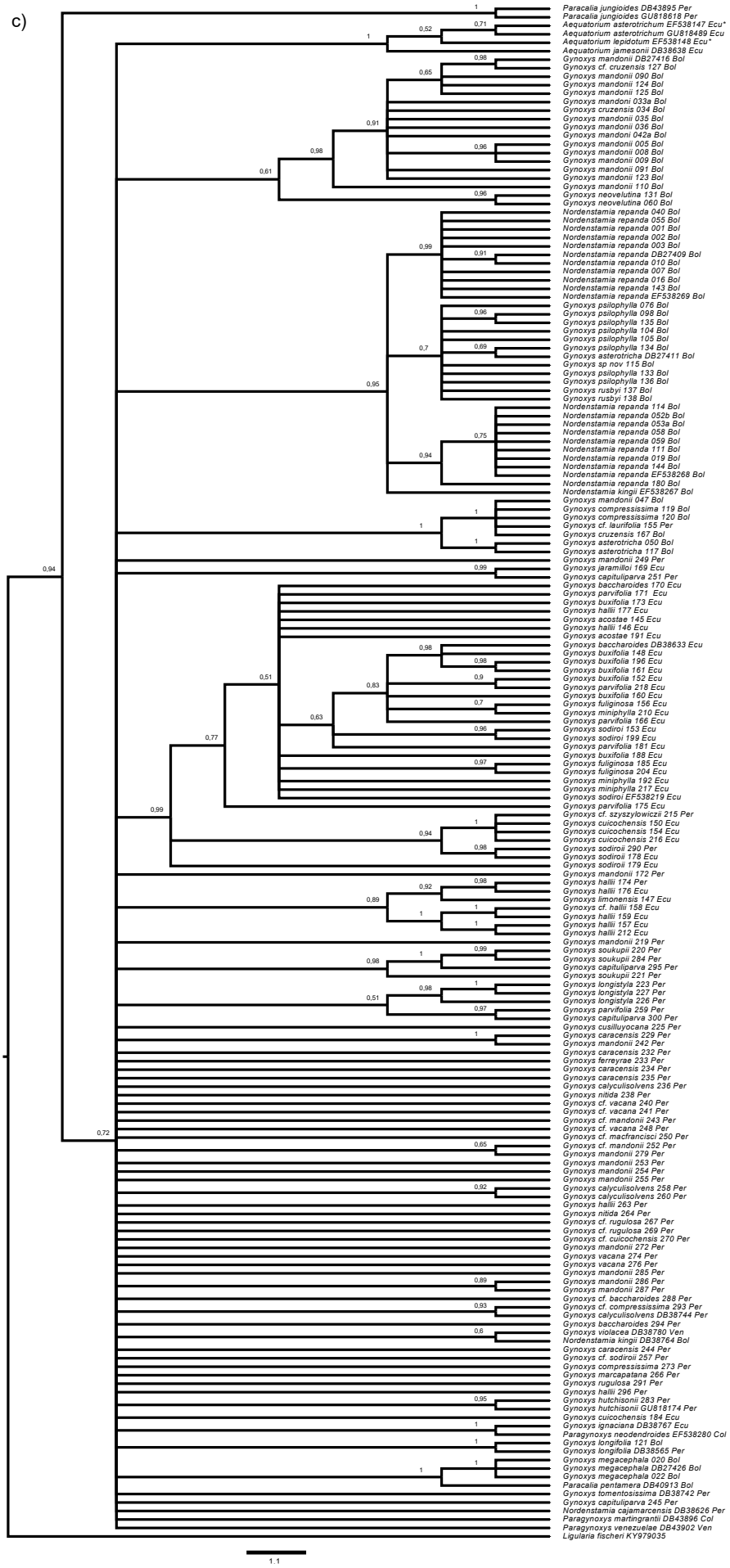
c)
Paracalia jungioides DB43895 Per
Paracalia jungioides GU818618 Per
Aequatorium asterotrichum EF538147 Ecu*
Aequatorium asterotrichum GU818489 Ecu
Aequatorium lepidotum EF538148 Ecu*
Aequatorium jamesonii DB38638 Ecu
Gynoxys mandonii DB27416 Bol
Gynoxys cf. cruzensis 127 Bol
Gynoxys mandonii 090 Bol
Gynoxys mandonii 124 Bol
Gynoxys mandonii 125 Bol
Gynoxys mandonii 033a Bol
Gynoxys cruzensis 034 Bol
Gynoxys mandonii 035 Bol
Gynoxys mandonii 036 Bol
Gynoxys mandonii 042a Bol
Gynoxys mandonii 005 Bol
Gynoxys mandonii 008 Bol
Gynoxys mandonii 009 Bol
Gynoxys mandonii 091 Bol
Gynoxys mandonii 123 Bol
Gynoxys mandonii 110 Bol
Gynoxys neovelutina 131 Bol
Gynoxys neovelutina 060 Bol
Nordenstamia repanda 040 Bol
Nordenstamia repanda 055 Bol
Nordenstamia repanda 001 Bol
Nordenstamia repanda 002 Bol
Nordenstamia repanda 003 Bol
Nordenstamia repanda DB27409 Bol
Nordenstamia repanda 010 Bol
Nordenstamia repanda 007 Bol
Nordenstamia repanda 016 Bol
Nordenstamia repanda 143 Bol
Nordenstamia repanda EF538269 Bol
Gynoxys psilophylla 076 Bol
Gynoxys psilophylla 098 Bol
Gynoxys psilophylla 135 Bol
Gynoxys psilophylla 104 Bol
Gynoxys psilophylla 105 Bol
Gynoxys psilophylla 134 Bol
Gynoxys asterotricha DB27411 Bol
Gynoxys sp nov 115 Bol
Gynoxys psilophylla 133 Bol
Gynoxys psilophylla 136 Bol
Gynoxys rusbyi 137 Bol
Gynoxys rusbyi 138 Bol
Nordenstamia repanda 114 Bol
Nordenstamia repanda 052b Bol
Nordenstamia repanda 053a Bol
Nordenstamia repanda 058 Bol
Nordenstamia repanda 059 Bol
Nordenstamia repanda 111 Bol
Nordenstamia repanda 019 Bol
Nordenstamia repanda 144 Bol
Nordenstamia repanda EF538268 Bol
Nordenstamia repanda 180 Bol
Nordenstamia kingii EF538267 Bol
Gynoxys mandonii 047 Bol
Gynoxys compressissima 119 Bol
Gynoxys compressissima 120 Bol
Gynoxys cf. laurifolia 155 Per
Gynoxys cruzensis 167 Bol
Gynoxys asterotricha 050 Bol
Gynoxys asterotricha 117 Bol
Gynoxys mandonii 249 Per
Gynoxys jaramilloi 169 Ecu
Gynoxys capituliparva 251 Per
Gynoxys baccharoides 170 Ecu
Gynoxys parvifolia 171 Ecu
Gynoxys buxifolia 173 Ecu
Gynoxys hallii 177 Ecu
Gynoxys acostae 145 Ecu
Gynoxys hallii 146 Ecu
Gynoxys acostae 191 Ecu
Gynoxys baccharoides DB38633 Ecu
Gynoxys buxifolia 148 Ecu
Gynoxys buxifolia 196 Ecu
Gynoxys buxifolia 161 Ecu
Gynoxys buxifolia 152 Ecu
Gynoxys parvifolia 218 Ecu
Gynoxys buxifolia 160 Ecu
Gynoxys fuliginosa 156 Ecu
Gynoxys miniphylla 210 Ecu
Gynoxys parvifolia 166 Ecu
Gynoxys sodiroi 153 Ecu
Gynoxys sodiroi 199 Ecu
Gynoxys parvifolia 181 Ecu
Gynoxys buxifolia 188 Ecu
Gynoxys fuliginosa 185 Ecu
Gynoxys fuliginosa 204 Ecu
Gynoxys miniphylla 192 Ecu
Gynoxys miniphylla 217 Ecu
Gynoxys sodiroi EF538219 Ecu
Gynoxys parvifolia 175 Ecu
Gynoxys cf. szyszylowiczii 215 Per
Gynoxys cuicochensis 150 Ecu
Gynoxys cuicochensis 154 Ecu
Gynoxys cuicochensis 216 Ecu
Gynoxys sodiroii 290 Per
Gynoxys sodiroii 178 Ecu
Gynoxys sodiroii 179 Ecu
Gynoxys mandonii 172 Per
Gynoxys hallii 174 Per
Gynoxys hallii 176 Ecu
Gynoxys limonensis 147 Ecu
Gynoxys cf. hallii 158 Ecu
Gynoxys hallii 159 Ecu
Gynoxys hallii 157 Ecu
Gynoxys hallii 212 Ecu
Gynoxys mandonii 219 Per
Gynoxys soukupii 220 Per
Gynoxys soukupii 284 Per
Gynoxys capituliparva 295 Per
Gynoxys soukupii 221 Per
Gynoxys longistyla 223 Per
Gynoxys longistyla 227 Per
Gynoxys longistyla 226 Per
Gynoxys parvifolia 259 Per
Gynoxys capituliparva 300 Per
Gynoxys cusilluyocana 225 Per
Gynoxys caracensis 229 Per
Gynoxys mandonii 242 Per
Gynoxys caracensis 232 Per
Gynoxys ferreyrae 233 Per
Gynoxys caracensis 234 Per
Gynoxys caracensis 235 Per
Gynoxys calyculisolvens 236 Per
Gynoxys nitida 238 Per
Gynoxys cf. vacana 240 Per
Gynoxys cf. vacana 241 Per
Gynoxys cf. mandonii 243 Per
Gynoxys cf. vacana 248 Per
Gynoxys cf. macfrancisci 250 Per
Gynoxys cf. mandonii 252 Per
Gynoxys mandonii 279 Per
Gynoxys mandonii 253 Per
Gynoxys mandonii 254 Per
Gynoxys mandonii 255 Per
Gynoxys calyculisolvens 258 Per
Gynoxys calyculisolvens 260 Per
Gynoxys hallii 263 Per
Gynoxys nitida 264 Per
Gynoxys cf. rugulosa 267 Per
Gynoxys cf. rugulosa 269 Per
Gynoxys cf. cuicochensis 270 Per
Gynoxys mandonii 272 Per
Gynoxys vacana 274 Per
Gynoxys vacana 276 Per
Gynoxys mandonii 285 Per
Gynoxys mandonii 286 Per
Gynoxys mandonii 287 Per
Gynoxys cf. baccharoides 288 Per
Gynoxys cf. compressissima 293 Per
Gynoxys calyculisolvens DB38744 Per
Gynoxys baccharoides 294 Per
Gynoxys violacea DB38780 Ven
Nordenstamia kingii DB38764 Bol
Gynoxys caracensis 244 Per
Gynoxys cf. sodiroii 257 Per
Gynoxys compressissima 273 Per
Gynoxys marcapatana 266 Per
Gynoxys rugulosa 291 Per
Gynoxys hallii 296 Per
Gynoxys hutchisonii 283 Per
Gynoxys hutchisonii GU818174 Per
Gynoxys cuicochensis 184 Ecu
Gynoxys ignaciana DB38767 Ecu
Paragynoxys neodendroides EF538280 Col
Gynoxys longifolia 121 Bol
Gynoxys longifolia DB38565 Per
Gynoxys megacephala 020 Bol
Gynoxys megacephala DB27426 Bol
Gynoxys megacephala 022 Bol
Paracalia pentamera DB40913 Bol
Gynoxys tomentosissima DB38742 Per
Gynoxys capituliparva 245 Per
Nordenstamia cajamarcensis DB38626 Per
Paragynoxys martingrantii DB43896 Col
Paragynoxys venezuelae DB43902 Ven
Ligularia fischeri KY979035
1.1

Appendix 4: Supplementary material for Chapter 4

Appendix 4.1: Specimens included in the phylogenetic analysis according to species determination. Bio material corresponds to the DNA extraction which are stored in B. SEN numbers correspond to the identifier in tree (Figure 4.1). Specimens marked with * represent the accessions used for the PCA analyses (Figure 4.2 and 4.3).

Gynoxys asterotricha: Bolivia: La Paz, Nor Yungas, bajando a Unduavi, 16 km desde la cumbre, subiendo ladera a la izquierda de la carretera, voucher: B100720926, bio material: DB 27411, Tree ID: SEN 11, B. Escobari, S. Beck & C. Beck 36*, 5.7.2016. Bolivia: La Paz, Nor Yungas, arriba de Unduavi, subiendo aproximadamente 1:15 hora hacia los bosques de Polylepis pepei, voucher: B100720937, bio material: DB 27464, Tree ID: SEN 50, B. Escobari 79*, 13.9.2016. Bolivia: La Paz, Nor Yungas, bajando a Unduavi, 16 km desde la cumbre, subiendo ladera a la izquierda de la carretera, voucher: LPB, bio material: DB 27417, Tree ID: SEN 12, B. Escobari 37, 5.7.2016. Bolivia: La Paz, Nor Yungas, bajando a Unduavi, 16 km desde la cumbre, subiendo ladera a la izquierda de la carretera, voucher: LPB, bio material: DB 27418, Tree ID: SEN 13, B. Escobari 38, 5.7.2016. Bolivia: La Paz, Nor Yungas, bajando a Unduavi, 16 km desde la cumbre, subiendo ladera a la izquierda de la carretera, voucher: LPB, bio material: DB 27419, Tree ID: SEN 14, B. Escobari 39, 5.7.2016. Bolivia: La Paz, Nor Yungas, bajando a Unduavi, 16 km desde la cumbre, subiendo ladera a la izquierda de la carretera, voucher: LPB, bio material: DB 27420, Tree ID: SEN 15, B. Escobari 40, 5.7.2016.

Gynoxys cf. asterotricha: Bolivia: La Paz, Nor Yungas, bajando a los Yungas, antes del tunel y de Unduavi, voucher: B 10 0720256, bio material: DB 38582, Tree ID: SEN 139, S.G. Beck 31966, 10.6.2006. Bolivia: Cochabamba, José Carrasco Torrico, camino al cerro Apacheta, Parque Nacional Carrasco, voucher: LPB, bio material: DB 38559, Tree ID: SEN 116, M. Zárate 599, 8.9.2000.

Gynoxys asterotricha × *mandonii:* Bolivia: La Paz, Larecaja, bosque de la localidad de Escalerani, voucher: B100720294, bio material: DB 38610, Tree ID: SEN 167, A. Palabral 732*, 8.11.2008. Bolivia: La Paz, Larecaja, Lipichi, 5 km pasando el cruce Lakatya-Lipichi camino a Anilea, arriba del campamento dela empresa Progresiva, que extraen antimonia y estano, voucher: B100720931, bio material: DB 27440, Tree ID: SEN 34, B. Escobari 59*, 7.8.2016. Bolivia: La Paz, Larecaja, 3,4 km subiendo a Lakatya, voucher: B100720932, bio material: DB 27441, Tree ID: SEN 35, B. Escobari 60, 7.8.2016. Bolivia: La Paz, Larecaja, 3,4 km subiendo a Lakatya, voucher: B100720933, bio material: DB 27442, Tree ID: SEN 36, B. Escobari 61, 7.8.2016. Bolivia: La Paz, Nor Yungas, arriba de Unduavi, subiendo aproximadamente 45 min hacia los bosques de Polylepis pepei, voucher: B100720936, bio material: DB 27459, Tree ID: SEN 47, B. Escobari 73*, 13.9.2016. Bolivia: La Paz, Franz Tamayo, Senda Pelechuco-Mojo, sector Tambo Quemado, a media hora del campamento siguiendo senda Pelechuco Moxos, voucher: LPB, bio material: DB 38570, Tree ID: SEN 127, N. Paniagua 5716*, 1.3.2003.

Gynoxys compressissima: Bolivia: La Paz, J Bautista Saavedra, Localidad de Puina, bosque de Quenuapata, voucher: LPB, bio material: DB 38562, Tree ID: SEN 119, G. Aguirre 83*, 22.8.2006. Bolivia: La Paz, Franz Tamayo, Ulla Ulla, cordillera Apolobamba cerca al pueblo de Pelechuco, voucher: LPB, bio material: DB 38563, Tree ID: SEN 120, P. Holt 32, 24.8.1986.

Gynoxys kingii: Bolivia: Cochabamba, Jose Carrasco Torrico, 5 km al NE de Monte Punco por el camino a Sihuenca, voucher: LPB, bio material: DB 38764, Tree ID: SEN 321, J.C. Solomon & M. Nee 18067*, 10.3.1988.

Gynoxys longifolia: Bolivia: La Paz, Jose M Camacho, Combaya, rio Khala paya, voucher: LPB, bio material: DB 38564, Tree ID: SEN 121, T. Ortuno 615, 12.6.2007.

Gynoxys mandonii: Bolivia: La Paz, Nor Yungas, Parque Cotapata Santa Bárbara, voucher: B 10 0720260, bio material: DB 38569, Tree ID: SEN 126, Campaña de recolección de madera 14, 27.4.1997. Bolivia: La Paz, Larecaja, 9 km pasando el desvío de Laripata-Lipichi, camino hacia Pacuni, voucher: B 10 0720929, bio material: DB 27434, Tree ID: SEN 29, B. Escobari 54, 7.8.2016. Bolivia: La Paz, Larecaja, 9 km pasando el desvío de Laripata-Lipichi, camino hacia Pacuni, voucher: B 10 0720930, bio material: DB 27438, Tree ID: SEN 33a, B. Escobari 58a, 7.8.2016. Bolivia: La Paz, Larecaja, pasando Laripata, camino hacia Pacuni-Chinchaya, voucher: B 10 0720935, bio material: DB 27448, Tree ID: SEN 42a, B. Escobari 68a, 7.8.2016. Bolivia: Cochabamba, Ayopaya, Cocapata, encima de Tiquipaya, voucher: B100763214; B100763215, bio material: DB 38533, Tree ID: SEN 90, B. Escobari 272*, 22.7.2017. Bolivia: Cochabamba, Ayopaya, Cocapata, encima de Tiquipaya, voucher: B100763216; B100763217, bio material: DB 38534, Tree ID: SEN 91, B. Escobari 273*, 22.7.2017. Bolivia: Cochabamba, Carrasco, Monte Punku, entrando hacia Yungas, voucher: B100763257; B100763258, bio material: DB 38553, Tree ID: SEN 110, B. Escobari 307*, 24.7.2017. Bolivia: La Paz, J Bautista Saavedra, Parque Nacional Madidi, Laji Sorapata, Cosnijmayu, Kanupata Interseccion de losrios Santa Elena y Laji alado de arroyo Kumamayu, voucher: MO-3151322, bio material: DB 27416, Tree ID: SEN 4, L. Cayola 5570, 29.6.2016. Bolivia: La Paz, Nor Yungas, Parque Nal Cotapata, Unduavi, sendero Sillutincara, ca de 1 km subiendo de la carretera, voucher: LPB, bio material: DB 38568, Tree ID: SEN 125, A. Fuentes 11933*, 30.5.2007. Bolivia: La Paz, J Bautista Saavedra, Parque Nacional Madidi, Laji Sorapata, Cosnijmayu, Kanupata Interseccion de losrios Santa Elena y Laji alado de arroyo Kumamayu, voucher: LPB, bio material: DB 27410, Tree ID: SEN 5, L. Cayola 5572, 29.6.2016. Bolivia: La Paz, J Bautista Saavedra, Parque Nacional Madidi, Laji Sorapata, Cosnijmayu, Kanupata Interseccion de losrios Santa Elena y Laji alado de arroyo Kumamayu, voucher: LPB, bio material: DB 27413, Tree ID: SEN 8, L. Cayola 5594, 29.6.2016. Bolivia: La Paz, J Bautista Saavedra, Parque Nacional Madidi, Laji Sorapata, Cosnijmayu, Kanupata Interseccion de losrios Santa Elena y Laji alado de arroyo Kumamayu, voucher: LPB, bio material: DB 27414, Tree ID: SEN 9, L. Cayola 5596, 29.6.2016. Bolivia: La Paz, J. Bautista Saavedra, Parque Nacional Madidi, Laji Sorapata, Cosñijmayu, Kañupata, Intersección de los ríos Santa Elena y Laji alado de arroyo Kumamayu, voucher: LPB, bio material: DB 27474, Tree ID: SEN 56, L. Cayola 5613, 29.6.2016. Bolivia: La Paz, J. Bautista Saavedra, Parque Nacional Madidi, Laji Sorapata, Cosñijmayu, Kañupata, Intersección de los ríos Santa Elena y Laji alado de arroyo Kumamayu, voucher: LPB, bio material: DB 27475, Tree ID: SEN 57, L. Cayola 5617, 29.6.2016. Bolivia: Cochabamba, Jose Carrasco Torrico, Siberia, voucher: LPB, bio material: DB 38566, Tree ID: SEN 123, R.F. Steinbach 214, 21.5.1966. Bolivia: La Paz, Larecaja, Municipio Sorata Comunidad Tucsa Jahuira Cerro Lakatya, voucher: LPB, bio material: DB 38567, Tree ID: SEN 124, M. Casas 5, 16.11.2006. Bolivia: La Paz, Larecaja, 9 km pasando el desvío de Laripata-Lipichi, camino hacia Pacuni, voucher: LPB, bio material: DB 27439, Tree ID: SEN 33b, B. Escobari 58b, 7.8.2016. Bolivia: La Paz, Larecaja, pasando Laripata, camino hacia Pacuni-Chinchaya, voucher: LPB, bio material: DB 27449, Tree ID: SEN 42b, B. Escobari 68b, 7.8.2016.

Gynoxys megacephala: Bolivia: La Paz, Nor Yungas entrando a la Ecovia 37,5 km desde la cumbre bajando a Unduavi a la derecha del sendero, voucher: LPB, bio material: DB 27426, Tree ID: SEN 21, B. Escobari 46, 5.7.2016. Bolivia: La Paz, Nor Yungas entrando a la Ecovia 37,5 km desde la cumbre bajando a Unduavi a la derecha del sendero, voucher: LPB, bio material: DB 27427, Tree ID: SEN 22, B. Escobari 47, 5.7.2016.

Gynoxys neovelutina: Bolivia: Cochabamba, Chapare, Inka Chaka, camino subiendo a hidroelectrica en propiedad privada, voucher: B100763054; B100763055, bio material: DB 38503, Tree ID: SEN 60, B. Escobari 133*, 16.7.2017. Bolivia: Cochabamba, Chapare, ca 8 km N Maycamayu, ca 70 km from Sacaba, voucher: LPB, bio material: DB 38574, Tree ID: SEN 131, M. Kessler 2905*, 12.8.1991.

Gynoxys psilophylla: Bolivia: Cochabamba, Quillacollo, Parque nacional Tunari, voucher: B100763142, bio material: DB 38519, Tree ID: SEN 76, B. Escobari 216, 20.7.2017. Bolivia: Cochabamba, Arani, Vacas, santuario de las Puyas, voucher: B100763231, bio material: DB 38541, Tree ID: SEN 98, B. Escobari 285, 23.7.2017. Bolivia: Cochabamba, Arani, Vacas, camino de bajada pasando el santuario de las Puyas, voucher: B100763238, bio material: DB 38547, Tree ID: SEN 104, B. Escobari 291, 23.7.2017. Bolivia: Cochabamba, Arani, Vacas, camino asfaltado a Mizque, voucher: B100763239; B100763240, bio material: DB 38548, Tree ID: SEN 105, B. Escobari 292*, 23.7.2017. Bolivia: La Paz, Inquisivi, climbing the forested slope of the Lower Cerro Chamaquiri N of the Rio Khatu Area knownas 'Huanhawira' ca 2 km SW of Quime, voucher: MO-1879966, bio material: DB 38577, Tree ID: SEN 134, M. Lewis 88971, 29.6.1988. Bolivia: Potosi, Charcas, voucher: LPB, bio material: DB 38576, Tree ID: SEN 133, G. Torrico 532, 20.6.1993. Bolivia: Cochabamba, Mizque, Canada Pucara Mayu a 37 km de Rodeo a Mizque entre Khewina Khasa y Pucara Khasa, voucher: LPB, bio material: DB 38578, Tree ID: SEN 135, S. Estenssoro 804, 8.5.1987. Bolivia: Chuquisaca, Jaime Zudanez, 25 km S Icla on Tarabuco - Azurduy road, voucher: LPB, bio material: DB 38579, Tree ID: SEN 136, M. Kessler 3222, 24.9.1991.

Gynoxys repanda: Bolivia: Cochabamba, José Carrasco Torrico, Monte Punco, camino a Sehuencas, a 15 min en auto de la entrada a Monte Punco, al lado izquiero del camino, en cultivo de papa, voucher: B 10 0720938, bio material: DB 27468, Tree ID: SEN 52b, B. Escobari 86b, 5.10.2016. Bolivia: Cochabamba, José Carrasco Torrico, Monte Punco, camino a Sehuencas, a 25 min en auto de la entrada a Monte Punco, al lado izquierdo del camino en una propiedad privada, voucher: B 10 0720939, bio material: DB 27469, Tree ID: SEN 53a, B. Escobari 87a, 5.10.2016. Bolivia: Cochabamba, Chapare, Inka Chaka, camino subiendo a hidroelectrica en propiedad privada, voucher: B 10 0763070, bio material: DB 38505, Tree ID: SEN 62, B. Escobari 147*, 16.7.2017. Bolivia: La Paz, Inquisivi, unos 8 km de Quime hacia Inquisivi, Camillaya arriba del pueblo, voucher: B100720276, bio material: DB 38623, Tree ID: SEN 180, S.G. Beck 24375*, 29.9.1997. Bolivia: La Paz, Nor Yungas, entrando a la Ecovia, 36 km desde la cumbre bajando a Unduavi, a la derecha del sendero, voucher: B100720927, bio material: DB 27421, Tree ID: SEN 16, B. Escobari 41*, 5.7.2016. Bolivia: La Paz, Nor Yungas, entrando a la Ecovia, 36 km desde la cumbre bajando a Unduavi, a la derecha del sendero, voucher: B100720928, bio material: DB 27424, Tree ID: SEN 19, B. Escobari 44*, 5.7.2016. Bolivia: La Paz, Larecaja, pasando Laripata, camino hacia Pacuni-Chinchaya, voucher: B100720934, bio material: DB 27446, Tree ID: SEN 40, B. Escobari 66*, 7.8.2016. Bolivia: Cochabamba, Chapare, Inka Chaka, camino subiendo a hidroelectrica en propiedad privada, voucher: B100763045, bio material: DB 38501, Tree ID: SEN 58, B. Escobari 129*, 16.7.2017. Bolivia: Cochabamba, Chapare, Inka Chaka, camino subiendo a hidroelectrica en

propiedad privada, voucher: B100763052; B100763053, bio material: DB 38502, Tree ID: SEN 59, B. Escobari 132*, 16.7.2017. Bolivia: Cochabamba, Carrasco, Monte Punku, entrando hacia Yungas, voucher: B100763259, bio material: DB 38554, Tree ID: SEN 111, B. Escobari 308*, 24.7.2017. Bolivia: La Paz, Nor Yungas, Ca 2 km sobre la Ecovia (antigua ferrovia planificada) hacia SW, despues subiendo hacia la cresta, voucher: US 01826012, bio material: DB 38557, Tree ID: SEN 114, S.G. Beck 29889, 10.6.2007. Bolivia: La Paz, Sud Yungas, Canton Yanacachi Mina Chojlla, camino de acceso de vehiculos a Kacapi, voucher: LPB, bio material: DB 38586, Tree ID: SEN 143, R. Sinani 264*, 28.7.2000. Bolivia: Cochabamba, Jose Carrasco Torrico, ca 6 km below Sehuencas, voucher: LPB, bio material: DB 38587, Tree ID: SEN 144, J.R.I. Wood 10093*, 30.7.1995. Bolivia: La Paz, J Bautista Saavedra, Parque Nacional Madidi, Laji Sorapata, Cosnijmayu, Waturuyuj Sobre la senda queva desde la interseccion de los rios Santa Elena y Laji hacia Chillkapampa, voucher: LPB, bio material: DB 27406, Tree ID: SEN 1, L. Cayola 5490, 23.6.2016. Bolivia: La Paz, J Bautista Saavedra, Parque Nacional Madidi, Laji Sorapata, Cosnijmayu, Waturuyuj Sobre la senda queva desde la interseccion de los rios Santa Elena y Laji hacia Chillkapampa, voucher: LPB, bio material: DB 27407, Tree ID: SEN 2, L. Cayola 5514, 23.6.2016. Bolivia: La Paz, J Bautista Saavedra, Parque Nacional Madidi, Laji Sorapata, Cosnijmayu, Waturuyuj Sobre la senda queva desde la interseccion de los rios Santa Elena y Laji hacia Chillkapampa, voucher: LPB, bio material: DB 27408, Tree ID: SEN 3, L. Cayola 5548, 23.6.2016. Bolivia: La Paz, Larecaja, 9 km pasando el desvío de Laripata-Lipichi, camino hacia Pacuni, voucher: LPB, bio material: DB 27435, Tree ID: SEN 3, B. Escobari 55, 7.8.2016. Bolivia: La Paz, J Bautista Saavedra, Parque Nacional Madidi, Laji Sorapata, Cosnijmayu, Kanupata Interseccion de losrios Santa Elena y Laji alado de arroyo Kumamayu, voucher: LPB, bio material: DB 27409, Tree ID: SEN 6, L. Cayola 5585, 29.6.2016. Bolivia: La Paz, J Bautista Saavedra, Parque Nacional Madidi, Laji Sorapata, Cosnijmayu, Kanupata Interseccion de losrios Santa Elena y Laji alado de arroyo Kumamayu, voucher: LPB, bio material: DB 27412, Tree ID: SEN 7, L. Cayola 5586, 29.6.2016. Bolivia: La Paz, J Bautista Saavedra, Parque Nacional Madidi, Laji Sorapata, Cosnijmayu, Kanupata Interseccion de losrios Santa Elena y Laji alado de arroyo Kumamayu, voucher: LPB, bio material: DB 27415, Tree ID: SEN 10, L. Cayola 5599, 29.6.2016. Bolivia: La Paz, Nor Yungas, entrando a la Ecovia, 36 km desde la cumbre bajando a Unduavi, A la derecha del sendero, voucher: LPB, bio material: DB 27422, Tree ID: SEN 17, B. Escobari 42, 5.7.2016. Bolivia: La Paz, Nor Yungas, entrando a la Ecovia, 36 km desde la cumbre bajando a Unduavi, A la derecha del sendero, voucher: LPB, bio material: DB 27423, Tree ID: SEN 18, B. Escobari 43, 5.7.2016. Bolivia: La Paz, Larecaja, pasando Laripata, camino hacia Pacuni-Chinchaya, voucher: LPB, bio material: DB 27447, Tree ID: SEN 41, B. Escobari 67, 7.8.2016. Bolivia: Cochabamba, José Carrasco Torrico, Monte Punco, camino a Sehuencas, a 25 min en auto de la entrada a Monte Punco, al lado derecho del camino, voucher: LPB, bio material: DB 27472, Tree ID: SEN 54, B. Escobari 88, 5.10.2016. Bolivia: La Paz, Franz Tamayo, area Natural de Manejo Integrado Apolobamba, Chullina, Comunidad Waira Pata (Sanachi), Kumamta, voucher: LPB, bio material: DB 27473, Tree ID: SEN 55, L. Cayola 5632, 5.7.2016. Bolivia: Cochabamba, José Carrasco Torrico, Siberia Oeste, Monte Hotel, voucher: LPB, bio material: DB 38584, Tree ID: SEN 141, S. Duran 102, 22.9.2003. Bolivia: La Paz, Franz Tamayo, Senda Pelechuco Mojo, sector Tambo Quemado, 15 minutos hacia abajo del campamento siguiendo senda Pelechuco Moxos, Parcela Temporal 88 (0,1 ha), voucher: LPB, bio material: DB 38585, Tree ID: SEN 142, N. Paniagua 5708, 29.4.2003. Bolivia: La Paz, Larecaja, pasando Laripata, camino hacia Pacuni-Chinchaya, voucher: LPB, bio material: DB 27450, Tree ID: SEN 42c, B. Escobari 68c, 7.8.2016. Bolivia: La Paz, Larecaja, pasando Laripata, camino hacia Pacuni-

Chinchaya, voucher: LPB, bio material: DB 27451, Tree ID: SEN 42d, B. Escobari 68d, 7.8.2016. Bolivia: La Paz, Larecaja, pasando Laripata, camino hacia Pacuni-Chinchaya, voucher: LPB, bio material: DB 27452, Tree ID: SEN 42e, B. Escobari 68e, 7.8.2016. Bolivia: Cochabamba, José Carrasco Torrico, Monte Punco, camino a Sehuencas, a 15 min en auto de la entrada a Monte Punco, al lado izquiero del camino, en cultivo de papa, voucher: LPB, bio material: DB 27467, Tree ID: SEN 52a, B. Escobari 86a, 5.10.2016. Bolivia: Cochabamba, José Carrasco Torrico, Monte Punco, camino a Sehuencas, a 25 min en auto de la entrada a Monte Punco, al lado izquierdo del camino en una propiedad privada, voucher: LPB, bio material: DB 27470, Tree ID: SEN 53b, B. Escobari 87b, 5.10.2016. Bolivia: Cochabamba, José Carrasco Torrico, Monte Punco, camino a Sehuencas, a 25 min en auto de la entrada a Monte Punco, al lado izquierdo del camino en una propiedad privada, voucher: LPB, bio material: DB 27471, Tree ID: SEN 53c, B. Escobari 87c, 5.10.2016.

Gynoxys rusbyi: Bolivia: La Paz, Inquisivi, Rio Mina Jahuira, river which runs from Mina Vieja with its mouth 05 km N of Choquetanga, voucher: LPB, bio material: DB 38580, Tree ID: SEN 137, M. Lewis 39240*, 15.7.1991. Bolivia: La Paz, Loayza, bajando de Viloco hacia Aguas Calientes (Choquetanga), voucher: LPB, bio material: DB 38581, Tree ID: SEN 138, N. Salinas 3315*, 16.8.1994.

Gynoxys: Bolivia: La Paz, Larecaja, 9 km pasando el desvío de Laripata-Lipichi, camino hacia Pacuni, voucher: LPB, bio material: DB 27436, Tree ID: SEN 31, B. Escobari 56, 7.8.2016. Bolivia: La Paz, Larecaja, 9 km pasando el desvío de Laripata-Lipichi, camino hacia Pacuni, voucher: LPB, bio material: DB 27437, Tree ID: SEN 32, B. Escobari 57, 7.8.2016. Bolivia: La Paz, Larecaja, pasando Laripata, camino hacia Pacuni-Chinchaya, voucher: LPB, bio material: DB 27443, Tree ID: SEN 37, B. Escobari 63, 7.8.2016. Bolivia: La Paz, Larecaja, pasando Laripata, camino hacia Pacuni-Chinchaya, voucher: LPB, bio material: DB 27444, Tree ID: SEN 38, B. Escobari 64, 7.8.2016. Bolivia: La Paz, Larecaja, pasando Laripata, camino hacia Pacuni-Chinchaya, voucher: LPB, bio material: DB 27445, Tree ID: SEN 39, B. Escobari 65, 7.8.2016. Bolivia: La Paz, Nor Yungas, arriba de Unduavi, subiendo aproximadamente 45 min hacia los bosques de Polylepis pepei, voucher: LPB, bio material: DB 27453, Tree ID: SEN 43, B. Escobari 69, 13.9.2016. Bolivia: La Paz, Nor Yungas, arriba de Unduavi, subiendo aproximadamente 45 min hacia los bosques de Polylepis pepei, voucher: LPB, bio material: DB 27454, Tree ID: SEN 44, B. Escobari 70, 13.9.2016. Bolivia: La Paz, Nor Yungas, arriba de Unduavi, subiendo aproximadamente 45 min hacia los bosques de Polylepis pepei, voucher: LPB, bio material: DB 27458, Tree ID: SEN 46, B. Escobari 72, 13.9.2016. Bolivia: La Paz, Nor Yungas, arriba de Unduavi, subiendo aproximadamente 45 min hacia los bosques de Polylepis pepei, voucher: LPB, bio material: DB 27460, Tree ID: SEN 48, B. Escobari 74, 13.9.2016. Bolivia: La Paz, Nor Yungas, arriba de Unduavi, subiendo aproximadamente 45 min hacia los bosques de Polylepis pepei, voucher: LPB, bio material: DB 27455, Tree ID: SEN 45a, B. Escobari 71a, 13.9.2016. Bolivia: La Paz, Nor Yungas, arriba de Unduavi, subiendo aproximadamente 45 min hacia los bosques de Polylepis pepei, voucher: LPB, bio material: DB 27456, Tree ID: SEN 45b, B. Escobari 71b, 13.9.2016. Bolivia: La Paz, Nor Yungas, arriba de Unduavi, subiendo aproximadamente 45 min hacia los bosques de Polylepis pepei, voucher: LPB, bio material: DB 27457, Tree ID: SEN 45c, B. Escobari 71c, 13.9.2016. Bolivia: La Paz, Nor Yungas, arriba de Unduavi, subiendo aproximadamente 45 min hacia los bosques de Polylepis pepei, voucher: LPB, bio material: DB 27461, Tree ID: SEN 49a, B. Escobari 75a, 13.9.2016. Bolivia: La Paz, Nor Yungas, arriba de Unduavi, subiendo aproximadamente 45 min hacia los bosques de Polylepis pepei, voucher: LPB, bio material: DB

27462, Tree ID: SEN 49b, B. Escobari 75b, 13.9.2016. Bolivia: La Paz, Nor Yungas, arriba de Unduavi, subiendo aproximadamente 45 min hacia los bosques de Polylepis pepei, voucher: LPB, bio material: DB 27463, Tree ID: SEN 49c, B. Escobari 75c, 13.9.2016. Bolivia: La Paz, Nor Yungas, arriba de Unduavi, subiendo aproximadamente 1:15 hora hacia los bosques de Polylepis pepei, voucher: LPB, bio material: DB 27465, Tree ID: SEN 51a, B. Escobari 80a, 13.9.2016. Bolivia: La Paz, Nor Yungas, arriba de Unduavi, subiendo aproximadamente 1:15 hora hacia los bosques de Polylepis pepei, voucher: LPB, bio material: DB 27466, Tree ID: SEN 51b, B. Escobari 80b, 13.9.2016. Bolivia: La Paz, Larecaja, 9 km pasando el desvío de Laripata-Lipichi, camino hacia Pacuni, voucher: LPB, bio material: DB 27435, Tree ID: SEN 30, B. Escobari 55, 42589.

Paracalia pentamera: Bolivia: La Paz, Sud Yungas, Municipio de Chulumani Localidad Rio Blanco Cerro Lambate, interior del bosque a 20 m del borde, voucher: LPB, bio material: DB 40913, Tree ID: SEN 389, S. Gallegos 3850, 23.11.2011.

Appendix 4.2: character state evaluation of vegetative characters on 99 specimens. Character abbreviations and states coding according Appendix 4.4. SEN number correspond to identifiers in the phylogenetic inference (Figure 4.1).

	Clade	Tree ID	Collector	Coll num	PCA ID	LHSC	LHSR	LHTR	LPVE	LPAL
1			Wood, J.R.I.	8047	ast_10	0	1	0	0	0
2			Loza, I.	883	ast_11	0	1	0	0	0
3			Feuerer, T.	11398	ast_12	0	0	1	0	0
4			Fuentes, A.	13625	ast_13	0	1	0	0	0
5			Fuentes, A.	16193	ast_3	0	1	0	0	0
6	ast-rus-psi	SEN11	Escobari, B., Beck, S. & Beck, C.	36	ast_6	0	1	0	0	0
7			Cayola, L.	3880	ast_7	0	1	0	0	0
8			Gutte, P.	424	ast_8	0	0	1	0	0
9	man 2	SEN50	Escobari, B., Beck, S. & Beck, C.	79	ast_9	0	1	0	0	0
10			Beck, S.	28794	new_B_11	0	1	0	0	1
11			Beck, S.	28794A	new_B_12	0	1	0	0	1
12			Müller, J.	7464	new_B_22	0	1	0	0	1
13			Fuentes, A.	15049	new_B_7	0	1	0	0	1
14			Beck, S.	21376	new_B_8	0	1	0	0	1
15			Loza, I.	754	com_1	0	0	1	0	0
16			Paco, P.	78	com_2	0	0	1	0	0
17	man 2	SEN119	Aguirre, G.	83	com_3	0	0	1	0	0
18			Rico, L., Windsor-Shaw, T., McRobb & Alvarez, L	1303	kin_1	0	1	0	0	0
19	kin	SEN321	Solomon, J.	18067	kin_2	0	1	0	0	1
20			Wood, J.R.I.	22990	kin_3	0	1	0	0	1
21			Wood, J.R.I.	9342	kin_4	0	1	0	0	1
22			Ortuño, T.	639	lon_1	0	1	0	0	0
23	man 1	SEN91	Escobari, B., Kilian, N., Villca, H. & Nieto, B.	273	man_10	0	0	1	0	0
24	man 1	SEN90	Escobari, B., Kilian, N., Villca, H. & Nieto, B.	272	man_11	0	0	1	0	0
25	man 1	SEN110	Escobari, B., Kilian, N. & Villca, H.	307	man_12	0	0	1	0	0

Appendix 4.2: continuation…

	Clade	Tree ID	Collector	Coll num	PCA ID	LHSC	LHSR	LHTR	LPVE	LPAL
26			Beck, S.	31967	man_13	0	0	1	0	0
27			Cayola, L.	3528	man_14	0	0	1	0	0
28			Samo, L.	41	man_15	0	0	1	0	0
29			Escobari, B., Beck, S. & Beck, C.	58	man_17	0	0	1	0	0
30			Escobari, B., Beck, S. & Beck, C.	68	man_20	0	0	1	0	0
31	man 1	SEN125	Fuentes, A.	11933	man_7	0	0	1	0	0
32	man 2	SEN47	Escobari, B., Beck, S. & Beck, C.	73	mas_10	0	0	1	0	0
33	man 2	SEN167	Palabral, A.	732	mas_11	0	0	1	0	0
34			Fuentes, A.	16905	mas_12	0	0	1	0	0
35			Fuentes, A.	15094	mas_13	0	0	1	0	0
36			Palabral, A.	285	mas_14	0	1	0	0	0
37			Saldias, M.	4632	mas_15	0	0	1	0	0
38			Fuentes, A.	8392	mas_16	0	0	1	0	0
39			Quisbert, J.	843	mas_17	0	0	1	0	0
40			Aldana, C.	510	mas_18	0	0	1	0	0
41			Solomon, J.	16497	mas_2	0	0	1	0	0
42			Paco, P.	19	mas_3	0	0	1	0	0
43			Fuentes, A.	16781	mas_4	0	1	0	0	0
44			Quisbert, J.	822	mas_5	0	0	1	0	0
45			Beck, S.	29440	mas_6	0	0	1	0	0
46	man 1	SEN127	Paniagua, N.	5716	mas_7	0	0	1	0	0
47	man 1	SEN34	Escobari, B., Beck, S. & Beck, C.	59	mas_8	0	0	1	0	0
48			Zarate, M.	621	mas_9	0	0	1	0	0
49			Fuentes, A.	15602	meg_1	0	1	0	0	0
50			Beck, S.	32686	meg_2	0	1	0	1	0
51			Müller, J.	7454	meg_3	0	1	0	0	0

Appendix 4.2: continuation…

	Clade	Tree ID	Collector	Coll num	PCA ID	LHSC	LHSR	LHTR	LPVE	LPAL
52	neo	SEN60	Escobari, B., Kilian, N. & Villca, H.	133	neo_1	0	0	1	0	0
53			Wood, J.R.I.	23092	neo_2	0	1	0	0	0
54	neo	SEN131	Kessler, M.	2905	neo_3	0	0	1	0	0
55			Hensen, I.	249	new_A_1	0	1	0	0	0
56			Wood, J.R.I.	19248	new_A_2	0	1	0	0	0
57			Cayola, L.	3873	new_C	1	0	0	0	0
58			Aedo, C.	14429	psi_1	0	1	0	0	0
59			Escobari, B., Kilian, N., Villca, H. & Nieto, B.	299	psi_10	0	1	0	0	0
60			Escobari, B., Kilian, N.	313	psi_11	0	1	0	0	0
61			Escobari, B., Kilian, N. & Villca, H.	176	psi_2	0	1	0	0	0
62			Escobari, B., Kilian, N. & Villca, H.	208	psi_3	0	1	0	0	0
63			Wood, J.R.I.	23288	psi_4	0	1	0	0	0
64			Escobari, B., Kilian, N., Villca, H. & Nieto, B.	247	psi_5	0	1	0	0	0
65			Escobari, B., Kilian, N., Villca, H. & Nieto, B.	277	psi_6	0	1	0	0	0
66			Escobari, B., Kilian, N., Villca, H. & Nieto, B.	279	psi_7	0	1	0	0	0
67			Escobari, B., Kilian, N., Villca, H. & Nieto, B.	289	psi_8	0	1	0	0	0
68	ast-rus-psi	SEN105	Escobari, B., Kilian, N., Villca, H. & Nieto, B.	292	psi_9	0	1	0	0	0
69	rep 1	SEN144	Wood, J.R.I.	10093	rep_1	0	1	0	0	1
70	rep 2	SEN143	Siñani, R.	264	rep_10	0	0	1	0	1
71			Escobari, B., Kilian, N. & Villca, H.	305	rep_13	0	0	1	0	1
72	rep 1	SEN111	Escobari, B., Kilian, N. & Villca, H.	308	rep_14	0	0	1	0	1
73			Cabrera, A.	33718	rep_15	0	0	1	0	1
74			Lewis, M.	39262	rep_16	0	0	1	0	1
75	rep 2	SEN16	Escobari, B., Beck, S. & Beck, C.	41	rep_17	0	0	1	0	1
76	rep 1	SEN19	Escobari, B., Beck, S. & Beck, C.	44	rep_18	0	0	1	0	1
77			Solomon, J.	6024	rep_19	0	1	0	0	1

Appendix 4.2: continuation…

	Clade	Tree ID	Collector	Coll num	PCA ID	LHSC	LHSR	LHTR	LPVE	LPAL
78			Solomon, J.	12372	rep_2	0	0	1	0	1
79	rep 2	SEN40	Escobari, B., Beck, S. & Beck, C.	66	rep_20	0	0	1	0	1
80			Cornejo M.	717	rep_21	0	0	1	0	1
81			Cornejo M.	772	rep_23	0	0	1	0	1
82			Cornejo M.	774	rep_24	0	0	1	0	1
83			Escobari, B., Beck, S. & Beck, C.	86	rep_25	0	0	1	0	1
84			Escobari, B., Beck, S. & Beck, C.	87	rep_26	0	0	1	0	1
85			Cornejo M.	915	rep_27	0	0	1	0	1
86			Cornejo M.	931	rep_28	0	1	0	0	1
87	rep 1	SEN58	Escobari, B., Kilian, N. & Villca, H.	129	rep_3	0	0	1	0	1
88			Smith, D.	13051	rep_4	0	1	0	0	1
89	rep 1	SEN59	Escobari, B., Kilian, N. & Villca, H.	132	rep_5	0	0	1	0	1
90	rep 1	SEN62	Escobari, B., Kilian, N. & Villca, H.	147	rep_6	0	0	1	0	1
91	rep 1	SEN180	Beck, S.	24375	rep_9	0	1	0	0	1
92	ast-rus-psi	SEN138	Salinas, N.	3315	rus_4	0	0	1	0	0
93			Lewis, M.	38940	rus_5	0	0	1	0	0
94	ast-rus-psi	SEN137	Lewis, M.	39240	rus_6	0	0	1	0	0
95			Escobari, B., Kilian, N. & Villca, H.	178	rus_7	0	1	0	0	1
96			Lewis, M.	35153	rus_cf_1	0	1	0	0	0
97			Lewis, M.	39352	rus_cf_2	0	1	0	0	0
98			Lewis, M.	881017	rus_cf_3	0	1	0	0	0
99			Palabral, A.	703	sor_1	0	1	0	0	0

Appendix 4.2: continuation…

	LPSU	LPOP	LSEL	LSLA	LSOL	LSOO	LSOV	LSOR	LMEN	LMDE	LMLO	LMRE	LMRV	LMBO	LBAC	LBOB	LBCO
1	0	1	1	0	0	0	0	0	1	0	0	0	0	0	0	0	0
2	0	1	0	0	0	0	1	0	1	0	0	0	0	0	0	0	0
3	0	1	1	0	0	0	1	0	1	0	0	0	0	0	0	0	0
4	0	1	0	0	0	0	1	0	1	0	0	0	0	0	0	1	0
5	0	1	1	0	0	0	1	0	1	0	0	0	0	0	0	0	0
6	0	1	0	0	1	0	1	0	1	0	0	0	0	0	0	0	0
7	0	1	1	0	0	0	1	0	1	0	0	0	0	0	0	1	0
8	0	1	0	0	0	0	1	0	1	0	0	0	0	0	0	1	0
9	0	1	0	0	0	0	1	0	1	0	0	0	0	0	0	1	0
10	0	0	1	0	0	0	0	0	1	0	0	0	0	0	0	0	1
11	0	0	0	0	0	1	0	0	0	0	0	1	0	0	0	0	0
12	0	0	1	0	0	0	0	0	1	0	0	0	0	0	0	0	0
13	0	0	1	0	0	0	0	0	0	0	0	1	0	0	0	0	1
14	0	0	1	0	0	1	0	0	1	0	0	0	0	0	0	0	1
15	0	1	1	0	0	0	0	0	1	0	0	0	0	0	0	0	0
16	0	1	0	0	0	0	1	0	1	0	0	0	0	0	0	0	0
17	0	1	1	0	0	0	1	0	1	0	0	0	0	0	0	0	0
18	0	1	0	0	0	0	1	0	0	0	1	0	0	0	0	0	1
19	0	0	0	0	0	0	1	0	0	0	1	0	0	0	0	0	1
20	0	0	0	0	0	0	1	0	0	0	1	0	0	0	0	0	1
21	0	0	0	0	0	0	1	0	0	0	1	0	0	0	0	0	1
22	0	1	0	0	1	0	0	0	1	0	0	0	0	0	1	0	0
23	0	1	0	0	0	0	1	0	1	0	0	0	0	0	0	0	0
24	0	1	0	0	0	0	1	0	1	0	0	0	0	0	0	1	0
25	0	1	0	0	0	0	1	0	1	0	0	0	0	0	0	1	0
26	0	1	0	0	0	0	1	0	1	0	0	0	0	0	0	0	0

Appendix 4.2: continuation…

	LPSU	LPOP	LSEL	LSLA	LSOL	LSOO	LSOV	LSOR	LMEN	LMDE	LMLO	LMRE	LMRV	LMBO	LBAC	LBOB	LBCO
27	0	1	0	0	0	0	1	0	1	0	0	0	0	0	0	0	0
28	0	1	0	0	0	0	1	0	1	0	0	0	0	0	0	0	0
29	0	1	0	0	0	0	1	0	1	0	0	0	0	0	0	0	0
30	0	1	1	0	0	0	1	0	1	0	0	0	0	0	0	0	0
31	0	1	0	0	1	0	0	0	1	0	0	0	0	0	0	1	0
32	0	1	1	0	0	0	1	0	1	0	0	0	0	0	1	0	0
33	0	1	0	0	1	0	0	0	1	0	0	0	0	0	0	0	0
34	0	1	0	0	0	0	1	0	1	0	0	0	0	0	0	1	0
35	0	1	0	1	0	0	0	0	1	0	0	0	0	0	0	0	0
36	0	1	1	0	0	0	0	0	1	0	0	0	0	0	0	0	0
37	0	1	0	1	0	0	0	0	1	0	0	0	0	0	0	0	1
38	0	1	0	0	0	0	1	0	1	0	0	0	0	0	0	0	0
39	0	1	1	0	0	0	0	0	1	0	0	0	0	0	0	0	0
40	0	1	0	0	0	0	1	0	1	0	0	0	0	0	0	0	0
41	0	1	0	0	0	0	1	0	1	0	0	0	0	0	0	0	0
42	0	1	1	0	0	0	0	0	1	0	0	0	0	0	0	0	0
43	0	1	0	1	0	0	0	0	1	0	0	0	0	0	0	0	1
44	0	1	0	0	0	0	1	0	1	0	0	0	0	0	0	0	1
45	0	1	0	0	0	0	1	0	1	0	0	0	0	0	0	0	0
46	0	1	0	1	0	0	0	0	1	0	0	0	0	0	0	0	0
47	0	1	0	0	1	0	0	0	1	0	0	0	0	0	0	0	1
48	0	1	1	0	0	0	0	0	1	0	0	0	0	0	1	0	0
49	1	1	0	0	0	1	0	0	1	0	0	0	0	0	1	0	0
50	0	0	1	0	0	0	0	0	1	0	0	0	0	0	1	0	0
51	0	1	1	0	0	0	0	0	1	0	0	0	0	0	1	0	0
52	0	1	0	0	0	0	1	0	1	0	0	0	0	0	0	0	0

Appendix 4.2: continuation…

	LPSU	LPOP	LSEL	LSLA	LSOL	LSOO	LSOV	LSOR	LMEN	LMDE	LMLO	LMRE	LMRV	LMBO	LBAC	LBOB	LBCO
53	0	1	0	0	0	0	1	0	1	0	0	0	0	0	0	0	1
54	0	1	0	0	0	0	1	0	1	0	0	0	0	0	0	1	0
55	0	1	0	0	0	0	1	0	1	0	0	0	1	1	0	0	1
56	0	1	0	0	1	0	1	0	1	0	0	0	1	1	0	0	1
57	0	1	0	0	1	0	1	0	0	0	0	1	0	0	0	0	0
58	0	1	0	0	0	0	1	0	1	0	0	0	0	0	0	0	0
59	0	1	0	0	0	0	1	0	1	0	0	0	0	0	0	0	0
60	0	1	0	0	0	0	1	0	1	0	0	0	0	0	0	0	0
61	0	1	1	0	0	0	0	0	1	0	0	0	0	0	1	0	0
62	0	1	1	0	0	0	0	0	1	0	0	0	0	0	0	0	0
63	0	1	0	0	0	0	1	0	1	0	0	0	0	0	0	0	0
64	0	1	1	0	0	0	0	0	1	0	0	0	0	0	1	0	0
65	0	1	1	0	0	0	0	0	1	0	0	0	0	0	1	0	0
66	0	1	1	0	0	0	0	0	1	0	0	0	0	0	0	0	0
67	0	1	1	0	0	0	0	0	1	0	0	0	0	0	0	0	0
68	0	1	0	0	0	0	1	0	1	0	0	0	0	0	0	0	0
69	0	1	0	0	0	0	1	0	0	1	0	0	0	0	0	1	0
70	0	0	1	0	0	0	1	0	0	1	0	0	0	0	0	0	1
71	0	0	1	0	0	0	1	0	1	0	0	0	0	0	0	1	0
72	0	0	0	0	0	0	1	0	0	1	1	0	0	0	0	0	0
73	0	0	1	0	0	0	0	0	0	0	0	1	0	0	1	0	0
74	0	0	0	0	0	1	0	0	1	0	0	0	0	0	0	0	1
75	0	0	1	0	0	0	0	0	1	0	0	0	0	0	0	1	0
76	0	0	1	0	0	0	0	0	0	1	0	0	0	0	0	0	0
77	0	0	1	0	1	0	0	0	0	1	0	0	0	0	1	0	0
78	0	0	1	0	0	0	0	0	0	0	0	1	0	0	0	0	1

Appendix 4.2: continuation…

	LPSU	LPOP	LSEL	LSLA	LSOL	LSOO	LSOV	LSOR	LMEN	LMDE	LMLO	LMRE	LMRV	LMBO	LBAC	LBOB	LBCO
79	0	0	1	0	0	0	0	0	1	0	0	0	0	0	0	1	0
80	0	0	0	0	1	0	1	0	1	0	0	0	0	0	0	0	1
81	0	0	0	0	1	0	0	0	1	0	0	0	0	0	0	0	0
82	0	0	0	0	1	0	0	0	1	0	0	0	0	0	0	0	1
83	0	0	0	0	0	0	0	1	0	0	1	0	0	0	0	0	0
84	0	0	1	0	0	0	0	0	1	0	0	0	0	0	0	1	0
85	0	0	1	0	1	0	0	0	1	0	0	0	0	0	0	0	1
86	0	0	0	0	1	0	0	0	1	0	0	0	0	0	0	0	0
87	0	0	1	0	0	0	0	0	1	0	0	0	0	0	0	1	0
88	0	0	1	0	0	0	0	0	1	0	0	0	0	0	0	0	1
89	0	0	1	0	0	0	0	0	1	0	0	0	0	0	0	1	0
90	0	0	1	0	0	0	0	0	0	0	0	1	0	0	0	0	1
91	0	0	1	0	0	1	0	0	0	1	0	0	0	0	0	0	1
92	0	1	0	0	0	0	1	0	1	0	0	0	0	0	0	0	0
93	0	1	1	0	0	0	1	0	1	0	0	0	0	0	1	0	0
94	0	1	1	0	0	0	0	0	1	0	0	0	0	0	0	1	0
95	1	0	1	0	0	0	0	0	1	0	0	0	0	0	1	0	0
96	0	1	0	0	0	0	1	0	1	0	0	0	0	0	0	0	0
97	0	1	0	0	0	0	1	0	1	0	0	0	0	0	0	0	0
98	0	1	0	0	0	0	1	0	1	0	0	0	0	0	0	0	0
99	0	1	0	0	1	0	0	0	1	0	0	0	0	0	0	0	0

Appendix 4.2: continuation…

	LBTR	LBRO	LAPE	LCPA	LCME	LCSU	LCCO	LLLE	LLWI	LLVI	LLVX	LPSE	LADA	LABA	LAPU	LAPA	LAPS	LATO
1	0	1	1	0	0	1	0	3,60	1,90	6	8	1	0	1	0	0	0	1
2	0	1	1	0	0	0	1	4,40	1,70	5	8	1	0	1	0	0	0	1
3	0	1	1	0	0	0	1	6,45	3,50	7	9	1	0	1	0	0	1	0
4	0	0	1	0	0	0	1	6,35	2,20	7	8	1	0	1	0	0	0	1
5	0	1	0	0	0	0	1	4,04	2,08	6	8	1	0	1	0	0	0	1
6	0	1	1	0	0	0	1	5,52	2,15	7	11	1	0	1	0	0	0	1
7	0	0	1	0	0	0	1	4,96	1,81	6	8	1	0	1	0	0	0	1
8	0	0	1	0	0	0	1	3,83	1,90	4	7	1	0	1	0	0	0	1
9	0	0	1	0	0	0	1	5,35	2,80	4	6	1	0	1	0	0	0	1
10	0	0	1	0	0	1	0	10,11	3,23	9	12	1	0	1	0	0	1	0
11	0	1	1	0	0	1	0	10,48	3,80	8	10	1	0	1	0	0	1	0
12	0	1	1	0	0	0	1	10,88	2,83	12	14	0	0	1	0	0	1	0
13	0	0	1	0	0	1	0	12,47	4,16	11	12	0	0	1	0	0	0	1
14	0	0	1	0	0	1	0	9,15	2,99	10	12	1	0	1	0	0	1	0
15	0	1	1	0	1	0	0	12,33	5,04	11	11	1	0	1	0	1	0	0
16	0	1	1	1	0	0	0	10,93	4,96	11	11	1	0	1	0	1	0	0
17	0	1	1	0	1	0	0	5,71	2,69	8	9	1	0	1	0	1	0	0
18	0	0	1	0	1	0	0	7,40	4,05	7	9	0	0	1	0	0	1	0
19	0	0	1	1	0	0	0	6,06	4,19	6	7	1	0	1	0	0	1	0
20	0	0	1	0	1	0	0	7,25	4,50	7	8	1	0	1	0	0	1	0
21	0	0	1	0	1	0	0	7,25	4,45	7	9	0	0	1	0	0	1	0
22	0	0	1	0	1	0	0	12,98	2,16	29	30	0	0	1	0	0	0	1
23	0	1	1	0	0	1	0	9,73	3,09	13	14	0	0	1	0	0	1	0
24	0	0	1	0	0	1	0	8,93	3,53	11	14	0	0	1	0	0	1	0
25	0	0	1	0	0	1	0	7,97	3,17	12	12	1	0	1	0	0	0	1
26	0	1	1	0	1	0	0	5,67	1,80	12	12	1	0	1	0	0	0	1

Appendix 4.2: continuation…

	LBTR	LBRO	LAPE	LCPA	LCME	LCSU	LCCO	LLLE	LLWI	LLVI	LLVX	LPSE	LADA	LABA	LAPU	LAPA	LAPS	LATO
27	0	1	1	0	0	1	0	9,19	3,02	12	14	0	0	1	0	0	0	1
28	0	1	1	0	1	0	0	7,93	3,01	10	12	0	0	1	0	0	1	0
29	0	1	1	0	1	0	0	9,43	3,87	9	10	0	0	1	0	0	1	0
30	0	1	1	0	0	1	0	11,19	2,64	10	11	0	0	1	0	0	0	1
31	0	0	1	0	1	0	0	10,10	2,90	11	12	0	0	1	0	0	0	1
32	0	0	1	0	0	1	0	7,25	3,70	7	9	0	0	1	0	0	1	0
33	0	1	1	0	0	1	0	5,60	2,10	8	10	0	0	1	0	0	1	0
34	0	0	1	0	0	1	0	8,56	3,20	12	14	0	0	1	0	0	1	0
35	0	1	1	0	0	1	0	6,70	2,35	9	11	0	0	1	0	0	1	0
36	0	1	1	0	0	1	0	9,15	3,00	10	12	1	0	1	0	0	1	0
37	0	0	1	1	0	0	0	11,50	4,50	13	15	0	0	1	0	0	1	0
38	0	1	1	0	0	1	0	5,50	2,70	8	9	0	0	1	0	0	1	0
39	0	1	1	1	0	0	0	7,20	5,00	10	11	0	1	1	0	0	1	0
40	0	1	1	1	0	0	0	6,85	2,55	11	11	0	0	1	0	0	1	0
41	0	1	1	0	0	1	0	7,15	3,00	10	12	0	0	1	0	0	1	0
42	0	1	1	0	0	1	0	9,25	3,65	11	11	1	0	1	0	0	1	0
43	1	0	1	0	0	1	0	8,75	3,60	8	9	1	0	1	0	0	0	1
44	1	0	1	0	0	1	0	10,25	4,70	12	13	0	0	1	0	0	1	0
45	0	1	1	0	1	0	0	12,41	5,26	11	12	0	0	1	0	0	0	1
46	0	1	1	0	0	1	0	8,30	2,80	11	13	0	0	1	0	0	1	0
47	1	0	1	1	0	0	0	4,25	2,10	8	9	0	1	1	0	0	0	1
48	0	0	1	0	0	1	0	6,10	2,12	10	11	0	0	1	0	0	1	0
49	0	0	1	0	0	1	0	4,34	2,24	5	5	0	0	1	0	0	0	1
50	0	0	1	0	0	1	0	2,65	1,51	5	5	0	0	1	0	0	0	1
51	0	0	1	0	0	0	1	2,62	1,48	6	6	0	0	1	0	0	0	1
52	0	1	1	0	0	0	1	8,23	3,49	11	11	1	0	1	0	0	0	1

Appendix 4.2: continuation…

	LBTR	LBRO	LAPE	LCPA	LCME	LCSU	LCCO	LLLE	LLWI	LLVI	LLVX	LPSE	LADA	LABA	LAPU	LAPA	LAPS	LATO
53	1	0	1	0	0	0	1	11,54	4,76	15	15	0	0	1	0	0	0	1
54	0	0	1	0	0	1	0	16,74	4,99	12	15	0	0	1	0	0	0	1
55	1	0	1	0	0	1	0	4,53	2,25	8	9	0	0	1	0	0	1	0
56	1	0	1	1	0	0	0	8,25	4,65	9	10	0	0	1	0	0	1	0
57	0	1	1	0	0	1	0	4,55	1,90	9	11	1	0	1	0	0	0	1
58	0	1	1	0	0	1	0	6,27	2,30	12	12	0	0	0	0	0	0	0
59	0	1	1	0	1	0	0	6,66	2,74	11	12	0	0	0	0	0	0	0
60	0	1	1	0	1	0	0	8,44	4,11	12	12	0	0	0	0	0	0	0
61	0	0	1	0	0	1	0	8,06	3,33	12	13	0	0	0	0	0	0	0
62	0	1	1	0	0	1	0	6,23	3,15	10	12	0	0	0	0	0	0	0
63	0	1	1	0	1	0	0	7,83	3,56	12	14	0	0	0	0	0	0	0
64	0	0	1	0	1	0	0	6,87	2,10	8	11	0	0	0	0	0	0	0
65	0	0	1	1	0	0	0	7,05	2,45	9	9	0	1	0	0	0	0	1
66	0	1	1	0	1	0	0	8,21	3,07	9	12	0	0	0	0	0	0	0
67	0	1	1	0	1	0	0	4,26	1,55	10	10	0	0	0	0	0	0	0
68	0	1	1	0	1	0	0	11,11	3,84	11	12	0	0	0	0	0	0	0
69	0	0	1	1	0	0	0	14,10	7,21	11	11	0	0	1	0	0	1	0
70	0	0	1	1	0	0	0	19,43	9,44	10	12	0	0	1	0	1	0	0
71	0	0	1	1	0	0	0	13,46	7,65	10	11	0	0	1	0	0	1	0
72	0	1	1	1	0	0	0	16,93	8,55	10	12	0	0	1	0	0	1	0
73	0	0	1	0	0	1	0	6,67	3,30	11	11	1	0	1	0	0	1	0
74	0	0	1	0	0	1	0	16,33	4,95	12	13	0	0	1	0	1	0	0
75	0	0	1	0	1	0	0	14,90	5,20	13	14	0	0	1	1	0	0	0
76	0	1	1	0	0	1	0	16,00	7,50	12	14	0	0	1	1	0	0	0
77	0	0	1	0	1	0	0	9,73	6,77	13	15	1	0	1	1	0	0	0
78	0	0	1	0	0	1	0	14,18	5,10	15	16	1	0	1	0	0	1	0

Appendix 4.2: continuation…

	LBTR	LBRO	LAPE	LCPA	LCME	LCSU	LCCO	LLLE	LLWI	LLVI	LLVX	LPSE	LADA	LABA	LAPU	LAPA	LAPS	LATO
79	0	0	1	0	1	0	0	14,73	5,06	13	14	1	0	1	1	0	0	0
80	0	0	1	0	0	1	0	12,50	4,85	10	12	0	0	1	0	0	1	0
81	0	1	1	0	0	1	0	10,80	4,50	8	11	0	0	1	0	0	1	0
82	0	0	1	0	0	1	0	12,27	5,17	10	11	0	0	1	0	0	1	0
83	0	1	1	1	0	0	0	10,91	5,70	10	11	0	0	1	0	0	1	0
84	0	0	1	1	0	0	0	16,63	8,63	13	16	0	0	1	0	0	1	0
85	0	0	1	0	0	1	0	14,05	4,50	12	13	0	0	1	0	1	0	0
86	0	1	0	0	0	0	1	6,73	2,20	10	11	0	0	1	0	0	1	0
87	0	0	1	1	0	0	0	14,94	6,31	15	16	0	0	1	0	0	1	0
88	0	0	1	0	0	0	1	6,84	2,26	7	9	1	0	1	0	0	1	0
89	0	0	1	1	0	0	0	12,77	5,74	9	11	1	0	1	0	0	1	0
90	0	0	1	1	0	0	0	11,85	5,63	10	11	0	0	1	0	0	1	0
91	0	0	1	0	1	0	0	13,03	4,77	12	14	0	0	1	0	0	1	0
92	0	1	1	0	0	1	0	7,30	2,80	9	11	0	1	1	0	0	1	0
93	0	0	1	0	0	1	0	8,25	3,85	9	10	0	1	1	0	0	1	0
94	0	0	1	1	0	0	0	7,50	2,90	9	10	0	0	1	0	0	1	0
95	0	0	1	0	0	1	0	6,96	2,11	9	11	0	0	1	0	0	0	1
96	0	1	1	0	0	1	0	4,60	2,00	7	9	0	0	1	0	0	1	0
97	0	1	1	0	0	1	0	7,55	3,75	9	11	0	0	1	0	1	0	0
98	0	1	1	0	0	1	0	6,25	2,95	8	9	0	0	1	0	0	1	0
99	0	1	1	0	0	1	0	11,57	3,20	13	15	1	0	1	0	0	0	1

Appendix 4.2: continuation…

	LTSU	LTSM	LTAS	LTAL	LTAT	LTAB	PELE	PEWI	PPNO
1	1	0	1	0	0	0	0,85	0,2	0
2	1	0	1	0	0	0	0,90	0,1	0
3	1	0	1	0	0	0	1,27	0,16	0
4	1	0	1	0	0	0	1,30	0,2	0
5	1	0	1	0	0	0	0,89	0,16	0
6	1	0	1	0	0	0	1,43	0,1	0
7	1	0	1	0	0	0	1,21	0,17	0
8	1	0	1	0	0	0	1,15	0,1	0
9	1	0	1	0	0	0	1,20	0,2	0
10	0	1	0	1	0	0	1,30	0,23	0
11	0	1	0	1	0	0	2,40	0,2	0
12	0	1	0	1	0	0	1,70	0,18	0
13	0	1	0	1	0	0	3,00	0,25	0
14	0	1	0	1	0	0	1,74	0,22	0
15	1	0	1	0	0	0	4,06	0,22	0
16	1	0	1	0	0	0	3,18	0,15	0
17	1	0	1	0	0	0	1,75	0,11	0
18	0	1	0	1	0	0	2,00	0,18	0
19	0	1	0	1	0	0	2,46	0,15	0
20	0	1	0	1	0	0	2,80	0,18	0
21	0	1	0	1	0	0	2,45	0,2	0
22	1	0	1	0	0	0	1,25	0,18	0
23	1	0	1	0	0	0	1,80	0,23	0
24	1	0	1	0	0	0	1,77	0,1	0
25	1	0	1	0	0	0	1,85	0,1	0
26	1	0	1	0	0	0	1,30	0,1	0

Appendix 4.2: continuation…

	LTSU	LTSM	LTAS	LTAL	LTAT	LTAB	PELE	PEWI	PPNO
27	1	0	1	0	0	0	2,06	0,19	0
28	1	0	1	0	0	0	2,10	0,12	0
29	1	0	1	0	0	0	2,47	0,2	0
30	1	0	1	0	0	0	1,69	0,15	0
31	1	0	1	0	0	0	1,83	0,2	0
32	1	0	1	0	0	0	2,70	0,14	0
33	1	0	1	0	0	0	2,30	0,1	0
34	1	0	1	0	0	0	1,54	0,14	0
35	1	0	1	0	0	0	1,8	0,08	0
36	1	0	1	0	0	0	1,50	0,1	0
37	0	1	0	0	1	0	3,50	0,2	0
38	1	0	1	0	0	0	1,75	0,12	0
39	1	0	1	0	0	0	2,75	0,1	0
40	1	0	1	0	0	0	1,23	0,16	0
41	1	0	1	0	0	0	2,80	0,15	0
42	1	0	1	0	0	0	2,50	0,2	0
43	1	0	1	0	0	0	1,90	0,2	0
44	1	0	1	0	0	0	2,65	0,18	0
45	1	0	1	0	0	0	2,78	0,2	0
46	1	0	1	0	0	0	2,15	0,13	0
47	1	0	1	0	0	0	1,25	0,2	0
48	1	0	1	0	0	0	1,81	0,15	0
49	1	1	1	1	0	0	0,44	0,2	0
50	0	1	0	0	0	1	0,48	0,14	0
51	0	1	0	0	0	1	0,40	0,14	0
52	1	0	1	0	0	0	1,78	0,21	1

Appendix 4.2: continuation…

	LTSU	LTSM	LTAS	LTAL	LTAT	LTAB	PELE	PEWI	PPNO
53	1	0	1	0	0	0	3,25	0,3	1
54	1	0	1	0	0	0	3,70	0,34	1
55	0	1	0	0	1	0	1,25	0,2	0
56	0	1	0	0	1	0	2,55	0,3	0
57	0	1	1	0	0	0	0,75	0,2	0
58	0	0	0	0	0	0	2,37	0,12	0
59	0	0	0	0	0	0	2,16	0,15	0
60	0	0	0	0	0	0	1,56	0,17	0
61	0	0	0	0	0	0	2,11	0,12	0
62	0	0	0	0	0	0	2,66	0,13	0
63	0	0	0	0	0	0	2,24	0,14	0
64	0	0	0	0	0	0	1,65	0,1	0
65	1	0	1	0	0	0	1,70	0,14	0
66	0	0	0	0	0	0	1,99	0,14	0
67	0	0	0	0	0	0	1,34	0,09	0
68	0	0	0	0	0	0	3,45	0,16	0
69	0	1	0	1	0	0	5,03	0,18	0
70	0	1	0	1	0	0	6,16	0,33	0
71	0	1	0	1	0	0	5,89	0,4	0
72	0	1	0	1	0	0	4,70	0,18	0
73	0	1	0	1	0	0	2,07	0,1	0
74	0	1	0	1	0	0	3,01	0,2	0
75	0	1	0	1	0	0	4,37	0,2	0
76	0	1	0	1	0	0	2,60	0,25	0
77	0	1	0	1	0	0	3,07	0,24	0
78	0	1	0	1	0	0	3,42	0,2	0

Appendix 4.2: continuation…

	LTSU	LTSM	LTAS	LTAL	LTAT	LTAB	PELE	PEWI	PPNO
79	0	1	0	1	0	0	4,62	0,24	0
80	0	1	0	1	0	0	2,80	0,2	0
81	0	1	0	1	0	0	2,65	0,2	0
82	0	1	0	1	0	0	2,63	0,15	0
83	0	1	0	1	0	0	4,43	0,2	0
84	0	1	0	1	0	0	5,90	0,27	0
85	0	1	0	1	0	0	1,15	0,1	0
86	0	1	0	1	0	0	1,30	0,13	0
87	0	1	0	1	0	0	4,71	0,18	0
88	0	1	0	1	0	0	0,93	0,13	0
89	0	1	0	1	0	0	4,52	0,22	0
90	0	1	0	1	0	0	4,34	0,14	0
91	0	1	0	1	0	0	2,5	0,2	0
92	1	0	1	0	0	0	3,03	0,08	0
93	1	0	1	0	0	0	2,30	0,1	0
94	1	0	1	0	0	0	2,60	0,1	0
95	0	1	0	1	0	0	2,37	0,1	0
96	1	0	1	0	0	0	1,00	0,14	0
97	1	0	1	0	0	0	2,95	0,09	0
98	1	0	1	0	0	0	1,50	0,13	0
99	1	0	1	0	0	0	1,70	0,26	0

Appendix 4.3: Character states evaluation of reproductive characters on 62 specimens. Characters abbreviations and states coding according Appendix 4.4. SEN number correspond to identifiers in the phylogenetic inference (Figure 4.1)

	Clade	Tree ID	Collector	Coll num	PCA ID	STCY	STCO	STPA	RESH	INLE	INWI	OPNU	OPLE
1			Wood, J.R.I.	8047	ast_10	0	1	0	1	0,80	1,25	2	0,70
2			Feuerer, T.	11398	ast_12	0	0	1	1	0,65	0,94	2	0,34
3	ast-rus-psi	SEN11	Escobari, B., Beck, S. & Beck, C.	36	ast_6	0	1	0	1	0,80	0,80	4	0,35
4			Cayola, L.	3880	ast_7	0	0	1	1	0,65	0,94	2	0,29
5	man 2	SEN50	Escobari, B., Beck, S. & Beck, C.	79	ast_9	0	1	0	1	0,80	0,90	2	0,40
6			Loza, I.	754	com_1	0	1	0	0	0,83	0,72	3	0,61
7			Paco, P.	78	com_2	0	1	0	0	0,92	0,56	2	0,71
8			Rico, L., Windsor-Shaw, T., McRobb & Alvarez, L	1303	kin_1	1	0	0	1	0,72	0,67	3	0,39
9	kin	SEN321	Solomon, J.	18067	kin_2	1	0	0	1	0,87	0,77	2	0,60
10			Wood, J.R.I.	22990	kin_3	1	0	0	1	0,65	0,68	3	0,40
11			Wood, J.R.I.	9342	kin_4	1	0	0	1	0,85	0,74	4	0,84
12	man 1	SEN91	Escobari, B., Kilian, N., Villca, H. & Nieto, B.	273	man_10	0	1	0	1	0,54	0,60	3	0,27
13	man 1	SEN90	Escobari, B., Kilian, N., Villca, H. & Nieto, B.	272	man_11	0	1	0	1	0,60	0,75	2	0,40
14			Cayola, L.	3528	man_14	0	1	0	1	0,68	0,62	3	0,30
15			Samo, L.	41	man_15	0	0	1	1	0,63	0,79	3	0,22
16			Escobari, B., Beck, S. & Beck, C.	58	man_17	1	0	0	1	0,70	0,70	4	0,35
17			Escobari, B., Beck, S. & Beck, C.	68	man_20	0	0	1	1	0,58	0,86	4	0,42
18	man 1	SEN125	Fuentes, A.	11933	man_7	0	1	0	1	0,60	0,60	4	0,49
19			Fuentes, A.	15094	mas_13	0	0	1	1	0,60	0,80	2	0,30
20			Palabral, A.	285	mas_14	0	0	1	1	0,77	1,04	3	0,40
21			Fuentes, A.	8392	mas_16	0	1	0	1	0,58	0,63	2	0,30
22			Quisbert, J.	843	mas_17	0	0	1	0	0,90	0,80	6	0,60
23			Solomon, J.	16497	mas_2	0	1	0	0	0,70	0,60	3	0,50
24			Paco, P.	19	mas_3	0	1	0	0	0,90	0,60	2	0,60
25			Fuentes, A.	16781	mas_4	0	0	1	1	0,70	1	5	0,45

Appendix 4.3: continuation…

	Clade	Tree ID	Collector	Coll num	PCA ID	STCY	STCO	STPA	RESH	INLE	INWI	OPNU	OPLE
26			Quisbert, J.	822	mas_5	0	1	0	0	0,70	0,50	4	0,70
27	man 1	SEN34	Escobari, B., Beck, S. & Beck, C.	59	mas_8	0	0	1	1	0,65	0,80	3	0,40
28			Zarate, M.	621	mas_9	0	0	1	1	0,61	0,65	5	0,28
29			Fuentes, A.	15602	meg_1	0	0	1	0	0,80	0,67	1	0,59
30			Beck, S.	32686	meg_2	1	0	0	0	0,87	0,67	4	0,60
31	neo	SEN60	Escobari, B., Kilian, N. & Villca, H.	133	neo_1	0	0	1	1	0,8	1,02	7	0,46
32			Wood, J.R.I.	23092	neo_2	0	0	1	1	0,73	0,72	7	0,43
33	neo	SEN131	Kessler, M.	2905	neo_3	0	0	1	1	0,88	0,92	7	0,43
34			Beck, S.	28794	new_B_11	1	0	0	0	0,57	0,41	3	0,28
35			Beck, S.	28794A	new_B_12	1	0	0	0	0,83	0,48	2	0,18
36			Müller, J.	7464	new_B_22	0	1	0	0	0,71	0,50	3	0,43
37			Beck, S.	21376	new_B_8	1	0	0	0	0,70	0,47	1	0,30
38			Cayola, L.	3873	new_C	0	1	0	1	0,65	0,60	3	0,50
39			Aedo, C.	14429	psi_1	0	0	1	1	0,82	0,98	2	0,75
40			Escobari, B., Kilian, N., Villca, H. & Nieto, B.	299	psi_10	1	0	0	1	0,73	1,05	2	0,55
41			Escobari, B., Kilian, N. & Villca, H.	176	psi_2	0	1	0	1	0,70	0,98	4	0,48
42			Escobari, B., Kilian, N. & Villca, H.	208	psi_3	0	1	0	1	0,74	1,06	2	0,67
43			Wood, J.R.I.	23288	psi_4	0	0	1	1	0,73	0,98	2	0,60
44			Escobari, B., Kilian, N., Villca, H. & Nieto, B.	247	psi_5	1	0	0	1	0,62	0,91	3	0,47
45			Escobari, B., Kilian, N., Villca, H. & Nieto, B.	277	psi_6	0	1	0	1	0,65	0,81	3	0,44
46			Escobari, B., Kilian, N., Villca, H. & Nieto, B.	289	psi_8	1	0	0	1	0,84	0,91	4	0,65
47	ast-rus-psi	SEN105	Escobari, B., Kilian, N., Villca, H. & Nieto, B.	292	psi_9	0	1	0	1	0,62	0,79	3	0,70
48	rep 1	SEN144	Wood, J.R.I.	10093	rep_1	0	1	0	0	0,70	0,45	2	0,31
49			Cabrera, A.	33718	rep_15	1	0	0	1	0,60	0,60	2	0,25
50			Lewis, M.	39262	rep_16	1	0	0	0	0,60	0,30	4	0,41
51	rep 2	SEN16	Escobari, B., Beck, S. & Beck, C.	41	rep_17	1	0	0	0	0,60	0,40	3	0,30

Appendix 4.3: continuation…

	Clade	Tree ID	Collector	Coll num	PCA ID	STCY	STCO	STPA	RESH	INLE	INWI	OPNU	OPLE
52			Solomon, J.	6024	rep_19	0	1	0	1	0,60	0,42	4	0,32
53			Solomon, J.	12372	rep_2	0	1	0	0	0,65	0,36	1	0,20
54			Escobari, B., Beck, S. & Beck, C.	86	rep_25	0	1	0	0	0,71	0,43	2	0,24
55			Escobari, B., Beck, S. & Beck, C.	87	rep_26	0	1	0	0	0,78	0,51	2	0,24
56			Cornejo M.	931	rep_28	0	1	0	0	0,60	0,37	3	0,27
57			Smith, D.	13051	rep_4	1	0	0	0	0,76	0,41	4	0,22
58	rep 1	SEN180	Beck, S.	24375	rep_9	0	1	0	0	0,87	0,59	3	0,58
59			Escobari, B., Kilian, N. & Villca, H.	178	rus_7	1	0	0	1	0,80	0,80	2	0,50
60			Lewis, M.	35153	rus_cf_1	0	1	0	1	0,56	0,60	3	0,60
61			Lewis, M.	39352	rus_cf_2	0	1	0	1	0,80	1	3	0,70
62			Lewis, M.	881017	rus_cf_3	0	0	1	1	0,80	0,90	2	0,40

Appendix 4.3: continuation

	OPWI	OSFI	OSOL	OSEL	OSOV	OSTR	OPAP	IPNI	IPLE	IPWO	IPWI	IPSC	IPAP	IPCM	IPCS	IPCC	CARA	FLNU	RFLE	RFTL	RFLW	RFVE
1	0,8	0	1	0	0	0	1	8	0,9	0,2	0,4	1	1	0	0	1	1	32	13,70	4,97	1,80	4,00
2	0,6	0	0	1	0	0	1	8	0,58	0,2	0,25	1	0	0	1	0	1	21	10,87	3,87	1,72	4,00
3	0,08	0	0	0	1	0	1	7	0,8	0,1	0,2	1	0	0	0	1	1	18	9,27	3,61	1,57	4,00
4	0,08	0	1	0	0	0	1	8	0,57	0,14	0,18	1	1	0	1	0	1	25	12,42	4,51	1,52	3,00
5	0,11	0	1	0	0	0	0	7	0,6	0,1	0,2	1	0	0	0	1	1	15	11,85	3,13	2,08	3,00
6	0,1	0	0	0	1	0	0	8	0,78	0,2	0,23	1	0	1	0	0	1	14	12,21	5,44	1,60	4,00
7	0,11	0	0	0	1	0	0	6	0,93	0,16	0,23	0	0	1	0	0	1	9	11,27	5,28	1,52	3,00
8	0,4	0	1	0	0	0	0	8	0,68	0,1	0,24	0	0	0	0	1	1	18	13,12	4,79	1,94	4,00
9	0,2	0	1	0	0	0	0	8	0,88	0,11	0,18	1	1	0	0	1	1	15	12,88	4,75	2,46	4,00
10	0,9	0	1	0	0	0	1	8	0,7	0,15	0,29	1	0	0	1	0	1	16	12,93	4,74	2,85	4,00
11	0,7	0	1	0	0	0	1	10	0,76	0,1	0,2	0	1	0	1	0	1	22	12,04	4,33	7,07	4,00
12	0,2	1	0	0	0	0	1	8	0,48	0,12	0,19	1	0	0	1	0	1	19	10,07	2,27	1,57	4,00
13	0,05	1	0	0	0	0	1	8	0,6	0,2	0,2	1	0	0	0	1	1	26	10,15	2,30	1,50	4,00
14	0,1	1	0	0	0	0	1	8	0,67	0,13	0,2	1	0	0	0	1	1	18	10,04	5,38	1,95	4,00
15	0,2	1	0	0	0	0	1	8	0,57	0,11	0,19	1	0	0	0	1	1	20	10,90	4,07	1,43	4,00
16	0,03	1	0	0	0	0	1	8	0,5	0,1	0,2	1	0	0	1	0	1	20	9,65	4,18	1,29	4,00
17	0,2	1	0	0	0	0	1	8	0,56	0,12	0,21	1	0	0	1	0	1	24	10,09	3,84	1,96	4,00
18	0,09	1	0	0	0	0	1	8	0,5	0,2	0,2	1	0	0	1	0	1	20	9,57	3,93	1,30	4,00
19	0,23	1	0	0	0	0	1	8	0,5	0,16	0,21	1	1	0	1	0	1	23	11,35	4,32	1,70	4,00
20	0,5	1	0	0	0	0	1	8	0,54	0,24	0,24	1	0	0	0	1	1	11	12,19	3,98	1,87	4,00
21	0,7	1	0	0	0	0	1	8	0,5	0,14	0,14	1	0	0	0	1	1	17	8,98	3,68	1,91	4,00
22	0,09	0	0	0	1	0	1	6	0,85	0,17	0,21	1	0	0	1	0	1	15	11,94	5,26	1,40	4,00
23	0,05	0	1	0	0	0	0	9	0,6	0,13	0,18	1	0	0	1	0	1	16	10,56	4,34	1,32	4,00
24	0,07	0	1	0	0	0	0	7	0,8	0,2	0,2	1	0	0	0	1	1	15	10,02	4,15	1,22	4,00
25	0,7	1	0	0	0	0	1	8	0,7	0,18	0,35	1	0	0	0	1	1	28	13,06	5,21	1,82	4,00
26	0,09	0	0	0	1	0	1	8	0,74	0,17	0,27	1	0	0	0	1	1	17	12,04	5,02	1,69	4,00

Appendix 4.3: continuation:

	OPWI	OSFI	OSOL	OSEL	OSOV	OSTR	OPAP	IPNI	IPLE	IPWO	IPWI	IPSC	IPAP	IPCM	IPCS	IPCC	CARA	FLNU	RFLE	RFTL	RFLW	RFVE
27	0,5	0	0	0	1	0	1	8	0,6	0,16	0,26	1	1	0	1	0	1	22	12,07	5,18	2,76	4,00
28	0,2	0	0	0	0	1	1	8	0,6	0,13	0,25	1	0	0	0	1	1	20	9,32	4,19	1,07	4,00
29	0,5	1	0	0	0	0	1	8	0,77	0,13	0,13	0	1	0	0	1	0	12	0,00	0,00	0,00	0,00
30	0,07	0	0	0	1	0	0	8	0,83	0,18	0,18	1	1	0	0	1	0	12	0,00	0,00	0,00	0,00
31	0,04	0	1	0	0	0	1	8	0,71	0,19	0,19	1	0	0	0	1	1	28	11,17	4,31	1,69	4,00
32	0,06	1	0	0	0	0	1	8	0,67	0,18	0,25	1	0	0	0	1	1	28	13,53	5,37	1,62	4,00
33	0,06	0	0	0	0	1	1	8	0,82	0,21	0,23	1	0	0	0	1	1	27	14,44	2,99	1,74	3,00
34	0,1	1	0	0	0	0	1	8	0,57	0,1	0,1	1	0	0	0	1	1	11	11,70	5,10	2,16	4,00
35	0,1	1	0	0	0	0	1	8	0,79	0,13	0,18	1	0	0	1	0	1	10	11,95	5,06	2,19	4,00
36	0,05	0	1	0	0	0	0	8	0,78	0,12	0,19	1	0	0	1	0	1	10	12,59	5,48	1,75	3,00
37	0,04	1	0	0	0	0	0	8	0,74	0,09	0,19	1	1	0	1	0	1	14	11,61	5,37	1,76	4,00
38	0,4	1	0	0	0	0	1	8	0,55	0,1	0,16	1	1	0	1	0	1	18	10,62	3,84	2,37	5,00
39	0,23	0	0	0	1	0	1	8	0,8	0,37	0,37	1	1	0	0	1	1	34	15,99	5,89	3,71	5,00
40	0,06	0	0	0	1	0	0	8	0,63	0,3	0,44	1	0	0	1	0	1	20	12,86	5,10	3,46	4,00
41	0,08	0	0	0	1	0	0	10	0,67	0,19	0,22	1	0	0	0	1	1	29	14,09	5,44	2,30	4,00
42	0,18	0	0	0	1	0	0	9	0,7	0,28	0,38	1	0	0	0	1	1	29	11,35	4,14	2,72	5,00
43	0,12	0	0	0	1	0	1	9	0,68	0,31	0,31	1	0	0	0	1	1	22	15,11	5,23	2,31	4,00
44	0,15	0	0	0	1	0	0	8	0,54	0,22	0,25	1	1	0	1	0	1	28	16,64	6,10	2,38	4,00
45	0,13	0	0	0	1	0	1	8	0,76	0,28	0,28	1	0	0	1	0	1	29	10,22	4,18	2,55	4,00
46	0,12	0	0	0	1	0	1	7	0,8	0,23	0,3	1	0	0	1	0	1	26	12,85	5,49	4,00	4,00
47	0,24	0	0	0	1	0	1	9	0,55	0,25	0,25	1	0	0	1	0	1	23	11,98	4,67	3,14	4,00
48	0,03	0	1	0	0	0	0	8	0,69	0,09	0,14	1	1	0	0	1	1	13	7,55	3,27	1,56	4,00
49	0,02	1	0	0	0	0	1	8	0,57	0,08	0,15	1	1	0	0	1	1	9	10,00	4,60	1,70	4,00
50	0,1	1	0	0	0	0	0	8	0,59	0,1	0,2	1	1	0	1	0	1	10	7,58	2,93	1,14	3,00
51	0,04	0	0	0	0	1	1	6	0,6	0,1	0,2	1	1	0	1	0	1	9	10,25	3,77	1,50	4,00
52	0,1	1	0	0	0	0	1	5	0,66	0,1	0,2	1	0	0	0	1	1	9	9,37	3,78	1,45	4,00

Appendix 4.3: continuation:

	OPWI	OSFI	OSOL	OSEL	OSOV	OSTR	OPAP	IPNI	IPLE	IPWO	IPWI	IPSC	IPAP	IPCM	IPCS	IPCC	CARA	FLNU	RFLE	RFTL	RFLW	RFVE
53	0,1	1	0	0	0	0	1	6	0,56	0,17	0,7	1	1	0	0	1	1	9	8,08	1,55	1,45	4,00
54	0,04	0	1	0	0	0	1	8	0,48	0,12	0,19	1	0	0	1	0	1	9	8,35	3,41	1,64	4,00
55	0,05	0	0	0	0	1	1	8	0,79	0,15	0,2	1	1	0	1	0	1	15	10,93	4,93	2,16	4,00
56	0,7	0	0	0	0	1	1	8	0,68	0,16	0,19	1	0	0	1	0	1	10	10,32	4,45	1,35	4,00
57	0,1	1	0	0	0	0	1	8	0,7	0,1	0,2	1	1	0	1	0	1	16	9,96	4,08	1,54	4,00
58	0,08	0	0	0	1	0	1	9	0,76	0,13	0,3	1	1	0	1	0	1	13	9,31	3,77	1,48	5,00
59	0,7	1	0	0	0	0	0	8	0,8	0,1	0,2	1	1	1	0	0	1	16	11,89	4,83	1,91	4,00
60	0,6	0	1	0	0	0	1	8	0,64	0,1	0,18	1	1	1	0	0	1	22	17,62	6,20	1,72	4,00
61	0,14	0	0	1	0	0	0	8	0,8	0,4	0,4	1	0	1	0	0	1	31	15,07	5,83	3,00	4,00
62	0,4	1	0	0	0	0	1	8	0,7	0,23	0,23	1	1	1	0	0	1	25	12,85	5,49	2,77	4,00

Appendix 4.3: continuation…

	RFTE	RFSL	RFIT	DFSH	DFNL	DFLC	DFLT	DFWT	DFWB	DFTB	DFLL	DFLO	DFSL	FILE	ANCO	ASSA	ASAU	ASRO	ANAP	ANLE	ANWI	STLE
1	3,00	0,00	0,00	1,00	5,00	10,07	3,97	0,33	0,89	0,00	4,80	1,29	0,00	3,50	0,68	1	0	0	0,00	3,35	0,43	10,75
2	3,00	1,00	1,00	1,00	5,00	7,68	3,11	0,50	0,73	1,00	2,40	2,57	1,00	2,61	0,38	0	0	1	0,00	2,06	0,39	6,45
3	3,00	1,00	0,00	1,00	5,00	5,16	1,95	0,27	0,54	0,00	2,47	1,48	0,00	2,42	0,31	1	0	0	0,00	1,70	0,22	5,60
4	2,00	1,00	1,00	1,00	5,00	7,39	2,46	0,36	0,65	1,00	3,08	2,09	0,00	2,59	0,61	1	0	0	1,00	2,43	0,36	7,83
5	2,00	0,00	1,00	1,00	4,00	10,50	4,00	0,50	0,50	1,00	5,20	2,27	0,00	3,00	0,00	1	0	0	1,00	3,10	0,40	6,45
6	3,00	0,00	0,00	1,00	5,00	10,03	5,01	0,61	1,90	1,00	4,32	1,81	0,00	3,23	0,50	0	1	0	0,00	3,19	0,43	12,50
7	3,00	1,00	0,00	1,00	5,00	8,58	4,40	0,36	0,75	1,00	2,79	2,59	1,00	2,96	0,45	0	0	1	1,00	2,61	0,43	9,47
8	3,00	1,00	0,00	1,00	5,00	7,44	3,22	0,36	0,91	0,00	3,83	0,92	0,00	2,49	0,48	1	0	0	0,00	2,29	0,24	8,47
9	3,00	0,00	0,00	1,00	5,00	7,21	2,83	0,35	1,04	0,00	3,98	1,43	0,00	3,50	0,54	1	0	0	0,00	2,30	0,31	7,46
10	3,00	1,00	0,00	1,00	5,00	6,45	2,50	0,47	0,87	1,00	3,38	1,81	1,00	1,96	0,50	0	1	0	0,00	2,46	0,28	8,45
11	3,00	0,00	0,00	1,00	5,00	7,15	1,98	0,34	0,61	1,00	4,30	1,51	0,00	3,09	0,57	0	1	0	1,00	2,10	0,31	7,57
12	3,00	1,00	0,00	1,00	5,00	7,08	2,85	0,39	0,78	1,00	3,09	1,45	0,00	2,47	0,51	1	0	0	0,00	1,97	0,37	7,31
13	3,00	1,00	0,00	1,00	5,00	7,00	2,90	0,40	0,90	1,00	3,20	1,70	0,00	2,90	0,50	1	0	0	1,00	2,35	0,30	8,60
14	3,00	0,00	0,00	1,00	5,00	7,75	3,39	0,36	0,72	1,00	3,58	1,23	0,00	4,10	0,54	1	0	0	0,00	2,38	0,34	9,08
15	3,00	0,00	1,00	1,00	5,00	5,94	2,47	0,28	0,58	1,00	2,78	1,72	0,00	2,17	0,56	1	0	0	0,00	2,02	0,35	8,20
16	2,00	0,00	0,00	1,00	5,00	6,24	2,38	0,42	0,73	1,00	3,04	1,38	0,00	2,22	0,53	0	1	0	1,00	2,18	0,37	7,37
17	3,00	1,00	0,00	1,00	5,00	6,34	2,61	0,56	0,88	1,00	3,30	1,47	0,00	2,83	0,41	1	0	0	0,00	2,36	0,32	7,28
18	3,00	0,00	0,00	1,00	5,00	6,20	2,40	0,50	0,50	1,00	3,35	1,30	0,00	2,95	0,40	0	1	0	1,00	2,30	0,30	8,45
19	3,00	1,00	0,00	1,00	5,00	6,75	2,94	0,36	0,75	1,00	3,20	1,87	0,00	3,42	0,44	0	1	0	0,00	2,02	0,28	8,63
20	3,00	1,00	0,00	1,00	5,00	10,65	3,70	0,52	0,84	1,00	4,47	2,76	0,00	3,51	0,90	0	1	0	0,00	2,88	0,36	9,44
21	3,00	1,00	1,00	1,00	5,00	4,71	2,15	0,43	0,52	1,00	2,20	1,65	0,00	2,27	0,40	0	1	0	1,00	2,15	0,28	6,76
22	3,00	0,00	0,00	1,00	5,00	10,07	4,24	0,41	0,56	1,00	3,86	2,23	0,00	2,87	0,55	0	0	1	0,00	3,21	0,36	9,06
23	3,00	1,00	1,00	0,00	5,00	9,30	4,04	0,32	0,56	1,00	4,01	1,68	0,00	3,00	0,44	0	1	0	0,00	2,99	0,40	11,21
24	3,00	0,00	0,00	1,00	5,00	8,26	4,41	0,59	0,72	1,00	2,90	1,60	0,00	1,54	0,56	1	0	0	0,00	2,66	0,44	9,85
25	3,00	1,00	1,00	0,00	5,00	7,92	3,17	0,42	0,67	1,00	4,18	1,57	0,00	3,22	0,45	0	1	0	0,00	2,75	0,29	9,81
26	3,00	1,00	1,00	0,00	5,00	8,47	3,47	0,43	0,64	1,00	3,79	2,18	1,00	2,69	0,49	1	0	0	1,00	3,24	0,37	8,71

Appendix 4.3: continuation…

	RFTE	RFSL	RFIT	DFSH	DFNL	DFLC	DFLT	DFWT	DFWB	DFTB	DFLL	DFLO	DFSL	FILE	ANCO	ASSA	ASAU	ASRO	ANAP	ANLE	ANWI	STLE
27	3,00	0,00	0,00	1,00	5,00	7,93	3,15	0,39	0,74	1,00	3,35	1,53	0,00	3,06	0,68	0	1	0	1,00	2,26	0,37	8,77
28	3,00	0,00	0,00	1,00	5,00	7,20	3,50	0,47	0,77	1,00	3,00	1,76	0,00	2,60	0,44	1	0	0	0,00	2,30	0,34	9,31
29	0,00	0,00	0,00	1,00	6,00	8,65	4,73	0,49	0,88	1,00	2,68	1,79	1,00	1,48	0,45	0	1	0	1,00	2,13	0,32	8,42
30	0,00	0,00	0,00	1,00	5,00	10,96	5,67	0,56	1,04	1,00	4,17	2,07	0,00	3,08	0,57	1	0	0	1,00	3,26	0,45	13,02
31	3,00	1,00	0,00	1,00	5,00	7,73	2,65	0,31	0,70	1,00	4,20	1,33	1,00	3,39	0,54	0	1	0	1,00	2,47	0,34	9,87
32	3,00	1,00	0,00	1,00	6,00	8,50	3,50	0,32	0,73	1,00	3,97	1,54	0,00	3,47	0,46	0	1	0	0,00	2,54	0,36	10,46
33	2,00	1,00	0,00	1,00	5,00	8,62	3,46	0,52	0,90	1,00	5,44	1,64	0,00	4,84	0,60	0	1	0	0,00	2,74	0,35	12,44
34	3,00	0,00	0,00	1,00	5,00	7,71	3,80	0,44	0,77	1,00	3,04	1,61	1,00	2,29	0,51	1	0	0	0,00	2,57	0,49	8,24
35	3,00	0,00	0,00	1,00	5,00	7,46	3,14	0,40	0,79	1,00	3,09	1,69	0,00	2,29	0,50	0	1	0	0,00	2,65	0,39	8,29
36	3,00	1,00	0,00	1,00	5,00	7,18	3,64	0,34	0,68	1,00	3,53	1,45	0,00	2,38	0,45	0	1	0	0,00	2,35	0,28	7,58
37	3,00	1,00	0,00	1,00	6,00	7,57	3,79	0,40	0,82	1,00	2,72	1,42	0,00	1,91	0,45	0	0	1	0,00	2,37	0,25	7,90
38	2,00	0,00	0,00	1,00	5,00	7,11	2,58	0,41	0,41	1,00	3,29	1,57	0,00	2,20	0,62	0	1	0	0,00	2,49	0,39	8,78
39	3,00	1,00	0,00	1,00	5,00	9,26	3,39	0,47	0,94	1,00	4,69	1,97	0,00	2,86	0,56	1	0	0	1,00	3,22	0,55	9,59
40	3,00	1,00	0,00	1,00	4,00	8,25	3,09	0,41	0,97	0,00	4,55	1,41	0,00	3,16	0,46	1	0	0	0,00	2,80	0,36	9,44
41	3,00	1,00	0,00	1,00	4,00	8,77	3,33	0,41	0,72	1,00	4,59	1,49	0,00	4,54	0,50	1	0	0	1,00	2,86	0,33	10,21
42	4,00	1,00	0,00	1,00	5,00	8,22	3,02	0,46	0,82	1,00	4,29	1,81	0,00	3,60	0,46	1	0	0	1,00	2,96	0,39	9,73
43	3,00	1,00	0,00	1,00	5,00	9,93	3,74	0,49	0,86	1,00	4,98	1,50	0,00	3,32	0,50	1	0	0	0,00	2,83	0,44	9,61
44	3,00	0,00	0,00	1,00	5,00	8,09	3,66	0,33	0,87	1,00	3,45	1,43	0,00	2,58	0,58	1	0	0	1,00	2,50	0,31	9,14
45	3,00	1,00	0,00	1,00	5,00	7,64	2,74	0,41	0,88	1,00	4,31	0,79	0,00	2,37	0,42	1	0	0	0,00	2,21	0,36	7,59
46	4,00	0,00	0,00	1,00	5,00	9,68	3,40	0,47	1,15	0,00	5,33	1,32	0,00	4,28	0,58	1	0	0	0,00	3,04	0,61	10,93
47	3,00	1,00	0,00	1,00	5,00	7,40	2,77	0,53	0,87	1,00	4,07	1,38	0,00	2,67	0,41	1	0	0	0,00	2,48	0,44	8,04
48	3,00	1,00	0,00	1,00	5,00	5,58	2,42	0,32	0,72	1,00	2,90	0,96	0,00	2,24	0,47	0	0	1	1,00	2,05	0,22	6,41
49	3,00	0,00	0,00	1,00	5,00	7,50	3,12	0,31	0,84	0,00	3,00	0,90	1,00	1,76	0,67	0	1	0	1,00	2,00	0,30	7,00
50	2,00	0,00	0,00	1,00	5,00	5,33	2,06	0,42	0,56	1,00	2,87	1,45	0,00	2,01	0,38	0	1	0	1,00	1,76	0,28	5,78
51	3,00	1,00	0,00	1,00	5,00	6,15	2,58	0,35	0,88	1,00	3,28	1,15	0,00	2,23	0,48	0	1	0	0,00	2,31	0,27	6,22
52	3,00	1,00	0,00	1,00	5,00	6,63	2,86	0,35	0,63	0,00	3,15	1,27	0,00	2,11	0,64	0	1	0	0,00	2,19	0,38	7,71

Appendix 4.3: continuation…

	RFTE	RFSL	RFIT	DFSH	DFNL	DFLC	DFLT	DFWT	DFWB	DFTB	DFLL	DFLO	DFSL	FILE	ANCO	ASSA	ASAU	ASRO	ANAP	ANLE	ANWI	STLE
53	3,00	1,00	0,00	1,00	5,00	5,54	2,17	0,26	0,58	0,00	2,95	1,05	0,00	1,77	0,40	0	1	0	0,00	2,14	0,36	5,40
54	3,00	1,00	0,00	1,00	5,00	6,06	2,73	0,35	0,90	0,00	2,49	1,36	0,00	1,74	0,43	0	1	0	0,00	1,97	0,27	5,94
55	3,00	1,00	0,00	1,00	5,00	7,33	3,46	0,34	0,92	0,00	3,64	1,13	0,00	2,62	0,51	0	1	0	0,00	2,31	0,25	8,28
56	3,00	1,00	0,00	1,00	5,00	7,06	3,21	0,32	0,92	1,00	3,21	1,47	1,00	2,21	0,61	1	0	0	1,00	2,46	0,34	8,12
57	2,00	1,00	0,00	0,00	5,00	7,11	3,50	0,36	0,64	1,00	2,76	1,38	1,00	1,81	0,48	0	1	0	0,00	2,50	0,39	8,14
58	3,00	1,00	0,00	1,00	5,00	5,93	3,40	0,32	1,20	0,00	2,87	0,93	0,00	1,91	0,57	0	1	0	0,00	2,06	0,32	7,16
59	3,00	0,00	0,00	1,00	5,00	8,25	3,02	0,34	0,57	1,00	4,37	1,51	0,00	3,22	0,69	1	0	0	0,00	2,72	0,28	8,80
60	3,00	1,00	0,00	1,00	5,00	9,95	4,25	0,25	1,10	1,00	5,14	2,09	0,00	5,25	0,20	1	0	0	0,00	3,16	0,30	10,79
61	3,00	1,00	0,00	0,00	5,00	9,26	3,93	0,35	0,92	1,00	3,96	1,51	0,00	3,16	0,48	1	0	0	1,00	2,90	0,38	10,42
62	3,00	1,00	0,00	1,00	5,00	9,09	3,28	0,35	0,73	1,00	4,19	1,79	0,00	3,16	0,51	1	0	0	0,00	2,99	0,35	11,65

Appendix 4.3: continuation…

	STBW	STSB	STSA	STSR	STST	ACLE	ACDI	PALE	PAWI
1	0,55	2,33	0	1,00	0	3,49	0,48	9,09	0
2	0,25	1,64	0	1,00	0	1,54	0,56	6,56	0
3	0,31	1,40	0	1,00	0	1,52	0,73	5,69	0
4	0,25	2,35	0	1,00	0	0,89	0,36	7,01	0
5	0,20	1,55	0	1,00	0	2,70	0,70	9,50	0
6	0,68	2,13	0	1,00	0	3,78	0,83	8,29	1
7	0,50	2,15	0	1,00	0	2,88	0,51	7,98	1
8	0,47	1,76	1,00	0	0	3,97	0,61	6,14	0
9	0,54	1,89	1,00	0	0	2,18	0,53	6,14	0
10	0,45	1,81	0	1,00	0	1,92	0,78	6,38	0
11	0,27	1,68	0	1,00	0	1,58	0,61	6,03	0
12	0,50	1,76	1,00	0	0	1,79	0,62	6,73	1
13	0,57	1,70	1,00	0	0	2,20	0,80	6,65	1
14	0,37	1,65	1,00	0	0	2,04	0,35	7,18	1
15	0,28	1,57	1,00	0	0	1,59	0,35	7,09	1
16	0,32	1,56	1,00	0	0	2,60	0,77	6,42	1
17	0,59	1,80	1,00	0	0	2,60	0,77	6,82	1
18	0,30	1,65	1,00	0	0	1,95	0,45	6,65	1
19	0,48	1,58	1,00	0	0	3,22	0,62	5,77	1
20	0,29	2,77	1,00	0	0	1,65	0,48	9,78	0
21	0,37	1,46	1,00	0	0	1,96	0,48	6,31	1
22	0,16	1,84	0	1,00	0	2,02	0,37	8,08	1
23	0,33	1,75	0	1,00	0	2,68	0,50	8,36	0
24	0,62	1,38	1,00	0	0	2,42	0,50	5,62	0
25	0,36	1,59	0	1,00	0	2,09	0,37	9,20	1
26	0,38	2,02	0	1,00	0	1,87	0,45	9,76	1

Appendix 4.3: continuation…

	STBW	STSB	STSA	STSR	STST	ACLE	ACDI	PALE	PAWI
27	0,51	1,42	1,00	0	0	1,82	0,55	6,22	1
28	0,55	1,64	1,00	0	0	2,24	0,65	6,12	1
29	0,52	2,50	1,00	0	0	1,65	0,68	6,32	0
30	0,70	3,33	1,00	0	0	2,63	1,08	8,42	0
31	0,18	1,48	0	1,00	0	1,51	0,58	7,46	0
32	0,55	1,49	1,00	0	0	2,40	0,52	8,22	1
33	0,60	1,63	0	1,00	0	2,76	0,82	8,10	1
34	0,51	2,20	0	1,00	0	2,44	0,62	7,66	0
35	0,49	2,14	0	1,00	0	2,46	0,64	7,95	0
36	0,28	2,23	0	1,00	0	1,98	0,53	7,24	1
37	0,38	1,98	0	1,00	0	1,55	0,54	7,84	1
38	0,26	1,49	1,00	0	0	1,43	0,27	6,90	1
39	0,60	1,61	1,00	0	0	2,94	0,84	8,95	0
40	0,78	1,65	0	1,00	0	3,14	0,93	7,46	0
41	0,38	1,76	1,00	0	0	1,99	0,64	8,47	0
42	0,43	2,16	1,00	0	0	2,60	0,71	7,89	0
43	0,53	2,26	1,00	0	0	2,74	0,75	8,43	0
44	0,55	1,81	1,00	0	0	2,73	0,70	6,59	0
45	0,52	1,39	0	1,00	0	2,22	0,74	6,80	1
46	0,65	2,00	0	1,00	0	4,31	0,96	7,80	0
47	0,56	1,92	0	1,00	0	2,11	0,81	7,35	0
48	0,27	1,73	0	1,00	0	1,44	0,54	5,58	1
49	0,40	1,84	1,00	0	0	1,80	0,60	6,00	0
50	0,36	1,73	0	1,00	0	1,26	0,35	4,94	0
51	0,51	1,51	1,00	0	0	2,44	0,50	5,82	0
52	0,33	1,87	0	1,00	0	1,49	0,34	6,12	0

Appendix 4.3: continuation…

	STBW	STSB	STSA	STSR	STST	ACLE	ACDI	PALE	PAWI
53	0,25	1,29	0	1,00	0	1,19	0,30	4,55	0
54	0,51	1,73	0	0	1,00	2,56	0,56	6,04	0
55	0,52	1,95	0	0	1,00	2,60	0,70	7,07	1
56	0,42	2,05	1,00	0	0	2,31	0,44	7,49	0
57	0,36	1,87	0	1,00	0	1,71	0,59	7,42	0
58	0,17	1,65	0	1,00	0	3,17	0,94	6,59	0
59	0,42	2,15	0	1,00	0	2,00	0,48	8,11	0
60	0,55	1,95	1,00	0	0	2,96	0,87	8,98	0
61	0,66	1,94	1,00	0	0	3,16	0,49	7,38	1
62	0,64	1,93	1,00	0	0	3,37	0,86	7,61	0

Appendix 4.4: List of vegetative and reproductive character including state character and abbreviations used in Appendix 4.2 and 4.3.

	Character	State	Abbrev.
	Habit	scandent	LHSC
		shrub	LHSR
		tree	LHTR
Leaves	Phyllotaxis	3-verticilate	LPVE
		alternate	LPAL
		subopposite	LPSU
		opposite	LPOP
	Shape	elliptic	LSEL
		lanceolate	LSLA
		oblong	LSOL
		obovate	LSOO
		ovate	LSOV
		suborbicular	LSOR
	Margin	entire	LMEN
		dentate	LMDE
		lobate	LMLO
		repand	LMRE
	Margin revolute	absent(0); present(1)	LMRV
	Margin border	brown(0); white(1)	LMBO
	Base	acute	LBAC
		oblique	LBOB
		cordate	LBCO
		truncate	LBTR
		rotund	LBRO
	Apex	obtuse(0); acute(1)	LAPE
	Consistence	papiraceous	LCPA
		membranaceous	LCME
		subcoriaceous	LCSU
		coriaceous	LCCO
	Length mean	na	LLLE
	Width mean	na	LLWI
	Secondary veins min	na	LLVI
	Secondary veins max	na	LLVX
	Pseudomargin	absent(0); present(1)	LPSE
	Adaxial surface indumentum	absent(0); present(1)	LADA
	Abaxial surface indumentum	absent(0); present(1)	LABA
	Abaxial surface indumentum type	puberulous	LAPU
		arachnoid	LAPA
		pubescent	LAPS
		tomentose	LATO
	Trichome structure	unicellular	LTSU

		multicellular	LTSM
	Trichome architecture	simple	LTAS
		stellate	LTAL
		T-shaped	LTAT
		branched (change term)	LTAB
Petiole	Length mean	na	PELE
	Width mean	na	PEWI
	Prominent nodes	absent(0); present(1)	PPNO
Synflorescence	Type	cymbiform	STCY
		corymbiform	STCO
		paniculiform	STPA
Receptacle	Shape	tubular (0); campanular (1)	RESH
Involucre	Length mean	na	INLE
	Width mean	na	INWI
Outer phyllaries	Number	na	OPNU
	Length mean	na	OPLE
	Width mean	na	OPWI
	Shape	filiform	OSFI
		oblong	OSOL
		elliptic	OSEL
		obovate	OSOV
		triangular	OSTR
	Apex	obtuse(0); acute(1)	OPAP
Inner phyllaries	Number	na	IPNI
	Phyllaries length mean	na	IPLE
	Outer row of inner phyllaries width mean	na	IPWO
	Inner row of inner phyllaries width mean	na	IPWI
	Scariose margin	absent(0); present(1)	IPSC
	Apex	obtuse(0); acute(1)	IPAP
	Consistence	membranaceous	IPCM
		subcoriaceous	IPCS
		coriaceous	IPCC
Capitula structure	Radiate capitula	absent(0); present(1)	CARA

Flowers	Total number of flowers (Radiate and Disc flowers)	na	FLNU
Ray flowers	Length mean	na	RFLE
	Tube lenght mean	na	RFTL
	Lobe width mean	na	RFLW
	Veins number	na	RFVE
	Terminal teeth number	na	RFTE
	Terminal teeths same length	absent(0); present(1)	RFSL
	Tube indumentum	absent(0); present(1)	RFIT
Disc flowers	Shape corolla	tubular (0); campanular (1)	DFSH
	Corolla lobes number	na	DFNL
	Corolla length mean	na	DFLC
	Tube length mean	na	DFLT
	Tube width mean	na	DFWT
	Tube base width mean	na	DFWB
	Tube base straight	abrupt (0); regular (1)	DFTB
	Limb length mean	na	DFLL
	Lobes length mean	na	DFLO
	Lobes shape	triangular (0); oblong (1)	DFSL
Filament	Length mean	na	FILE
Anthers	Collar anthers length mean	na	ANCO
	Base shape	sagittate	ASSA
		auriculate	ASAU
		rounded	ASRO
	Apex fused to teca	absent(0); present(1)	ANAP
	Length mean	na	ANLE
	Width mean	na	ANWI
Style	Lenght Aver	na	STLE
	Base width mean	na	STBW
	Style branches lenght mean	na	STSB
	Shape of apex	acute	STSA
		rotund	STSR
		truncated	STST
Achens	Length mean	na	ACLE
	Diameter mean	na	ACDI
Papus	Length mean	na	PALE
	Wider apex	absent(0); present(1)	PAWI